Institut für Geowissenschaften
Mathematisch-Naturwissenschaftliche Fakultät
Universität Potsdam

LAKE-LEVEL FLUCTUATIONS AND LATE-QUATERNARY CLIMATE CHANGE IN THE CENTRAL KENYA RIFT

Dissertation

zur Erlangung des akademischen Grades
Doktor der Naturwissenschaften (Dr. rer. nat.)
in der Wissenschaftsdisziplin Geologie

eingereicht an der
Mathematisch-Naturwissenschaftlichen Fakultät
der Universität Potsdam

von
Andreas G. N. Bergner

Potsdam, im November 2003.

To my family,
with gratitude for all the years of support.

ABSTRACT

In this work, an approach of paleoclimate reconstruction for tropical East Africa is presented. After giving a short summary of modern climate conditions in the tropics and the East African climate peculiarity, the potential of reconstructing climate from paleolake sediments is discussed. As demonstrated, the hydrologic sensitivity of high-elevated closed-basin lakes in the Central Kenya Rift yields valuable guaranties for the establishment of long-term climate records. Temporal fluctuations of the limnological characteristics saved in the lake sediments are used to define variations in the Quaternary climate history. Based on diatom analyses in radiocarbon- and $^{40}Ar/^{39}Ar$-dated sediments, a chronology of paleoecologic fluctuations is developed for the Central Kenya Rift -lakes *Nakuru, Elmenteita* and *Naivasha*. At least during the penultimate interglacial (around 140 to 60 kyr BP) and during the last interglacial (around 12 to 4 kyr BP), these lakes experienced several transgression-regression cycles on time intervals of about 11,000 years. Additionally, a long-term trend of lake evolution is found suggesting the general succession from deep freshwater lakes towards more saline waters during the last million years. Using ecologic transfer functions and a simple lake-balance model, the observed paleohydrologic fluctuations are linked to potential precipitation-evaporation changes in the lake basins. Though also tectonic influences on the drainage pattern and the effect of varied seepage are investigated, it can be shown that already a small increase in precipitation of about 30±10 % may have affected the hydrologic budget of the intra-rift lakes within the reconstructed range. The findings of this study help to assess the natural climate variability of East Africa. They furthermore reflect the sensitivity of the Central Kenya Rift -lakes to fluctuations of large-scale climate parameters, such as solar radiation and sea-surface temperatures of the Indian Ocean.

KURZFASSUNG

Diese Arbeit beschäftigt sich mit der Rekonstruktion von Klima in historischen Zeiten im tropischen Ostafrika. Nach einer Übersicht über die heutigen klimatischen Bedingungen der Tropen und den Besonderheiten des ostafrikanischen Klimas, werden die Möglichkeiten der Klimarekonstruktion anhand von Seesedimenten diskutiert. Es zeigt sich, dass die hoch gelegenen Seen des Zentralen Keniarifts, als Teil des Ostafrikanischen Grabensystems, besonders geeignete Klimaarchive darstellen, da sie sensibel auf klimatische Veränderungen reagieren. Veränderungen der Seechemie, wie sie in den Sedimenten aufgezeichnet werden, eignen sich um die natürlichen Schwankungen in der Quartären Klimageschichte Ostafrikas nachzuzeichnen. Basierend auf der guten $^{40}Ar/^{39}Ar$- und ^{14}C-Datierbarkeit der Seesedimente wird eine Chronologie der paläoökologischen Bedingungen anhand von Diatomeenvergesellschaftungen restauriert. Dabei zeigen sich für die Seen *Nakuru, Elmenteita* und *Naivasha* kurzfristige Transgression/ Regressions-Zyklen im Intervall von ca. 11.000 Jahren während des letzten (ca. 12.000 bis 6.000 J.v.H.) und vorletzten Interglazials (ca. 140.000 bis 60.000 J.v.H.). Zusätzlich kann ein allgemeiner, langfristiger Trend der Seeentwicklung von großen Frischwasserseen hin zu stärker salinen Gewässern innerhalb der letzen 1 Mio. Jahre festgestellt werden. Mittels Transferfunktionen und einem hydro-klimatischen Modellansatz können die restaurierten limnologischen Bedingungen als klimatische Schwankungen des Einzugsgebietes interpretiert werden. Wenngleich auch der zusätzliche Einfluss von tektonischen Veränderungen auf das Seeeinzugsgebiet und das Gewicht veränderter Grundwasserströme abgewogen werden, zeigt sich, dass allein geringfügig erhöhte Niederschlagswerte von ca. 30±10 % zu dramatischen Seespiegelanstiegen im Zentralen Keniarift führen. Aufgrund der etablierten hydrologisch-klimatischen Wechselwirkungen werden Rückschlüsse auf die natürliche Variabilität des ostafrikanischen Klimas gezogen. Zudem wird die Sensitivität der Keniarift-Seen in Bezug auf die Stärke der äquatorialen Insolation und hinsichtilch variabler Oberflächenwassertemperaturen des Indischen Ozeans bewertet.

INDEX

TABLE OF CONTENTS

APPENDIX B

LIST OF FIGURES

LIST OF TABLES

PREFACE

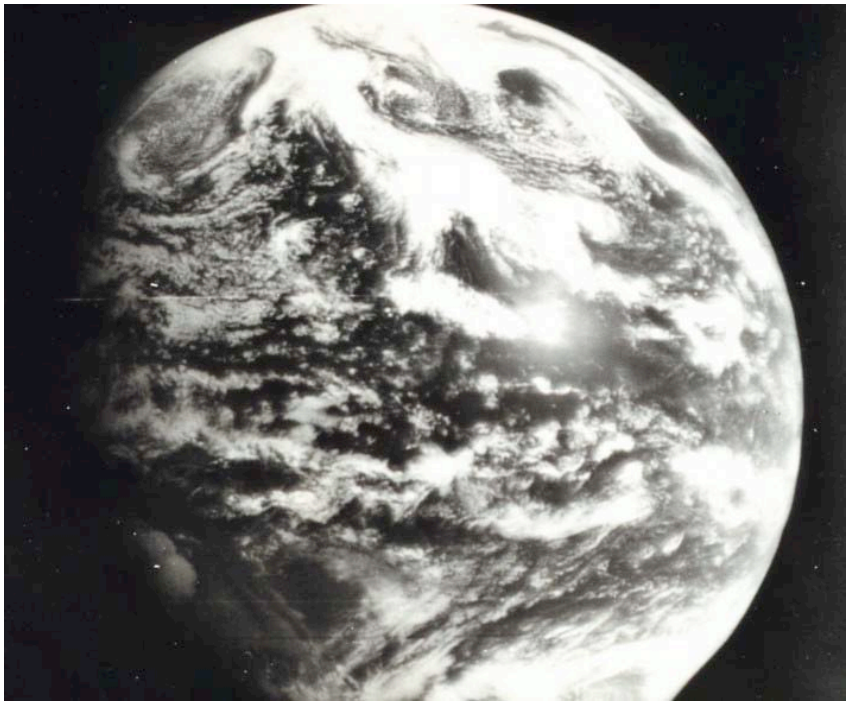

The changing Planet Earth, as seen from the sky. Early image of the Earth from Applications Technology Satellite 1 (ATS-1), December 1966 (NOAA).

Environmental conditions on Planet Earth have been varied and still vary on different temporal and spatial scales. On geologic time scales, volcano-tectonic processes and changes in the orbital constellations caused large variations in the lithosphere and atmosphere: the uplift of the Tibetan Plateau initialized the Indian monsoon system, the closure of the Panama Isthmus intensified the Gulf stream, whereas periodically weak solar insolation forced the ice age cycles of the last million years (Milankovitch, 1941; Imbrie and Imbire, 1979; Berger, 1992; Prell and Kutzbach, 1992; Haug and Tiedemann, 1998). On shorter time scales, climate changes are related to intensity fluctuations, but also by anthropogenic influences, i.e., emission of greenhouse gases and deforestation. Living communities were always affected by the environmental changes: during the last 3 million years, human evolution was strongly associated with African climate change (Vrba et al., 1995; deMenocal, 1995); during the last hundreds of thousands of years ice age climates dramatically affected human habitats in Eurasia and Northern America (Roberts, 1998; Oldfield and Alverson, 2003); during the last 2,000 years, climate-induced changes in humidity, floods and droughts influenced food

and water supply in several, mostly tropical regions of the world (Nieuwolt, 1986; Verschuren et al., 2000; Haug et al., 2003).

In contrast to the long history of climate change, our knowledge on the Earth's climate is limited and mainly based on short instrumental records and few simplified models. The understanding of the full natural variability of climate change and its causes requires the investigation of longer archives of climate history. In this context, the study of natural climate archives such as ice cores, tree rings, speleothems, marine and terrestrial sediments provides a solid basis for a better understanding of the mechanisms and causes of climate change (Harjes and Walter, 1999; Alverson et al., 2001; Saltzmann, 2002). Without an understanding of the effect of external forcing and internal interactions of the most relevant components of the Earth's climate system we will never be able to fully anticipate and predict future changes of our environment and our place in it.

Where will we go? Photograph of the 3.6 million year old Laetoli footprints giving the first evidence for the existence of *Australopithecus afarensis*, one of the first ancestors of modern man; photo by John Reader

ACKNOWLEDGEMENTS

This project was funded by two grants to Martin Trauth and Manfred Strecker by the German Research Foundation (DFG). I thank my supervisor Martin Trauth who achieved a great deal teaching me how to become a scientist, how to obtain reliable information and how to sell the results of my investigations. I thank him and Manfred Strecker for their confidence, constructive critics and huge support at all time.

My particular gratitude goes to Françoise Gasse, Françoise Chalié and Cathrin Brüchmann for their help with diatom taxonomy and interpretation as well as for many inspiring discussions. These experts helped me to learn the language of the diatoms and made me a good friend of the 'petits bestiols' or 'kleine Scheißerchen'. *Merci beaucoup pour votre persistance! Danke für die unglaubliche Geduld!*

I want to express many thanks to all my colleagues, co-workers, reviewers of this manuscript and friendly assistants in Potsdam, Aix-en-Provence and San Francisco struggling with me for best results and continuous progress in the research. In particular I am very grateful to the students Anke, Jan and Gordon as well as to Peter Blisniuk, Bodo Bookhagen, Axel Bronstert, Alan Deino, Miriam Dühnforth, Jörg Erzinger, Birgit Fabian, Christine Fischer, Anke Friedrich, Gerald Haug, Antje Müller, Roland Oberhänsli, Birgit Tiersch and Christine Vallet-Coulomb. I thank the government of Kenya and the Kenya Wildlife Service for research permits. I acknowledge Thomas Schlüter, Malte Ibs-von Seht, Sarah Higgins and Dirk Verschuren, the Kenyan colleagues at the University of Nairobi and our friends in Naivasha for their friendly support and help. *Asante sana*, thank you very much!

I want to say 'tausend Dank' and many thanks to all my friends in Potsdam, especially to those who were always present when their help was required. *Ein dickes Dankeschön* to Eckat, Carola, Barbara, Kai, Susan, Antje, Molli, Dagmar, Annett, analleDok and to all the others.

At least - and this might be the most important acknowledgement - I have to thank my family. It was a wonderful experience getting their support whenever it was necessary and without even having to ask for. *Danke dir liebes Mütterchen, Dad, Berit, den Großeltern und dem Rest der 'buckligen' Verwandtschaft*. Thank you ever so much!

CHAPTER 1

SOCIETAL RELEVANCE AND THE POTENTIAL OF PALEOENVIRONMENTAL RESEARCH

Fig. 1.1 Pupils of the Kenyata Primary School in Rumuruti, Kenya, waiting for water distribution during the year-2000-drought of East Africa (photograph by J. Bobert).

More than two thirds of the world's population lives in the tropics (UN, 2003). Most of the tropical countries strongly depend on agricultural production as a major source of food supply, employment and foreign exchange. Since relatively stable high temperature is not the limiting factor of food production in the tropics, the total amount and the regional distribution of rainfall is the most important factor controlling the availability of adequate food and fresh water (Troll, 1959; Nieuwolt, 1986; Nieuwolt, 1989). Short-term variations in the tropical rainfall pattern provoked severe floods and droughts, which repeatedly affected societies and their socio-economic stability in the past as well as in present-day (Vrba et al., 1995; Birkett et al., 1999; Verschuren, 1999; Phillips and McIntyre, 2000; Galvin et al., 2001; Haug et al., 2003). The effective understanding of factors controlling regional climate variability would enable countries to prepare for the effects of extreme climate events.

Natural rainfall variability in the tropics

Those approximately 40% of the Earth's surface bounded by the 23.5° latitudes, the so-called Tropics of Cancer and Capricorn (from Greek tropos = turn), are commonly defined as the *tropics* or *low latitudes* (Fig. 1.2). Since the latitudinal parallels refer to the limits of the area where the sun can be in a zenith position, the geographic division implies a climatic characterization, too. The tropics are therefore often defined by the prevailing climate (Hartmann, 1994; McGregor and Nieuwolt, 1998).

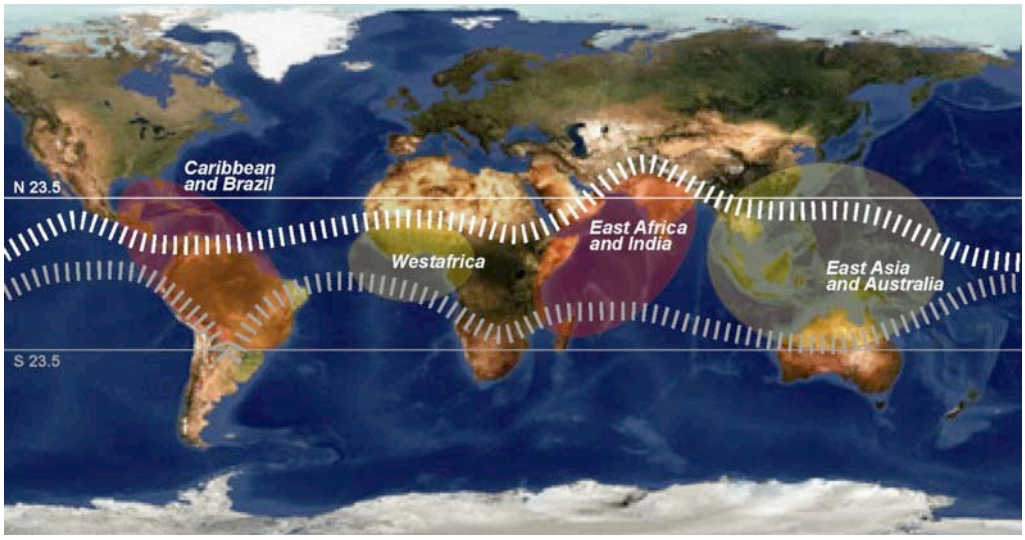

Fig. 1.2 Composite satellite image of the world (NOAA) showing natural vegetation and the position of the tropics between the 23.5° latitudes with aligned equatorial low-pressure cells (*Intertropical Convergence Zone* - ITCZ) forming after the transition of the overhead sun in July (North) and January (South); shaded areas indicate main regions of trade wind/ monsoonal influence (modified after McGregor and Nieuwolt, 1998)

A *tropical climate* in Vladimir Köppen's scheme of climate classification is defined as a non-arid climate in which all twelve months have mean temperatures above 18°C (McGregor and Nieuwolt, 1998). Additionally, the description of tropical climates is classically related to the definition of the Hadley-cell principles (Hartmann, 1994; McGregor and Nieuwolt, 1998). Following the highest sun, hot and moist air rises in the Intertropical Convergenze Zone (ITCZ), flows towards higher latitudes, subsides at about 30° latitude and returns as trade winds or monsoons (Hartmann, 1994; Leroux, 2001). The trade winds attracted by the ITCZ commonly collect large volumes of water vapor while they pass over large open water surfaces of the world's oceans. The higher the evaporation over the oceans, i.e., the warmer the sea surface temperatures, the wetter

are the trade winds and the more water vapor is produced in the convergence centers (Hartmann, 1994). High topographic relief on the adjacent continents functions as a natural barrier for the trade winds. If the moist air masses are lifted over topographic heights and lifting is sufficient for reaching the condensation level, cloudiness of the convective type occurs. Prominent continental topography and prevailing warm ocean currents are thus the main causes for the pronounced humidity of many tropical regions (McGregor and Nieuwolt, 1998) (Fig. 1.2).

There has been much debate about the general character of the ITCZ, focusing on a distinction between single physical parameters, such as surface temperature, air pressure and cloudiness. Although all these parameters are distinctive within the ITCZ, it is now well accepted that the term *intertropical convergence* refers to the zone of converging trade winds, maximum cloudiness and rainfall (Hastenrath and Lamb, 1977; Hastenrath, 1985; Waliser and Gautier, 1993; Vincent, 1994). This zone generally follows the position of the solar zenith with a delay of about one month. In that sense, the propagation of the ITCZ defines the timing of the onset, duration and cessation of the rainy season in many tropical regions (McGregor and Nieuwolt, 1998). Caused by both, the long-term and synoptic variability of the determinants of the ITCZ, the amount of rainfall naturally fluctuates dramatically in the tropics. On geologic timescales, the intensity of the ITCZ is controlled by (a) intensified solar heating of the tropics in the course of changing orbital parameters, (b) increased sea-surface temperatures (SST) and (c) changes in ocean circulation (e.g., Prell and Kutzbach, 1987; Clemens et al., 1991; Clement et al., 1999; Cane and Molnar, 2001; Seidov et al., 2001; Trauth et al., 2003). In contrast, short-term fluctuations are mostly attributed to the intensity of the El Niño/Southern Oscillation (ENSO), variations of the North Atlantic Dipole (NAO) influence and changes of the stratospheric wind circulation (quasi-biennial oscillation - QBO) (e.g., Hastenrath and Rosen, 1983; Hastenrath, 1985; Haigh, 1994; Clement et al., 1999; Indeje et al., 2000). In particular, Indian and Pacific Ocean SST anomalies caused some of the most extreme floods during the last 100 years (Suplee, 1999) (Fig. 1.3).

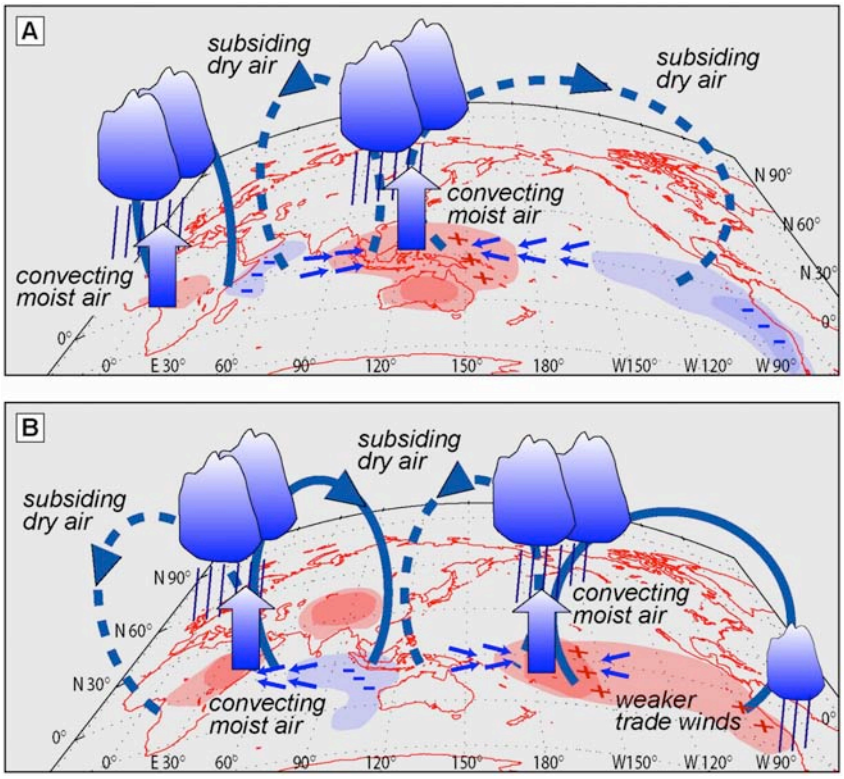

Fig. 1.3 General pattern of the ENSO variation over the Indian and Pacific Ocean. Under normal conditions (A) trade winds maintain a balance between warm western Pacific and cool eastern Pacific waters; high convection over Indonesia causes an equatorial eastward circulation in the Indian Ocean (arrows) and cools sea-surface at the coast (-); Under El-Niño conditions (B) weaker easterly trade winds over the Pacific Ocean cause higher sea-surface temperatures along the coast of South America (+); warm Pacific-Ocean water migrates eastward; convection is highest over Tahiti; in the Indian Ocean, local high surface air-pressure forms over Australia causing westward migration of the equatorial ocean currents (arrows); convection is high at the East African coast (modified after Suplee, 1999).

Temporal and spatial distribution of rainfall in East Africa

In contrast to many other tropical regions, low rainfall throughout the year characterizes most parts of East Africa. This might be surprising because of the equatorial position of the subcontinent, reaching from 14° N to 11° S (Fig. 1.4). Whereas dense rain forests typify other equatorial regions, the representative vegetation in East Africa is open savanna. The main reasons for the pronounced aridity causing this type of vegetation are (a) the topographically-controlled isolation of East Africa from westerly flows and (b) relatively cold oceans at Indian-Ocean origin of the trade winds (Camberlin, 1995; Nicholson, 1996; Nicholson, 2000; Leroux, 2001). As a consequence, East Africa receives most of the annual rainfall when the ITCZ is directly located over East Africa, i.e., in Northern Hemisphere spring during the *long rains* from April to May, and in fall,

during the *short rains* from October to November. During Northern Hemisphere summer, the southwesterly trade winds from the southern Indian Ocean prevail, but air masses carried by these winds released most of their moisture along the coast of Madagascar before reaching the continent. Thus, rainfall from June to September is restricted to the coastal regions and the higher mountains of East Africa, e.g., Mt. Kilimanjaro (5,895 m a.s.l.) and Mt. Kenya (5,199 m). In winter, the northeasterly trade winds pass over the stabilizing cold Somali current and cause significant rainfall only in Southern Tanzania (Griffiths, 1972; Rodhe and Virji, 1976; Gatebe et al., 1999; Nicholson, 2000) (Fig. 1.4).

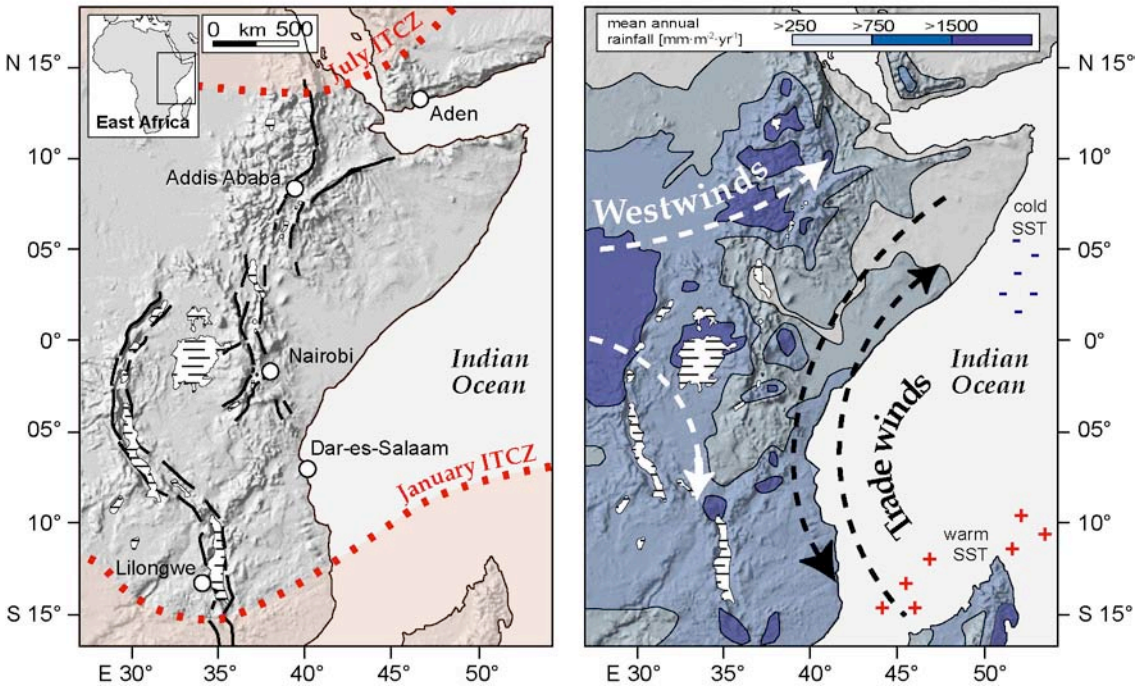

Fig. 1.4 Shaded relief map of East Africa (Gtopo-30 data from U.S.G.S. EROS Data Center in Sioux Falls, South Dakota) showing (left) topography, location of large lakes and major faults of the East African Rift System (EARS) as well as the position of the ITCZ in Northern Hemisphere summer (July) and winter (January); (Right) airflow pattern and precipitation of East Africa; contours of seasonal precipitation show rainfall maxima in northern (Ethiopia) and southern East Africa (Madagascar), which are mainly controlled by topography and sea-surface temperatures (SST) of the Indian Ocean; for comparison: mean annual precipitation of Jakarta (6° 11' S; 106° 50' E): 1,755 mm (Heyer, 1993). The predominating circulation systems of the SE- and NE-trade winds as well as westwind streams only indirectly affect the rainfall pattern of East Africa. Modified after Survey of Kenya (1991).

Whereas the large-scale airflow pattern and the distribution of rainfall in East Africa are now well understood, changes in local rainfall as a consequence of global and regional climate fluctuations are often difficult to predict. Long records of instrumental data to investigate the relationship between local hydrological changes and large-scale climate processes are scarce. However, much work has been done on the history of East African

lakes responding to climate changes on time scales of years up to thousands of years (cf., Gasse, 2000). Herein it is assumed that, e.g., specific fossil plants grew under the same preferred climatic conditions than their modern equivalents, the temporal succession of typical floral communities would suggest climate changes (Cronin, 1999). In that sense, particular closed-basin lakes are excellent recorders of past climate changes (Taub, 1996; Bradley, 1999; Battarbee, 2000; Yuretich and Ervin, 2002). Their water storage as well as all hydrochemical parameters strongly depend on the surrounding environment. Small temporal and spatial changes in the distribution of rainfall in the catchment cause changes in river discharge, vegetation, soil coverage, supply of dissolved and suspended river load. These changes are in turn recorded in the deposits of the lake, which is therefore a natural archive of past climate fluctuations. The investigation of lake sediments including all kinds of biological, mineralogical and geochemical environmental indicators therefore provides the unique opportunity to study the consequences of global and regional climate shifts on local water budgets and environmental changes (cf., Battarbee, 2000; Gasse, 2000; Gasse, 2001).

Reconstructing climates from paleolake sediments

Linking the sedimentological and paleontological information contained in lake deposits to past climate conditions is one of the main objectives of paleolimnological research (Last et al., 2002; Cohen, 2003). During the last decades, numerous indirect indicators of climate have been identified in lake deposits and used to reconstruct past climate changes (e.g., clay minerals, diatom and pollen assemblages) (Battarbee, 2000; Alverson et al., 2003). Also in East Africa, a large number of investigations have been carried out on lake histories (e.g., Müller, 1903; Hustedt, 1949; Talling and Talling, 1965; Beadle, 1974; Eugster and Jones, 1979; Yuretich, 1982; Gasse, 1986). The studies established a number of valuable proxy data, i.e., climate-dependent indicator values recording changes of the past climatic conditions in lake sediments (Fig. 1.5). Based on the comparison between modern and paleo-inventories transfer functions were established, e.g., for pollen or diatoms (unicellular silica algae of the class *Bacillariophyceae*) relating single taxa to values of hydrochemical preference (Guiot, 1990; Gasse et al., 1995). In closed-basin lakes, where the lake's hydrochemistry is closely linked to the precipitation-evaporation (*P-E*) balance in the catchment, transfer-

function based reconstructions of paleowater chemistry provide a direct estimate of the past climate conditions in the lake catchment (Taub, 1996; Cohen, 2003) (Fig. 1.5).

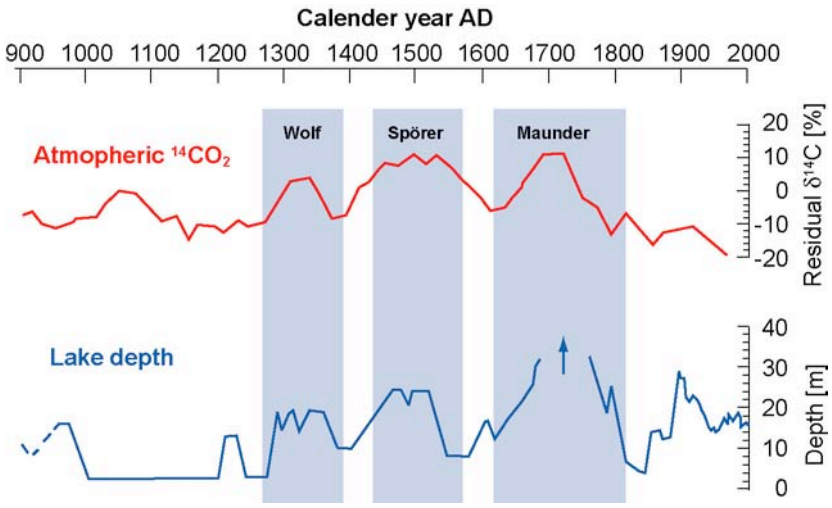

Fig. 1.5 Comparison of the lake level of Lake Naivasha, Kenya, (as reconstructed from sediment characteristics; Verschuren et al., 2000) with changes in solar radiation (inferred from $\Delta^{14}C$ of atmospheric CO_2; Stuiver and Reimer, 1993).

Depending on the character of the lake basin, hydrologic changes of a lake are also influenced by processes such as changes in basin geometry and river network caused by tectonic movements and volcanic processes (Yuretich, 1982; Bradley, 1999; Hoelzmann et al., 2001; Renaut and Ashley, 2002; Saltzmann, 2002). Second, direct and indirect anthropogenic influences on the hydrology of the lake, vegetation in the catchment and river discharge may have a significant impact on the lake's history on shorter time scales. In particular, the knowledge about the influence of natural and man-made changes in vegetation on the *P-E* balance of lakes in East Africa is still very limited (cf., Barron and Moore, 1994; Kubatzki et al., 2000; Rensen and Lautenschlager, 2000). Interpreting climate proxies from lake sediments, it has to be considered that always a complex mixture of climatic, geologic and anthropogenic influences controls the individual lake evolution (Taub, 1996; Carrol and Bohacs, 1999; Last et al., 2002).

Finally, while reconstructing climate change from lake sediments, it has to be considered that different processes in the catchment cause changes in the lake basin on different timescales. The approximate response (or relaxation) time in a lake system is a measure of the time it would hypothetically take for dissipative processes (acting in the absence of continoud forcing) to balance departures from equilibrium (Saltzmann,

2002) (Fig. 1.6). For example, hydrochemical parameters adapt relatively quickly, whereas the formation of massive fluvial deposits and paleo-shorelines acts on longer timescales (Renaut and Ashley, 2002; Last et al., 2002; Saltzmann, 2002). Although lake sediments represent powerful tools for constructing scenarios of the biotic, hydrologic and climatic evolution of closed-basin lakes, the validity of these scenarios has always to be carefully tested by independent sources of information.

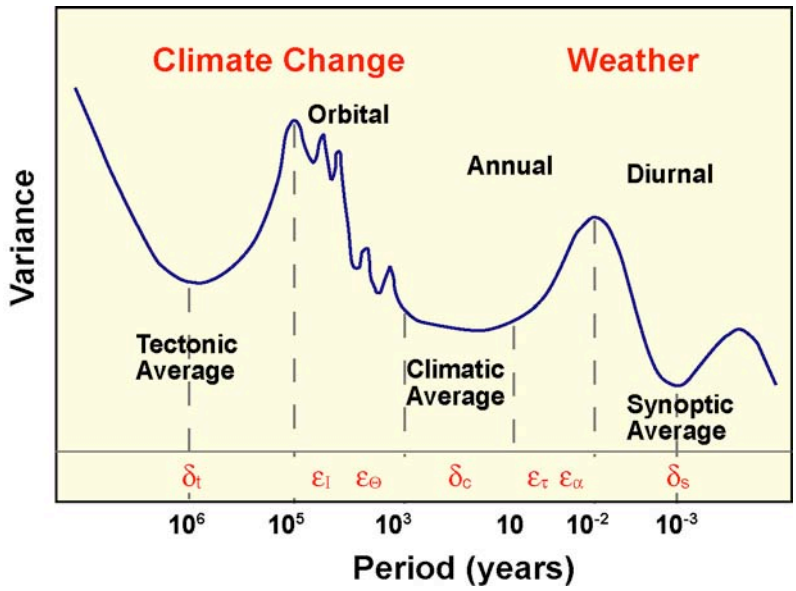

Fig. 1.6 Large-scale example for a hypothetical, highly idealized, spectrum of atmospheric thermal variance at an individual point over the age of the Earth. □, □ and □ denote the synoptic, climatic and tectonic averaging interval, respectively, and □, □, □ and □ denote the approximate response times for the atmosphere, oceanic mixed layer, deep ocean and ice sheets, respectively. This sample has to be adapted to the time resolution of each system (modified after Saltzmann, 2002).

CHAPTER 2

RECONSTRUCTING PALEOCLIMATE IN THE CENTRAL KENYA RIFT

Fig. 2.1 Photograph from the eastern escarpment towards the rift graben of the Central Kenya Rift (*CKR*) with Mt. Longonot, one of the central volcanoes, whose ashes have periodically intercalated the *CKR*-lake sediments.

During the last three years the Kenya research group at the University of Potsdam focused on the establishment of a long-term continental record for East Africa climate change. Such records are important, because (contrasting several precise reconstructions of Holocene climate change) detailed information for the time period prior to 10,000 BP are scarce (Gasse, 2000; Alverson et al., 2003; Trauth et al., 2003). The lack of paleoclimatic information from continental records is mostly related to either the limited time resolution of the investigated paleoclimate archives, the shortness of records with higher temporal resolution or insufficient age control. Therefore, climate information for the Pleistocene is mainly based on the interpolation from marine records and Global Climate Modeling (*GCM*) results (Alverson et al., 2003; Trauth et al., 2003).

The Central Kenya Rift (*CKR;* 0°15' to 1°00' S and 35°45' to 36°45' E) is the highest part of the volcanically and tectonically active eastern branch of the East African Rift System (*EARS*) (Figs. 1.4, 2.1, 2.2). In this area, lake sediments from closed-basin intra-rift lakes were continuously deposited at least during the last one million years. Since

abundant and precisely dateable volcanic ashes periodically intercalate the sediments, they provide excellent prospects to extract paleoenvironmental data. In addition, the hydrologic sensitivity of the closed-basin lakes offers a net correlation between the (paleo-) limnologic and climate conditions.

Already at the beginning of the last century, intensive geologic mapping of paleolake sediments started in the *CKR* (e.g., Leakey, 1931; Nilsson, 1931; Thompson and Dodson, 1963). In the middle of the century, radiometric age determinations provided a temporal framework for the environmental histories as reconstructed from the lake deposits (e.g., Bone, 1985; Blisniuk, 1988; Clarke et al., 1990; Strecker, 1991; Trauth, 1992). South of modern Lake Naivasha (today 1,889 m a.s.l.) in the Ol Njorowa Gorge, the analyses of a 60 m-thick profile suggested that lake-level highstands, as indicated by massive diatom-bearing deposits coincide with periods of wetter climates (Trauth and Strecker, 1996) (Fig. 2.2, 2.4). On the other hand, intermittent lowstands, as inferred from hydrochemically altered lake deposits, were interpreted as to reflect increased alkalinity and the formation of brine solutions during more arid conditions (Trauth, 1992; Trauth and Strecker, 1996). Based on these findings, the first long-term paleoclimate record of the *CKR* was established (Trauth et al., 2001).

In 2000, we started a new project, sponsored by the German Research Foundation (*DFG*) focusing on the internal causes of the lake-level changes in the 3,400 km^2-large Naivasha basin (Fig. 2.2). The main goal of this new project was to analyze (a) the hydrochemical evolution of each lake-level highstand, (b) their relation to environmental changes in the catchment area and (c) the correlation of these hydrological changes with synchronous changes in the neighboring Lake Nakuru-Elmenteita basin.

Geologic and hydrologic settings

The *EARS* is the major morphologic and geologic feature of the East African continent, which has been geologically active at least during the past 45 million years. Although the geologic evolution of *CKR* is not older than 15 Ma, present-day volcanic and

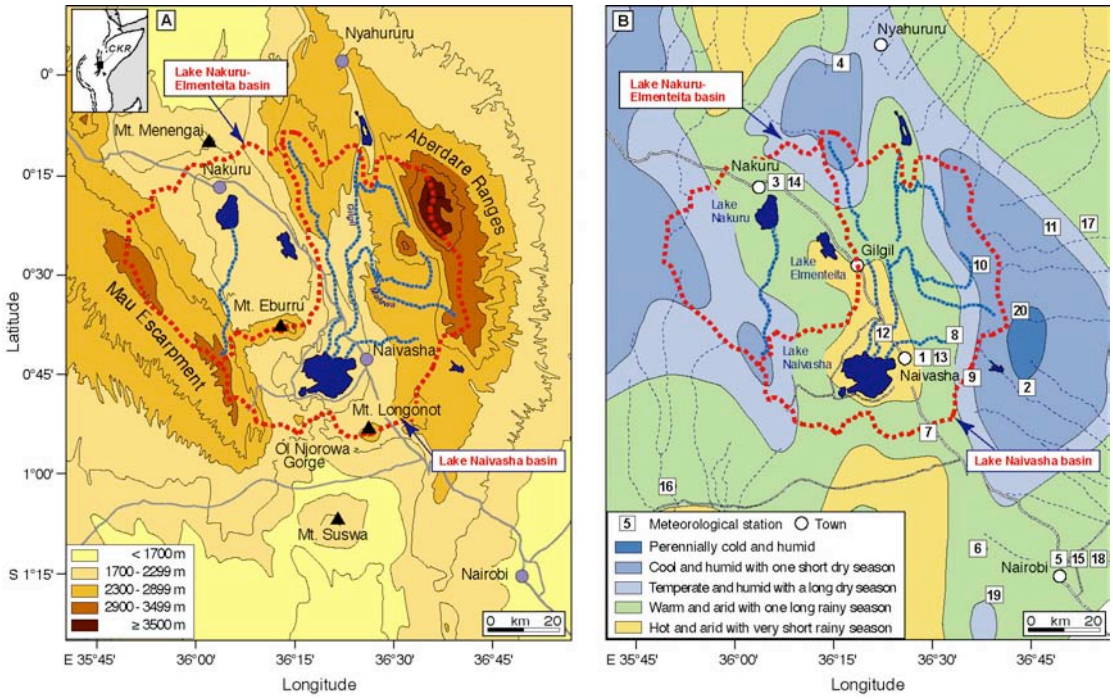

Fig. 2.2 Maps of the Central Kenya Rift showing the location of the Naivasha and Nakuru-Elmenteita basins, main rivers, cities and (A) topography and (B) climate conditions; location of meteorological stations (1) Naivasha W.D.D., (2) Kimakia Forest Station, (3) Nakuru Met. Station, (4) Nyahuhuru, (5) Nairobi Dagoret Corner, (6) Muguga K.A.R.I., (7) Kedong Ranch, (8) Naivasha Mkungi, (9) Longonot Carnell, (10) Aberdare West Gate, (11) Aberdare East Gate, (12) Naivasha Morendat, (13) Naivasha Kongoni Farm, (14) Nakuru, (15) Nairobi Int.Airport, (16) Narok, (17) Nyeri, (18) Kiambu, (19) Ngong, (20) S. Kinangop (Ndiara); climate information from KMD (2000; stations 1 to 7), Vincent et al. (1989; stations 8 to 11, 13), Vincent et al. (1979; station 12), GDS (1994) and ISMCS (1995; stations 14 to 17), Rodhe and Virji (1976; stations 18 to 19), Ojany and Ogendo (1988; station 20).

tectonic events are concentrated to the rift floor, with acidic volcanism from small eruption centers and NNE-SSW orientated faulting with offset rates of about 5 cm per 1,000 years (Baker and Wohlenberg, 1971; Clarke et al., 1990; Strecker et al., 1990; Strecker, 1991; Roessner and Strecker, 1997; Ebinger et al., 2000). The present-day morphology of the *CKR* is dominated by longitudinal bordering rift escarpments, i.e. the Aberdare Range (4,403 m a.s.l.) to the East and the Mau Escarpment (3,080 m) to the West, and Late Pleistocene to Holocene volcanic domes, such as Mt. Suswa (2,357 m), Mt. Longonot (2,776 m), Mt. Eburru (2,840) and Mt. Menengai (2,278), erupted in the rift graben (Fig. 2.1 and 2.2)

Climatologically, the *CKR* is located between the influences of the Congo air mass and the trade wind/monsoon circulation over the Indian Ocean (Nicholson, 1996; Leroux, 2001) (cf., Fig. 1.4). Due to their NNW-SSE orientation, the high-elevated rift shoulders block both, the Congo westwinds and the trade winds from the North- and Southeast (Nicholson, 1996). As a consequence, only the flanks of the rift receive high amounts of

orographic rain nearly throughout the year. Precipitation on the rift floor only results from convective rainfall during the short-time transition of the *ITCZ* (Rodhe and Virji, 1976; Vincent et al., 1979; KMD, 2000). Annual rainfall exceeds 1,750 $mm \cdot yr^{-1}$ on the rift shoulders (Jätzold, 1981; KMD, 2000). In contrast, the fairly flat and wind-stressed graben is characterized by a negative moisture budget with rainfall averaging ~650 $mm \cdot yr^{-1}$ and evaporation of ~1,900 $mm \cdot yr^{-1}$ (Jätzold, 1981; KMD, 2000) (Fig. 2.2).

Three intra-rift lakes - Lake Nakuru (1,758 m a.s.l.), Lake Elmenteita (1,786 m) and Lake Naivasha (1,989 m) - are located in the *CKR*. They belong to two different drainage basins, the Nakuru-Elmenteita and the Naivasha basins (Fig. 2.2). Since the lakes are all located in the evaporation-stresses rift graben, they loose between 25 to 50% of their water storage through vaporization. To compensate this water output, the lakes strongly depend on sufficient freshwater supply by river discharge from high-elevated upstream catchments (Milbrink, 1977; Gaudet and Melack, 1981; Verschuren, 1999). The temporal variance of these freshwater supplies, related to short-term fluctuations in the precipitation pattern causes significant lake-level fluctuations to the hydrologically sensitive lakes (Vincent et al., 1979; Becht and Harper, 2002).

Lake Naivasha, the largest and highest-elevated lake of the *CKR*, is unique among the others. The modern lake contains about 0.85 km^3 of water and covers an area of about 180 km^2. Around 20% of the lake surface is covered by papyrus swamps. Whereas Lake Elmenteita and Lake Nakuru (1,758 m) are both highly alkaline, Lake Naivasha contains fresh water with a pH of ~7.9 and conductivity values fluctuating between 250 and 500 $\mu S \cdot cm^{-1}$ (Gasse et al., 1995; Verschuren, 1999). Because of the regional importance of Lake Naivasha for fishery, tourism and horticulture industry, several studies focused on the calculation of its water balance (e.g., Hastenrath and Kutzbach, 1983; Vincent et al., 1989; Becht and Harper, 2002). It is now well established that the water quality of the lake can in part be attributed to mineral precipitation and biochemical removal at the sediment-water interfaces. This process is controlled by significant lake-level fluctuations in the range of ±2 meters (Milbrink, 1977; Gaudet and Melack, 1981). Additionally, significant seepage lost through permeable volcanic subsurface rocks and the perennial freshwater supply from the Malewa and Gilgil rivers account for a large part of the dilution (Darling et al., 1990; Ojiambo and Lyons, 1996;

Becht and Harper, 2002). However, it could sufficiently be attested that the lake responds extremely sensitive to any changes in the moisture availability in its drainage area (Vincent et al., 1979; Harper et al., 1990; Becht and Harper, 2002). Interestingly, a similar dependency was found for historical lake-level fluctuations (Hastenrath and Kutzbach, 1983; Verschuren et al., 2000). The lake system, i.e., the water reservoir and the related catchment or drainage area reveal a close hydrologic association. Lake Naivasha therefore can be used to link paleohydrologic fluctuations with past climate changes (Fig. 2.3).

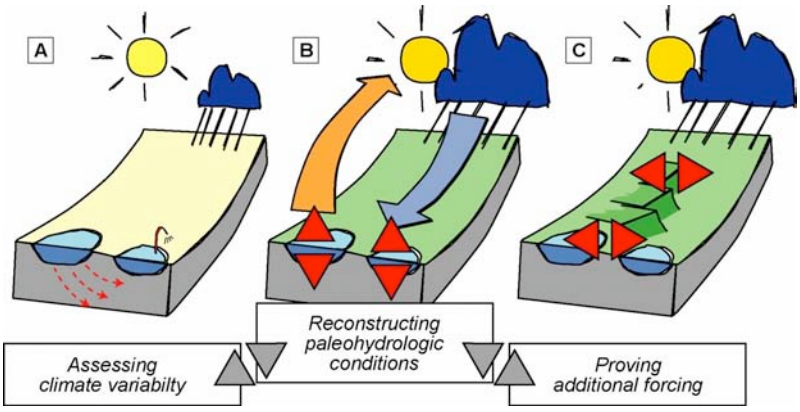

Fig. 2.3 Conceptional drawing of the hypothesized relationship between *CKR* lakes and their drainage area: (A) Under modern conditions the lakes of the *CKR* are highly dependent on the moisture availability in the catchments; hydrologic differences can be attributed to local variations, such as seepage or water consumption. For a direct linkage of (B) past hydrologic changes to paleoclimate variations, the *CKR* lakes have to show similar paleohydrologic fluctuations, otherwise (C) additional forcing factors, such as tectonic or volcanic activity have to be considered.

Linking lake sediments to paleoclimates in the *CKR*

The older history of hydrologic fluctuations at Lake Naivasha was mainly derived from paleolake sediments exposed in the Ol Njorowa Gorge (Figs. 2.2, 2.4). The gorge comprises an erosional feature through mostly volcanic material forming the southern rim of the Naivasha basin. Since lacustrine deposits repeatedly intercalate the pyroclastic material, it was inferred that the shoreline of Lake Naivasha was more extended to the south in the past (Bone, 1985; Trauth et al., 2001). Obviously, the ongoing extrusion of several volcanic domes farther north forced the lake to migrate northwards (Washbourn-Kamau, 1977; Bergner, 2000). On the other hand, the high frequency of volcanic eruptions, partly depositing their extrusives directly into the lake, provides an excellent age control of the timing of lacustrine periods. A definite age

determination of six independent periods of elevated lake-levels (i.e., paleo-Lake Naivasha highstands IX to IV) contributed essential fundamentals to the laterally developed chronology of paleohydrologic variability (Trauth et al., 2001; Trauth et al., 2003) (Fig. 2.4).

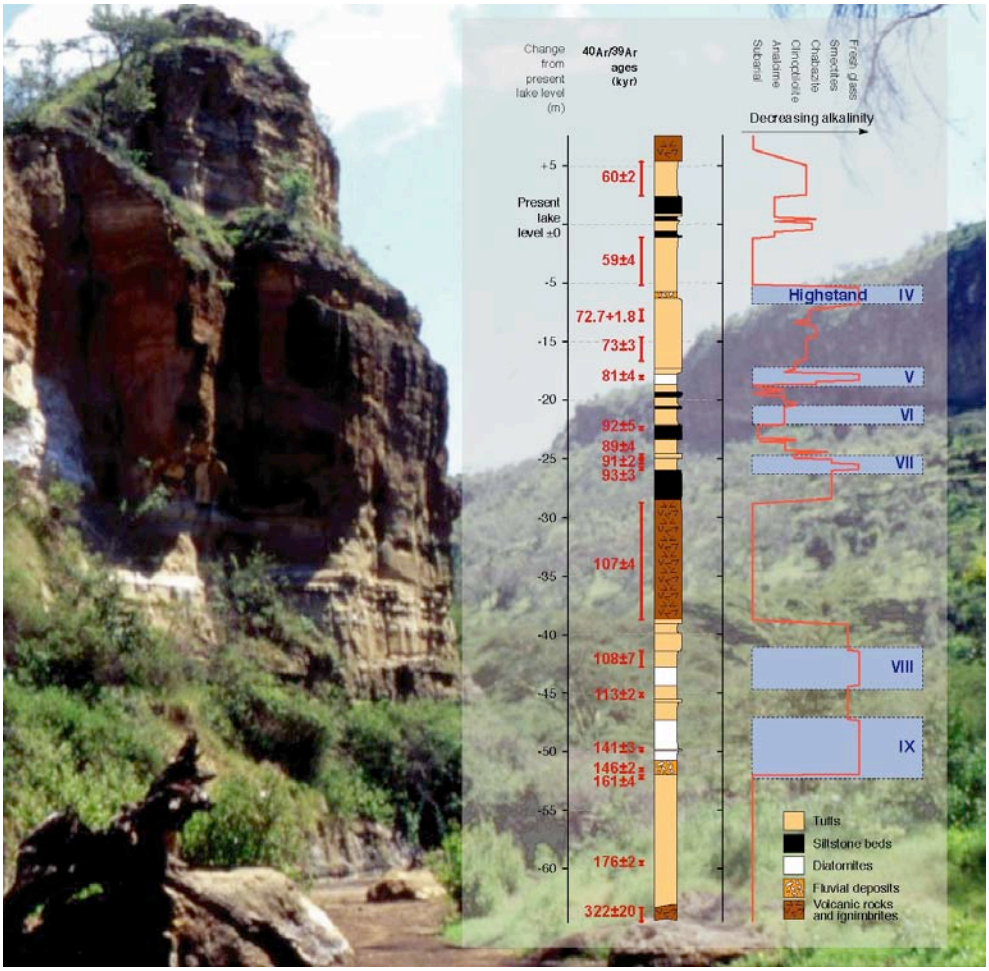

Fig. 2.4 (Back) Photograph of the Ol Njorowa Gorge south of modern Lake Naivasha, showing the lateral exposition of massive volcanic rocks intercalating diatomaceous lake deposits. (Insert) Composite profile of the Ol Njorowa Gorge showing major lithologic units and inferred lake-level fluctuations based on diatom interpretation and analyses of geochemical alteration phases (Trauth et al., 2001).

More detailed information about the development of paleo-Lake Naivasha was obtained from the identification of fossil diatom assemblages contained in the lake sediments of the Ol Njorowa Gorge (Fig. 2.4). Diatoms are unicellular silica algae of the class *Bacillariophyceae*, which are found in nearly every habitat where water is present (Stoermer and Smol, 1999). They are very sensitive indicators of various environmental parameters such as pH, salinity and nutrient concentration (vanDam, 1994; Gasse et al., 1995). Diatoms prefer distinct water depths and their grow-up is related to specific

environments, including turbidity (effectiveness of light), oxygen requirements (mixing stage of the lake) and the existence of higher plants for epiphytic growth (vanDam, 1994; Gasse et al., 1995; Stoermer and Smol, 1999) (Fig. 2.5). Since changes of these conditions are mainly linked to lake-level changes and thus climate variability, diatom assemblages provide indirect insights into the changes of the precipitation-evaporation balance in a area catchment (Stoermer and Smol, 1999; Battarbee, 2000).

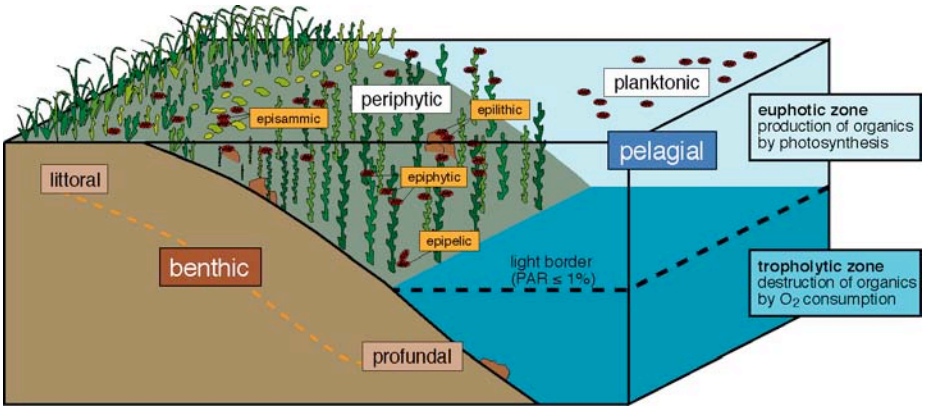

Fig. 2.5 Sketch illustrating the main occurrence of diatoms in lake environments. Planktonic species live near the surface of the lake, indicating no limitation to the littoral habitats, meaning the lake shore. Periphytic diatoms include both benthic species, i.e. diatoms living on the lake bottom (episammic, epipelic, epilithic) and all diatoms which grow up on higher plants (epiphytic). Because of their restrictions to grow up on something, periphytic diatoms are generally more often related to the littoral. Some diatoms are able to live as planktonic and periphytic (i.e., fakultative planktonic diatoms). Modified after Lampert and Sommer (1993).

In our approach, presented here as chapter 3 (cf., p. 21 ff.), we used an exact determination of the relative abundance of single diatom taxa within the paleolake deposits of the Ol Njorowa Gorge to achieve an estimate of the environmental conditions during lake highstands (Bergner et al., subm.). Precise information about the paleohydrologic parameters, such as pH, alkalinity and conductivity (as a measure of lake salinity) were derived from the application of diatom transfer functions (Gasse et al., 1995). From these results, we obtained an approximation of (a) the general hydrochemical character and (b) the morphologic extension of paleo-Lake Naivasha during the three highstand periods at ~135, ~110 and ~80 kyr BP (cf., Fig 2.4). Comparing our results with results from a 28 m-long sediment core from Lake Naivasha (Richardson and Richardson, 1972; Richardson and Dussinger, 1986) and lake-level reconstructions of Washbourn-Kamau (1975; 1977), we found that the lake highstand at ~135 kyr BP was similar to an Early Holocene lake highstand between 12 and 4 kyr BP. Interestingly both highstand periods coincide with maximum sea surface temperatures in the Indian Ocean as well as maximum δD values in the Arctic ice shields and

therefore suggest a strong influence of the intensity of solar radiation and intensified equatorial convergence on the water balance of the Lake Naivasha catchment.

In a second step, presented here as chapter 4 (cf., p. 48 ff.), we correlated the reconstructed paleohydrologic conditions of paleo-Lake Naivasha to paleoclimatic changes in the drainage area using a lake-balance model (Bergner et al., 2003). Such models relate the water storage of a lake to the regional hydrologic conditions in its catchment. Expressed differently, basin precipitation and evaporation are balanced so that the difference between them accounts for the river discharge into the lake. Using lake-balance models, the volumetric change of the water body of a lake may be explained as a change in the precipitation-evaporation (*P*-*E*) ratio in the catchment (Barron and Moore, 1994; Saltzmann, 2002). If the lake-balance model sufficiently simulates the modern conditions, the adaptation onto paleoscenarios provides interesting insights into the relationships between the paleolake extensions and the changing *P*-*E* ratio (Fig. 2.6).

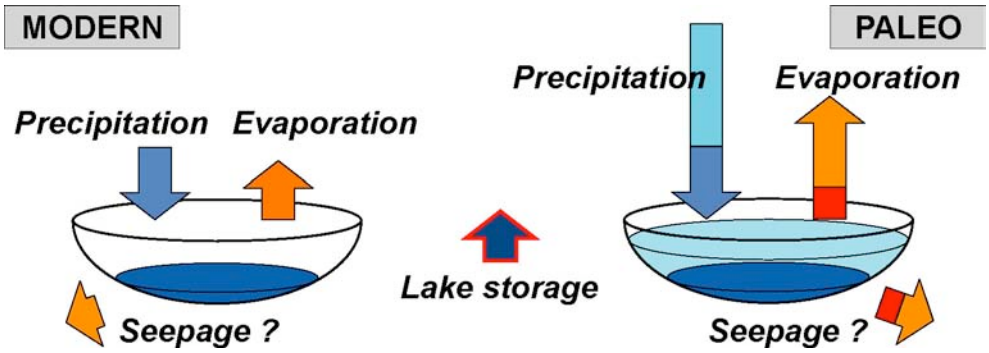

Fig. 2.6 Principles of lake-balance modeling: (Left) Modern run of the model for steady-state equilibrium between precipitation and evaporation (minus seepage) in the catchment; (Right) After a significant change of both precipitation and evaporation, the lake equilibrates on a higher level.

For the Naivasha basin, we applied a lake-balance model, which has been designed for a landslide-dammed lake in NW Argentina (Blodgett et al., 1997; Bookhagen et al., 2001). We first adapted the model to the present-day condition using the outline of the modern lake and 20-yr-averaged values of climatic and environmental data. After the application of the model to the modern conditions, we simulated the hydrologic conditions for the most prominent highstands (135 and 9 kyr BP) in order to infer the *P*-*E* balance for these time slices. Herein, the volumetric expansion of the paleolakes, as

reconstructed using a stratigraphically-constrained three-dimensional elevation model (Bergner, 2000), was fixed. Then, the paleoclimatic parameters were modified until the paleolake extensions were reached. The results of this simulation suggest a 30±10% increase of precipitation for both highstands compared to the present. The combined paleohydrologic-paleoclimate modeling are in line with the results from the analysis of diatom assemblages suggesting similar conditions in the Naivasha basin at ~135 and ~9 kyr BP (Bergner et al., 2003; Trauth et al., 2003).

As a third aspect, discussed in chapter 5 (cf, p. 72 ff.), we correlated the hydrological changes in the Naivasha basin with fluctuations in the neighboring Nakuru-Elmenteita basin (Bergner et al., in prep.). Similar to Lake Naivasha, the paleo-Lake Nakuru-Elmenteita experienced a significantly (~180 m) higher water level during the Early Holocene compared to the present (Washbourn-Kamau, 1970; Dühnforth, 2001; Dühnforth et al., in prep.). Although the dimension of the lake as well as the diatom flora were similar to those of Lake Naivasha, the results from lake-balance modeling for this basin suggest a much higher precipitation increase of about 45%. The disparity to our results is backed by a newly investigated diatomite profile in the Nakuru-Elmenteita basin, dated as to be 138±11 kyr old (Bergner et al., in prep.). Again, the flora contained in these sediments precisely matches the diatom assemblages observed in the Late Pleistocene sediments exposed in the Ol Njorowa Gorge. Taking into account the similar paleohydrologic evolution in the neighboring lake basins and the same present-day climate conditions, stronger regional climatic differences in the past do not seem reasonable.

Consequently, we tried to assess the influence of tectonic movements on the segmentation of the lake catchments and hence a shift in the relative river discharge between the freshwater Lake Naivasha and alkaline Lakes Nakuru and Elmenteita. Geologic investigations in the vicinity of the modern Lake Elmenteita indeed suggest that ongoing normal faulting has caused a deflection of significant river discharges towards the modern Lake Naivasha (P. Blisniuk and M. Strecker, pers. comm.). The capture of considerable parts of the Nakuru-Elmenteita drainage area would have resulted in a more negative P-E ratio in this basin, whereas the P-E ratio for modern Lake Naivasha catchment would have become more positive (cf., Behrensmeyer et al.,

2002). The hypothesized continuously preferential feeding of the Naivasha basin could help to explain the hydrologic similarities of the two lake basins in the past and the modern hydrochemical differences. Furthermore, the close vicinity of highly-alkaline and freshwater lakes in comparable regional climates has important consequences for reconstructing past climates from lake sediments in comparable tectonically active regions. Particularly in East Africa, the study of past climates always requires basin-to-basin correlation of hydrologic changes and a careful investigation of volcano-tectonic processes.

Note to the reader

While compiling this thesis, I realized that some of the paragraphs in the following three chapters 3, 4 and 5 contain some repeats of former writings. This fact has to be attributed to the composition of the chapters as former stand-alone articles, published or to-be-published in different international journals. Since chapters 1 and 2 already give a summary of the regional setting, I have marked the corresponding pieces of text as *italics*. Additionally, I changed the numbering of illustration according to the layout used in this compendium. Some of the figures are now given in original colored labels, which are drawn black and white in the publications. Finally, I added some remarks referring to helpful comments or figures in other chapters. I hope that these edits make the reading of the thesis more clear and comprehensible.

CHAPTER 3

QUANTITATIVE RECONSTRUCTION OF PALEOHYDROLOGIC AND HYDROCHEMICAL CHARACTERISTICS DURING LAKE-HIGHSTAND PERIODS OF LAKE NAIVASHA

---

extended version submitted to **Palaeogeography, Palaeoclimatology, Palaeoecology** (29.07.03), entitled as Bergner, A.G.N and Trauth, M.H.: Comparison of the hydrologic and hydrochemical evolution of Lake Naivasha (Kenya) during three highstands between 175 and 60 kyr BP.

Fig. 3.1 Photograph of my colleague Hendrik Wulf, posing in front of the ~135 kyr-old diatomite (highstand IX) in the Ol Njorowa Gorge, south of modern Lake Naivasha. The groove within the diatomite refers to the position of the intercalated tuff, dated as to be 141±3 kyr old (see insert).

Abstract

Three diatomite beds exposed in the Ol Njorowa Gorge south of Lake Naivasha, Central Kenya Rift, document three major lake-level highstands between 175 and 60 kyr BP. Diatom transfer-function estimates of hydrologic and hydrochemical parameters suggest that a deep and large freshwater lake existed during the highstands at ~135 and ~80 kyr BP. In contrast, a shallower but more expanded freshwater lake existed at ~110 kyr BP. The best analog for the most extreme highstand at ~135 kyr BP is the highstand during the well-established early Holocene humid period between 12 and 4 kyr BP. The environmental conditions as reconstructed from diatom assemblages indicate relatively stable environmental conditions during these periods of increased humidity. This contrasts the modern situation with an extremely shallow lake characterized by rapid

water level fluctuations within a few decades. The most likely cause for the differences in the magnitude of the highstands since 175 kyr BP are orbitally-driven insolation changes on the equator and increased lateral moisture transport from the oceans.

Introduction

Diatoms are very sensitive indicators of various environmental parameters in a lake such as water depth, chemistry, turbidity and nutrient supply (Gasse et al., 1995). Typical assemblages of these algae were intensely studied in modern lakes, but also from cores and dry surface outcrops of paleolake sediments all over the world. Diatomite as sediment, comprising mainly fossil diatom skeletons, is the ideal archive of the conditions in a lake through time. Since changes of these conditions are mainly linked to climate, diatom assemblages provide indirect insights into the variability of the precipitation-evaporation balance in a catchment. A quantitative estimate of the environmental conditions through time is gained using diatom transfer functions (Gasse et al., 1995). Although lateral transport of the diatom frustules, selective dissolution of diatom taxa, diagenetic alteration of the biogenic silica after deposition cause significant distortions of the paleoenvironmental signal, cross-validation of the environmental reconstructions based on diatom assemblages with other proxies emphasize the validity of this method (Gasse et al., 1997).

In the Central Kenya Rift (Fig. 2.2), diatoms have been studied already for a long time to reconstruct environmental changes in lake basins and hence climate changes on a variety of time scales (i.e., Nilsson, 1931; Richardson and Richardson, 1972; Trauth et al., 2001; Barker et al., 2002). As identified in Late Pleistocene and Holocene deposits of Lake Naivasha, the diatom-based paleohydrologic reconstructions helped to manifest periods of high water levels and low alkalinity at around 135, 110, 80 and 9 kyr BP (Richardson and Dussinger, 1986; Trauth et al., 2003). The timing of these highstands is now well defined (Trauth et al., 2003) and the precipitation-evaporation ratio during the most extreme highstands at ~9 and ~135 kyr BP has been determined using a lake-balance model (cf., chapter 4; Bergner et al., 2003). However, the natural variability during such a highstand, the short-term trends as well as the bandwidth of hydrochemical fluctuations on time scales of years to thousands of years has not been

investigated. We therefore studied the diatom assemblages contained in three diatomite layers exposed in the Ol Njorowa Gorge south of the present lake. Using diatom transfer functions, we compared three highstands at ~135, ~110 and ~80 kyr BP with both the well-known highstand at around 9 kyr BP and the modern setting. The results provide valuable insights into the internal dynamics of the lake system and its response to regional and global climate change.

Setting

Located at 1,890 m above sea level, Lake Naivasha is the highest water body in the Central Kenya Rift (0°55'S 36°20'E) (Fig. 2.2). The tectonically-initiated lake basin is bounded by rift escarpments to the east and west, Mt. Eburru volcano to the north and Mt. Longonot volcano and the Olkaria Volcanic Complex to the south. The history of the Naivasha basin began at about 320 kyr BP, when Olkaria lava flows closed the southern basin outlet between the flanks of the 400 kyr-old Mt. Longonot and the escarpment to the west (Clarke et al., 1990) (Fig. 3.2). These effusive bodies are unconformably overlain by an up 60 m-thick fluvio-lacustrine sequence, between 175 and 60 kyr old, suggesting that the basin was covered by a lake tree-times bigger than the modern Lake Naivasha (Trauth et al., 2001, 2003; Bergner et al., 2003). After the regression of this lake in the Late Pleistocene, ongoing volcanic activity in the Olkaria Complex produced most of the present relief covering the lake deposits (Clarke et al., 1990). Their exposure was only realized in the Early Holocene, when the Ol Njorowa Gorge was formed by headward erosion of the outlet of another lake highstand, which had an overflow to the southern Akira plains (Washbourn-Kamau, 1977). Today, the sediments are laterally continuous over a distance of more than 7 km and can be sampled in excellent dry sample outcrops of the gorges walls.

The modern Lake Naivasha is unique among the other lakes in the Central Kenya Rift because of its low pH of ~7.9 and depleted conductivity values, fluctuating between 250 and 500 $\mu S \cdot cm^{-1}$ (Gasse et al., 1995; Verschuren, 1999). The freshness of the lake can be attributed to a significant groundwater seepage through permeable volcanic subsurface rocks and to the perennial freshwater supply from the Malewa and Gilgil rivers. The two streams drain a ~3,200 km^2 large catchment area, which includes moist

mountain ranges of the eastern (2,200 to 2,500 m a.s.l.) and western escarpments (up to 4,400 m elevation). Whereas annual rainfall exceeds 1,750 mm·yr^{-1} in these regions, the fairly flat and wind-stressed Lake Naivasha basin is characterized by a negative moisture budget with rainfall averaging ~650 mm·yr^{-1} and evaporation of ~1,900 mm·yr^{-1} (Jätzold, 1981; KMD, 2000).

Temporal variations in the hydrologic budget of Lake Naivasha are mainly controlled by changes in precipitation, which is in turn linked to the seasonal migration of equatorial convergence zones, i.e., the Intertropical Convergence Zone (ITCZ) and the Congo Air Boundary (Nicholson, 1996). Although heaviest rainfalls occur during April-May and October-November after the transition of the ITCZ, prevailing SE trade winds and westerly winds during summer, as well as NE trade winds and northwesterly air flow during winter cause minor rainfall in the Naivasha basin (Fig. 1.3). The short-term variability in the intensity of these wind systems is directly related to sea-surface temperature variations in the Indian, Pacific and Atlantic Oceans (Camberlin, 1995). In particular, the El Niño/Southern Oscillation (ENSO) accounts for a significant part of hydrologic fluctuations in the catchment (Camberlin, 1995; Nicholson, 1996; Indeje et al., 2000).

As a consequence of these variations, the lake level is subjected to significant fluctuations, which particularly affect sediment-water interfaces of the shallow nearshore portions of the lake (Gaudet and Melack, 1981; Tarras-Wahlberg et al., 2002). Related sedimentation and biochemical exchange processes account for much of the ionic removal and therefore may provide further explanation for the freshness of the lake (Gaudet and Melack, 1981). The modern waters of Lake Naivasha are classified as low chloride, high fluoride, sodium bicarbonate water, where the acquisition of solutes by weathering of the surrounding feldspathoidic bedrocks masks the chemical composition of the rain (Gaudet and Melack, 1981; Tarras-Wahlberg et al., 2002). Due to the heavy afternoon winds, the water body of Lake Naivasha is polymictic and not thermally stratified (Verschuren, 1999). The intense mixing of the water column is also reflected in the modern diatom assemblages, collected from both, sediment and surface-water (i.e., plankton) samples. Herein, the typical modern diatom flora is dominated by Aulacoseira ambigua, Aulacoseira granulata var. angustissima and Synedra acus (Richardson and Richardson, 1972; Gaudet and Melack, 1981; Gasse et al., 1995).

Methods

We sampled the diatomite beds exposed in the 60 m-thick onshore sediment section of the Ol Njorowa Gorge south of Lake Naivasha (Fig. 3.2). The diatomites are the only diatomaceous sediments, deposited during three out of nine prominent periods of high lake levels, low alkalinity and wetter climates (Trauth et al., 2001). According to a composite chronology of lake-level fluctuations, the oldest diatomites, 340 and 120 cm in diameter, were accumulated during highstands IX (~135 kyr BP) and VIII (~110 kyr BP), whereas the youngest diatomite, around 15 cm thick, documents highstand V (~80 kyr BP) (Fig. 2.3; Trauth et al., 2003). Since the diatomites are laterally continuous on a length of several kilometers without substantial variation in thickness and also no evidence for erosional unconformities is observed within the diatomite layers, these sediments most likely represent continuous records of the three major highstands between 175 and 60 kyr BP.

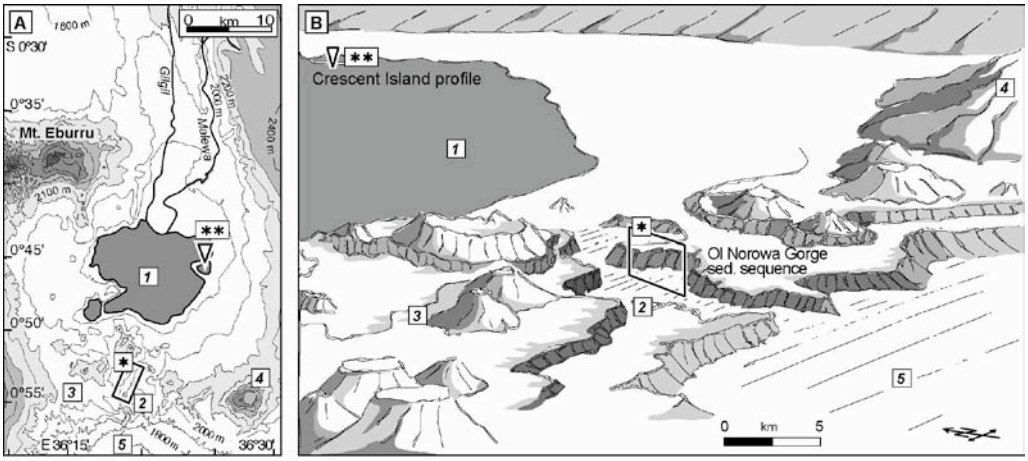

Fig. 3.2 (A) Map of the Naivasha basin showing present-day topography, extension of modern Lake Naivasha, main rivers, location of surface outcrops in the Ol Njorowa Gorge (square indicated by ✻) and sediment core at Crescent Island (triangle indicated by ✻✻) (Richardson and Richardson, 1972). (B) Present-day relief and lake area obtained from digital-elevation modeling. The idealized landscape ignores vegetation coverage, but shows the southern rim of the Naivasha basin as seen towards NE with (1) Lake Naivasha, (2) NNE-SSW orientated Ol Njorowa Gorge, volcanic complexes of (3) Olkaria and (4) Longonot, as well as (5) Akira plains. Location of sediment sequence in the Ol Njorowa Gorge (✻) and sediment core profile at Crescent Island (✻✻).

Depending on the quality of the sediment, the diatom analysis was performed at 10 to 30 cm-intervals for highstand IX and VIII, and at 2.5 cm-intervals for highstand V. In order to average potential seasonal variations in the species assemblages, we integrated 2.5 cm-thick slices of sediment for the investigation of the long-term trends. The dry sample material was washed in distilled water, organic matter was oxidized by H_2O_2 and

carbonates were removed using HCl. Diatom slides were mounted in Naphrax and analyzed using a Leica optical microscope at magnification x1,000. Because of the limited preservation of the diatoms, we counted between 300 to 1,000 valves per sample. We also estimated the content of detrital material and the percentage of broken valves for each sample relative to the total sum of counted valves. Furthermore, we documented the occurrence of phytoliths and sponge spicules as indicators of a nearshore deposition. The ratio of broken diatoms, the amount of clastic debris as well as the phytolith content were regarded as a proxy for littoral conditions of the sampling site (e.g., Hecky and Kilham, 1973; Barker et al., 1990; Gasse et al., 1997). Since several sections of the profiles show strong laminations, high-resolution sampling and separate analysis were investigated in a 15 cm-thick continuous slice of diatomite to distinguish between the dark-brown thin layers and intercalated white bands

The diatom identification followed the principles of Hustedt (1949), Gasse (1986) and Krammer and Lange-Bertalot (1991a, 1991b, 1997a, 1997b). For paleohydrologic and environmental interpretations the identified taxa were chross-checked with the species listed in the modern East African Diatom Database, where both taxa counts and environmental variables of the sampling site are included (data from F. Gasse, pers. comm. 2001; results published in Gasse et al., 1995). Using this database, diatom-inferred conductivity, pH, cation and anion ratios were derived by transfer functions (cf., data in the appendix). Secondly, principle component analysis (PCA) and hierarchical cluster analysis have been used to identify groups of diatoms with comparable chemical and habitat characteristics. The routine pca of the Matlab® PLS_Toolbox provided by Eigenvector Research Inc., Manson, was used to perform PCA on the auto-scaled data, implying all variables were put on an equal basis in the analysis (Swan and Sandiland, 1995; Wise et al., 2002). This was important because the ecologic parameters of the diatoms show large differences in the absolute values of mean and variance. Next, we employed the Matlab® routine cluster on the auto-scaled data to define groups of diatoms.

Results

Long-term trends in facies and diatom assemblages

The diatomites can be subdivided into tree lithologic facies: (a) pure white diatomite, (b) diatomite with a moderate clastic component concentrated in thin clayey laminae, and (c) grayish diatomite with a relatively high clastic component, but without clear laminations (Fig. 3.3). Microscopic analyses of sedimentological parameters and the preservation of diatom frustules support this macroscopic classification. The preservation of the diatom frustules and the number of phytoliths and sponge spicules change parallel to the occurrence of clastic particles. Although the laminated sections show large fluctuations, they generally contain more well-preserved diatom valves and only minor amounts of phytolithes and sponge spicules. Within the non-laminated sections, this pattern is reversed and significant amounts of broken valves occur more frequently. However, the total amount of clastic debris is generally low and never exceeds the amount of diatom valves. Phytoliths and sponge spicules also only appear in subordinate amounts, i.e., less than one percent of the number of diatoms. In contrast, breakage of the diatom frustuls is a frequent feature and some samples may suggest some minor syn- or post-sedimentary reworking of the skeletons.

A much more detailed picture of the paleolimnologic trends we obtained from the analyses of the diatom assemblages. A first-order estimate for the hydro-ecologic changes in the lake can be best illustrated by the ratio of planktonic vs. littoral species. Calculated for each highstand separately, this parameter nicely correlates with the changes in the diatomite facies as outlined above. The combined usage of these two proxies already provides a valuable approximation of the hydrologic history of paleo-Lake Naivasha during the highstands on time scales of hundreds and thousands of years. As a next step, high-resolution analyses of the laminated sections yield important information about the internal dynamics of the lake system on decadal and annual time scales (Fig. 3.3).

For the analysis of long-term hydrologic trends, we first investigated 39 diatom samples in 10 to 30 cm intervals. Within the samples, the algae assemblages are relatively diverse, but the same taxa were consistently abundant from level to level. The diatom

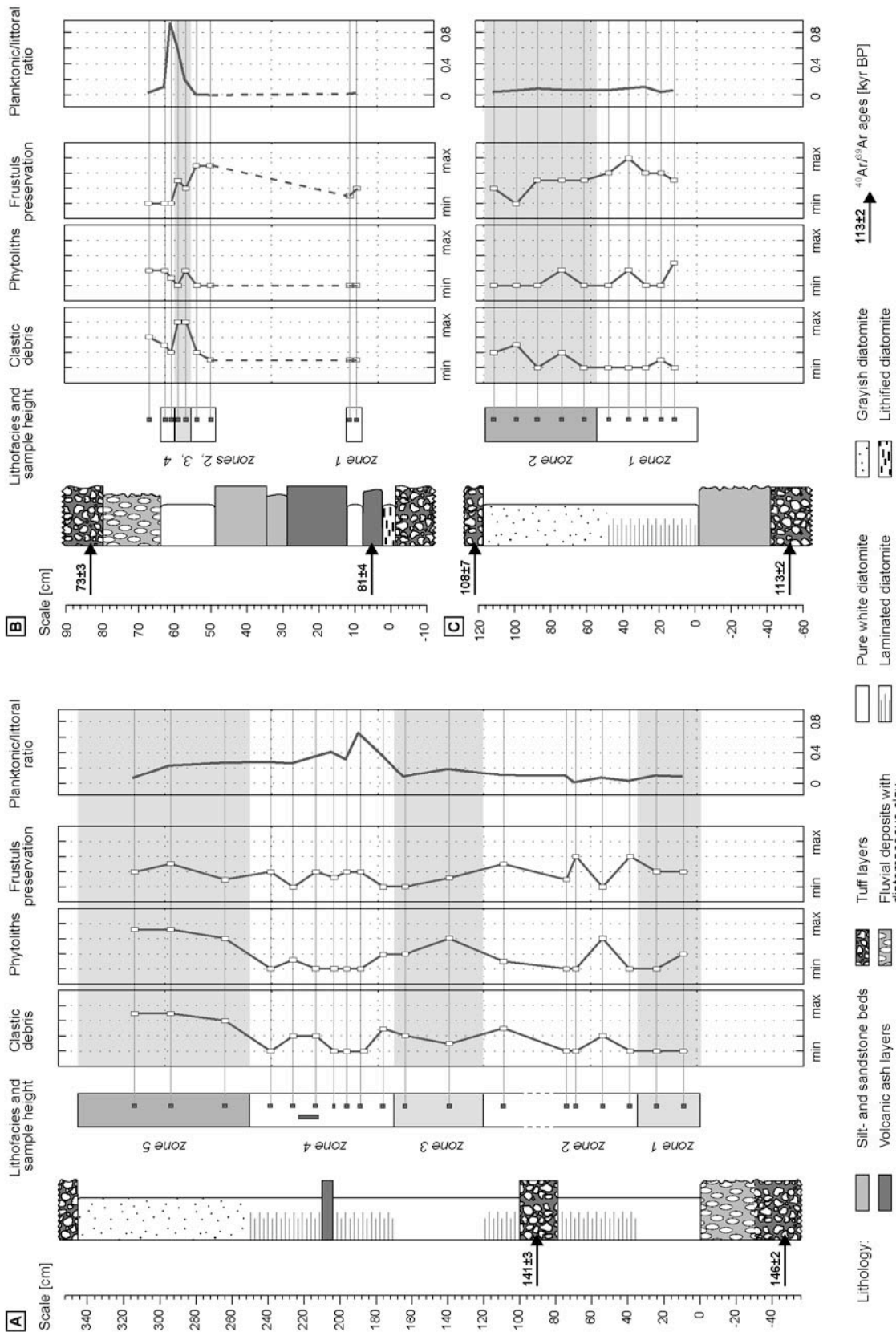

Fig. 3.3 Lithostratigrapic profiles of diatomites of (A) highstand IX (146±2 to ~120 kyr BP), (B) highstand VIII (113±2 to 108±7 kyr BP) and (C) diatomites and diatomaceous silts of highstand V (81±4 to 73±3 kyr BP). Age control from $^{40}Ar/^{39}Ar$ dating on sanidine phenochrysts from intercalated volcanic tuff beds (Trauth et al., 2001, 2003). Semi-quantitative plots of sedimentological parameters obtained from thin-section analysis. Planktonic-littoral ratio of diatom taxa reflecting the fraction of planktonic species within the identified diatom assemblages. Environmental information corresponds to the dataset of East African diatoms (Gasse et al., 1995).

flora covers a wide range of habitats between planktonic and facultative planktonic species, including such genera as *Aulacoseira, Cyclotella, Fragilaria* and *Thalassiosira*, and benthic-littoral genera, such as *Epithemia, Cymbella* and *Gomphonema*. Although planktonic and littoral species appear together in nearly all samples, comparable analogs to the lithologic trends are found within the diatom assemblages for the selected stratigraphic levels of the profiles. Highstand IX is composed of five stratigraphic zones (Fig. 3.3 and 3.4a): The lowest non-laminated part of the diatomite, i.e., zone 1 extending from the base until the height of 35 cm, comprises littoral diatoms such as *Epithemia adnata, Epithemia sorex, Gomphonema intricatum* and *Cymbella cistula*, but the assemblage is clearly dominated by facultative planktonic species such as *Fragilaria pinnata* and *F. construens*. Deep-water indicators like *Aulacoseira granulata, Cyclotella glomerata* and *Nitzschia tropica* are rare. Within a laminated zone 2 between 35 and 120 cm, the diatom assemblage contains abundant facultative planktonic diatoms of the genus *Fragilaria*, with high amounts of *Fragilaria brevistriata*. In this level, increased percentages of planktonic *Aulacoseira spp.* and *Cyclotella ocellata* are observed, but also littoral diatom species of *Gomphonema intricatum* occur in great numbers. At zone 3, a less or non-laminated section between 120 and 170 cm, the portion of the facultative planktonic *Fragilaria spp.* is systematically reduced, whereas *Cocconeis placentula*, typical for epiphytic habitats, and littoral *Epitemia sorex*, *Gomphonema intricatum* and *Mostogloia elliptica* become more frequent. At the same level, also planktonic diatoms including *Cyclotella ocellata, Aulacoseira granulata* and *Nitzschia tropica* increase in numbers. Zone 4, between 170 and 250 cm above the diatomite base, is again laminated and characterized by predominant planktonic species, mainly of *Aulacoseira spp.* and *Cyclotella spp.* Epiphytic taxa, such as *Achnanthes minutissima, Amphora pediculus, Cocconeis placentula*, *Gomphonema intricatum* are more abundant, than facultative planktonic genera such as *Fragilaria* and *Synedra*. In contrast, in the upper part of zone 4, above 235 cm the facultative planktonic *Fragilaria spp.* return to the diatom assemblage, but *Aulacoseira spp.* and *Cocconeis placentula* become less abundant. At zone 5, the uppermost siltic and non-laminated part of the diatomite, *Fragilaria spp.* with mainly *Fragilaria construens* dominate the assemblage. Planktonic species are represented by *Aulacoseira granulata*, *Cyclotella ocellata* and *Nitzschia lancetulla*, whereas small percentages of *Epithemia sorex* and *Cymbella*

muellerii, as well as *Gomphonema gracile* also reflect nearshore, littoral habitats (Fig. 3.4a).

In the diatomite profile of highstand VIII a similar, but much less distinct trend is observed within the diatom assemblages (Fig. 3.4b): Planktonic species, like *Aulacoseira granulata* or *Nitzschia vanoyei*, and facultative planktonic diatoms, such as *Cyclotella stelligera* and *Synedra ulna* are concentrated in the lower, more laminated section of the profile (zone 1). The maximum in the planktonic-littoral ratio occurs at around 30 cm above the diatomite base, corresponding to a decrease in the occurrence of phytoliths and sponge spicules. In this section, also the preservation of the diatom frustules is good, and only minor amounts of clastic debris are observed. In contrast to highstand IX, the entire profile is characterized by a stronger dominance of littoral genera, such as *Fragilaria, Gomphonema* and *Epithemia*. In the upper part of the profile, where this dominance gets striking, the content of clastic debris as well as the number of phytoliths and sponge spicules increases, whereas the fraction of planktonic diatoms is low and never exceeds 8%.

The diatomaceous beds of highstand V do not show any laminations. However, even these units reveal similarities between sedimentological facies and the relative abundance of diatom taxa (Fig. 3.4b). Like in the profiles of highstands IX and VIII, epiphytic and facultative planktonic diatoms predominate in the diatom assemblages. *Fragilaria brevistriata, F. construens* and *F. pinnata, Epithemia adnata* and *E. sorex*, as well as *Cyclotella ocellata* contribute around 70% to the algae assemblage. Only within a distinctive, narrow zone between 58 and 64 cm above the base of the diatomite (zone 4), an abrupt increase in planktonic, freshwater diatoms of *Aulacoseira ambigua* (up to 40%), accompanied by abundant *Aulacoseira granulata* and *Cyclotella stelligera*, is observed. Interestingly, the amount of clastic debris is significantly reduced in this section. However, a few centimeters below this level in zone 3, higher amounts of *Thalassiosira faurii* and *Cyclotella meneghiana* suggest much more saline conditions. Higher numbers of *Rhopalodia gibberula* and *Cymbella cistula* imply a more nearshore character of this sequence, that nicely correlates with the appearance of phytoliths and sponge spicules at the same level. At the top of the diatomite, again *Fragilaria spp.* and *Epithemia spp.* dominate the diatom assemblages, and the occurrence of *Cyclotella meneghiniana* and *Rhopalodia gibberula* reflect the return of more saline conditions.

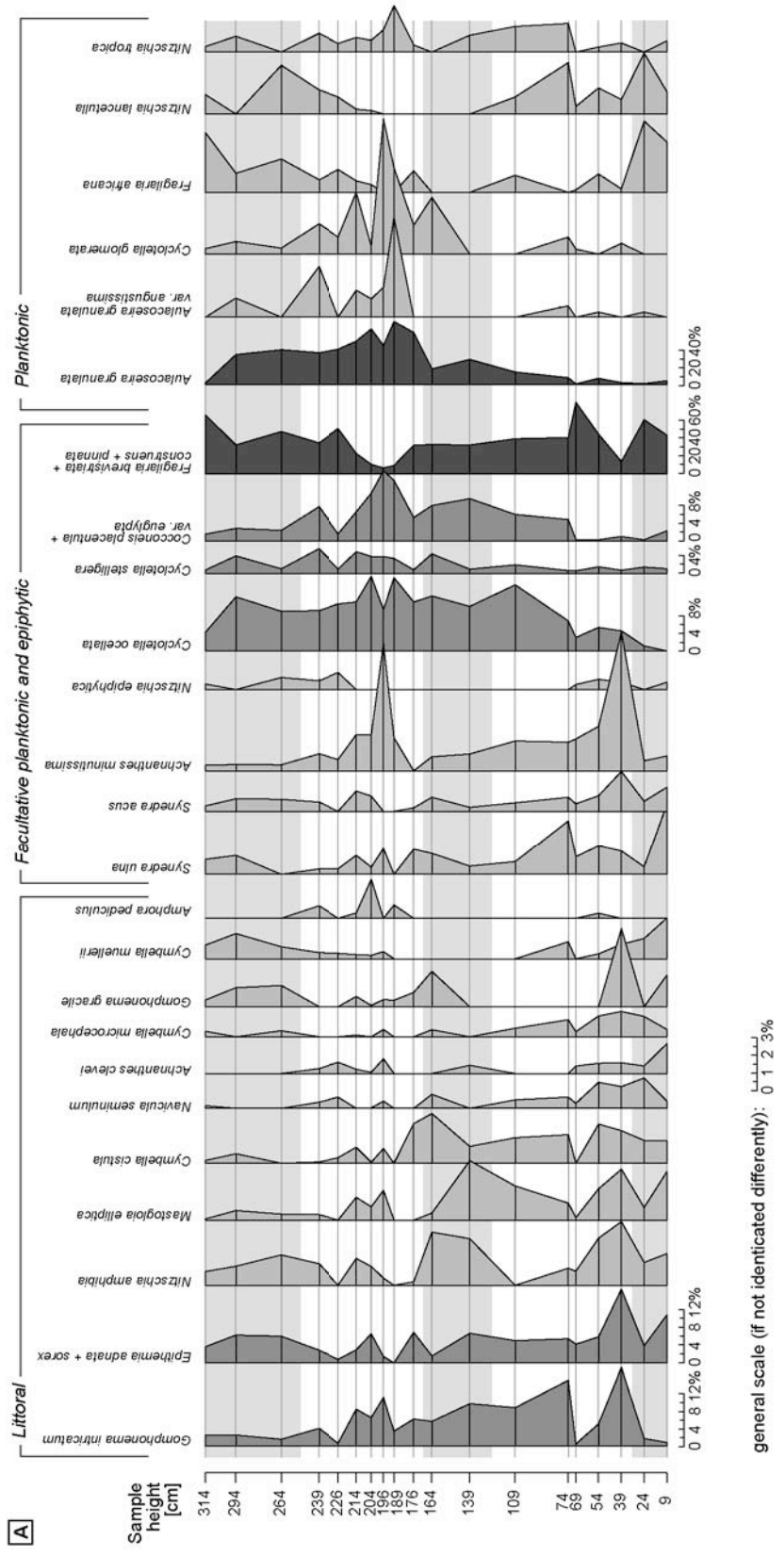

Fig. 3.4 (A) Relative abundance of selected diatom species in profiles of highstand IX. Shadings correspond to lithologic facies (cf., Fig. 3.3).

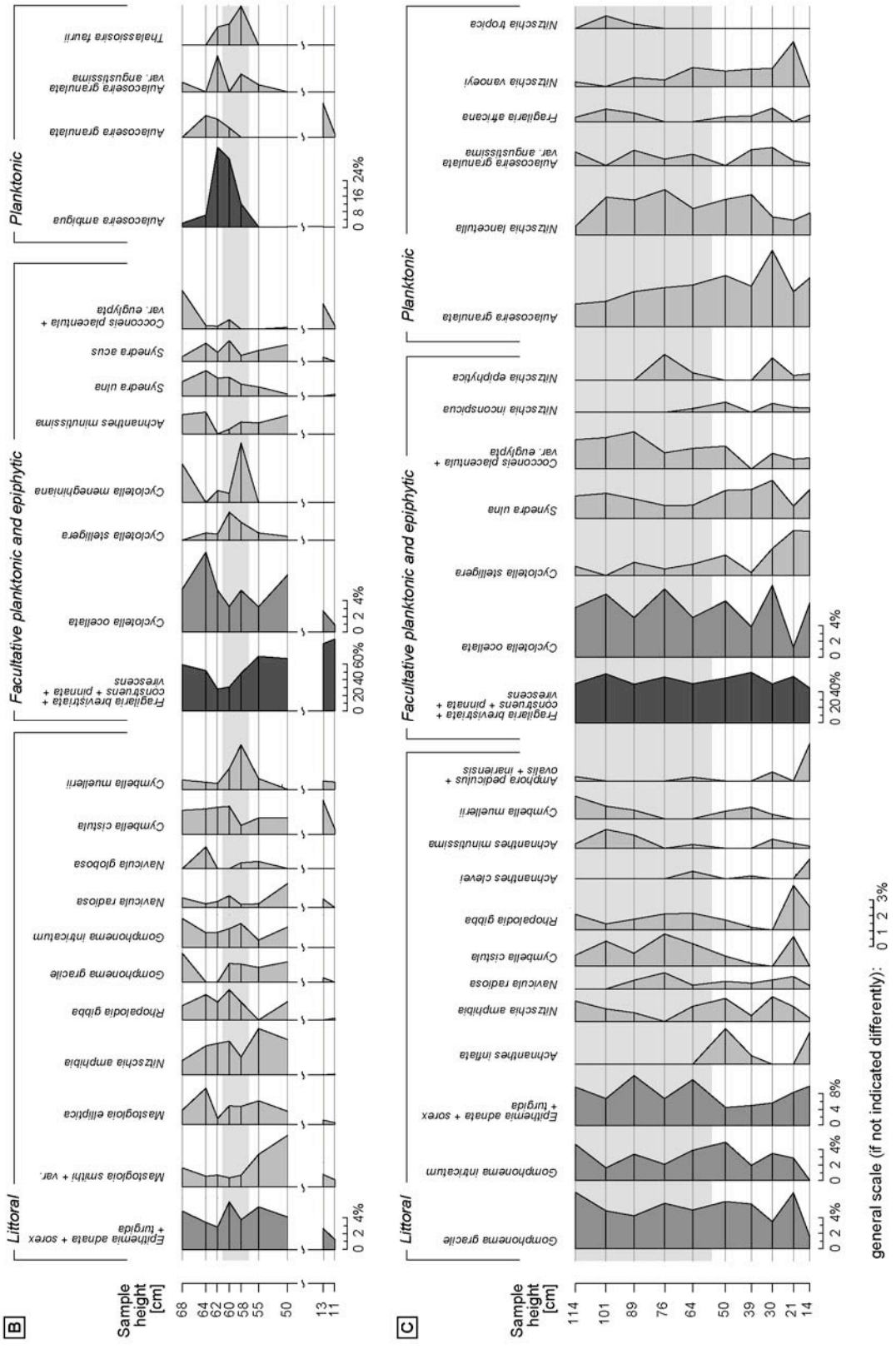

Fig. 3.4 (B-C) Relative abundance of selected diatom species in profiles of (B) highstand VIII and (C) highstand V. Shadings correspond to lithologic facies (cf., Fig. 3.3).

Short-term fluctuations

In order to assess the short-term variability of the diatom assemblages within the laminated parts, a short section of the highstand-IX diatomite, between 212 and 225 cm above its base, was analyzed in 0.25 cm-intervals and from thin sections (Fig. 3.5). The main purpose of this analysis was to assess the relative importance of short-term variations in the flora on annual to decadal time scales vs. the long-term fluctuations. The comparison of the species assemblages within pure-white sediment layers and brownish clay-rich layers indicates a clear anti-correlation between the amount of clastic material and the numbers of planktonic diatom taxa. Moreover, increasing numbers of phytoliths and sponge spicules correlate with higher amounts of well-preserved diatom frustules and predominant littoral taxa. From thin section analysis it can also be concluded that clay-rich, dark layers document nearshore sedimentary conditions, dominated by littoral and facultative-planktonic diatoms, whereas the pure-white layers reflect deep-water conditions with abundant planktonic species.

Although the understanding of the internal dynamics of the lake system would require a much more detailed investigation of the laminated part of the section, these preliminary results help to interpret the observed long-term trends in the diatom flora. As reflected in the planktonic-littoral ratio, all highstands are characterized by long-term trends from more littoral, shallow-water conditions to deeper freshwater environments. This trend is overlain by short-term fluctuations, as indicated by the highly varying sedimentological and paleontologic parameters in the laminated sections of the profile. In these sections, littoral species get more abundant where brownish silt layers alternate with pure-white diatomite. The relative importance of littoral taxa inversely correlates with the thickness of the white layers, as it can best be studied in the laminated, basal part of the highstand-VIII diatomite.

Unfortunately, the analysis of the laminated sections yields no detailed information about the mechanism causing the layering. Since several blooms of algae were identified within one couplet of white and brown layers, it can only be speculated that the laminae do not corresponds to one year of lake history. An alternative explanation would be that the brownish layers record increased clastic influx during the spring and/

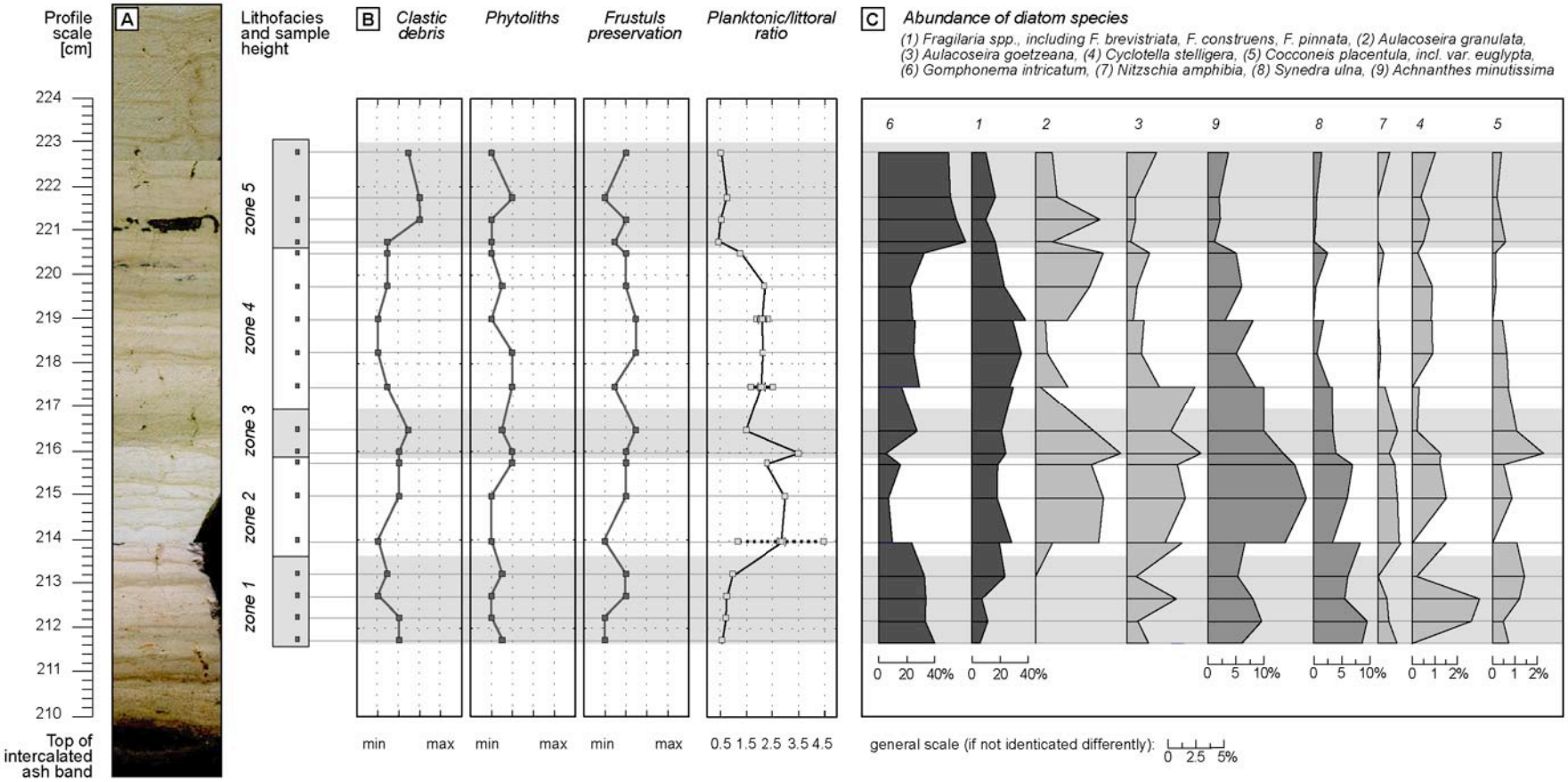

Fig. 3.5 Results of high-resolution analysis of laminated highstand-IX diatomite. (A) The investigated slice of diatomite shows strong laminations with alternating pure-white and brownish clay-rich layers. Analyses were performed in ~0.25-cm intervals, for comparison between the characteristics of the laminae and diatom assemblages. (B) Variance of sedimentological parameters and planktonic-littoral ratio. (C) Relative abundance of selected diatom species.

or fall rainy seasons, according to the hypothesis by Nilsson (1931) and Richardson and Richardson (1972). We suggest a more complex interpretation of the laminae including a bimodal precipitation signal, which is modulated by a strong ENSO-type influence (cf., Damnati and Taieb, 1995).

Paleohydrologic and hydrochemical reconstructions

Estimation of paleoenvironmental parameters

After having determined the species assemblages and their temporal variations for the three diatomite layers, we used this data matrix for the reconstruction of the hydrochemical trends during each highstand. The East African Diatom Database was used as a modern analog for the diatoms observed in our samples (Gasse et al., 1995). Applying multivariate transfer techniques, we calculated estimates of conductivity, pH, cation ($Na^+ + K^+ / Ca^{2+} + Mg^{2+}$) and anion ($CO_3^{2-} + HCO_3^- / Cl^- + SO_4^{2-}$) ratios for each fossil sample. As a first result, we observe only minor changes in the hydrochemical parameters within the diatomites, suggesting relatively stable environmental conditions over long time periods. The presence of pure white diatomite layers supports this interpretation since such deposits typically reflect relatively undisturbed hydrochemical and sedimentary conditions (Harwood, 1999).

In order to separate various environmental influences on the evolution of the diatom assemblages and increase the signal-to-noise ratio of the data, principle-component analysis and hierarchical cluster analysis (CA) have been used to identify groups of diatoms indicating similar chemical and habitat characteristics (Swan and Sandilands, 1995). Using the Mahalanobis distance of the graphical output of the CA, seven main groups were identified for a number of 102 diatom species. Only 15 species with no and 7 species with incomplete ecologic information were excluded from the CA. Between 86% and 100% of the diatom species identified in the different stratigraphic levels are listed in the East African Diatom Database. The seven groups of diatoms as defined from cluster analysis can therefore be regarded as to be representative for the true flora of the paleolakes and can be used for our environmental reconstructions. As a first step, arithmetic means of the pH, conductivity values, anion and cation ratios were calculated

for each diatom cluster separately (Tab. 3.1). Whereas groups 1 to 6 obviously reflect freshwater conditions with a preferred pH between 7.3 and 8.0, and conductivity values between 150 and ≤2,000 µS·cm^{-1}, only diatom species comprising cluster 7 prefer strongly alkaline conditions with pH values of ≥9.0 and conductivity values above 5,000 mS·cm^{-1}. Taken into account the close similarities of group 1 and 2, and 5 and 6, respectively, the clusters were merged to five fields of hydrochemical preference based on their pH and conductivity values (Fig. 3.6a). Moreover, the genus *Fragilaria* was excluded from the clusters, because of their predominance in nearly all samples. After this pretreatment of the data, new graphs were created showing the occurrence of the diatoms for each cluster reflecting the hydrochemical conditions vs. depth (Fig. 3.6b-d; Fig. 3.7). These plots characterized by a higher signal-to-noise ratio now provide a much better base for the paleohydrologic interpretation.

cluster	number of diatom species	means of pH	conductivity (mS·cm^{-1})	cation-ratio (log)	anion-ratio (log)
1	17	*8.02*	*1,900*	*0.53*	-0.39
2	4	*7.94*	*2,200*	*0.38*	-0.35
mean (1+2)		**7.98**	**2,000**	**0.46**	**-0.37**
3	21	**7.99**	**850**	**0.30**	**0.02**
4	20	**7.84**	**300**	**0.30**	**0.29**
5	14	*7.49*	*200*	*0.18*	0.56
6	4	*7.26*	*150*	*-0.09*	0.75
mean (5+6)		**7.37**	**180**	**0.05**	**0.67**
7	7	**9.24**	**13,800**	**1.58**	**-0.36**

Tab. 3.1 Results of the cluster analyses on identified diatom taxa of all highstands (total124 taxa); input values comprises means and standard deviation of conductivity, pH, cat- and anion ratio; classes were derived by nearest neighbor-likelihood method using 'cluster' routine in Matlab® (autoscaling and PCA on data, nr. of principle elements eq. 1)

While interpreting the results from this analysis, it has to be kept in mind, that the fossil flora apparently only represents an incomplete picture of the original assemblage. The limited preservation of at least some of the samples suggests that this factor could be of some relevance in the Ol Njorowa Gorge sequence. Above all, breaking of larger *Navicula*, *Pinnularia* or *Synedra* frustules is a problem throughout the sequences and thin-walled frustules are less abundant then morphologically stable diatoms. Moreover,

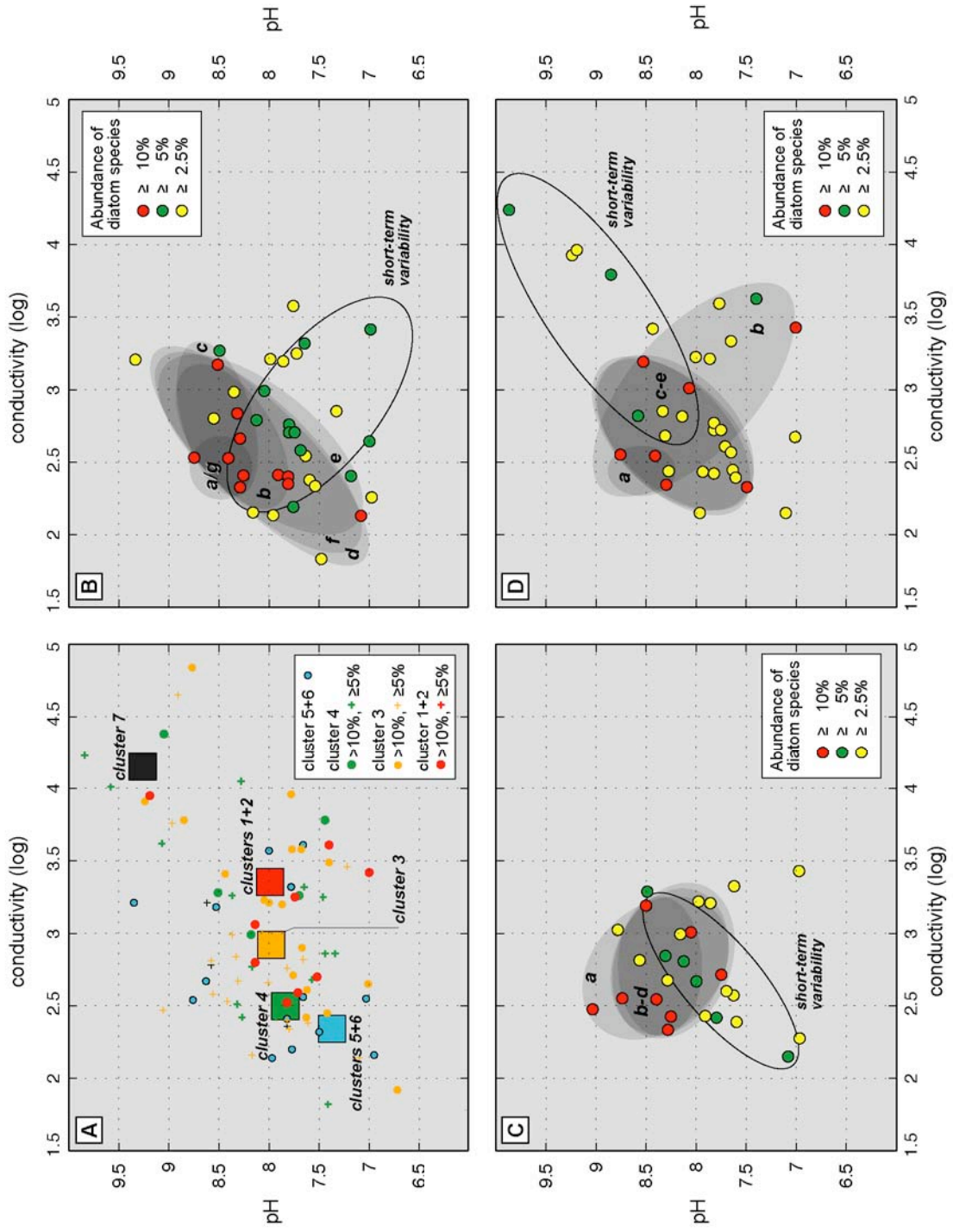

Fig. 3.6 Paleohydrology inferred from diatom assemblages. (A) Principle-component and hierarchical cluster analyses defining five groups of diatom species with distinctive hydrochemical preference. Large squares refer to calculated means (cf., Tab. 3.1), small symbols indicate individual values of single diatom species (cluster 7 not indicated). Temporal variation of hydrochemical conditions in the reconstructed paleolakes as derived from abundance of hydrochemical clusters for (B) highstand IX, (C) highstand VIII and (D) highstand V showing prevailing diatom species (circles) vs. time. Time slices as corresponding to subdivision of sediment profiles based on typical diatom assemblages (cf., Fig. 3.7).

the treatment of the dry sample material for diatom slides may have affected fragile skeletons. However, the comparison of diatom slides with smear slides and thin sections yields no significant difference in the preservation of the diatom frustules. Obviously the damage of the valves has to be explained by the sedimentary regime of the paleolakes. Since the location of the Ol Njorowa Gorge section is believed to represent the littoral part of a lake, reworking of diatom frustules may be of some importance (Hecky and Kilham, 1973; Gasse et al., 1997).

Implications for environmental changes

The variations in the importance of each diatom cluster through time nicely correlates with the facies zonation as described above as well as with the planktonic-littoral ratio (Fig. 3.7). In the lowest section of the profile of highstand IX (i.e., zones 1 and 2), the flora is clearly dominated by diatom taxa indicating a pH of ~8.5 and conductivity values of almost around 500 $mS \cdot cm^{-1}$. Towards the top of zone 2, i.e., at around 100 cm above the base of the diatomite unit, diatom taxa tolerating slightly higher conductivity values get more abundant. Within zone 3, these diatom species are replaced by taxa reflecting pronounced freshwater conditions. In the lithologic zone 4, between +170 cm and +200 cm, diatoms of a very low pH dominate the community, whereas euhalobe-alkalibionte species are almost absent. Between +200 cm and +260 cm, around ~50% of diatoms preferring a pH of ≤7.5 and abundant diatoms of intermediate pH and conductivity of ≤400 $mS \cdot cm^{-1}$ (i.e., cluster 4) indicate that relatively stable freshwater conditions have been established over a relatively long period of time. Interestingly, *Fragilaria spp.* return to the diatom community at the top of zone 4, whereas similar alkaliphile taxa never reach the high numbers as observed in the lower part of the profile. Zone 5 is characterized by diatom assemblages indicating more alkaline, mixosaline conditions towards the termination of this highstand.

As already indicated by the planktonic-littoral ratio, the diatom assemblages of highstand VIII are completely different from highstand IX. The less pronounced temporal variations of the diatom clusters suggest that the lake experienced only minor changes in hydrochemistry during this highstand (Fig. 3.6c and 3.7). Throughout the profile, pH fluctuates around ~8.0 to ~8.5, whereas conductivity values vary between

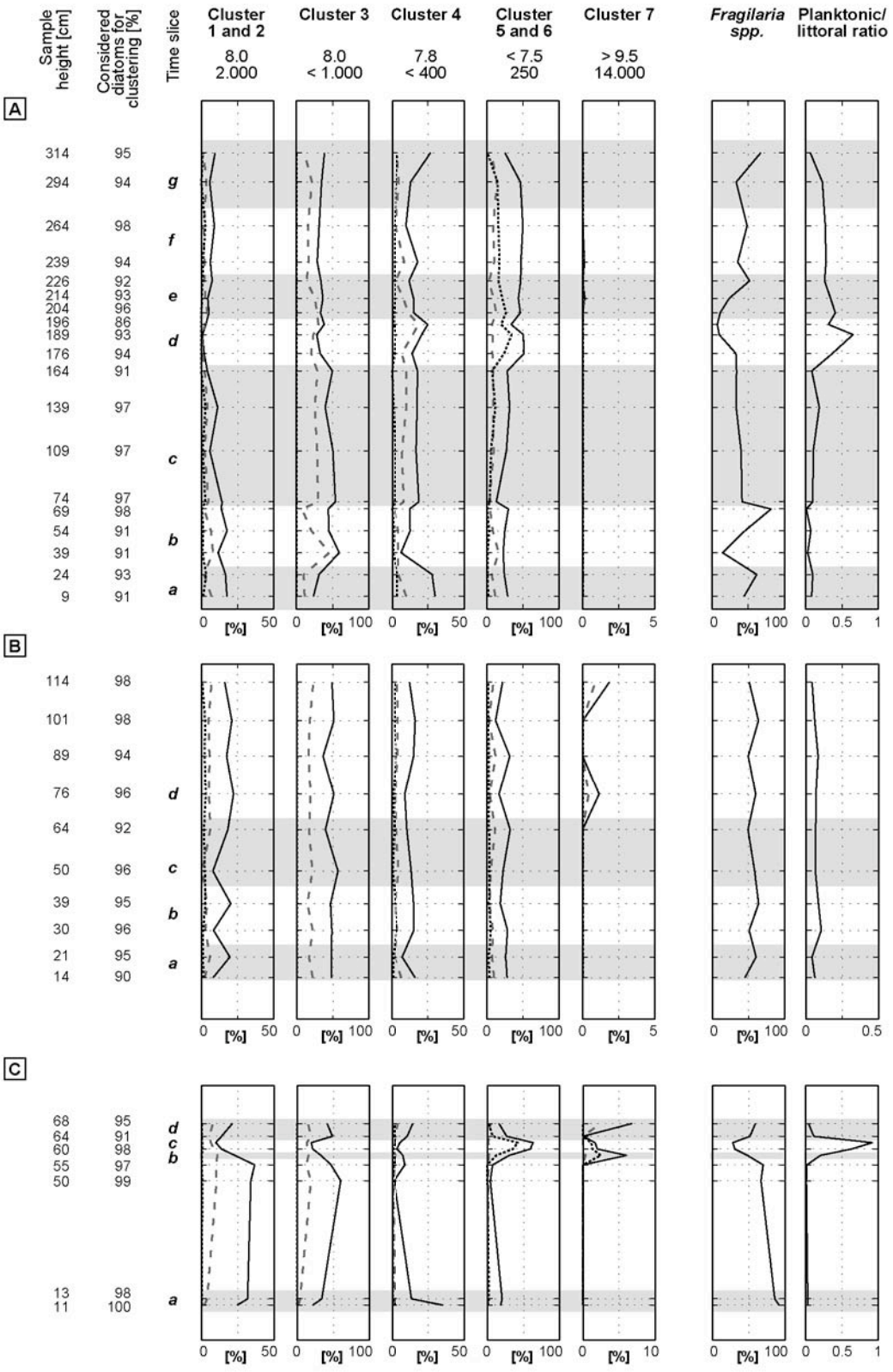

Fig. 3.7 Temporal variation of hydrochemical diatom clusters denotes total fraction of species belonging to one cluster (in %), fraction of littoral (dashed) and planktonic species (dotted). Fraction of non-considered Fragilaria spp. and plot of planktonic-littoral ratio for comparison. Shadings correspond to subdivision of profiles from typical diatom assemblages.

300 to 1,000 mS·cm^{-1}. Diatoms preferring freshwater conditions with lower pH, as represented by clusters 5 and 6, never appear in greater numbers and only reach ~25% in zone 1. In contrast, alkali- and halophile species appear in zone 2, reflecting increasing eusaline-eualkaline condition towards the end of this highstand. Similar to highstand IX, also in this profile the section of optimal freshwater conditions correlates with the maximum planktonic-littoral ratio (at around 30 cm above the diatomite base; cf., Fig. 3.7).

In contrast to the previous highstands, the relative importance of the diatom clusters through time indicates generally more saline conditions during highstand V (Fig. 3.6d and 3.7). Within zone 1, means of pH of ~8.5 and conductivity values of around 300 μS·cm^{-1} are still in the same order of magnitude as during the initiation of highstands IX and VIII. As suggested by abundant taxa belonging to clusters 1 to 3, from this point the evolution of highstand V continued on much higher salinity levels during zones 2, 3 and 4 compared to the corresponding zones of the previous highstands. The diatom assemblages clearly indicate prevailing eusaline conditions with conductivity values of more than 1,000 to 3,000 mS·cm^{-1} (Fig. 3.7). On the other hand, two distinct maxima in the occurrence of planktonic species suggest that also this highstand went through a period with deep-water conditions. The abrupt shift from halophil *Thalassiosira faurii* towards freshwater-preferring *Aulacoseira ambigua* emphasizes the rapid changes in hydrochemistry typical for this lake period.

Temporal evolution of the highstands

It has been shown that the diatomites exposed in the Ol Njorowa Gorge contain valuable information about the temporal evolution of three highstands of Lake Naivasha between 175 and 60 kyr BP. The first highstand initiated at around 146±2 kyr BP recorded by diatomaceous clays with intercalated pumice lapilli tuffs (Trauth et al., 2001, 2003). These deposits continuously grade into the diatomite of highstand IX. The lower part of this diatomite documents a littoral sedimentary regime with intermediate pH and conductivity of a relatively shallow lake (zone 1). The lake gradually deepens during a period of stabilizing alkalinity and salinity (zone 2) reaching an optimum with deep lake conditions and low alkalinity (zone 3). Clearly, the lake deposits reflect the

environmental conditions of the southernmost nearshore habitat of the paleolake. The observed disturbances of clastic layers are attributed to periodically rainfall events increasing the suspension of the lake. This hypothesis is emphasized by (a) the morphologic lake reconstruction, suggesting a flat marginal basin for the study side (cf., chapter 4; Bergner et al., 2003) and the dominance of littoral diatoms in the detritus-enriched laminae (Fig. 3.8). In that context, the occurrence of thick dark-brown layers within the diatomite suggests that the lake period was initialized by several extreme flood events dramatically decreasing both pH and conductivity. After this pronounced dilution, relatively stable freshwater conditions lasted for a long period of time (zone 4), before the lake level declined slowly (zone 5) and a long period of low water levels and higher alkalinity occurred in the lake basin.

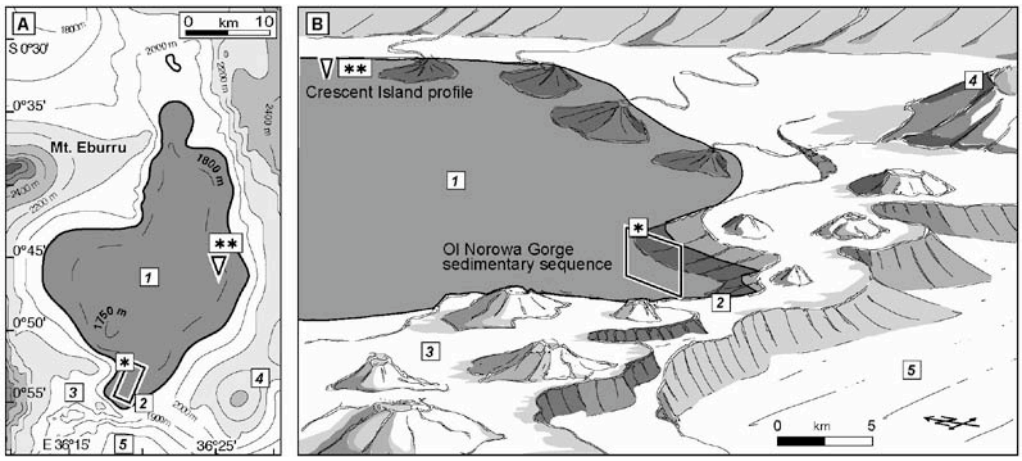

Fig. 3.8 Reconstruction of maximum extension of paleo-Lake Naivasha, as inferred from the results of this study and reconstruction of the bathymetry based on geologic field data (Bergner et al., 2003). (A) Map of estimated topography of the Naivasha basin with 100 m-contour interval; 1,900 m a.s.l. corresponds to maximum lake level at ~135 kyr BP. (B) Relief-sketch of the southern rim of the paleobasin derived from digital-elevation modeling outlining the extension of the paleo-Lake Naivasha and spatial relation of the sediment profiles. (1) paleo-Lake Naivasha. (2) location of later Ol Njorowa Gorge, (3) Olkaria Volcanic Complex, (4) Mt. Longonot, (5) Akira plains. Location of sediment sequence in the Ol Njorowa Gorge (*) and sediment core profile at Crescent Island (**).

The exact timing for the development of the highstand is difficult to be estimated. Since there is no evidence for an unconformity within the diatomite, neither from field observations nor from the diatom analyses, the ~80 cm of diatomite between the base of the diatomite and the 141±3 kyr-old tuff have to be deposited within at least 5,000 yrs. Unfortunately, the second ash layer of the profile at around 200 cm above the diatomite base, is not datable (A. Deino, pers. comm. 2003). Since also the high-resolution analysis of the thinly-layered diatomite could not prove the laminae as varves or multi-year couplets, we can only speculate about the timing of this highstand. Typical

sedimentation rates for diatomite range from ~1 to 10 mm·yr^{-1}, depending on the productivity of the lake (Richardson and Richardson, 1972; Owen and Renault, 1981; Tellford and Lamb, 1999; Stager and Johnson, 2000; Chalié and Gasse, 2002; Owen, 2002). Assuming a sedimentation rate of ~1mm·yr^{-1} for the lower part of highstand-IX diatomite, we found a significant discrepancy between the corresponding theoretical time interval of deposition and the true time span as inferred from the radiometric age control points. Taken into account the uncertainties in $^{40}Ar/^{39}Ar$ dating, the best approximation for the sedimentation rate is around 0.2 mm·yr^{-1}. Due to the thicker laminae in the upper part of the profile, higher rates of sedimentation are postulated for this section. Herein, a value of 0.5 mm·yr^{-1} would correspond to our observation from the thin-section studies. This value would also be in the same order of magnitude as sedimentation rates calculated for the paleo-Lake Abiyata, an Ethiopian crater lake of similar hydrochemical characteristics as Lake Naivasha (Chalié and Gasse, 2002). Therefore, we assume that the onset of the paleolake highstands was characterized by low sedimentation rates, whereas the period of stabilized deep-water conditions corresponds to higher sedimentation rates. Assuming the postulated sedimentation rates, the highstand-IX paleolake lasted between 7,000 to 15,000 years from the first manifestation of lacustrine conditions until its complete regression.

After the termination of highstand IX, the water level of Lake Naivasha was extremely low for a long period of time. It cannot be excluded that the lake disappeared for at least part of this time interval, because no lake deposits are described for the time between the regression of highstand IX and the transgression of highstand VIII. Only ~25 to ~30 kyr after the previous lake-level maximum, paleo-Lake Naivasha experienced a second period of an extreme water level. The results from diatom analyses of highstand VIII indicate significant differences to the previous, but also to the later lake period. The shallow lake does not show significant fluctuations neither in the morphologic nor in the hydrochemical parameters (Fig. 3.6). As documented by the lower, laminated part of the profile, this lake highstand was again initialized by pronounced flood events. Laminae thickness increases with time suggesting higher productivity in a constantly deepening lake. In contrast to highstand IX, the conductivity and pH of the lake water did not significantly decrease and it can be speculated if the freshwater influx was not high enough to significantly change the hydrochemistry. On the other hand, diatoms

preferring freshwater conditions occur in greater numbers (Fig. 3.7). Since these species mostly represent littoral habitats, we believe that the lake was not large enough to support a significant growth of planktonic freshwater algae. However, during the highstand-VIII, paleo-Lake Naivasha certainly stands at a level well above the modern level for at least several hundred years. The flora in the upper part of the diatomite bed indicates that environmental conditions in the catchment should have changed considerably, allowing favorable hydrologic conditions and constantly high lake levels over such a long time span.

After an interval of ~30 kyr without prominent lacustrine phases, Lake Naivasha experienced a third and last lake-level highstand documented by diatomite deposits in the Ol Njorowa Gorge. According to the thickness of the lake deposits, the 80 kyr BP-highstand lasted only for a short time, but the diatom assemblages suggest rapid changes from shallow conditions to a deeper and larger lake. Obviously, the evolution of this highstand was strongly affected by pyroclastic input during a period of volcanic activity. The dissolution of silicic volcanic glass may have influenced the hydrochemistry, and thus would partially account for the constant variation of the pH and conductivity values within the eualkaline-eusaline field. However, even during this period the lake experienced a short-term shift towards a higher water level and lower alkalinity compared with today (Fig. 3.7). The most significant difference between this high lake and modern Lake Naivasha is again the relative stability of the hydrologic conditions through time.

Paleoclimate implications of the reconstructed highstand periods

The detailed analysis of three diatomite profiles exposed in the Ol Njorowa Gorge reveals the enormous hydrologic variability of the present-day shallow, but freshwater Lake Naivasha. Our results as well as data from investigations of a 28 m-long sediment core (Richardson and Richardson, 1972) suggest that the lake experienced at least two major, two intermediate and several less pronounced lake-level highstands during the last 175 kyr (Fig. 3.9). The continuous deposition of diatomaceous silts and diatomites characterize four of these highstands as periods of stable lacustrine conditions over long time spans, with moderate water chemistry. Diatom analyses reveal that the high lakes

at ~135 kyr and ~9 kyr BP were clearly dominated by abundant planktonic diatom species typical for deep freshwater lakes. The sediments of both highstands document the existence of high lake levels during a period of several thousand years. Beach pebbles and paleoshorelines as well as basin reconstructions indicate that Lake Naivasha was up to 150 m deeper than today at that time (cf., chapter 4 and figure 3.8; Washbourn-Kamau, 1975; Bergner et al., 2003). Since the lake also contributed water to the northern Nakuru-Elmenteita basin and to the southern Akira plains at least during the highstand at ~9 kyr BP (Washbourn-Kamau, 1977; Dühnforth, 2001; Dühnforth et al., 2001), we conclude that Lake Naivasha at ~135 kyr and ~9 kyr BP went through the most extreme hydrologic conditions during the last 175 kyr.

Whereas the diatom assemblages during the 135 and the 9 kyr BP-highstands show great similarities, significant differences are observed between the flora of the 110 and 80 kyr BP-highstands. The 110 kyr BP-highstand has no analog during the last 175 kyr, with respect to the diatom flora. In contrast, diatom assemblages of the 80 kyr BP-highstand and the flora preserved in the modern sediment imply comparable environmental conditions during these periods. Diatom analyses on short sediment cores from the modern lake reflect a similar temporal trend in the evolution of diatom assemblages since the last 5,000 yr as during the 80 kyr BP-highstand (Richardson and Richardson, 1972). Starting from a predominant alkalophil flora, the diatom assemblages develop toward a freshwater-preferring community. This similar pattern reflects a similar freshening of the lakes with time and comparable environmental conditions. On the other hand, the higher fraction of planktonic species during the 80 kyr BP-highstand suggests a slightly deeper lake during the Late Pleistocene. From morphologic constraints, we furthermore believe that the 80 kyr BP-paleolake was larger in the open-water area.

In contrast to all other lake periods when diatomite has been deposited, the 110 kyr BP-highstand does not show a dominance of planktonic algae. The diatom flora much more reflects nearshore lake habitats, and also the reconstructed paleoenvironmental conditions suggest a freshwater swamp and not a deep lake. Although the hydrologic conditions at ~110 kyr BP were different from those during the other highstands, the sedimentary facies is similar, but different from the modern deposits. Whereas the

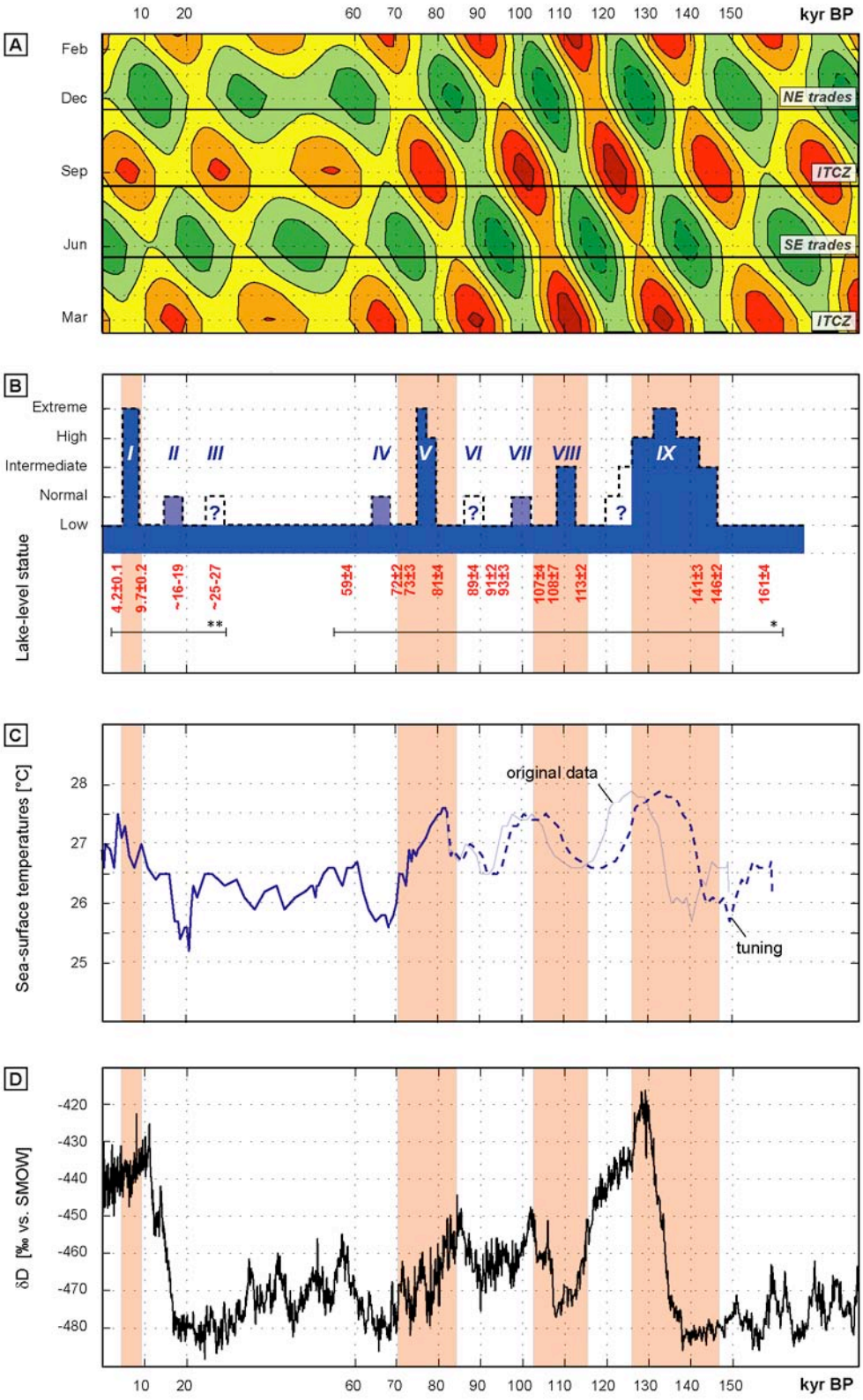

Fig. 3.9 Correlation of lake-level changes of Lake Naivasha and orbitally-induced changes of climatic parameters. (A) Contour plot of the anomalous heat flux ($W \cdot m^{-2}$) onto the equator (contour interval is 20 $W \cdot m^{-2}$). Seasons of prevailing airflow pattern indicated by horizontal bars (cf., Fig. 1.3). (B) Composite chronology of hydrologic changes in the Central Kenya Rift; highstand periods as indicated corresponding to (*) this study, Trauth et al. (2001, 2003) and (**) Richardson and Richardson (1972), Richardson and Dussinger (1986). (C) $U^{37}K$-based Indian Ocean sea-surface temperatures (marine core MD85674; Bard et al., 1997); solid line according to tuning on SPECMAP timescale; dashed line according to timing of Termination II by Shackleton et al. (2003). (D) Vostok deuterium content of ice as a proxy for atmospheric temperature (Petit et al., 1999).

modern Lake Naivasha is characterized by permanent sediment mixing due to wind-driven resuspension (Verschuren, 1999), the laminated deposits of the paleolake imply wind-sheltered sedimentation in a (most probably) deeper lake environment. In that sense, the 110 kyr BP-highstand can be regarded as an intermediate stage between the highest lake-levels and the modern lowstand conditions.

Comparing our results with other lake-level records derived from several sediment cores in the Naivasha and Nakuru-Elmenteita basins, an interesting chronology of lake-level fluctuations can be compiled for the last 175 kyr (Fig. 3.9). Since important tectonic movements did not affect the Naivasha basin during that time, the hydrologic changes are interpreted as to reflect variations in the precipitation-evaporation balance in the catchment. The compilation suggests that the hydrologic variations can best be explained by orbitally-induced changes in solar radiation on the equator, but the lake-level fluctuations also correlate with variations in the Indian Ocean sea-surface temperatures (SST). Since the short-term variability of the present-day climate in East Africa is mainly controlled by such large-scale influences, changes of those factors provide a partial explanation of the hydrologic fluctuations in the Central Kenya Rift.

Obviously, the chronology of lake-level highstands in the Naivasha basin at 10-11 kyr intervals follows the maximum equatorial March and September insolation (Trauth et al., 2003). The increased heating of the continent attracts more moisture to East Africa. In that context, both more intense spring and fall rainy seasons provoke higher water tables in the catchment. Interestingly, there is no one-to-one correlation between the amplitudes of maximum March and September insolation and the magnitude of the highstands. Moreover, assuming the $^{40}Ar/^{39}Ar$ chronology of our record is correct, significant differences between the timing of these highstands and solar radiation can be observed. We therefore believe that equatorial insolation is the most important but not the sole cause for hydrologic changes in the Central Kenya Rift.

Comparing our chronology with tropical Indian-Ocean SST records as inferred from alkenones (Bard et al., 1997), periods of higher SST's tend to correlate with the highest lake levels of Naivasha. Higher ocean temperatures cause higher moisture availability and hence higher lateral water transport to the African continent. At present, lateral

moisture transport during the short rains in fall is even stronger during ENSO-warm (i.e., El-Niño) events (cf., figure 1.2; Camberlin, 1995; Nicholson, 1996; Indeje et al., 2000; Nicholson, 2000). In the past, periods of stronger ENSO as triggered by maximum lower latitude insolation may provide an additional source of increased humidity in the Central Kenya Rift (Clement et al., 1999). The rhythmic lamination of the diatomites provide some evidence for such an ENSO-type influence. Taken into account these observations we infer that the present-day hydrologic situation with mostly hypersaline and only a few shallow freshwater lakes represents a narrow snapshot of the lower end of the hydrologic variability. The enormous environmental changes in the past certainly had important consequences and feedbacks on regional, but maybe also for global climates. The record of hydrologic changes in the Naivasha basin therefore confirm earlier work in the region and yield valuable insights for future water- and climate-related research in equatorial East Africa.

CHAPTER 4

ASSESSING CLIMATE INFLUENCES ON THE SUCCESSION OF PALEO-LAKE NAIVASHA

extended version published in **Global and Planetary Change, vol. 36, p. 117-136** (2003), entitled as
Bergner, A.G.N, Trauth, M.H., Bookhagen, B.: Paleoprecipitation estimates for the Lake Naivasha basin (Kenya) during the last 175 k.y. using a lake-balance model.

Fig. 4.1 View from the southern shore of Lake Naivasha towards the Aberdare Range

Abstract

We modeled the two most extreme highstands of Lake Naivasha during the last 175 kyr to estimate potential precipitation/evaporation changes in this basin. In a first step, the bathymetry of the paleolakes at ~135 and ~9 kyr BP was reconstructed from sediment cores and surface outcrops. Second, we modeled the paleohydrologic budget during the highstands using a simplified coupled energy mass-balance model. Our results show that the hydrologic and hence the climate conditions at ~135 and ~9 kyr BP were similar, but significantly different from today. The main difference is a ~15% higher value in precipitation compared to the present. An adaptation and migration of vegetation in the cause of climate changes would result in a ~30% increase in precipitation. The most likely cause for such a wetter climate at ~135 and ~9 kyr BP is a more intense intertropical convergence and increased precipitation in East Africa.

Introduction

In East Africa, Quaternary climatic changes are recorded in lacustrine sediments reflecting changes in water level and hydrochemistry (e.g., Richardson and Richardson, 1972; Gasse et al., 1989; Johnson et al., 2000; Talbot and Lærdal, 2000; Verschuren et al., 2000; Barker et al., 2001; Trauth et al., 2001). To determine the magnitude of such climate changes, lake-balance modeling is now a widely used and accepted tool (e.g., Barron and Moore, 1994; Bookhagen et al., 2001; Nicholson and Yin, 2001). Since the water storage of a lake is directly related to regional hydrologic conditions, these models provide important insights into the relationship between various components of the catchment (i.e., basin geometry, climate, vegetation and subsurface conditions) and can therefore also be used to predict future freshwater supply.

Lake-balance models have to be adjusted to the environmental conditions in the basin; this calibration is more precise if several natural scenarios in the same basin are available for different time slices. Unfortunately, instrumental climate records in East Africa are short and do not document the full natural variability in a lake basin. Moreover, the interference of natural changes and human impact on lake-level fluctuations during the last hundred years causes further difficulties. To overcome this problem, environmental conditions can be reconstructed using natural climate archives such as lake sediments. Paleoenvironmental data can help to define extreme hydrologic scenarios and the potential magnitude of precipitation-evaporation changes in the catchment. In such an environment, water-balance modeling provides the opportunity to give precise answers about the absolute values of climate changes in the past.

Widespread lacustrine deposits in the Naivasha basin record multiple lake-level highstands and intermittent lowstands during the last 175 kyr BP (cf., chapter 3; Richardson and Richardson, 1972; Richardson and Dussinger, 1986; Trauth and Strecker, 1996; Trauth et al., 2001) (Fig. 2.2). High-precision $^{40}Ar/^{39}Ar$ age data of intercalated tuffs provide a precise age control for these hydrological changes. The two most extreme highstands during the last 175 kyr occurred during the Late Pleistocene between 139 and 133 kyr BP and in the early Holocene between 12 and 4 kyr BP (Richardson and Richardson, 1972; Trauth et al., 2001). Although timing and magnitude

of the hydrologic changes are well-known, the climate conditions during these times are not well defined. Results from earlier lake-balance modeling for the early Holocene wet period contradict in the magnitude of climate changes and suggest an increase in precipitation by 10 to 17% (Hastenrath and Kutzbach, 1983) or 20 to 55%, respectively (Vincent et al., 1989). For the Late Pleistocene, the climate conditions for East Africa have to be interpolated from large-scale general circulation model (GCM) results that suggest changes in the same order of magnitude (Prell and Kutzbach, 1987; deNoblet et al., 1996; Dong et al., 1996). To obtain a more precise estimate for the hydrologic variability in the Central Kenya Rift, we reconstructed the geometry of the water body of Lake Naivasha at around 135 kyr and 9 kyr BP. Using a water-balance model, we show that a significantly higher precipitation-evaporation ratio is the most likely cause for these two highstands.

Regional settings

Temporal variances in the hydrologic budget of the Central Kenya Rift lakes are mainly controlled by changes in precipitation, which is in turn linked to the seasonal migration of the Intertropical Convergence Zone (ITCZ) (Nicholson, 1996). This pronounced equatorial low-pressure cell is caused by the zenith of the overhead sun and therefore reaches its maximum value during March and September in the Central Kenya Rift. While surface temperatures coincide with maximum solar radiation, the time of maximum rainfall follows the latitudinal position of the ITCZ with a time lag of about four weeks. Local rainfall mainly results from moisture transport from the Indian Ocean and/or westerly winds from the Congo basin (Fig. 1.3). Both wind circulation systems are attracted by the ITCZ, crossing East Africa and causing convective rainfall in the center of the ITCZ. Heaviest rains occur in spring, when the trade winds parallel the rift margins and thunderstorms occur every afternoon.

Located at 1,890 m above sea level, Lake Naivasha is the highest lake in the Central Kenya Rift (0°55'S 36°20'E). The Mau Escarpment (3,080 m a.s.l.) and the volcano Mt. Eburru (2,840 m) bound the closed-basin lake to the west. To the north and east (Kinangop Plateau), the basin is bordered by Plio-Pleistocene fault scarps, whereas the volcano Mt. Longonot (2,776 m) and the Olkaria Volcanic Complex (2,440 m) define a

southern barrier. The history of the Naivasha basin began at about 320 kyr BP, when lava flows at Olkaria closed the southern outlet between the flanks of the 400-kyr-old Mt. Longonot and the Mau Escarpment. However, a large lake did not exist before ~146 kyr BP (Trauth et al., 2001). Modern Lake Naivasha contains ~0.85 km^3 of water and covers an area of about 180 km^2. Around 20% of the lake surface is covered by papyrus swamps. Whereas most of the Kenya Rift lakes such as Lake Elmenteita (1,776 m) and Lake Nakuru (1,758 m) are highly alkaline, Lake Naivasha is fresh and has a pH of ~8.1 (Åse, 1987). Since the lake area only receives 600 mm·yr^{-1} of rainfall and potential evapotranspiration is about 1,900 mm·yr^{-1} (Clarke et al., 1990), the low pH can only be a consequence of the high water influx from the Malewa and Gilgil rivers draining the Kinangop Plateau and the 4,400-m-high Aberdare Range to the east. In these areas, evapotranspiration is low due to a thin vegetation coverage up to elevations of 2,600 m and high water runoff on steep slopes with poorly-developed soils (Griffiths, 1972; Jätzold, 1981; KMD, 2000) (Fig. 2.2). In contrast, high elevated afro-montane forests of the Aberdare Range play a major role in storing huge amounts of moisture (Jätzold, 1981). As shown by experiments in water wells, almost the entire amount of water received from the rift margins reaches Lake Naivasha after a very short time (e.g., Vincent et al., 1979; Onacha, 2000). Infiltrating into the lake, about fifteen percent of the river input leaves the lake by underground seepage through porous volcanic material. Although the total amount of this subsurface outflow is still a matter of debate, this process is certainly important in the hydrochemical budget and the solute export from the lake (e.g., Gaudet and Melack, 1981; Ojiambo-Bwire and Lyons, 1996)

Methods

The model employed in this study computes an equilibrium lake level of a closed-basin lake using the balance between basin-averaged precipitation and evaporation. As in most lake-balance models, evaporation is the most critical component, but difficult to determine. Our model uses a energy-budget method evaluating incoming and outgoing radiation at the earth's surface. The algorithm was first developed by Blodgett et al. (1997), but significantly modified, translated into Matlab® code and applied to a landslide-dammed lake in the Central Andes by Bookhagen et al. (2001). The most important differences in the application of the model to the semi-arid intra-andean basin

and Lake Naivasha were the importance of seepage and a potential vegetation feedback in the lake basin.

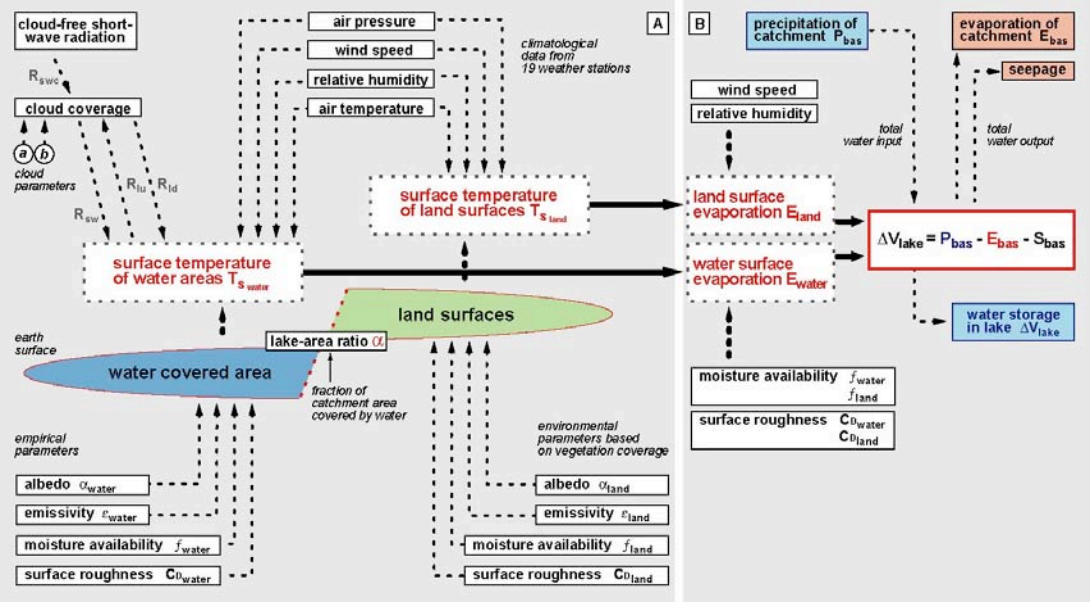

Fig. 4.2 Concept of lake-balance model based on Blodget et al. (1997) and Bookhagen et al. (2001) showing the major components of the hydrologic system. The model is a combination of an (A) energy-budget approach, where the potential evaporation rate of the earth surface is calculated from radiation-controlled and climate-triggered energy transformations at the lower atmosphere boundary. Based on the differences between water- and vegetation-covered areas, two values of potential evaporation are obtained and introduced into a (B) mass-balance equation. Herein, the total of the catchment evaporation is balanced with the values of basin-averaged precipitation and seepage. In the case of a hydrologic steady state, the change in the water storage of the closed-basin Lake Naivasha is zero.

The steady state hydrological budget for a closed-basin lake system can be written as:

$$\Delta V_{lake} = P_{bas} - [E_w \cdot \alpha_w + E_l(1 - \alpha_w)] - S_{bas} = 0 \qquad (1)$$

where ΔV_{lake} is the volumetric change in the water body, P_{bas} is the basin-averaged precipitation, E_w and E_l denote the evaporation over water and land, respectively, α_w is the lake-area ratio, or the fraction of the catchment covered by water and S_{bas} is the basin-integrated seepage (Fig. 4.2). Whereas the modern values for P_{bas}, E_w and S_{bas} are easy to determine, E_l is difficult to estimate mainly due to the complexity of related parameters and their spatial variability in the catchment. On the other hand, the equation clearly indicates that higher lake levels and larger lakes are always the consequence of increased precipitation and/or reduced evaporation and seepage, as long as no important tectonic movements affected the basin geometry during the studied time-period.

For the hydrologic modeling, we used a two-step approach. First, the present-day lake was modeled using modern climate parameters. The result was intensely tested for robustness and sensitivity to all parameters. Then, the reconstructed paleolakes were modeled by changing the climate parameters until the paleolake levels were reached. During the modeling, changes in the radiation pattern due to variations in the earth's orbit as well as changes in vegetation in the cause of climate shifts were considered (Kutzbach and Webb, 1993; Kutzbach et al., 1996; Carrington et al., 2001). From all solutions, the scenarios consistent with results from pollen analyses and large-scale GCM's were preferred (e.g., Maitima, 1991; Street-Perrott and Perrott, 1993; deNoblet et al., 1996; Dong et al., 1996).

Paleolake reconstruction techniques

The chronology of the lake-level fluctuations in the Naivasha basin is based on the correlation of lake-sediment outcrops at twelve locations in the Lake Naivasha basin (Washbourn-Kamau, 1975; Bone, 1985; Clarke et al., 1990; Trauth et al., 2001) (Fig. 4.3). In the Ol Njorowa Gorge within the southern rim of the basin, a 60-m-thick succession of lake sediments, between 146 and 60 kyr old, is used as a reference section for the Late Pleistocene lake highstands (Trauth and Strecker, 1996). The deposits of the early Holocene highstand were described in a sediment core from the present lake (Richardson and Richardson, 1972; Richardson and Dussinger, 1986) and additional unpublished core logs from water wells (S. Higgins, pers. comm. 2000) (Fig. 4.3).

The geometry of the water body for the 135 and 9 kyr BP-time slices was reconstructed from the elevation of the youngest sediments deposited during these highstands. A set of elevation reference points was obtained by correlating the different outcrops and profiles. The altitude of each reference point was corrected for tectonic movements and erosion using the chronology by Bosworth and Strecker (1997). The typical offsets of normal faults for the last 175 kyr are in the order of a few meters (Strecker et al., 1990; Bosworth and Strecker, 1997). The reference points were embedded into a digital elevation model (DEM) of the present-day Naivasha basin. Because of their significantly older tectonic history, it is assumed that the higher-elevated parts of the catchment were not subjected to important morphological changes

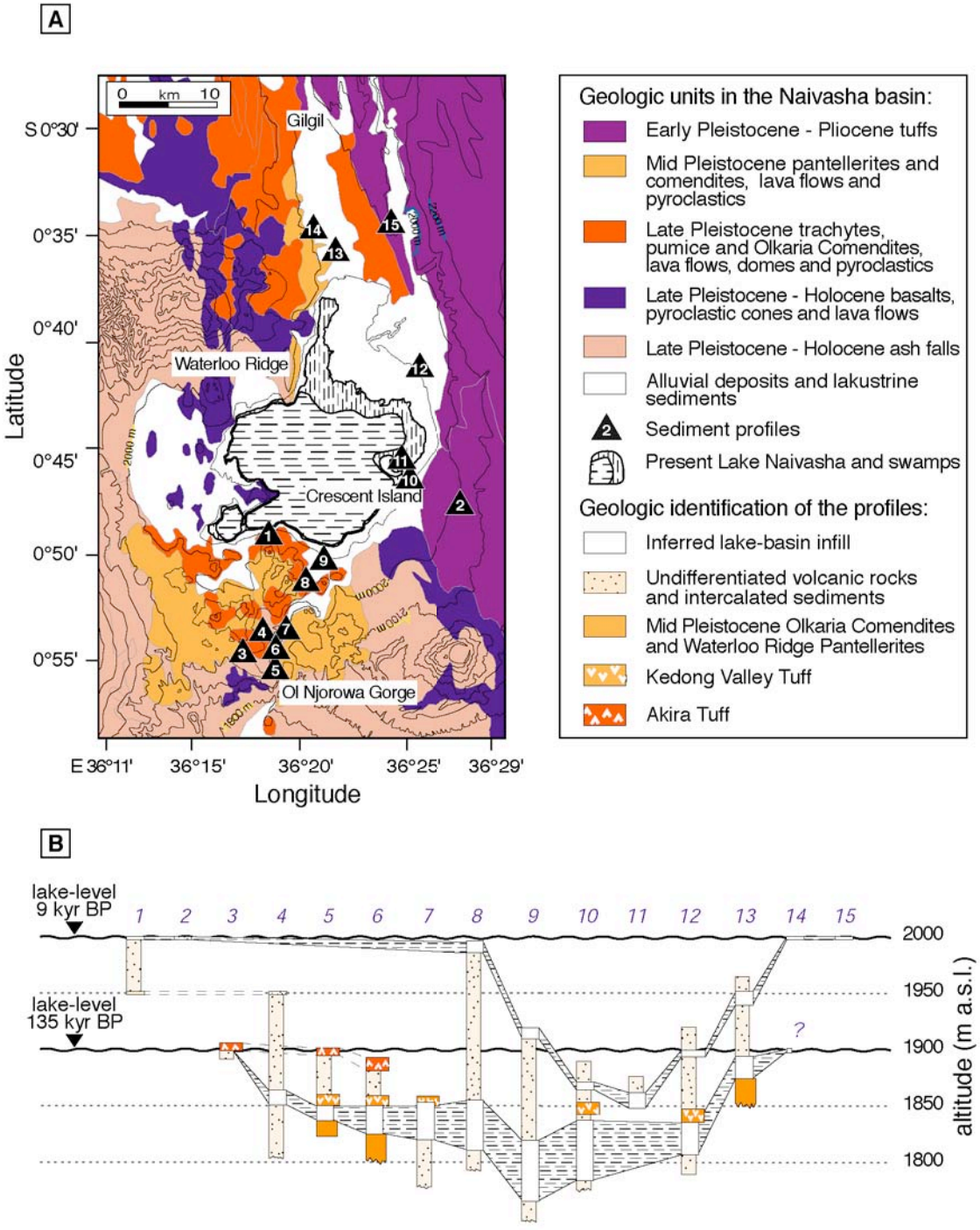

Fig. 4.3 Geology of the Naivasha basin; (A) map showing lithologic units (after Clarke et al., 1990) and key outcrops in the vicinity of the modern lake for paleolake reconstruction; (B) stratigraphic correlation for bathymetry reconstructions with inferred paleolake levels and corresponding sediments (dashed). (1) Oserian Farm (Washbourn-Kamau, 1975); (2) Munyu railway cut (Washbourn-Kamau, 1975); (3) Lolonito North (Bone, 1985); (4) Ololbutot North (Bone, 1985); (5) Ol Njorowa Gorge (Trauth et al., 2001); (6) Ol Njorowa Gorge II (Clarke et al., 1990); (7) Maasai Gorge (Clarke et al., 1990); (8) Gorge Farm North (Clarke et al., 1990); (9) Lake Naivasha South (Bone, 1985); (10) Lake Naivasha South II (private sediment core by S. Higgins, pers. comm. 2000); (11) Crescent Island (Richardson and Richardson, 1972); (12) Naivasha East (unpublished core data by the Kenyan Government, pers. comm. 2000); (13) Waterloo Ridge (Clarke et al., 1990); (14) Gilgil railway cut (Washbourn-Kamau, 1975); (15) Malewa railway cut (Washbourn-Kamau, 1975)

during the last 300 kyr (Baker and Wohlenberg, 1971; Strecker et al., 1990; Bosworth and Strecker, 1997). All present elevation data are based on digitized topographic maps at a scale of 1:250,000 and 1:50,000.

The paleolakes were computed by triangulation between the reference points using bilinear and t-spline interpolation techniques. The t-spline technique uses Green's functions for a spline in tension (Wessel and Bercovici, 1998). The inclusion of a tension *t* greatly improves the stability of the method relative to conventional gridding routines without tension, e.g., undesirable oscillations between data points. The value of *t* can vary between t=0 (corresponding to the biharmonic spline solution; Sandwell, 1987) and t=1 equivalent to bilinear interpolation.

Algorithm for modeling modern and paleoevaporation

The energy-budget equation after Brutsaert (1982) and Shuttleworth (1988) assumes that the difference between incoming and outgoing radiation at the earth surface, the net heating rate, is zero:

$$R_{sw} - R_{lu} + \varepsilon \cdot R_{ld} - H - L \cdot E = 0 \tag{2}$$

where R_{sw} is the net short-wave radiation down, R_{lu} the long-wave radiation up, ε the surface emissivity, R_{ld} the long wave radiation down, H the sensible heating rate, L the latent heat of vaporization, and E is rate of evaporation. Solving for E , the equation becomes:

$$E = \frac{H - \varepsilon \cdot R_{ld} + R_{lu} - R_{sw}}{L} \tag{3}$$

where H is calculated by

$$H = \frac{p \cdot C_D \cdot U \cdot c_p}{R \cdot T_a}(T_s - T_a) \tag{4}$$

with p for the air pressure, C_D for the surface drag coefficient, U refers to wind speed, c_p is the specific heat of dry air, R the gas constant of dry air and T_a and T_s corresponding

to the air and surface temperature, respectively (Brutsaert, 1982). The net long-wave radiation down R_{ld} is obtained by:

$$R_{ld} = 1.24\left(\frac{rh \cdot es(T_a)}{100 T_a}\right)^{\frac{1}{7}} \sigma T_s^4 (1 - a' \cdot cc^{b'}) \tag{5}$$

where rh is the relative humidity, $es(T_a)$ the saturation vapour pressure depending on temperature, σ reflects the Stefan-Boltzmann constant, and a' and b' refer to long wave cloud parameters; whereas the net long wave radiation up R_{lu} can be given as:

$$R_{lu} = \varepsilon \cdot \sigma \cdot T_s^4 \tag{6}$$

where ε corresponds to the surface emissivity (Brutsaert, 1982). The net short wave radiation down R_{sw} is calculated from the cloud free short-wave radiation R_{sws}, the surface albedo α, two values referring to short wave cloud parameters a and b, and the cloud cover cc (Brutsaert, 1982):

$$R_{sw} = R_{swc}(1 - \alpha)\left[1 - (a + b \cdot cc)\right] \tag{7}$$

Independently from the energy-budget equation, the potential evaporation can be calculated using a bulk transfer method as described by Brutsaert (1982):

$$E_{pot} = \frac{0.622 C_D \cdot U \cdot \rho}{R \cdot T_a}[es(T_s) - rh \cdot es(T_a)] \tag{8}$$

where E_{pot} is the potential evaporation and f is the soil moisture availability; both parameters are given in volumetric units.

Combining equations (3) and (8), evaporation in the Naivasha catchment can be estimated from very few environmental parameters. Assuming that radiation-controlled energy transformations at the atmosphere-lithosphere boundary are the triggering mechanism for evaporation from the surface, evaporation clearly depends on the characteristics of the boundary layer. Since the high topographic relief of the 3,400 km^2 large Naivasha catchment forces spatially varying environmental conditions, we resampled all parameters to a 1 km by 1 km regular grid using t-spline interpolation techniques (Wessel and Bercovici, 1998). Climatic data were obtained by averaging data sets for the last twenty years from nineteen weather stations (GDS, 1994; ISMCS,

1995; KMD, 2000; Fig. 2.2b) and expanding this dataset by contoured values from climatological maps (Griffiths, 1972; Jätzold, 1981; Ojany and Ogendo, 1988; Survey of Kenya, 1991). The present-day vegetation coverage was obtained from vegetation maps and field observations published by Jätzold (1981), Ojany and Ogendo (1988) and the Survey of Kenya (1991) and additional information from satellite images and field mapping.

Based on basin-averaged values, the modern hydrologic budget for Lake Naivasha was computed using equation (1). For the paleoclimatic scenario, the corresponding climate parameters were determined according to orbital-induced insolation changes and limited environmental data such as vegetation reconstructions based on Holocene pollen data (Maitima, 1991; Street-Perrott and Perrott, 1993). For some parameters, such as wind speed and cloud coverage, modeling results from GCM results provided important constraints. Since several parameters were only determined for the 9 kyr, but not for the 135 kyr BP-time slice, we used the 9 kyr BP-conditions as a starting point also for the Late Pleistocene model run.

Reconstruction of paleolakes

In contrast to the rift-shoulder areas, i.e., the Aberdare Range and the Mau Escarpment, tectonism and volcanism during the last 300 kyr significantly modified the inner-graben part of the catchment. At around 300 kyr BP, the inner-rift depression reached a maximum altitude near Gilgil (at 2,010□m today), separating the Nakuru-Elmenteita and Naivasha basins (Thompson and Dodson, 1963) (Fig. 2.2). From this point, the rift floor descends north- and southward with a ~2% gradient. Late Pleistocene trachytes, like the Gilgil Trachytes in the North (~950 kyr old) and the Limuru Trachytes in the South (~2.01 to 1.88 Myr old), as well as the Kinangop Tuffs in the East and the Mau Tuffs in the West (both ~4.5 to 3.4 Myr old) were the most prominent geologic units deposited in the inner rift (Clarke et al., 1990). The majority of the mid Pleistocene Olkaria Comendites, the Ol Njorowa Pantellerites and the Olongonot Volcanics were erupted well-before 320 kyr BP closing the Naivasha basin towards the south (Trauth and Strecker, 1996). The volcanic barrier reached a minimum elevation of around 1,950□m

and was laterally overlain by lake deposits. The base of these lake sediments documents the earliest history of Lake Naivasha after ~146 kyr BP (Fig. 4.3).

The 135 kyr BP-highstand is documented by a sequence of lake sediments containing two diatomite beds and intercalated waterlain tuffs. The sequence reaches ~20□m in the Ol Njorowa Gorge and thickens toward the deepest point of the paleolake up to 80±10□m (cf., chapter 3). The sediments are covered by the 106±4 kyr old Kedong Valley Tuff (Trauth et al., 2001). This tuff can be easily identified in most of the other outcrops and sediment cores north of the gorge and represents an excellent paleobathymetric marker horizon (Fig. 4.3). This marker defines the position of the lake bottom at 1,840□m in the location of the Ol Njorowa Gorge, descending northward to around 1,750□m near the center of the present lake. North of the present Lake Naivasha, lake sediments overlying volcanic rocks of a similar age as the Olkaria volcanic rocks define an elevation of 1,875□m for the lake bottom (Clarke et al., 1990). Sedimentary indicators, such as authigenic minerals and diatoms at the southern end of the Ol Njorowa Gorge suggest that the paleolake level remained at around 1,900±10□m for a long time span. The large lake deepened toward the center, but expanded into much shallower areas in the south and northeast. This geometry is corroborated by results from diatom analysis indicating shallow- and deep-water environments (Trauth and Strecker, 1996; Trauth et al., 2001).

Taking into consideration that the maximum lake level reached approximately 1,900□m, the best approximation for the true paleolake size was obtained using the t-spline method with t=0.2. The paleolake then covers an area of about 520□km^2 and the volume of the water body is ~55□km^3 (Tab. 4.1). In comparison with the present-day lake, the paleolake was three times larger with a volume of the water body 60 times larger. At its deepest point, the paleolake was 150□meters deep, in comparison with nine meters for the present-day lake (Fig. 4.4).

In contrast to the Pleistocene conditions, the early Holocene morphology of the Naivasha basin was not much different from the present-day situation. The activity of the Eburru Volcanic Center and the inner-graben volcanoes terminated before the Holocene lake-level highstand. Only a few volcanic centers of the Olkaria Complex

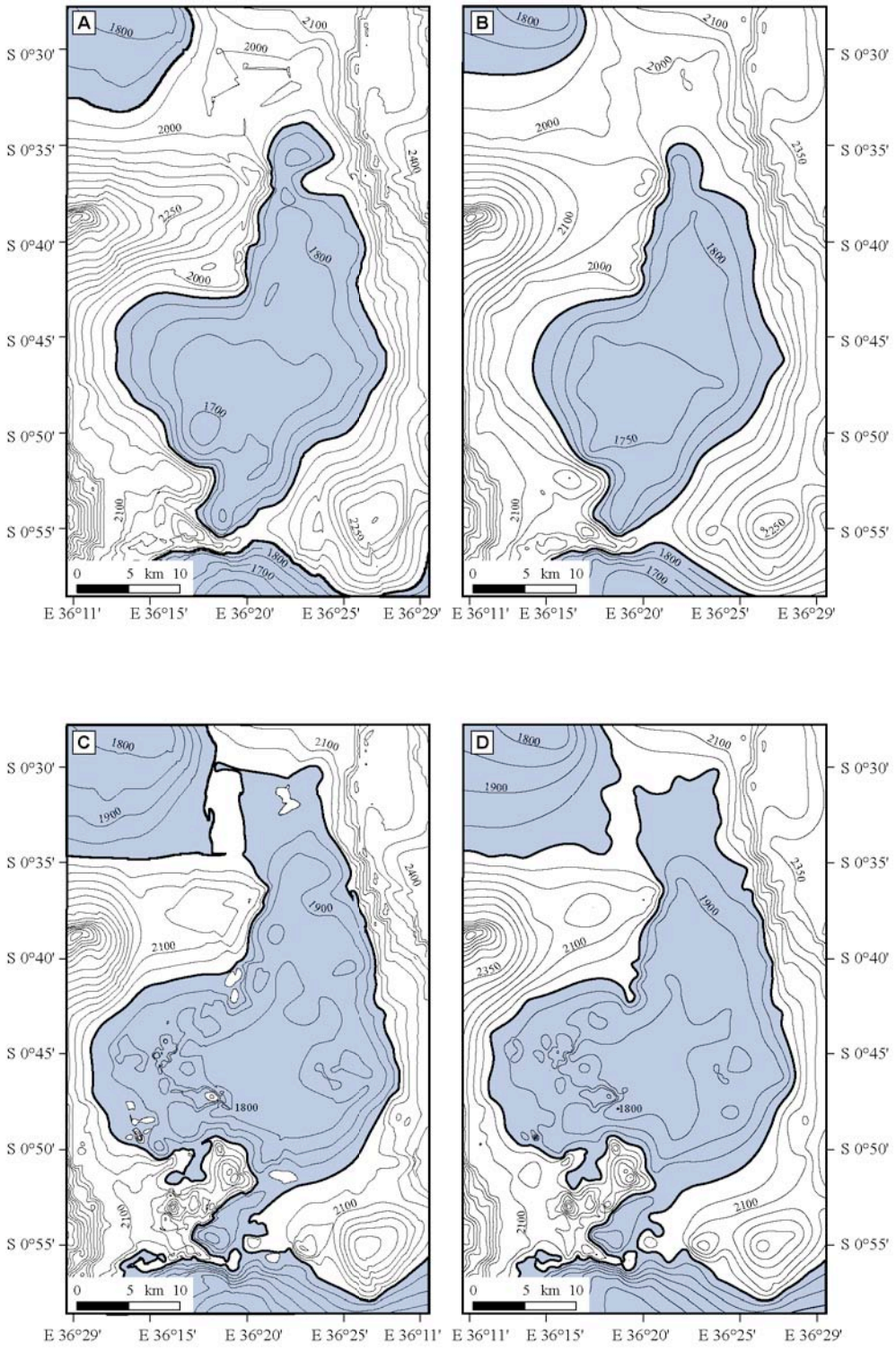

Fig. 4.4 Results of the paleobathymetric reconstructions showing (A and B) contour maps of the Late Pleistocene Naivasha-basin morphology as obtained by (A) quintic interpolation and (B) t-spline interpolation (t=0.2); (C - D) show the contour maps of the basin bathymetry for the Holocene lake period, as derived from (C) quintic interpolation and (D) t-spline interpolation (t=0.7); see text for more details.

erupted after this event (Clarke et al., 1990). The onset of the 9 kyr BP- highstand was documented in a sediment core obtained in the Crescent Island Crater, where deposits of this age were described at ~28□m depth below the present-day lake bottom (Richardson and Richardson, 1972). The 12 to 4 kyr-old sediment layer has a thickness of about 14□m at an altitude of 1,848 to 1,862□m. Equivalent sediments were neither identified in the Ol Njorowa Gorge nor in the deposits of the Olkaria or Mt. Longonot volcanic complex. Only in the outcrops close to the present shoreline, Holocene lake sediments were identified (cf., chapter 5; Bone, 1985; Clarke et al., 1990; S. Higgins, pers. comm. 2000). In addition, beach gravels inferred to correspond to this lake highstand, were found in several localities at an elevation of about 2,000□m (cf., chapter 5; Washbourn-Kamau, 1975; Bone, 1985). From morphologic observations and the distribution of lake deposits we infer that the maximum thickness of these highstand deposits occurs near the deepest point of the present-day Lake Naivasha, and thins out toward the shore lines. The past-6 kyr BP-sediments only slightly modify the early Holocene lake bathymetry, since they are ≤ 20 m thick (Richardson and Richardson, 1972; Clarke et al., 1990) (Fig. 4.3).

Tab. 4.1 Summary of reconstructed basin geometry using various interpolation techniques

Method	**9 kyr BP-time slice**		**135 kyr BP-time slice**	
	Lake size (km^2)	Volume (km^3)	Lake size (km^2)	Volume (km^3)
t-spline (t=0.1)	693.3	64.9	525.4	57.0
t-spline (t=0.2)	692.6	64.3	**518.5**	**55.4**
t-spline (t=0.7)	**684.5**	**59.3**	472.6	46.8
t-spline (t=0.9)	667.7	54.3 *	442.6 *	40.6 *
Linear with 1 x 10^{-2} km^2 grid cells	627.6 *	55.1	476.6	45.9
Quintic	697.2	63.6	525.9	56.4
Mean	677.2	60.3	493.6	50.4
Mean without values indicated by (*)	687.1	61.4	503.8	52.3

All calculations were done in Matlab® using 1km by 1km regular grids of elevation reference-points. Values for the size and volume of the paleowater bodies of Lake Naivasha during the 9 and 135 kyr BP-highstands were obtained from different interpolation techniques. T-spline interpolation uses Green's functions for a spline in tension (Wessel and Bercovici, 1998), where *t* varies between t=0 (equivalent to biharmonic spline solution; Sandwell, 1987) and t=1 (equivalent to bilinear interpolation). The quintic method refers to a fifth order cubic interpolation method. Best estimates for the true paleolake extensions are closest to the median and written in bold letters (t-spline interpolation with t=0.7 for the 9 kyr BP-highstand and t=0.2 for the 135 kyr BP-highstand).

Although beach gravels suggest that the lake remained at the observed elevations for a longer time, a second stable lake occurred at a deeper elevation. At the time when the paleolake reached 2,000□m, overflowing water partly eroded the southern barrier and began to form the modern Ol Njorowa Gorge. Subsequently, the lake level dropped gradually, until it stabilized again at about 5,700 BP (Richardson and Richardson, 1972). This second stable paleolake level is inferred from paleoshorelines at 1,950±10□m (Washbourn-Kamau, 1975). Assuming the maximum Holocene lake level

at an elevation of 2,000±10 m, the most likely lake size was around 685 km^2. In contrast to the Pleistocene lake reconstructions, the best result was obtained using a t-spline interpolation with t=0.7, where the curvature of the modeled bathymetry is at a minimum. The volume of this water body is approximately 59 km^3 (Tab. 4.1; Fig. 4.4 c,d). For the lower stable lake level at ~1,950 m the corresponding values were 480 km^2 for the lake area and 34 km^3 for volume.

Validation of the hydrologic model for the present-day Lake Naivasha

Due to the high relief and large lateral vegetation changes, the present-day Lake Naivasha basin shows extreme gradients for single environmental parameters (Jätzold, 1981). In order to take into account this spatial heterogeneity, basin-averaged values for the Lake Naivasha catchment were obtained using two different techniques; climatological parameters, such as insolation, precipitation, air pressure, wind speed, cloud coverage, relative humidity, and air temperature were calculated by interpolation between climate stations within and in the vicinity of the catchment (Fig. 2.2). The basin-averaged value for temperature is 13.5±0.5°C, whereas annual precipitation varies between 950 and 1,050 mm·yr^{-1}. Wind speed for the Lake Naivasha basin was obtained from the climatic stations Nyahururu, Nakuru, Naivasha and Nairobi (GDS, 1994; ISMCS, 1995; KMD, 2000). From these data sources, a basin-averaged value of 2.5±0.3 m·s^{-1} was determined, which is consistent with results from Nicholson (1996), as well as measurements by R. Hennemann (pers. comm., 2001). The solar radiation was set to 415±3 W·m^{-2} according to Berger and Loutre (1991); cloudiness was 65±5% and relative humidity was 65±5% using the information given in Rodhe and Virji (1976), GDS (1994), ISMCS (1995) and KMD (2000). The values for the short- and long-wave cloud coefficients, which symbolize the predominant character of clouds in the catchment, were obtained as described in Bookhagen et al. (2001) (Tab. 4.3).

In contrast to the climatological parameters, all environmental parameters depending on surface characteristics, such as emissivity, soil moisture availability, albedo and surface roughness, were compiled for water-covered and land-surface regions separately (Fig. 4.2). Six classes of different surface patterns were determined, distinguishing between water surfaces, regions covered by afro-alpine heath and bogs, bamboo-tree dominated

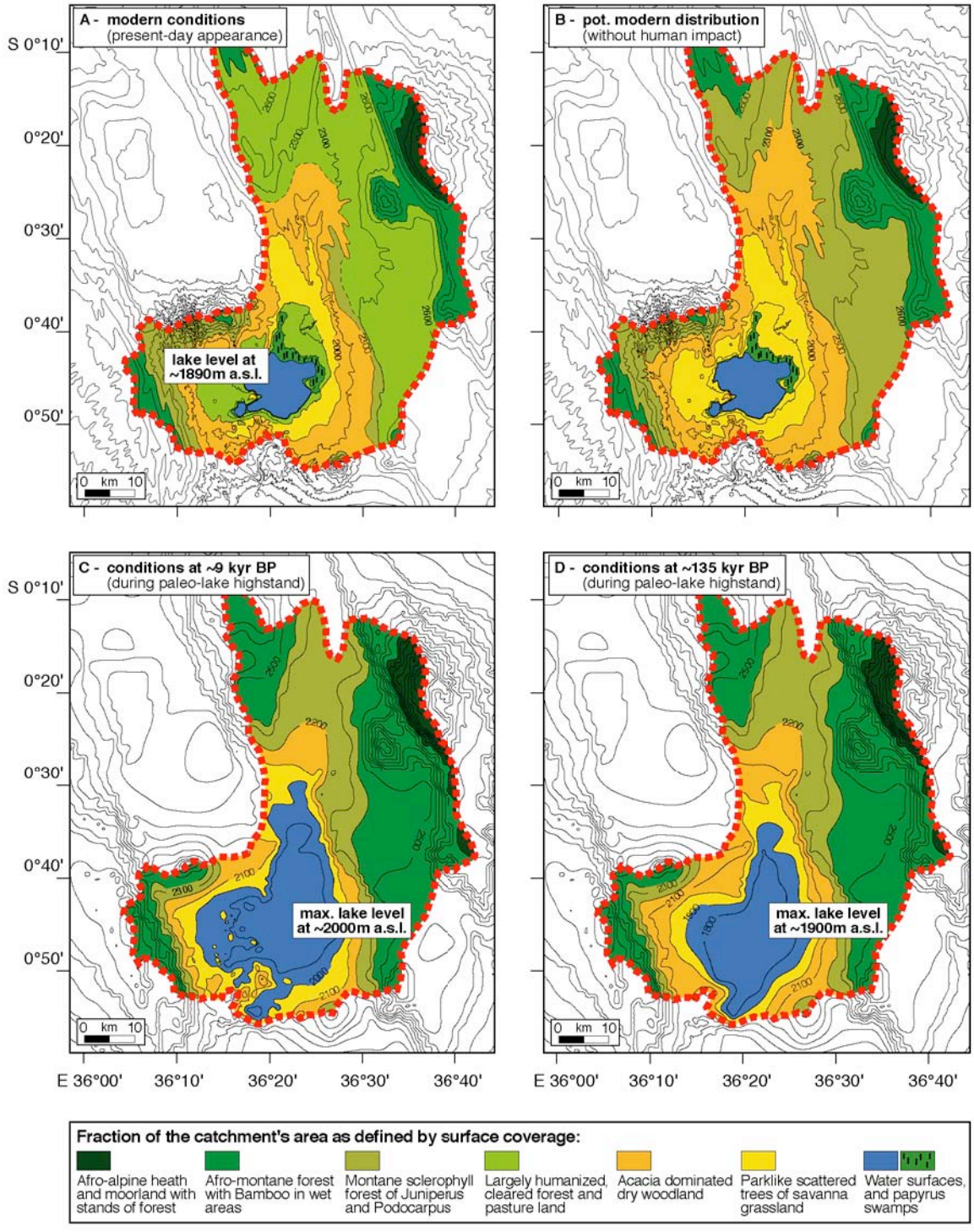

Fig. 4.5 Comparison of the modern and reconstructed paleoconditions for Lake Naivasha and the catchment. Upper graphs show the present-day morphology and vegetation coverage compiled from topographic and vegetation maps, satellite-images and field observations. Elevation contours were generated at different scales for the outer (1:250,000) and inner part (1:50,000) of the basin. Whereas the actual vegetation distribution, as shown in (A), was used for the present-day hydrologic modeling, (B) illustrates the estimated modern vegetation coverage without human impact.
Paleoreconstructions (lower graphs) were obtained from 3D-landscape computations based on geologic field data and t-spline interpolation techniques with (C) t=0.7 for 9 kyr BP highstand and (D) t=0.2 for 135 kyr BP highstand. Paleovegetation reconstructions are based on published pollen data for the Holocene. The reconstructed 9 kyr BP vegetation coverage was also applied to the 135 kyr BP situation, based on significant similarities in the large-scale climate conditions.

forests, the sclerophyll forests of *Juniperus* and *Podocarpus*, intensively used areas with pastures and farming, *Acacia* dominated dry woodland and open-savanna land with scattered shrubs and trees (Jätzold, 1981) (Fig. 4.5). The fraction of the catchment area defined by each surface pattern was calculated from a raster-based mapping of vegetation coverage, where each cell represents an area of 1 km by 1 km. From this mapping, weighting-averaged values for albedo, surface roughness, emissivity and soil moisture availability were determined following the principles outlined in Schmugge and André (1991). Basin-averaged albedo $\alpha = 0.16 \pm 0.02$ and surface roughness, reflected by the surface drag coefficient $C_D = 4.0 \pm 0.2 \cdot 10^{-3}$, represent the predominant savanna-type and deforested environments in the present-day catchment (Jätzold, 1981; Schmugge and André, 1991). Although, nearly 80% of the former sclerophyll forests are cleared for agricultural use, basin-averaged values for emissivity $\varepsilon = 0.96 \pm 0.02$ and soil moisture availability $f = 0.35 \pm 0.05$ are more or less unaffected and reflect prevailing occurrence of water-unsaturated soils (Brutsaert, 1982; Schmugge and André, 1991) (Tab. 4.2).

While the majority of all parameters could easily be determined, the amount of subsurface outflow from the lake bottom is a matter of debate. Gaudet and Melack (1981) and Ojiambo-Bwire and Lyons (1996) use such a subsurface outflow as a partial explanation for the low alkalinity of the lake. Assuming, about 36 million cubic meters of the direct water loss from Lake Naivasha is contributed to seepage, they also postulate an even higher value for precipitation in the hydrologic budget of the lake. Consequently, the given basin-averaged precipitation varies between 900 and 1,100 $mm \cdot yr^{-1}$ (Griffiths, 1972; Ojany and Ogendo, 1988; Survey of Kenya, 1991; GDS, 1994; ISMCS, 1995; KMD, 2000). In the present-day hydrologic simulation, we used a basin-averaged value of 100 $mm \cdot yr^{-1}$ reflecting the entire basin seepage, although this value is only attributed to subsurface outflow in the lake area itself.

Applying the input parameters for the present-day conditions (Tab. 4.3), the model computes a hypothetical lake precisely at the modern level of Lake Naivasha at 1,890 m (Fig. 4.6). The modeled evaporation rates were 1,880±30 $mm \cdot yr^{-1}$ over open water, but 915±100 $mm \cdot yr^{-1}$ over land. In order to maintain a stable lake level, the value of precipitation has to reach 970±100 $mm \cdot yr^{-1}$. This value increases to about

1,070 mm·yr^{-1}, as soon as the model allows a significant subsurface outflow as suggested by Ojiambo-Bwire and Lyons (1996).

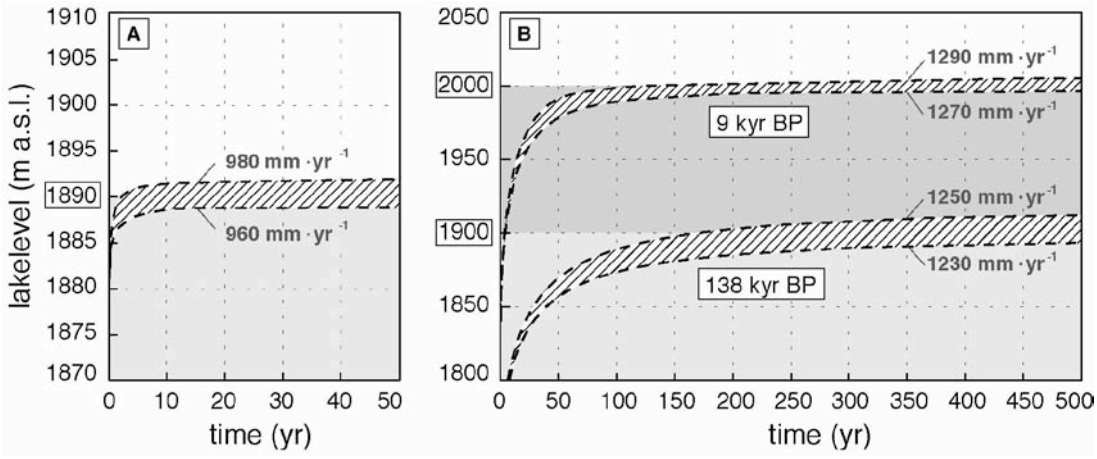

Fig. 4.6 Modeled lake-fill curves for (A) the modern lake reaching the 1,890 m-contour and (B) the paleo-lakes at 2,000 m (9 kyr BP) and 1,900 m (135 kyr BP).

Intense sensitivity testing of our results was done for the model-input parameters such as solar radiation, temperature, cloud coverage, relative humidity, wind speed and the surface-drag coefficient. The influence of each single coefficient was expressed as the deviation of the inferred rainfall value from the modern precipitation estimate. Considering the confidence of the coefficients and their natural variability, the sensitivity tests yield an uncertainty of the modeled precipitation between 2.5 and 10%. Whereas surface roughness is of particular importance, introducing large uncertainties, cloud coverage, wind speed and relative humidity are less important for the final result (Fig. 4.7). Summing up all uncertainties in definition of the paleoenvironmental parameters and the natural variability of the modern climate indices, the error in the final results most likely is not more than 15%. Thus, a careful adjustment of the model to the paleoconditions starting from the modern values in small steps leads to reasonable results and provides some valuable informations about the dynamics and sensitivity of the lake system.

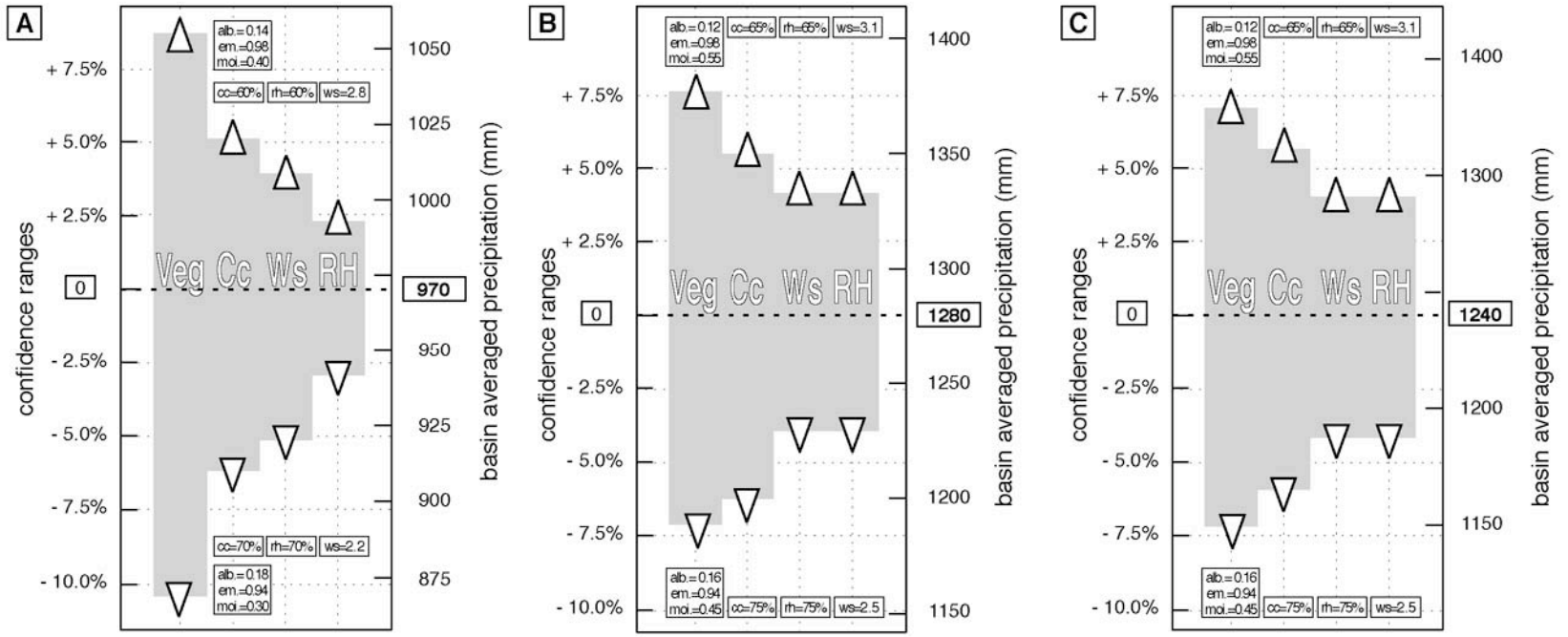

Fig. 4.7 Results of sensitivity tests for model parameters with important impact on the final result; veg - vegetation coverage, cc - cloud coverage, ws – wind speed, rh - relative humidity. Fluctuations in vegetation coverage introduce larger changes in the modeled precipitation values as compared to all other parameters. In the paleomodeling, the higher portion of water-covered areas reduces the influence of vegetation, whereas all general climatic parameters, i.e., cloud coverage, wind speed and relative humidity, show higher degrees of uncertainty.

Modeling the paleolake highstands

First we tried to model the Late Pleistocene and early Holocene lakes using the modern values for precipitation and evaporation (Tab. 4.3). The resulting hypothetical lakes cover an area similar to the modern lake but the volume of the water bodies are 4.5 and 2.3 km^3, respectively, due to the differences in bathymetry. With the selected input parameters, the Late Pleistocene lake does not reach the southern basin boundary and rises only up to the 1,760±5 m-contour, whereas the early Holocene lake reaches 1,855±5 m. The enormous discrepancies between the modeled lakes and the reconstructed geometry of the paleolakes imply significant differences in the hydrologic budget and hence the climatic boundary conditions of the catchment area.

The most effective mechanism changing the lake hydrology is either higher lateral moisture transport increasing precipitation or reduced basin-averaged temperatures lowering evaporation. Applying these arguments to the modeling, as a first test all environmental parameters were kept at their modern values assuming that the entire change in the hydrologic budget is attributed to a change in rainfall. The simulation of the 135 kyr BP-highstand suggests an increase of 11% rainfall (1,075 $mm \cdot yr^{-1}$), whereas the 9 kyr BP-paleolake can be simulated using an increase of 16% (1,125 $mm \cdot yr^{-1}$) (Tab. 4.3).

Such dramatic changes require the adaptation of many other environmental factors, such as wind speed, cloudiness and higher relative humidity. A realistic scenario for the region of the Naivasha basin is an increase of these parameters by 10% according to similar investigations by Kutzbach et al. (1996). Another consequence of higher moisture levels is a significant change in vegetation of the present-day grassland areas. Climate modeling experiments have shown that vegetation feedbacks can dramatically influence local climatic conditions (e.g., Doherty et al., 2000; Renssen and Lautenschlager, 2000; Carrington et al., 2001). Unfortunately, no Pleistocene vegetation reconstructions are available, but pollen analysis covering the Holocene suggests more extensive woodlands, at least for the more elevated parts of the Lake Naivasha catchment (Maitima, 1991; Street-Perrott and Perrott, 1993). Such vegetation changes

Tab. 4.2 Characterization of catchment area today and during lake highstands

Surface pattern and parameters				Catchment area characterized by specific vegetation provinces (%)			
α	ε	*f*	z_0 (cm)	Modern		9-k.y. BP time slice	135-k.y. BP time slice
				Actual coverage	Potential coverage	Reconstructed coverage	
(1) Water surfaces							
0.06	0.99	0.97	0.01	0.05	0.05	0.20 (+ 287%)	0.15 (+ 192%)
(2) Savanna grassland							
0.25	0.98	0.05	5.0	0.07	0.14	0.10 (- 28%)	0.07 (- 50%)
(3) Dry woodlands							
0.20	0.96	0.10	10.0	0.20	0.25	0.09 (- 62%)	0.17 (- 31%)
(4) Pastures and farming							
0.15	0.95	0.30	20.0	0.44	0	0	0
(5) Sclerophyll forests							
0.12	0.96	0.50	30.0	0.08	0.37	0.20 (- 46%)	0.20 (- 45%)
(6) Afro-montane forests							
0.09	0.96	0.80	50.0	0.13	0.17	0.34 (+ 96%)	0.37 (+ 115%)
(7) Afro-alpine heath, bogs							
0.20	0.97	0.30	10.0	0.02	0.02	0.04 (+ 75%)	0.04 (+ 67%)

Means for surface patterns	α	ε	*f*	z_0	C_D	α	ε	*f*	z_0	C_D
Mean, land surfaces (2 - 7)	0.16	0.96	0.35	22.5	4.0×10^{-3}	0.14	0.96	0.50	32.0	4.4×10^{-3}
Confidence range	± 0.02	± 0.02	± 0.05	± 5.0	0.2×10^{-3}	± 0.02	± 0.02	± 0.05	± 5.0	0.2×10^{-3}

Surface patterns terminology correspond to the mapping of (1) water covered areas in the catchment of Lake Naivasha and (2-7) six classes of land-surface areas distinguished by predominant vegetation coverage (cf., Jätzold, 1981). Corresponding environmental parameters were derived from empirical data and tables as outlined in Brutsaert (1982) and Schmugge and André (1991); a reflects the surface albedo, e the surface emissivity, *f* the soil moisture availability and z_0 corresponds to the roughness length (according to Schmugge & André (1991) with $CD = k^2 \cdot \ln(z_r / z_0)^{-2}$, with $k = 0.4$ and $z_r = 1.30 \cdot 10^4$ cm). The portion of the catchment area characterized by a particular vegetation coverage is calculated from raster-based maps. The actual modern vegetation coverage includes changes by human influence, whereas the potential coverage of present-day is hypothetical as predicted by the altitudinal variation of vegetation (Jätzold, 1981; Maitima, 1991). Paleovegetation was inferred from pollen data (Maitima, 1991; Street-Perrott and Perrott, 1993). The difference between modern and past vegetation is expressed as percentage from the potential modern conditions (in brackets).

Tab. 4.3 Summary of all input parameters and corresponding modeling results for modern and paleo- Lake Naivasha

Parameter	Units	Modern	9-k.y. BP time slice		135-k.y. BP time slice		Confidence	Ref.
			Without vegetation feedback	With vegetation feedback	Without vegetation feedback	With vegetation feedback		
Catchment area	km^2	3400					± 100	a
Maximum lake level	m a.s.l.	1889	2000 ± 10		1900 ± 10		--	a
Water body	km^3	0.85	59.3		55.4		± 5	a
Lake area	km^2	178.6	684.5		518.5		± 15	a
Portion of basin covered by lake	--	0.052	0.201		0.152		± 0.05	a
Cloudfree shortwave radiation	$W \cdot m^{-1}$	415					± 3	b
Shortwave cloud parameters	--	0.39, 0.38					ñ	c
Longwave cloud parameters	--	0.22, 2.0					ñ	c
Air pressure	Pa	815 10^5					ñ	d
Cloud coverage	--	0.65	0.65	0.70	0.65	0.70	± 0.05	d
Relative humidity	--	0.65	0.65	0.70	0.65	0.70	± 0.05	d
Windspeed	$m \cdot s^{-1}$	2.5	2.5	2.8	2.5	2.8	± 0.3	d
Air temperature	C	13.5	13.5	13.0	13.5	13.0	± 0.5	d
Surface temperature	C	18.3	18.3	15.7	18.3	15.7	± 0.5	e
Lake-surface water temperature	C	17.4	17.4	16.1	17.4	16.1	± 0.5	e
Surface drag coefficient	--	4.0×10^{-3}	4.0×10^{-3}	4.4×10^{-3}	4.0×10^{-3}	4.4×10^{-3}	$\pm 0.2 \times 10^{-3}$	f
Surface albedo over water, land	--	0.06, 0.16	0.06, 0.16	0.06, 0.14	0.06, 0.16	0.06, 0.14	± 0.02	f
Surface emissivity over water, land	--	0.99, 0.96	0.99, 0.96	0.99, 0.96	0.99, 0.96	0.99, 0.96	± 0.02	f
Soil moisture over water, land	--	0.97, 0.35	0.97, 0.35	0.97, 0.5	0.97, 0.35	0.97, 0.5	± 0.05	f
Evaporation over water	$mm \cdot yr^{-1} \cdot m^{-2}$	1880	1880	1850	1880	1850	± 30	e
Evaporation over land	$mm \cdot yr^{-1} \cdot m^{-2}$	915	915	1125	915	1125	± 100	e
Precipitation	$mm \cdot yr^{-1} \cdot m^{-2}$	970	1125	1280	1075	1240	± 100	e
Precipitation including expected basin drainage	$mm \cdot yr^{-1} \cdot m^{-2}$	1070	1225	~1380	1175	~1340	--	g

All input parameters are derived from available climate data sets (see references). Listed values correspond to basin-averaged values, which were obtained by interpolation between weather stations within and in the vicinity of the catchment; surface-pattern related parameters are derived from vegetation mappings (see text for further explanations). All hydrologic modelings were done in Matlab® using the lake-balance-modeling concept published by Blodget et al. (1997) and Bookhagen et al. (2001); final modeling results for a steady state of the lake-balance are given in bold letters. Indices reflect: (a) values taken from digital elevation model; (b) Berger and Loutre (1991); (c) Bookhagen et al. (2001); (d) Rodhe and Virji (1976), GDS (1994), ISMCS (1995) and KMD (2000); (e) calculated value for given parameters in the modeling run; (f) surface-pattern related parameters as attributed to vegetation mappings (cf., Tab. 4.2); (g) modeled precipitation values including a postulated basin-averaged seepage of S_{bas}=100 $mm \cdot yr^{-1}$.

would have caused a lower surface albedo, higher soil moisture availability, surface emissivity and surface drag coefficient.

Starting from the grid-based mapping of present-day vegetation coverage, we computed a basin-wide interpolation of paleovegetation using the Holocene pollen records (Maitima, 1991; Street-Perrott and Perrott, 1993). Although, this interpolation can only reflect a very rough estimate of the paleovegetation change, it provides important insights into the potential environmental change due to a more humid climate in the Naivasha basin. Whereas the fraction of the catchment area covered by afro-alpine elements, as well as wet montane forests dramatically increased (+70 to +100%), areas of dry woodlands and savanna habitats were reduced by –30 to –60% (Tab. 4.2; Fig. 4.5). Following the principles outlined by Schmugge and André (1991), surface roughness of the paleo-Naivasha basin was increased to $C_D=4.4\pm0.2\cdot10^{-3}$, whereas basin-averaged albedo was reduced to a =0.14±0.02; the basin-averaged emissivity was e =0.96±0.02, whereas soil moisture availability reached $f=0.5\pm0.05$.

The Holocene pollen assemblages also indicate a basin-wide temperature reduction (Street-Perrott and Perrott, 1993) that is most likely attributed to the vegetation change rather than insolation changes (Maitima, 1991; Kutzbach et al., 1996; Renssen and Lautenschlager, 2000). Although, the absolute value of this temperature change is not known, large-scale GCM results imply a reduction on the order of –0.5 to -2°C (deMenocal and Rind, 1993; Jolly et al., 1998). Since, mean-annual insolation does not significantly differ from the present-day value, we used a basin-averaged temperature reduction of –0.5±0.5°C as a realistic model input for the early Holocene simulation as well as for the Late Pleistocene model run. Following the same argument, we applied the paleovegetation reconstruction to both time-slices (Tab. 4.3).

In consideration of all feedback mechanisms, the time to fill the lake basin after a hypothetical abrupt climate change towards the reconstructed conditions would have been longer by a factor of ten as compared to the present (Fig. 4.6). The modeled value for the basin-averaged precipitation is 1,240±100□mm·yr-1 (+28%) for the 135□kyr□BP-lake level, and 1,280±100□mm·yr-1 (+32%) for the 9□kyr□BP-highstand, respectively. Variations of the input parameters within the defined confidence ranges indicate that

changes in the vegetation-controlled parameters introduce a lower degree of uncertainty into the modeling results than during the modern run (Fig. 4.7). The higher portion of water-covered areas during the paleohighstands reduces the hydrologic influence of vegetation. In contrast, general climatic parameters, i.e., cloud coverage, wind speed and relative humidity, show a higher degree of uncertainty for the paleomodeling results (±4 to ±6%).

Our model runs do not consider changes in the subsurface outflow. However, during the 9 kyr BP-highstand the lake had at least a temporary overflow through the Ol Njorowa Gorge (Washbourn-Kamau, 1977). As there are good arguments for a subsurface outflow under the present lake, a potential change in the amount of groundwater infiltration was discussed (cf., chapter 5; Gaudet and Melack, 1981; Ojiambo-Bwire and Lyons, 1996; R.Becht, pers. comm. 2000). It is assumed that infiltration should have been comparable to its present-day value during the paleolake highstands, or even less due to more water-saturated grounds, higher water tables and lower groundwater gradients. Although, exact values of the overflow and subsurface outflow are unknown, the modeled values for paleoprecipitation for both highstands are believed to be minimum estimates.

Paleoclimate implications

The dimension of Lake Naivasha during the two highstands at ~135 and ~9 kyr BP compared to present illustrates the extreme variability of climate and hydrology in the Central Kenya Rift. Since the Naivasha basin was not affected by important tectonic movements or volcanic activity during the last 175 kyr, the observed lake-level fluctuations document long-term changes in the precipitation/evaporation balance. Our modeling results suggest that precipitation was increased by 11 to 16% compared to the present-day value. Starting from the modern climate conditions, such an increase in humidity would result in a stable lake at the reconstructed level after a minimum time of 200 years. This change toward more humid conditions, however, would also cause changes in vegetation in the catchment. If the adaptation and migration of vegetation and subsequent higher transpiration are introduced into the model, the hydroclimatic conditions in the catchment would be characterized by a 28 to 32% increase in mean-

annual precipitation. A change in the amount of subsurface outflow from the lake would lead to further changes in the paleohydrologic budget; but since no strong arguments support such changes, our modeling results reflect minimum, but realistic estimates of the precipitation/evaporation change.

For the early Holocene climate optimum, our modeling results are in the same order of magnitude as climate parameters modeled by Hastenrath and Kutzbach (1983) for this region. The authors use a more generalized energy-budget method and found a minimum precipitation change of 10% in the catchment. Vegetation changes in the cause of such a more humid climate would increase this value to 17% (Hastenrath and Kutzbach, 1983). In contrast, Vincent et al. (1989) found a 350□mm·yr-1 (+55%) increase in rainfall, similar to the results from GCM experiments (deMenocal and Rind, 1993) and run-off calculations by Butzer et al. (1972). However, these results seem to overestimate the regional precipitation changes because they do not take into account the large spatial heterogenities in rainfall in the Central Kenya Rift. Our grid-based lake-balance model allows a precise assessment of local rainfall anomalies and large gradients in the environmental parameters. The modeled precipitation changes of 16 to 32% are therefore believed to be a better estimate for the true paleoclimatic conditions in the Central Kenya Rift.

In contrast to the detailed paleoclimatic information for the Early Holocene, climate records for the late Pleistocene are scarce (Richardson and Richardson, 1972; Trauth et al., 2001). The history of Lake Naivasha suggests that although the causes for the highstands at ~135 and ~9 kyr BP were different (Richardson and Dussinger, 1986; Trauth et al., 2001), the hydroclimatic conditions in the Naivasha Basin during these highstands show significant similarities. Whereas the 135 kyr BP-highstand seems to be the result of maximum March insolation on the equator resulting in a strong intertropical convergence and high precipitation during the April/May rains (Trauth et al., 2001), the 9 kyr BP-highstand correlates with maximum Northern Hemisphere insolation and a strong summer monsoonal circulation (Richardson and Dussinger, 1986; Gasse, 2000). Herein, a stronger influence of westerly flows may be speculated. However, an important factor for both highstands seems to be higher intra-annual fluctuations in air temperature. More precipitation during the rainy seasons and

decreased evaporation during the dry season would result in a more positive net moisture budget in the course of a year.

The magnitude of the hydrologic changes in the Naivasha basin provides valuable insights into the sensitivity of this natural system. Obviously the present-day character of the modern lake only represents a snapshot of its natural variability and the climate system. As demonstrated by our modeling, a relatively small change in humidity can rise the lake level from less than 10 to more than 100 meters, an area three-time larger would be flooded by water. Paleoclimatic reconstructions from other basins suggest, that high and large lakes are a common feature in East Africa at least during the Early Holocene (Street-Perrott and Perrott, 1993; Jolly et al., 1998; Gasse, 2000). During this time, open water surfaces or papyrus swamps covered most of the inner-graben region. These dramatic environmental changes certainly had important consequences and feedbacks on regional, but maybe also for global climates. Such relationships between East African climate and the global implications should be the subject for future large-scale GCM experiments.

CHAPTER 5

INFLUENCE OF TECTONICS VS. CLIMATE ON THE EVOLUTION OF LAKES IN THE CENTRAL KENYA RIFT

---

to be submitted to **Geology**, entitled as
Bergner, A.G.N., Blisniuk, P.M., Deino, A., Dühnforth, M., Strecker, M.R., Trauth, M.H.: Tectonics vs. climate influences on the evolution of the lakes in the Central Kenya Rift.

Fig. 5.1 Photograph of Maasai children in front of tilted fault-scarp blocks east of Lake Elmenteita. Ongoing tectonic movements on listric faults along the eastern rim of the Nakuru-Elmenteita basin may affect segmentation of the drainage areas of the Central Kenya Rift lakes.

Introduction and settings

The Cenozoic East African Rift System (*EARS*) is a major morpho-tectonic feature that transverses East Africa from the Gulf of Aden to Mozambique (Fig. 5.2). The development of approximately north-south trending grabens, the uplift of rift shoulders and internal rift segmentation as well as the eruption of massive volcanic edifices during the last 45 million years has resulted in a pronounced accentuation of local climates in tropical East Africa (e.g., Baker et al., 1972; Strecker et al., 1990; KRISP Working Party, 1991; Morley, 1994; George et al., 1998; Prodehl et al., 1997; Ebinger et al., 2000; Macdonald et al., 2001). As a consequence of the rift-related volcano-tectonic processes and the topographically controlled distribution of rainfall a series of

sedimentary basins formed in the *EARS* providing complex geometries, catchment areas and drainage networks (Yuretich, 1982; Tiercellin and Lezzar, 2002). Whereas sediments in these basins often document similar lake histories through time, modern lakes of the *EARS* exhibit a considerable variety in size and hydrochemical characteristics (Yuretich, 1982; Schlüter, 1993). The western branch of the *EARS* contains several large and deep lakes. In contrast, much smaller and more alkaline lakes characterize the eastern branch (Schlüter, 1993) (Fig. 5.2a). The difference between the large freshwater lakes of the western branch and the shallow lakes of the eastern rift has been attributed to differences in (a) the tectonically-controlled relief, (b) the composition of the volcanic surface rocks in the catchment and (c) climate conditions (Talling and Talling, 1965; Yuretich, 1982; Johnson and Odada, 1996; Tiercelin and Lezzar, 2002). Although these aspects are well-accepted as important factors having influenced the evolution of East African rift-lakes on long time scales (>10^4 years), short-term hydrologic fluctuations on time scales of 10^3 to 10^4 years are generally attributed to climate variations (e.g., Roberts, 1990; Street-Perrott and

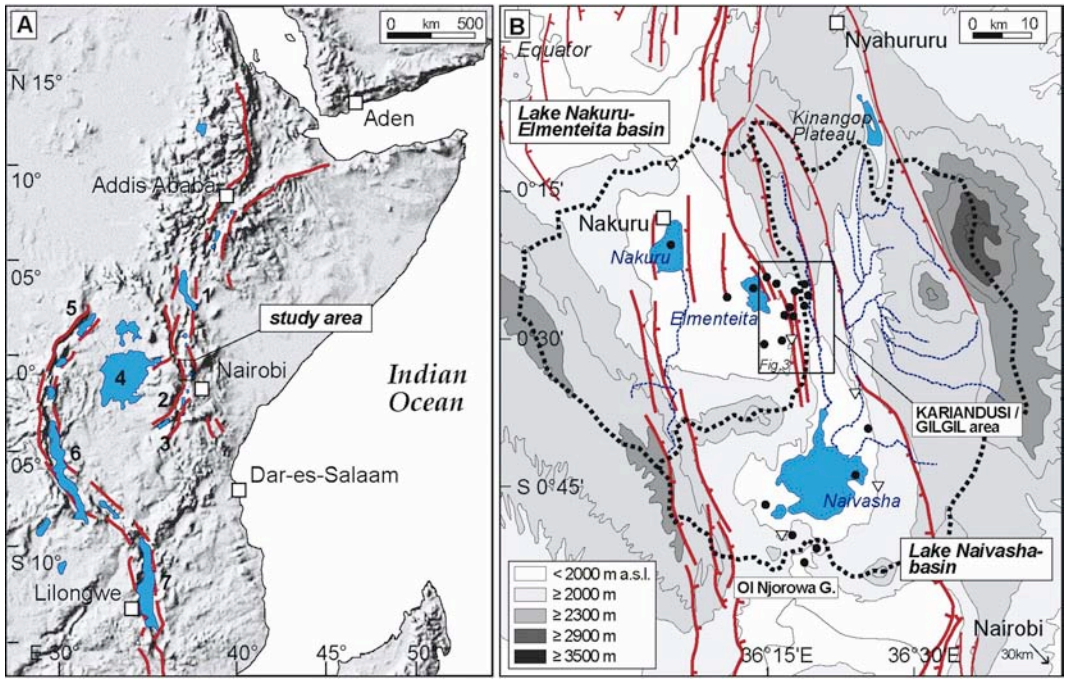

Fig. 5.2 Regional settings of the study area; (A) Shaded relief map of East Africa (GTOPO30 data from USGS EROS Data Center in Sioux Falls, South Dakota) showing topography, location of large lakes, major faults of the East African Rift System (EARS) and location of the Central Kenya Rift (study area); (1) Lake Turkana, (2) Lakes Magadi and Natron, (3) Lake Eyasi, (4) Lake Victoria, (5) Lake Albert, (6) Lake Tanganyika, (7) Lake Malawi. (B) Topographic map of the Central Kenya Rift (150 m elevation contours) showing modern Lakes Nakuru, Elmenteita and Naivasha, modern drainage divides (dashed black line), main rivers and the location of investigated lake-sediments outcrops (dots) and paleo-shorelines (triangle) (see Tab. 5.2 and Fig. 5.5 for details); red lines mark principal areas of active tectonics during the last one million years.

Perrott, 1993; LeTurdu et al., 1999; Gasse, 2000; Verschuren et al., 2000; Chalié and Gasse, 2002). However, the influence of tectonic movements and magmatic activities on hydrological fluctuations was generally not considered in paleoclimate reconstructions for the last 20,000 years (cf., Carroll and Bohacs, 1999; Behrensmeyer et al., 2002; Yuretich and Ervin, 2002; Gierlowski-Kordesch and Buchheim, 2003).

In the Central Kenya Rift (*CKR*), the highest part of the eastern branch of the *EARS* the history of the neighboring Nakuru-Elmenteita and Naivasha basins demonstrates that both rift-related tectonic processes and climate influence are important while interpreting environmental changes on all time scales (Fig. 5.2). Although the geologic settings as well as the climatic conditions are very similar in these two basins, hydrologic characters of the modern lakes suggest significant differences. Whereas the modern Nakuru and Elmenteita lakes (1,758 and 1,786 m a.s.l.) are both highly alkaline, relatively small (40 and 24 km^2) and less than 2 m deep, Lake Naivasha (1,889 m) is fresh, covers an area of ~150 km^2 and is up to 9 m deep (Milbrink, 1977; Verschuren, 1999) (Tab. 5.1). The dissimilarities have been generally explained by differences in the size of the catchment areas (2,400 vs. 3,400 km^2), basin precipitation and discharge, combined with a reduction of the alkalinity by precipitation of minerals and significant seepage through porous pyroclastic material (Milbrink, 1977; Gaudet and Melack, 1981; Ojiambo and Lyons, 1996; Becht and Harper, 2002). Interestingly, the older history of the lakes, as reconstructed from ^{14}C-dated Holocene lake deposits and paleo-shorelines, indicates rather similar hydrologic conditions between 12 to 4 kyr BP (Washbourn-Kamau, 1970, 1975; Richardson and Dussinger, 1986). At that time, the Naivasha and the Nakuru-Elmenteita basins hosted lakes, which were almost 200 m deep and more than 650 km^2 in area (Washbourn-Kamau, 1970, 1975; Dühnforth, 2001; Bergner et al., 2003; Dühnforth et al., in prep.). Furthermore, these deep paleolakes showed striking similarities in hydrochemistry (Richardson and Dussinger, 1986). The similar lake character and the temporal coincidence of the lake highstands with the timing of the Early Holocene climate optimum suggested that higher moisture levels in the course of wetter climates were the most likely cause for higher lake levels in the *CKR* (Hastenrath and Kutzbach, 1983; Bergner et al., 2003).

modern catchments	Nakuru-Elmenteita basin		Naivasha basin
drainage area [km^2]	2,390		3,400
modern lakes	Nakuru	Elmenteita	Naivasha
lake level [m a.s.l.]	1,760	1,786	1,888
lake area [km^2]	40	26	146
max. lake depth [m]	2	0.5	8
pH	9.7	10.9	7.8
conductivity [µS·cm^{-1}]	25,000	30,000	250
paleolakes			
Holocene:			
max. lake level [m a.s.l.]		1,940	2,000
max. lake area [km^2]		755	685
max. lake depth [m]		180	130
Late Pleistocene:			
max. lake level [m a.s.l.]		*~ 1,900*	1,900
max. lake area [km^2]		*~ 500*	520
max. lake depth [m]		*~ 100*	150

Tab. 5.1 Physical parameters of the Nakuru-Elmenteita and Naivasha basins. Modern data from Gasse et al. (1995) and this work. The geometry of the paleo-waterbodies was obtained from DEM-based reconstructions (Bergner et al., 2003; Dühnforth et al., in prep., Bergner et al., in prep.).

In this article, we try to assess the relative influence of climate vs. tectonic processes on the hydrologic evolution of the two lake basins. We extended the paleolimnologic history of the Nakuru-Elmenteita and Naivasha lakes back to around one million years before present (BP). We used thirteen diatomite profiles in the Nakuru-Elmenteita basin and six profiles in the Naivasha basin with $^{40}Ar/^{39}Ar$ age-control to test the hypothesis that the difference in the modern hydrology of the two basins is the consequence of tectonic activity resulting in a segmentation of drainage areas. The analysis of diatom assemblages contained in the sediments of similar age from both basins helps us to trace characteristic trends of hydrochemical and hydrologic lake evolution. The comparison of these trends between the two basins helps us to separate rift-related and climatic influences on lake history. This study therefore exemplarily illustrates the importance of an understanding of volcano-tectonic processes while reconstructing climate in such an (tectonically active) environment.

Reconstructing lake history in the Central Kenya Rift

Nineteen onshore exposures of diatomaceous lake sediments, as well as four paleo-shorelines and ancient beach cliffs were studied in the Nakuru-Elmenteita and Naivasha basins. The lacustrine deposits, comprising pure diatomite as well as diatom-rich clays and silts are located in the modern lake basins between 1,800 m and 2,000 m a.s.l. (Fig. 5.2 and 5.5; Tab. 5.2). The newly investigated lacustrine sequences were supplemented by data from three older lake-sediment cores taken at the intra-rift lakes (Richardson and Richardson, 1972; Richardson and Dussinger, 1986). Age control was obtained from radiocarbon dates of freshwater snail shells contained in the sediments and $^{40}Ar/^{39}Ar$ single-crystal dating on intercalated tuffs. Periods of lake-level highstands and intermittent lowstands were reconstructed from sediment characteristics and fossil diatom assemblages. The diatomaceous deposits were sampled at 5 to 50 cm intervals, depending on total sediment thickness. All diatomite samples were treated with HCl and H_2O_2, cleaned and suspended in destilled water and mounted in Naphrax. Species identification was performed using optical and scanning electron microscopes following the principles of Hustedt (1949), Gasse (1986) and Krammer and Lange-Bertalot (1991a, b; 1997a, b).

Based on the individual determination of fossil diatom assemblages in each stratigraphic level, a paleolimnologic classification of the flora was carried out in two steps. First, typical diatom assemblages were defined from averaging corresponding stratigraphic levels of all relevant sediment sections. Herein, age control and sequence characteristics were used to obtain a cross-basin average of sequence-specific lake evolution. Using the standardized diatom communities, the major phases in paleolake evolution were defined as initial, intermediate, highstand and final stage. In a second step, the diatom assemblages of similar lake stages were compared at different time-slices to assess the long-term change of prevailing hydrochemical characteristics in the lake history. After having identified the diatom assemblages in each sediment sequence, we found that all stratigraphic levels contain similar diatom assemblages characterized by a mixture of planktonic and epiphytic species. The lake deposits therefore suggest near-shore habitats providing favorable conditions to both, littoral (mostly epiphytic) and planktonic diatoms (Lampert and Sommer, 1993; Taub, 1996; Battarbee, 2000). In such an environment, the relative fraction of eu-planktonic vs. facultative planktonic and

epiphytic diatoms provide significant information on the depth of the paleolake. The ecologic preference of the most prominent taxa, such as diatom-specific habitat, oxygen requirement and trophic state, provides some additional constraints for the geometry of the water body, i.e., water depth and lake area (Gasse, 1986; VanDam et al., 1994). The approximation of the hydrochemical conditions was derived from optimum values, such as pH and conductivity of the most frequent diatoms (Hecky and Kilham, 1973; Gasse, 1980; Fritz et al., 1991; VanDam et al., 1994; Gasse et al., 1995).

Nr.	Local name	Elevation [m a.s.l.]	Age [kyr BP]	Dating method and reference	Sequence thickness [cm]	Sediment characteristics
Nakuru-Elmenteita basin						
sediment profiles:						
--	Nakuru core	1,750 ±5	6.5 ±0.1	(C^{14}; top) Richardson and Dussinger, 1986	500 [3]	diatomaceous gytia
			12.2 ±0.2	(C^{14}; base) Richardson and Dussinger, 1986		
--	Elmenteita core	1,780 ±5	3.8 ±0.3	(C^{14}; top) Richardson and Dussinger, 1986	300 [3]	diatomaceous gytia
			12.9 ±0.2	(C^{14}; base) Richardson and Dussinger, 1986		
D01	Kariandusi road cut	1,910 ±10	9.5 ±0.2	(C^{14}; top) Dühnforth et al., in prep.	40	diatom. silts
D02	Karterit	1,930 ±10	11.1 ±0.9	(C^{14}; base) Dühnforth et al., in prep.	70	siltic diatomite
D03	Lemulug	1,930 ±10	12.3 ±0.4	(C^{14}; top) Dühnforth et al., in prep.	90	siltic diatomite
D04	Soysambu	1,880 ±10	138 ±11	(Ar^{40}/Ar^{39}; intercal.) this work	450	soft diatomite
D05	Kariandusi road cut	1,900 ±10	900 ±50	(stratigraphic corr.) [2] new Ar^{40}/Ar^{39} age in prep.	140	soft diatomite
D06	Elmenteita road cut	1,860 ±10	900 ±50	(stratigraphic correlation) [2]	100	soft diatomite
D07	Elmenteita gorge	1,830 ±10	900 ±50	(stratigraphic correlation) [2]	600	pure white diatomite
D08	Elmenteita river gully	1,860 ±10	900 ±50	(stratigraphic correlation) [2]	> 150	pure white diatomite
D09	Kariandusi river gully	1,880 ±10	900 ±50	(stratigraphic correlation) [2]	> 200	pure white diatomite
D10	Prehistoric top	1,880 ±10	900 ±50	(stratigraphic correlation) [2]	> 160	pure white diatomite
D11	Prehistoric site	1,870 ±10	974 ±07	(Ar^{40}/Ar^{39}; base) Behrensmeyer et al., 2002 [1,2]	300	pure white diatomite
D12	Elmenteita beach	1,790 ±10	1,000 ±50	(stratigraphic correlation) [2]	> 500	pure white diatomite
D13	Kariandusi mine	1,840 ±10	946 [3]	(Ar^{40}/Ar^{39}; top) Evernden & Curtis, 1965 [2]	3500	pure white diatomite
			1,050 [3]	(Ar^{40}/Ar^{39}; base) Strecker, 1991 [2]		
paleoshore lines:						
S01	Karterit	1,935 ±10	12 - 6 ±2	(stratigraphic correlation) Dühnforth et al., in prep.		
S02	Menengai	1,940 ±10	12 - 6 ±2	(stratigraphic correlation) Washbourn-Kamau, 1967		
Naivasha basin						
sediment profiles:						
--	Naivasha core	1,880 ±5	4.2 ±0.1	(C^{14}; top) Richardson and Richardson, 1972	400 [3]	diatomaceous gytia
			12.3 ±0.2	(C^{14}; base) Richardson and Richardson, 1972		
D14	Oserian Farm	1,950 ±10	12 - 6 ±2	(stratigraphic correlation) this work	70	siltic diatomite
D15	Mundui Estate	1,960 ±10	12 - 6 ±2	(stratigraphic correlation) this work	80	siltic diatomite
D16	Central Tower	1,860 ±10	81 ±4	(Ar^{40}/Ar^{39}; top) Trauth et al., 2001	60	soft diatomite
			73 ±3	(Ar^{40}/Ar^{39}; base) Trauth et al., 2001		
D17	Ol Njorowa Gorge II	1,840 ±10	108 ±7	(Ar^{40}/Ar^{39}; top) Trauth et al., 2001	120	pure white diatomite
			113 ±2	(Ar^{40}/Ar^{39}; base) Trauth et al., 2001		
D18	Malewa river	1,930 ±20	110 ±30	(stratigraphic correlation) this work	200	soft diatomite
D19	Ol Njorowa Gorge I	1,830 ±10	141 ±3	(Ar^{40}/Ar^{39}; top) Trauth et al., 2001	350	soft diatomite
			146 ±2	(Ar^{40}/Ar^{39}; base) Trauth et al., 2001		
paleoshore lines, beach gravels:						
S03	Oserian Farm	2,000 ± 20	12 - 6 ±2	(stratigraphic correlation) Washbourn-Kamau, 1975		
S04	Munyu railway	2,005 ± 10	12 - 6 ±2	(stratigraphic correlation) Washbourn-Kamau, 1975		
S05	Malewa river	1,980 ± 20	12 - 6 ±2	(stratigraphic correlation) Washbourn-Kamau, 1975		

Tab. 5.2 Catalog of investigated paleolake sediments in the Nakuru-Elmenteita and Naivasha basins and reference core logs (without ID) listing topographic elevation, age determinations, dating methods and general sediment characteristics. Notes: (1) dated by geochemical fingerprinting (A. Deino, pers. comm.); (2) references: Blisniuk, 1988; Bergner et al., in prep.; (3) published without error bars

Character of the paleolakes as inferred from diatom assemblages

Based on the radiometric age determinations, the deposition of the lake sediments occurred during three major lacustrine events: a Mid Pleistocene period around one

million years ago (Evernden and Curtis, 1965; McCall, 1967), a Late Pleistocene period between around 150 and 60 kyr BP (Trauth et al., 2001; 2003), and a Holocene period between around 12 and 4 kyr BP (Washbourn-Kamau, 1970; 1975). Only during these times, diatomites and diatomaceous deposits were formed in the *CKR*, suggesting stable lacustrine conditions with prevailing freshwater conditions over a long period of time (Harwood, 1999; Owen, 2002). Beside the so defined time slices, some less pronounced periods of higher lake-levels were inferred from fine-grained, well-sorted siltic beds, but no diatomaceous deposits accumulated during these times. The investigated diatomite profiles are therefore unique and most likely document periods of most pronounced lake levels.

Mid Pleistocene lake period (~1 million years BP)

The oldest studied lake deposits are the pure white diatomites exposed in the southeastern part of the Nakuru-Elmenteita basin (Fig. 5.2 and 5.5; Tab. 5.2). At several localities, e.g. near the shore of modern Lake Elmenteita the deposits accumulate on top of ~1.05 million-year-old trachytes erupted in this part of the basin (Blisniuk, 1988; Strecker et al., 1990). The sediments can best be studied in the diatomite mine near Kariandusi (Fig. 5.2 and 5.5). Here, the diatomite is up to 40 m thick and unconformably overlain by ~0.946 million-year-old tuffs (Evernden and Curtis, 1965). Since the volcanic unit defines the end of the paleolake highstand, the lacustrine period most likely occurred between ~1 million to ~950,000 years before present BP.

From the point of sedimentological characteristics the lake period is characterized by the purity of the diatomite and the excellent preservation of diatom frustules. Although a series of normal faults with small offsets in the order of 0.1 to 1.0 m and a number of neptunic dykes indicate some post-depositional tectonic activity, no clear evidence for distinct chemical solution of the fossil material was observed throughout the sequences (McCall et al., 1967; Blisniuk, 1988; Flower 1993; Gasse et al., 1997). Typical diatom assemblages at Kariandusi are characterized by abundant planktonic *Stephanodiscus transylvanicus*, *S. niagarae* and *Aulacoseira granulata* during the stage of highest lake level (Fig. 5.3). Littoral species are represented by abundant facultative planktonic *Fragilaria construens*, *F. brevistiata* and *F. pinnata*, whereas epiphytic genera, such as

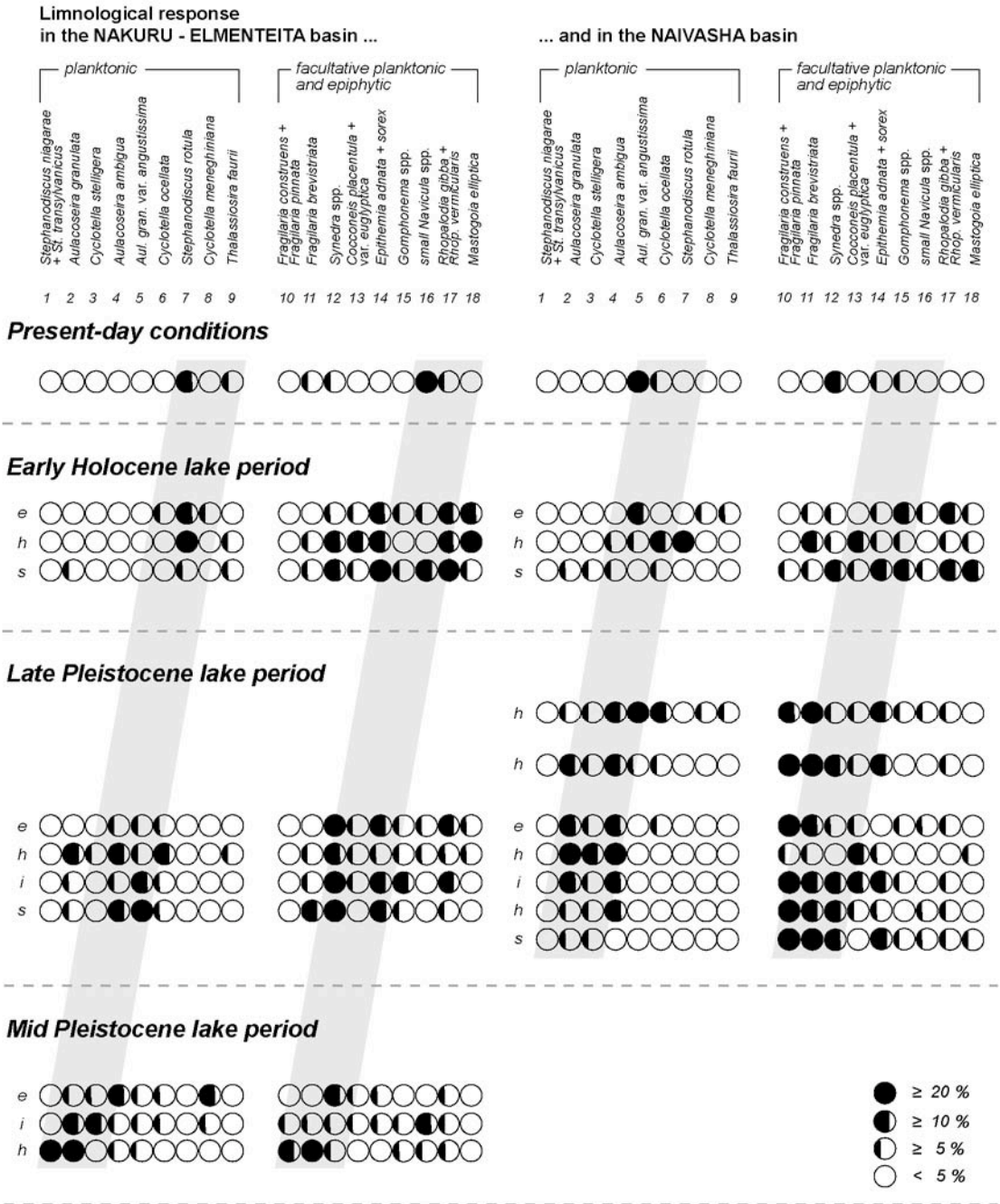

Fig. 5.3 Results of diatom investigations in the deposits of paleolakes Nakuru-Elmenteita and Naivasha showing long-term trend of increasing pH and salinitiy. Diatom taxa are sorted with respect to their habitat (deep water vs. shallow water preference and preferred conductivity values (data from Gasse, 1980; vanDam et al., 1994; Gasse et al., 1995). Relative abundance of selected diatom species correspond to averaged values from corresponding samples in selected stratigraphic levels (s: begin, i: intermediate, h: highstand, e: final stage of lake succession); circles reflect <5%, ≥5%, ≥10% and ≥20% of all identified diatom species per level.

Epithemia and *Rhopalodia* are rare. Hydrochemical optima adapted to diatom assemblages during the highstand state indicate slightly alkaline conditions with prevailing pH of ~7 to 7.5 and conductivity values well below 500 □S·cm^{-1}.

Late Pleistocene lake period (150 to 60 kyr BP)

Lake deposits at Soysambu (west of Lake Elmenteita) and three diatomite sequences in the Ol Njorowa Gorge, south of Lake Naivasha document multiple lake-level highstands in the Nakuru-Elmenteita and Naivasha basins during the Late Pleistocene (Fig. 5.2; Tab. 5.2). The oldest of these highstands is doccumented by a ~4 m thick diatomite unit in both basins, intercalated by ~140 ±5 kyr BP old tuffs and containing almost identical diatom assemblages. In the Naivasha basin, two diatomite beds, ~110, and ~80 kyr BP old, document younger highstands in the *CKR* that were not observed in the Nakuru-Elmenteita basin (Tab. 5.2). Compared to the oldest diatomite unit, these two layers contain more abundant phytoliths and clastic particles and are characterized by a reduced preservation of the diatom frustules.

The flora of the Late Pleistocene lakes is dominated by abundant facultative planktonic and epiphytic diatoms. Compared to the Mid Pleistocene lake period, the ratio between littoral vs. planktonic species is significantly higher (Fig. 5.3). In the Late Pleistocene sequences, abundant *Fragilaria* spp., *Synedra* spp., *Cocconeis placentula*, *Gomphonema* spp. and *Epithemia* spp. predominate. During the state of highest lake level, the characteristic diatom assemblage is characterized by a predominance of the planktonic genus *Cyclotella* spp., i.e., *C. ocellata, C. stelligera* and *C. meneghiniana*. In contrast to the Mid Pleistocene assemblages, the importance of *Aulacoseira ambigua* and *A. granulata* var. *angustissima* increases. Remarkably, also halophile diatoms, such as *Thallasiosira faurii* and *Mastogloia elliptica* occur at some stages of lake evolution reflecting that more saline conditions established in the lake basins compared to the Mid Pleistocene (Fig. 5.3).

Holocene lake period (12 to 4 kyr BP)

Holocene lake sediments in the Nakuru-Elmenteita and Naivasha basins exposed in the vicinity of the modern lakes are generally characterized by a relatively small thickness

(less than 80 cm). The deposits generally contain a significant amount of clastic particles, phytoliths and sponge spicules and the diatom preservation is often limited (Tab. 5.2). The compilation of paleoenvironmental data extracted from these onshore sediments and sediment-core data from Richardson and Richardson (1972) and Richardson and Dussinger (1986) suggests that the Holocene lake period was characterized by similar hydrologic conditions in both lake basins. The investigated shorelines and beach pebbles imply water depths of 180 m in the Naivasha basin and 130 m in the Nakuru-Elmenteita basin, respectively (Washbourn-Kamau, 1970, 1975; Bergner, 2000; Dühnforth, 2001; Bergner et al., in review). Reconstructions of the ancient water bodies suggest that the lakes were three- to four-times larger than today, and had 50 to 60 times greater volumes (Dühnforth et al., 2001; Bergner et al., 2003).

Compared to the diatom communities in Mid- and Late-Pleistocene sediments, the Early Holcoene flora contains more littoral diatoms, even during the highest lake levels. Numerous *Epithemia* spp., *Rhopalodia* spp., smaller *Nitzschia* spp. and *Navicula* spp. are accompanied by planktonic *Stephanodiscus rotula, Aulocoseira agassizii* and facultative planktonic *Synedra* spp. Frequent halophile *Thallasiosira faurii, Aulacoseira granulata* var. *angustissima* and *Mastogloia elliptica*, but absent *Fragilaria construens* and less abundant *Cyclotella ocellata* reflect an increasing salinity in both lake basins. The reconstructed hydrochemical parameters show a much higher variability between the initial, culminate and final stages of the lake period, respectively. Conductivity estimates obtained from the predominant diatom taxa fluctuate between 750 and 2,000 $\mu S \cdot cm^{-1}$. The estimated pH in the paleolakes was probably higher than 9.0 during most of the time, but was reduced to about 8.0 during the highstand of the lake (Fig. 5.4).

Morphologic frame of paleolake evolution

The paleohydrologic information derived from sediment characteristics and diatom assemblages suggest a rather similar hydrologic evolution in the *CKR* lake-basins during the last million years. Mid Pleistocene diatomites are only exposed in the Nakuru-Elmenteita basin, but equivalent sediments are most likely buried underneath younger volcanic rocks and pyroclastics in the Naivasha basin. The diatom flora dominated by large *Stephanodiscus* spp. and *Aulacoseira* spp. is typical for large

freshwater lakes, as they are reconstructed from lake sediments of similar age in the Kenyan and Ethiopian rifts (e.g., Gasse, 1980, 1990; Owen, 2002). Assuming the paleohydrologic similarities oft these lakes, a single several-hundred-meter-deep lake may have existed during the Mid Pleistocene in the *CKR*, too. Based on current knowledge of the geologic history of the rift valley, the paleolake expanded to the (future) Naivasha and Nakuru-Elmenteita basins, which are now separated by the Late Pleistocene Mt. Eburru volcanic complex (Baker and Wohlenberg, 1971; Baker et al., 1972; Clarke et al., 1990; Strecker et al., 1990; Strecker, 1991) (Fig. 5.5).

By ~950 kyr BP, major tectonic activity had ceased along the Kinangop Plateau, east of modern Lake Elmenteita, and massive trachytic volcanism accompanied by repeated faulting have resulted in more localized drainage basin developments in the graben region (Baker and Wohlenberg, 1971; Baker et al., 1988; Bosworth and Strecker, 1997). After the closure of the Naivasha basin by Mt. Eburru in the north (~400 kyr BP, Clarke et al., 1990) and the Olkaria Volcanic Complex in the south (~320 kyr BP, Trauth et al., 2001), and the closure of the Nakuru-Elmenteita basin by Mt. Menengai Caldera probably at around the same time, separate lakes with similar histories developed in the two basins (Trauth et al., 2001, 2003; Bergner and Trauth, in review). Although no paleo-shorelines could be identified for the time span between 150 kyr to 60 kyr BP, a stratigraphically-constrained, 3-dimensional reconstruction of the paleobathymetry indicates up to 150 m-deep lakes, which must have been approximately 3 to 4 times larger then their modern equivalents (Bergner et al., 2003). The extreme hydrologic conditions in the Late Pleistocene lake basins are reflected in massive fluvial sediments deposited in an erosional channel cutting through the Mid Pleistocene diatomites at Kariandusi (Fig. 5.5a). Reworked ~500 kyr-old handaxes contained in these deposits define a maximum age for this cut-and-fill event (Gowlet and Crompton, 1994). However, stratigraphic correlation with interfingering deposits suggests a slightly younger, but probably pre-Holocene age. The thickness of the fluvial deposits and the depth of the erosional channel suggest a significantly higher discharge of the rivers draining the escarpment into Lake Elmenteita compared to present. This hypothesis is supported by results of lake-balance modeling in the *CKR* suggesting a long-term increase in precipitation as the main cause of lake-level highstands (Bergner et al., 2003).

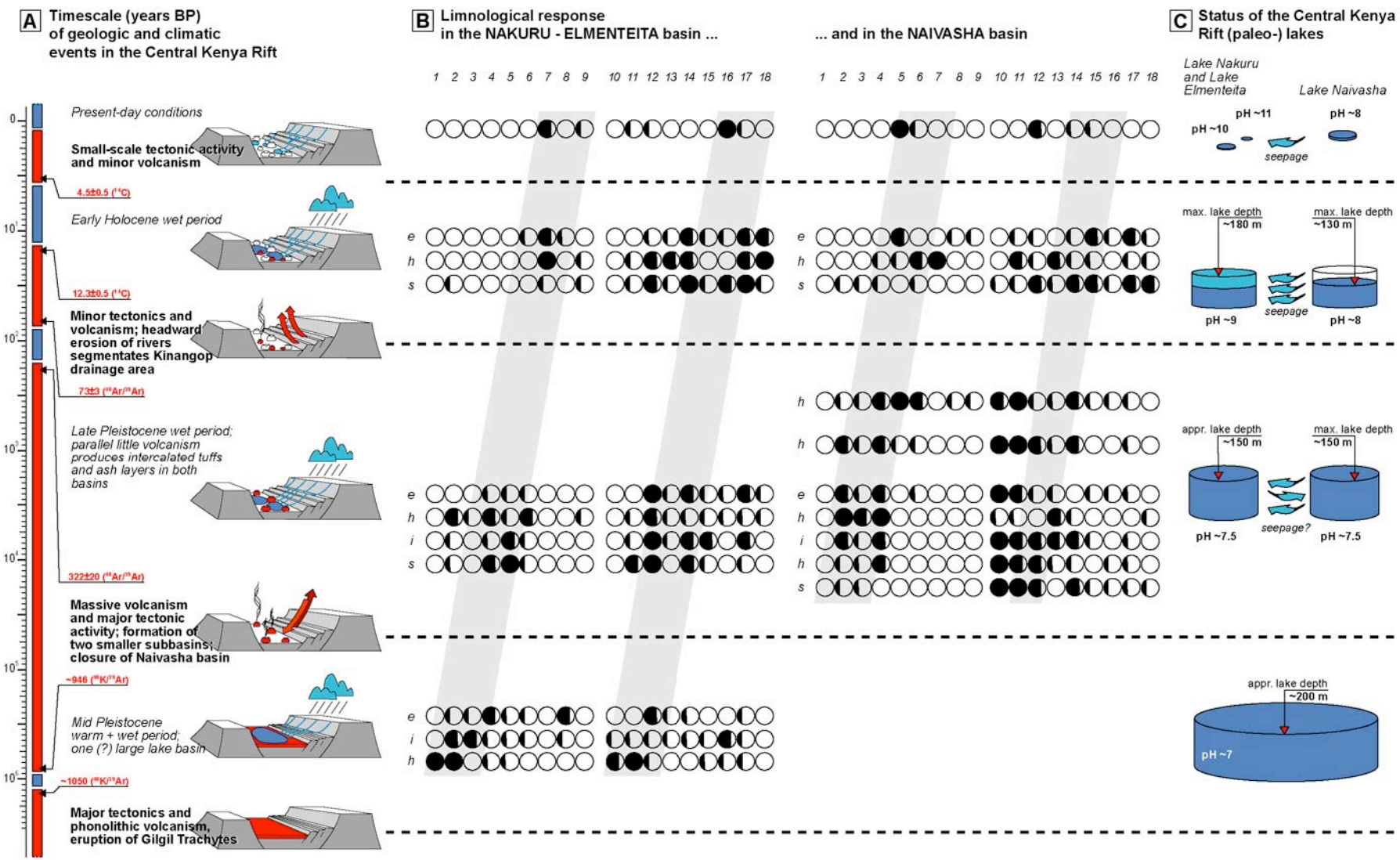

Fig. 5.4 Compilation of (A) timing of large-scale geologic and climate events influencing the lake evolution in the Central Kenya Rift; (B) results of diatom investigations in the deposits of paleolakes Nakuru-Elmenteita and Naivasha indicating the paleohydrologic response of the intra-rift lakes (cf., fig. 5.3 for corresponding diatom taxa and details); and (C) Paleolake characteristics as inferred from diatom assemblages and sediment characteristics. Estimates of paleo-hydrochemistry were derived by applying chemical optima of modern species to typical assemblages of highest lake levels; non-scaled sketches of lake size illustrate the relative change of lake dimensions.

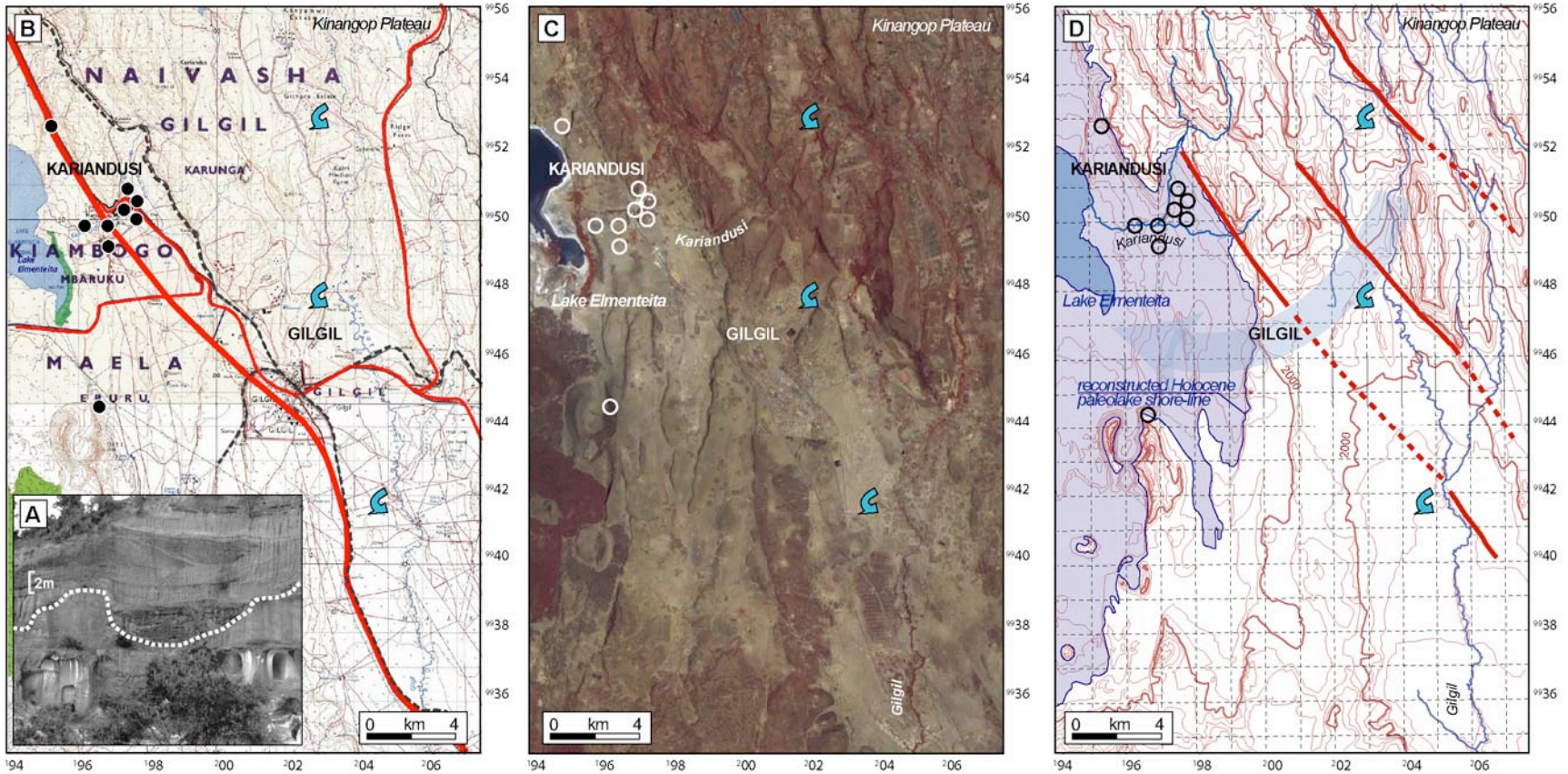

Fig. 5.5 Illustration of morphologic indicators implying tectonically-controlled changes in drainage patterns of the Central Kenya Rift basins: (A) Photograph of Late Pleistocene fluviatile sediments near Kariandusi, deposited in a fluviatile channel which has eroded into Mid Pleistocene diatomites; equivalent modern rivers miss large catchment areas and therefore would not be capable to produce comparable deposits. (B) Topographic map showing the location of important sediment outcrops studied in this project (see table for details). (C) ASTER Satellite image (NOAA) and (D) Contour map (20-m elevation contours) of the area between Gilgil and Kariandusi showing perennial river flow, regional distribution of listhric faults blocks and transfer faults as well as extension of Holocene paleo lake during max. highstand. Geologic structures in this area are believed to have affected river flow directions by continuous propagation of convergent fault systems towards each other (cf., Arrowsmith et al., 2000). Possible deflection of the Giligil river is indicated by blue arrows.

In contrast to the Mid to Late Pleistocene volcano-tectonic activities, the lake basins were not affected by significant changes in geometry during the last 60 kyr (Strecker et al., 1990). However, minor faulting may have caused continued segmentation of the high-elevated lake catchments and reorganization of river networks (cf., Baker et al., 1988; Roessner and Strecker, 1997; Arrowsmith et al., 2000). The most dramatic change during the last 60 kyr was to progressive capture of large parts of the Nakuru-Elmenteita drainage system through a combination of headward erosion and tectonic deflection of the Gilgil river (Fig. 5.5). The capture of moisture-bearing drainage areas dramatically reduced discharge to the Nakuru-Elmenteita Basin and caused a significant decline of the precipitation-evaporation (*P*-*E*) ratio. Recent hydrologic modeling comparing synchronous lake-level highstands during the Early Holocene provides some additional evidence for the hypothesis of drainage piracy (Dühnforth et al., in prep.): Whereas the sedimentary inventory document rather similar conditions of the Holocene paleo-Lakes Nakuru-Elmenteita and Naivasha, lake-balance modeling suggests a different hydrologic response if assuming the same climate change. That implies that synchronous highstands in both basins required a significant groundwater exchange between the basins (Dühnforth et al., in prep.). In contrast to the extreme paleolake conditions, water seepage and groundwater flow does not balance the differences in the hydrologic conditions of the modern lakes.

Linking hydrologic changes to climate and tectonics

The hydrologic changes in the Nakuru-Elmenteita and Naivasha basins through time suggest both climate and tectonic influences on lake history. On long-term scales, the succession of typical diatom assemblages as well as changing sediment characteristics indicates a tendency of increasing salinity (and pH) as well as shrinking water depth in both lake basins (Fig. 5.4). From the point of sediment characteristics, the absolute thickness of the diatomaceous lake-sediment sequences and the purity of the diatomites decrease continuously from Pleistocene units towards the Holocene most likely suggesting a decrease in duration and importance of the lacustrine phases. The trend towards more detritus in the youngest deposits is accompanied by the reduction in the preservation of diatom frustules. Since detrital content and diatom preservation correlate with the proximity of the sampling site to the shoreline, these observations also reflect

continuously decreasing water depths towards the modern times (cf., Hecky and Kilham, 1973; Owen, 2002).

This long-term trend towards declining water levels, decreasing lake areas and increasing alkalinity is a common feature in many East African lake basins (e.g., Hecky and Kilham, 1973; Stoffers and Hecky, 1978; Eugster and Jones, 1979; Gasse et al., 1997; Owen, 2002; Yan et al., 2002). This phenomenon is commonly explained as a consequence of decreasing subsidence rates, high sediment supply and thus the restricted accommodation space (Yuretich, 1982; Carroll and Bohacs, 1999; Tiercellin and Lezzar, 2002). In the *CKR*, the process can to be attributed to (a) relaxed basin subsidence and (b) ongoing filling of the basins with volcanic edifices since the Mid Pleistocene (Baker and Wohlenberg, 1971; Strecker et al., 1990; Bosworth and Strecker, 1997; Prodehl et al., 1997; Ebinger et al., 2000). Additionally, the tectonically controlled segmentation of upstream drainage areas has resulted into a hydrologic spreading of the former rather similar lake systems. The differences between the lake basins become more obvious during periods of drier climates, since then the *P-E* deficit of the Nakuru-Elmenteita basin cannot be balanced by sufficient water supply from the neighboring Naivasha basin.

Short-term fluctuations of the water levels, however, are most likely caused by climatic changes. The temporal coincidence of lake highstands during the Late Pleistocene and Holocene with periods of maximum equatorial insolation suggests a stronger intertropical convergence, higher precipitation and hence an increase in the *P-E* ratio in the rift basins (Trauth et al., 2001, 2003; Bergner et al., 2003). Higher Indian Ocean sea-surface temperatures may have an additional influence on lake highstands in the *CKR* (Bergner and Trauth, in review). But since no one-to-one correlation between the individual parameters could be established, their singular importance can only be speculated. As shown by this study, both tectonic and climate influences control the hydrologic evolution in the *CKR*. Rift-relative processes mainly act on longer timescales, whereas climate changes cause short-term fluctuations of lake levels. However, tectonically-controlled changes in the catchments and drainage networks change thresholds and alter the hydrologic conditions in a relatively short period of time. Lakes sediments in the Central Kenya Rift certainly represent excellent natural

archives of climate change. However, the interpretation of paleolimnologic proxies in similar environments requires a careful assessment of tectonic influences on lake history even on timescales of 10^3 to 10^4 years.

SUMMARY

Fig. 6.1 Romantic view of Cresent Island Crater in Lake Naivasha taken in year 2003 from the terrace of the Lake Naivasha Yacht Club. Only 5,000 years, this area was flooded by a more than 100 m-deep lake expanding during a periods of pronounced wetter climates.

The study of diatomaceous lake sediments in the Central Kenya Rift (*CKR*) reveals that the intra-rift lakes Naivasha, Elmenteita and Nakuru have been subjected to significant hydrologic fluctuations during the Late Quaternary. The variations are expressed as changes of water depth and lake area, hydrochemistry and ecology. As indicated by fossil diatom assemblages, the amplitude of these fluctuations decreased in the *CKR* during the last million years. At about one million years ago, large freshwater lakes, several hundred meters deep, covered most of the inner graben. In the Late Pleistocene and Early Holocene, diatom assemblages and paleo-shorelines indicate up to 150 m deep lakes in the same area. Today, only small alkaline lakes, a few meters deep, and the shallow freshwater Lake Naivasha exist in the *CKR*. This long-term trend towards shallow alkaline lakes also exists for other lake basins in the Ethiopian and Kenyan Rifts (Taieb et al., 1987; Street-Perrott and Perrott, 1993; leTurdu et al., 1999; Gasse, 2000; Behrensmeyer et al., 2002). Since the phenomenon develops at timescales of about 10^5 to 10^6 years, it is usually attributed to the tectonically and volcanically affected availability of accommodation space in the lake basin (Yuretich, 1982;

Behrensmeyer et al., 2002). However, the observation that tectonic activity also caused a rearrangement of drainage systems in parts of the *CKR* reflects that ongoing tectonics may significantly influence the character of rift lakes even on relatively short time scales.

Diatom assemblages in the Late Pleistocene and Holocene lake sediments of the Naivasha and Nakuru-Elmenteita basins show that the general geologically-controlled trend in lake evolution is overlain by pronounced short-term fluctuations on timescales of thousands of years. In the *CKR*, several lake-level highstands, which occurred at time intervals of 10-11 kyr, were interrupted by lake lowstands (Trauth et al., 2001, 2003; Bergner and Trauth, in review). Applying transfer functions to the diatom assemblages of the most prominent highstands, we found that relatively stable freshwater conditions with a low pH and reduced conductivity characterizes these periods. The synchronous evolution of similar hydrologic conditions in the Naivasha and in the Nakuru-Elmenteita basin suggests that regional climate changes are the most plausible cause for the short-term environmental fluctuations. Furthermore, the timing of the highstand periods during global interglacial stages and the periodicity of the transgression-regression cycles at 10-11 kyr intervals imply that orbitally induced changes in solar radiation triggered climate and hydrologic fluctuations in the *CKR*. The results of lake-balance modeling emphasize that already small changes in the moisture balance of the lake catchments may have caused the observed hydrologic fluctuations. Our best estimate for a basin-averaged precipitation increase of about 30±10% is in a good agreement with similar investigations hypothesizing moisture changes as an important factor influencing the hydrology of East African rift lakes (e.g., Butzer et al., 1972; Gasse, 1977; Bonnefille, 1983; Gasse et al., 1989; Damnati and Taieb, 1995; Bergonzini et al., 1997; Barker et al., 2001; Behrensmeyer et al., 2002; Chalié and Gasse, 2002).

After having assessed the relative importance of rift-related and climate processes as main factors controlling the hydrology, we conclude that the lake sediments of the *CKR* are valuable archives of environmental change. As shown by our results, the intra-rift lakes of the *CKR* respond to the interior tectonic activity as well as to large-scale climate fluctuations. It reveals that hydrologic alterations are not the sole consequence of climate change but also reflects changes in basin geometry, size of the catchment and

river network. The sedimentary records from the *CKR* are therefore difficult to read but provide valuable insights into the complex hydrologic processes in a tectonically active region. The postulated mechanisms relating limnological to environmental changes can help to explain the modern hydrologic dependency of the intra-rift lakes. Furthermore, they provide useful tools to assess the amplitude of natural climate variability in East Africa. Taking into account the large need of long-term climate archives, similar *CKR*-deposits of even higher temporal resolution, such as sediment cores from volcanic crater lakes, provide excellent prospects for further paleoclimate investigations. Since East African population strongly depends on changes in water and food supply, more research should be done on the understanding of environmental and future climate change.

REFERENCES

Alverson, K.D., Bradley, R.S., Pedersen, T.F., 2001. PAGES - Hydrologic variability. IGBP Science Series, 3, 20-21.

Alverson, K.D., Bradley, R.S., Pedersen, T.F. (Eds.), 2003. Paleoclimate, Global change and the future. Springer.

Arrowsmith, J.R., Hilley, G.E., Strecker, M.R., 2000. Mechanisms for the association of large drainage basins with structural steps in compressional and extensional tectonic settings. Eos Trans. AGU Fall Meeting, 81 (48), Abstract T71E-02.

Åse, L.-E., 1987. A note on the water budget of Lake Naivasha. Geographiska Annaler, 69A, 415-429.

Baker, B.H., Mitchell, J.G., Williams, A.J., 1988. Stratigraphy, geochronology and volcano-tectonic evolution of the Kedong-Naivasha-Kinangop region, Gregory Rift Valley, Kenya. Journal of the Geological Society, London, 145, 107-116.

Baker, B.H., Mohr, P.A., Williams, L.A.J., 1972. Geology of the eastern rift system of Africa, Geol. Soc. Am. Spec. Pap., 136.

Baker, B.H., Wohlenberg, J., 1971. Structure and evolution of the Kenya Rift Valley. Nature, 229, 538-542.

Bard, E., Rostek, F., Sonzogni, C., 1997. Interhemispheric synchrony of the last deglaciation inferred from alkenone paleothermometry. Nature 385, 707-710.

Barker, P.F., Gasse, F., Roberts, N., Taieb, M., 1990. Taphonomy and diagenesis in diatom assemblages; a Late Pleistocene palaeoecological study from Lake Magadi, Kenya. Hydrobiologia, 214, 267-272.

Barker, P.A., Street-Perrott, F.A., Leng, M.J., Greenwood, P.B., Swain, D.L., Perrott, R.A., Telford, R.J., Ficken, K.J., 2001. A 14,000-Year Oxigen Isotope Record from Diatom Silica in Two Alpine Lakes on Mt. Kenya. Science, 292, 2307-2310.

Barker, P., Telford, R., Gasse, F., Thevenon, F., 2002. Late Pleistocene and Holocene paleohydrology of Lake Rukwa, Tanzania, inferred from diatom analysis. Palaeogeography, Palaeoclimatology, Palaeoecology, 187, 295-305.

Barron, E.J., Moore, G.T., 1994. Climate Modell Applications in Paleoenvironmental Analysis. Society for Sedimentary Geology, Tulsa, USA.

Battarbee, R.W., 2000. Paleolimnological approaches to climate change, with special regard to the biological record. Quaternary Science Reviews, 19, 107-124.

Beadle, L.C., 1974. The inland waters of East Africa. Longman, London.

Becht, R., Harper, D., 2002. Towards an understanding of human impact upon the hydrology of Lake Naivasha. Hydrobiologia, 488, 1-11.

Behrensmeyer, A.K., Potss, R., Deino, A., Ditchfield, P., 2002. Olorgesaille, Kenya: A million years in the life of a rift basin. In: Renaut, R.W., Ashley, G.M., (Eds.), 2002. Sedimentation in continental rifts. SEPM Special Publications, 73, 97-106.

Berger, A., 1992. Astronomical theory of paleoclimates and the last glacial-interglacial cycle. Quaternary Science Reviews, 11, 571-582.

Berger, A., Loutre, M.F., 1991. Insolation values for the climate of the last 10 million years. Quaternary Science Reviews, 10 (04), 297-317.

Bergner, A.G.N., 2000. Rekonstruktion und Modellierung Pleistozäner Seespiegelschwankungen des Lake Naivasha, Kenia, im Rahmen von insolationsgesteuerten Klimaveränderungen. Unpublished diploma thesis, University of Potsdam.

Bergner, A.G.N., Deino, A., Trauth, M.H., in prep. Evidence for synchronous high lake-levels in the Central Kenya Rift at Termination II, 135 kyr BP.

Bergner, A.G.N., Trauth, M., Bookhagen, B., 2003. Paleoprecipitation estimates for the Lake Naivasha basin (Kenya) during the last 175 k.y. using a lake-balance model. Global and Planetary Change, 36, 117-136.

Bergonzini, L., Chalié, F., Gasse, F., 1997. Paleoevaporation and paleoprecipitation in the Tanganyika basin at 18,000 years B.P. inferred from hydrologic and vegetation proxies. Quaternary Research, 47, 295-305.

Birkett, C., Murtugudde, R., Allan, T., 1999. Indian ocean climate event brings floods to East Africa's lakes and the Sudd Marsh. Geophysical Research Letters, 26 (8), 1031-1034.

Blisniuk, P.M., 1988, Geologie des Lake Elmenteita Gebiets, zentrales Kenya Rift. Unpublished diploma thesis, University of Karlsruhe.

Blodgett, T.A., Lenters, J.D., Isacks, B.L., 1997. Constraints on the origin of paleolake expansions in the central Andes. [available online at http://www.earthinteractions.org].

Bookhagen, B., Haselton, K., Trauth, M.H., 2001. Hydrological modeling of a landslide-dammed lake in the Santa Maria basin, NW Argentina. Palaeogeography, Palaeoclimatology, Palaeoecology, 169 (1-2), 113-127.

Bone, B.D., 1985. The geological evolution of the S.W. Naivasha volcanic complex, Kenya. Ph.D. Thesis, University of Lancaster, UK.

Bonnefille, R., 1983. Evidence for a cooler and drier climate in the Ethiopian uplands towards 2.5 Myr ago. Nature, 303, 487-492.

Bosworth, W., Strecker, M., 1997. Stress field changes in the Afro-Arabian rift system during the Miocene to recent period. Tectonophysics, 278, 47- 62.

Bradley, R.S., 1999. Paleoclimatology - reconstructing climates of the Quaternary. Academic Press.

Brutsaert, W., 1982. Evaporation into the Atmosphere. D. Reichel Publishing Company, Dortrecht.

Butzer, K.W., Isaac, G.L., Richardson, J.L. & Washbourn-Kamau, C., 1972. Radiocarbon Dating of East African Lake Levels. Science, 175, 1069-1076.

Camberlin, P., 1995. June-September rainfall in North-Eastern Africa and Atmospheric signals over the tropics: a zonal perspective. International Journal of Climatology, 15, 773-783.

Cane, M.A., Molnar, P., 2001. Closing of the Indonesian seaway as a precursor to East African aridification around 3-4 million years ago, Nature, 411, 157-162.

Carrington, D.P., Gallimore, R.G., Kutzbach, J.E., 2001. Climate sensitivity to wetlands and wetland vegetation in mid-Holocene North Africa. Climate Dynamics, 17, 151-157.

Carroll, A.R., Bohacs, K.M., 1999. Stratigraphic classification of ancient lakes: Balancing tectonic and climatic controls. Geology, 27 (2), 99-102.

Chalié, F., Gasse, F., 2002. Late Glacial-Holocene diatom record of water chemistry and lake level change from the tropical East African Rift Lake Abiyata (Ethiopia). Palaeogeography, Palaeoclimatology, Palaeoecology, 187, 259-283.

Clarke, M.C.G., Woodhall, D.G., Allen, D., Darling, G., 1990. Geological, volcanological and hydrogeological controls on the occurrence of geothermal activity in the area surrounding Lake Naivasha, Kenya. British Geological Survey Report and Govt. of Kenya - Ministry of Energy, Nairobi, Kenya.

Clemens, S., Prell, W., Murray, D., Shimmield, G., Weedon, G., 1991. Forcing mechanisms of the Indian Ocean Monsoon. Nature, 353, 720-725.

Clement, A.C., Seager, R., Cane, M.A., 1999. Orbital controls on the El Niño/Southern Oscillation and the tropical climate. Paleoceanography, 14, 441-456.

Cohen, A.S., 2003. Paleolimnology – the history and evolution of lake systems. Oxford University Press.

Damnati, B., Taieb, M., 1995. Solar and ENSO signatures in laminated deposits from Lake Magadi (Kenya) during the Pleistocene/ Holocene transition. Journal of African Earth Sciences, 21, 373-382.

Darling, W.G., Allen, D.J., Armannsson, H., 1990. Indirect detection of subsurface outflow from a Rift valley lake. Journal of Hydrology, 113, 297-305.

deMenocal, P.B., 1995. Plio-Pleistocene African climate. Science, 270, 53-59.

deMenocal, P.B., Rind, D., 1993. Sensitivity of Asian and African climate to variations in seasonal insolation, glacial ice cover, sea surface temperature and Asian orography. Journal of Geophysical Research, 98, 7265-7287.

deNoblet, N., Braconnot, P., Joussaume, S., Masson, V., 1996. Sensitivity of simulated Asian and African monsoons to induced variations in insolation 126, 115 and 6 kBP. Climate Dynamics, 12, 589-603.

Doherty, R., Kutzbach, J., Foley, J., Pollard, D., 2000. Fully coupled climate/dynamical vegetation model simulations over Northern Africa during the mid-Holocene. Climate Dynamics, 16 (8), 561-573.

Dong, B., Valdes, P.J., Hall, N.M.J., 1996. The changes of monsoonal climates due to earth's orbital perturbations and ice age boundary conditions. Paleoclimates, 1, 203-240.

Dühnforth, M., 2001. Rekonstruktion, Modellierung und Charakterisierung eines früh-holozänen Seespiegelhochstandes im Nakuru-Elmenteita-Becken, Kenia. Unpublished diploma thesis, Humboldt-Universität Berlin.

Dühnforth, M., Bergner, A.G.N., Trauth, M.H., 2001. Hydrological modeling of the 10 kyr BP paleo-lake in the Nakuru-Elmenteita basin, Central Kenya Rift. Conference contribution to PAGES-PEP III meeting, August 27-31, Aix-en-Provence, p. 76.

Dühnfort, M., Bergner, A.G.N., Strecker, M.R., Trauth, M.H., in prep. The influence of the Early Holocene wet period on the hydrological budget of the Nakuru-Elmenteita basin, Central Kenya Rift.

Ebinger, C.J., Yemane, T., Harding, D.J., Tesfaye, S., Kelley, S., Rex, D.C., 2000. Rift deflection, migration, and propagation: linkage of the Ethiopian and Easter rift, Africa. GSA Bulletin, 112 (2), 163-176.

Eugster, H.P., Jones, B.F., 1979. Behavior of major solutes during closed-basin brine evolution. American Journal of Science, 279, 609-631.

Evernden, J.G., Curtis, G.H., 1965. The potassium-argon dating of late Cenozoic rocks in East Africa and Italy, Current Anthropology, 6, 177-189.

Flower, R.J., 1993. Diatom preservation: experiments and observations on dissolution and breakage in modern and fossil material. Hydrobiologia, 269/270, 473-484.

Fritz, S.C., Juggins, S., Battarbee, R.W., Engstrom, D.R., 1991. Reconstruction of past changes in salinity and climate using a diatom-based transfer function. Nature, 352, 706-708.

Galvin, K.A., Boone, R.B., Smith, N.M., Lynn, S.J., 2001. Impacts of climate variability on East African pastoralists: linking social science and remote sensing. Climate Research, 19, 161-172.

Gasse, F., 1977. Evolution of Lake Abhé (Ethiopia and TFAI), from 70,000 b.p. Nature, 265, 47-45.

Gasse, F., 1980. Les diatomées lacustres Plio-Pléistocenes du Gadeb (Éthiopie). Revue Algologique, mémoire hors-série 3, Paris.

Gasse, F., 1986. East African diatoms - Taxonomy, ecological distribution. Bibliotheca diatomologica 11. Cramer, Stuttgart.

Gasse, F., 1990. Tectonic and climatic controls on lake distribution and environments in Afar from Miocene to present. In: Katz, B.J. (Ed.), Lacustrine Basin Exploration, Case Studies, and Modern Analogs. AAPG Memoir, 50.

Gasse, F., 2000. Hydrological changes in the African tropics since the Last Glacial Maximum. Quaternary Science Reviews, 19, 189-211.

Gasse, F., 2001. Hydrological changes in Africa. Science, 292, 2259-2260.

Gasse, F., Barker, P., Gell, P.A., Fritz, S.C., Chalié, F., 1997. Diatom-inferred salinity in paleolakes: an indirect tracer of climate change. Quaternary Science Reviews, 16, 547-563.

Gasse, F., Juggins, S., Ben Khelifa, L., 1995. Diatom-based transfer functions for inferring past hydrochemical characteristics of African lakes. Palaeogeography, Palaeoclimatology, Palaeoecology, 117, 31-54.

Gasse, F., Lédée, V., Massault, M., Fontes, J.C., 1989. Water-level fluctuations of Lake Tanganyika in phase with oceanic changes during the last glaciation and deglaciation. Nature, 342, 57-59.

Gatebe, C.K., Tyson, P.D., Annegarn, H., Piketh, S., Helas, G., 1999. A seasonal air transport climatology for Kenya. Journal of Geophysical Research, 104 (D12), 14,237-14,244.

Gaudet, J.J., Melack, J.M., 1981. Major ion chemistry in a tropical lake basin. Freshwater Biology, 11, 309-333.

George, R.M.M., Rogers, N.W., Kelley, S., 1998. Earliest magmatism in Ethiopia: evidence for two mantle plumes in one flood basalt province, Geology, 26, 923-926.

Gierlowski-Kordesch, E.H., Buchheim, H.P., 2003. Lake basins as archives of continental tectonics and paleoclimate: introduction. Journal of Paleolimnology, 30, 113-114.

Global Daily Summary (GDS) - Temperature and Precipitation, CD-Rom Vers. 1.0, 1994. Federal Climate Complex Asheville, National Oceanic and Atmospheric Administration, Department of Commerce, Washington, USA.

Gowlett, J.A.J., Crompton, R.H., 1994. Kariandusi: Acheulean morphology and the question of allometry. The African Archaeological Review, 12, 3-42.

Griffiths, J.F., 1972. Climates of Africa. World Survey of Climatology, 10, Elsevier, Amsterdam.

Haigh, J.D., 1994. The role of stratospheric ozone in modulating the solar radiative forcing of climate. Nature, 370, 544-546.

Harjes, H.-P., Walter, R. (Eds.), 1999. Die Erde im Visier. Springer.

Harper, D.M., Mavuti, K.M., Muchiri, S.M., 1990. Ecology and management of lake Naivasha, Kenya, in relation to climate change, alien specie's introductions, and agricultural development. Environmental Conservation, 17 (4), 328-336.

Hartmann, D.L., 1994. Global Physical Climatology. Academic Press, San Diego, USA.

Harwood, D.M., 1999. Diatomite. In: Stoermer, E.F., Smol, J.P. (Eds.), The diatoms. University Press, Cambridge, 436-443.

Hastenrath, S., 1985. Climate and Circulation of the tropics. D. Reidel, Dortrecht.

Hastenrath, S., Lamb, P.J., 1977. Climate atlas of the tropical Atlantic and Eastern Pacific Ocean. Madison, Wisconsin.

Hastenrath, S., Kutzbach, J.E., 1983. Paleoclimatic Estimates from Water and Energy Budgets of East African Lakes. Quaternary Research, 19, 141-153.

Hastenrath, S., Rosen, A., 1983. Patterns of Indian monsoon rainfall anomalies. Tellus, 35A, 324-331.

Haug, G.H., Günther, D., Peterson, L.C., Sigman, D.M., Hughen, K.A., Aeschlimann, B., 2003. Climate and the collapse of Maya civilization. Science, 299, 1731-1735.

Haug, G.H., Tiedemann, R., 1998. Effect of the formation of the Isthmus of Panama on Atlantic Ocean thermohaline circulation. Nature, 393, 673-676.

Hecky, R.E., Kilham, P., 1973. Diatoms in alkaline, saline lakes: Ecology and geochemical implications. Limnology and Oceanography, 18 (1), 53-71.

Hoelzmann, P., Keding, B., Berke, H., Kröpelin, S., Kruse, H.-J., 2001. Environmental change and archaeology: lake evolution and human occupation in the Eastern Sahara during the Holocene. Palaeogeography, Palaeoclimatology, Palaeoecology, 169, 193-217.

Hustedt, F., 1949. Süßwasserdiatomeen aus dem Albert-Nationalpark in Belgisch Kongo. In: Damas, H. (Ed.), Exploration du Parc National Albert (1935-1936). Hayez, Bruxelles.

Imbrie, J., Imbrie, K.P., 1979. Ice ages - solving the mystery. Harvard University Press.

Indeje, M., Semazzi, F.H.M., Ogallo, L.J., 2000. ENSO signals in East African rainfall seasons. International Journal of Climatology, 20, 19-46.

International Station Meteorological Climate Summary (ISMCS), CD-Rom Vers. 3.0, 1995. Federal Climate Complex Asheville, National Oceanic and Atmospheric Administration, Department of Commerce, Washington, USA.

Jätzold, R., 1981. Klimageographie - Ostafrika, Kenya, Uganda, Tanzania) 2°N – 2°S, 32°-38°E. In: Freitag, U. (Ed.), Afrika-Kartenwerk, Serie E, Beiheft zu Blatt 5. Bornträger, Berlin.

Johnson, T.C., Kelts, K., Odada, E., 2000. The Holocene history of Lake Victoria. Ambio 29 (1), 2-11.

Johnson, T.C., Odada, E. (Eds.), 1996. The Limnology, Climatology and Paleoclimatology of the East African Lakes, The International Decade for the East African Lakes (IDEAL).

Jolly, D., Harrison, S.P., Damnati, B., Bonnefille, R., 1998. Simulated climate and biomes of Africa during the Late Quaternary: Comparison with pollen and lake status data. Quaternary Science Reviews, 17, 629-657.

Kenya Meteorological Department, 2000. Unpublished synoptic and rain station data. Ministry of Information, Transport and Communications, Nairobi, Kenya.

Krammer, K., Lange-Bertalot, H., 1991a. Bacillariophyceae - 3. Teil: Centrales, Fragilariaceae, Eunotiaceae. In: Ettl, H., Gerloff, J., Heynig, H., Mollenhauer, D. (Eds.), Süßwasserflora von Mitteleuropa, 2/3. Gustav Fischer, Stuttgart.

Krammer, K., Lange-Bertalot, H., 1991b. Bacillariophyceae - 4. Teil: Achnanthaceae, Kritische Ergänzungen zu Navicula (Lineolatae) und Gomphonema, Gesamtliteraturverzeichnis Teil 1-4. In: Ettl, H., Gerloff, J., Heynig, H., Mollenhauer, D. (Eds.), Süßwasserflora von Mitteleuropa, 2/4. Gustav Fischer, Stuttgart.
Krammer, K., Lange-Bertalot, H., 1997a. Bacillariophyceae - 1. Teil: Naviculaceae. In: Ettl, H., Gerloff, J., Heynig, H., Mollenhauer, D. (Eds.), Süßwasserflora von Mitteleuropa, 2/1. Gustav Fischer, Stuttgart.

Krammer, K., Lange-Bertalot, H., 1997b. Bacillariophyceae - 2. Teil: Bacillariaceae, Epithemiaceae, Surirellaceae. In: Ettl, H., Gerloff, J., Heynig, H., Mollenhauer, D. (Eds.), Süßwasserflora von Mitteleuropa, 2/2. Gustav Fischer, Stuttgart.

KRISP Working Party, 1991. Large scale variations in lithospheric structure along and across the Kenya Rift. Nature, 354, 223.

Kubatzki, C., Montoya, M., Rahmstorf, S., Ganopolski, A., Claussen, M., 2000. Comparison of the last interglacial climate simulated by a coupled global model of intermediate complexity and an AOGCM. Climate Dynamics, 16, 799-814.

Kutzbach, J., Bonan, G., Foley, J., Harrison, S.P., 1996. Vegetation and soil feedbacks on the response of the African monsoon to orbital forcing in the early to middle Holocene. Nature 384, 623-626.

Kutzbach, J.E., Webb III, 1993. Conceptual Basis for understanding Late-Quaternary Climates. In: Wright jr., H.E. (Ed.), Global climates since the Last Glacial Maximum. University of Minnesota Press, Minnesota, 5-11.

Lampert, W., Sommer, U., 1993. Limnoökologie. Georg Thieme, Stuttgart.

Last, W.M., Smol, J.P., Birks, H.J.B. (Eds.), 2002. Tracking environmental change using lake sediments, vol. 01. Kluwer Academic Publishers.

Le Turdu, C., Tiercelin, J.-J., Gibert, E., Travi, Y., Lezzar, K.-E., Richert, J.-P., Massault, M., Gasse, F., Bonnefille, R., Decobert, M., Gensous, B., Jeudy, V., Tamrat, E., Mohammed, M.U., Martens, K., Atnafu, B., Chernet, T., Williamson, D., Taieb, M., 1999. The Ziway-Shala lake basin system, Main Ethiopian Rift: Influence of volcanism, tectonics, and climatic forcing on basin formation and sedimentation. Palaeogeography, Palaeoclimatology, Palaeoecology, 150, 135-177.

Leakey, L.S.B., 1931. East African Lakes. Geographical Journal, 497-514.

Leroux, M., 2001. The meteorology and climate of Tropical Africa. Springer Praxis Publishing.

Macdonald, R., Rogers, N.W., Fitton, J.G., Black, S., Smith, M., 2001. Plume-Lithosphere interaction in the generation of the basalts of the Kenya Rift, East Africa. Journal of Petrology, 42(5), 877-900.

Maitima, J.M., 1991. Vegetation response to climatic change in Central Rift Valley, Kenya. Quaternary Research, 35, 234-245.

McCall, G.J.H., Baker, B.H., Walsh, J., 1967. Late Tertiary and Quaternary sediments of the Kenya Rift Valley. In: Bishop, W.W., Clark, J.D. (Eds.), Background to evolution in Africa, University of Chicago Press, 191-220.

McGregor, G.R., Nieuwolt, S., 1998. Tropical Climatology. John Willey & Sons, Chichester.

Milankowitch, M., 1941. Canon der Erdbestrahlung und seine Anwendung auf das Eiszeitenproblem. Royal Serbian Academy Special Publications, 132, Section of Mathematical and Natural Sciences, 33.

Milbrink, G., 1977. On the limnology of two alkaline lakes (Nakuru and Naivasha) in the East Rift Valley System in Kenya. Int. Revue ges. Hydrobiology, 62 (1), 1-17.

Morley, C.K., 1994. Interaction of deep and shallow processes in the evolution of the Kenya rift, Tectonophysics, 236, 81-91.

Müller, O., 1903-1910. Berichte über die botanischen Ergebnisse der Nyassa-See und Kinga-Gebirgs-Expedition der Herman- und Elise- geb. Heckmann-Wentzel-Stiftung. VV. Bacillariaceen aus dem Nyassalande und einigen benachbarten Gebieten. In: Engler, A. (ed.): Beiträge zur Flora von Afrika - XXVI. Engler's Botanisches Jahrbuch für Pflanzengesellschaften und Pflanzengeographie.

Nicholson, S.E., 1996. A review of climate dynamics and climate variability in Eastern Africa. In: Johnson, T.C., Odada, E. (Eds.), The Limnology, Climatology and Paleoclimatology of the East African Lakes, The International Decade for the East African Lakes (IDEAL). Gordon and Breach Publishers, 25-56.

Nicholson, S.E., 2000. The nature of rainfall variability over Africa on time scales of decades to millenia. Global and Planetary Change, 26, 137-158.

Nicholson, S.E., Yin, X., 2001. Rainfall conditions in equatorial East Africa during the Nineteenth century as inferred from the record of Lake Victoria. Climatic Change, 48, 387-398.

Nieuwolt, S., 1986. Agricultural droughts in the tropics. Theoretical Applications of Climatology, 37, 29-38.

Nieuwolt, S., 1989. Estimating the agricultural risks of tropical rainfall. Agric. For. Met., 45, 251-263.

Nilsson, E., 1931. Quaternary glaciations and pluvial lakes in British East Africa. Geographiska Annaler, 13, 249-349.

Ojany, F.F., Ogendo, R.B., 1988. A study in physical and human geography. Longman Kenya, Nairobi.

Ojiambo-Bwire, S., Lyons, W.B., 1996. Residence of major ions in Lake Naivasha and their relationship to lake hydrology. In: Johnson, T.C., Odada, E. (Eds.), The limnology, climatology and paleoclimatology of the Eastern African lakes. Gordon and Breach Publishers, Amsterdam, 267-278.

Oldfield, F., Alverson, K., 2002. The societal relevance of paleoenvironmental research. In: Alverson, K.D., Bradley, R.S., Pedersen, T.F. (Eds.), Paleoclimate, Global change and the future. Springer, 1-11.

Onacha, S.A., 2000. Use of electrical resistivity methods to evaluate the hydrogeology of the Lake Naivasha Basin. In: Ogola, J.S., Behr, H.-J. (Eds.), Saline-alkaline lakes in Eastern and Southern Africa, workshop proceedings. University of Nairobi.

Owen, R.B., 2002. Sedimentological characteristics and origins of diatomaceous deposits in the East African Rift System. SEPM Special Publication, 73, 233-246.

Petit, J.R., Jouzel, J., Raynaud, D., Brkov, N.I., Barnola, J.-M., Basile, I., Bender, M., Chappellaz, J., Davis, M., Delaygue, G., Delmotte, M., Kotlyakov, V.M., Legrand, M., Lipenkov, V.Y., Lorius, C., Pépin, L., Ritz, C., Saltzmann, E., Stievenard, M., 1999. Climate and atmospheric history of the past 420,000 years from the Vostok ice core, Antarctica. Nature, 399, 429-436.

Phillips, J., McIntyre, B., 2000. ENSO and interannual rainfall variability in Uganda: implications for agricultural management. International Journal of Climatology, 20, 171-182.

Prell, W.L., Kutzbach, J.E., 1987. Monsoon variability over the past 150,000 years. Journal for Geophysical Research, 92 (D7), 8411-8425.

Prell, W.L., Kutzbach, J.E., 1992. Sensitivity of the Indian monsoon to forcing parameters and implications for its evolution. Nature, 360, 647-652.

Prodehl, C., Ritter, J.R.R., Mechie, J., Keller, G.R., Khan, M.A., Jacob, B., Fuchs, K., Nyambok, I.O., Obel, J.D., Riaroh, D., 1997. The KRISP 94 lithospheric investigation of southern Kenya - the experiments and their main results. Tectonophysics, 278, 121-147.

Renaut, R.W., Ashley, G.M. (Eds.), 2002. Sedimentation in continental rifts. SEPM Special Publications, 73.

Renssen, H., Lautenschlager, M., 2000. The effect of vegetation in a climate model simulation on the Younger Dryas. Global and Planetary Change, 26, 423-443.

Richardson, J.L., Dussinger, R.A., 1986. Paleolimnology of mid-elevation lakes in the Kenya Rift Valley. Hydrobiologia, 143, 167-174.

Richardson, J.L., Richardson, A.E., 1972. History of an African Rift Lake and its climate implications. Ecological Monographs, 42, 499-534.

Roberts, N., 1990. Ups and downs of African lakes. Nature, 346, 107.

Roberts, N., 1998. The Holocene. Blackwell Publishers, Oxford.

Rodhe, H., Virji, H., 1976. Trends and Periodicities in East African Rainfall Data. Monthly Weather Review, 104, 307-315.

Roessner, S., Strecker, M., 1997. Late Cenozoic tectonics and denudation in the Central Kenya Rift: quantification of longterm denudation rates. Tectonophysics, 278, 83-94.

Saltzmann, B., 2002. Dynamical Paleoclimatology. Academic Press.

Sandwell, D.T., 1987. Biharmonic spline interpolation of Geos-3 and Seasat altimeter data. Geophysical Research Letters, 14(2), 139-142.

Schmugge, T.J., André, J.C., ed., 1991. Land Surface Evaporation – Measurement and Parameterisation. Springer, New York.

Seidov, D., Haupt, B.J., Maslin, M.A. (Eds.) 2001. The oceans and rapid climate change: past, present and future. AGU Geophysical Monograph Series, 126.

Schlüter, T., 1993. Comparison of the mineral composition of the lakes of the East African Rift System (Western Rift and Gregory Rift). In: Thorweihe, U., Schandelmeier, H. (Eds.), Geoscientific Reseach in Northeast Africa. Balkema, Rotterdam, 657-662.

Schlüter, T., 1997. Geology of East Africa. Bornträger.

Shackleton, N.J., Sanchez-Goñi, M.F., Pailler, D., Lancelot, Y., 2003. Marine Isotope Substage 5e and the Eemian Interglacial, Global and Planetary Change, 36, 151-155.

Shuttleworth, W.J., 1988. Parameterization schemes of land-surface processes for mesoscale atmospheric models. In: Schmugge, T.J., André, J.C. (Eds.), Land Surface Evaporation – Measurement and Parameterisation. Springer, New York.

Stager, J.C., Johnson, T.C., 2000. A 12,400 ^{14}C yr offshore diatom record from east central Lake Victoria, East Africa. Journal of Paleolimnology, 23, 373-383.

Stager, J.C., Mayewski, P.A., 1997. Abrupt Early to Mid-Holocene climatic transition registered t the equator and the poles. Science, 276, 1834-1836.

Stoermer, E.F., Smol, J.P. (Eds.), 1999. The diatoms. University Press, Cambridge.

Stoffers, P., Hecky, R.E., 1978. Late Pleistocene-Holocene evolution of the Kivu-Tanganyika Basin. In: Matter, A., Tucker, M.E. (Eds.), Modern and ancient lake sediments. Int. Assoc. Sed. Spec. Pub. 2, 43-55.

Strecker, M.R., 1991. Das zentrale und südliche Kenya-Rift unter besonderer Berücksichtigung der neotektonischen Entwicklung. Unpublished thesis, University of Karlsruhe.

Strecker, M., Blisniuk, P., Eisbacher, G., 1990. Rotation of extension direction in the central Kenya Rift. Geology, 18, 299-302.

Street-Perrott, F.A., Perrott, R.A., 1993. Holocene Vegetation, Lake Levels and Climate of Africa. In: Wright jr., H.E., Kutzbach, J.E., Webb III, T., Ruddimann, W.F., Street-Perrott, F.A., Bartlein, P.J. (Eds.), Global Climates since the Last Glacial Maximum. University of Minnesota Press, Mineapolis, 318-356.

Stuiver, M., Reimer, P.J., 1993, Extended 14C data base and revised Calib. 3.0 14C age calibration program. Radiocarbon, 35, 215-230.

Suplee, C., 1999. El Niño/ La Niña. National Geographic, 195 (3), 72-95.

Survey of Kenya, 1991. National Atlas of Kenya. Kenya Government, 4th edition.

Swan, A.R.H., Sandilands, M., 1995. Introduction to geological data analysis. Blackwell Sciences, Oxford.

Taieb, M., Casanova, J., Fritz, B., Hillaire-Marcel, C., Icole, M., Manega, P., Page, N., Zins, P., 1987. Paléohydrologie dans le rift d'Afrique orientale de 240,000 ans B.P. à l'Actuel. Géodynamique, 2 (2), 145-147.

Talbot, M.R., Lærdal, T., 2000. The Late Pleistocene - Holocene palaeolimnology of Lake Victoria, East Africa, based upon elemental and isotopic analyses of sedimentary organic matter. Journal of Paleolimnology, 23, 141-164.

Talling, J.F., Talling, I.B., 1965. The chemical composition of African lake waters. Int. Rev. Ges. Hydrobiol., 50, 421-463.

Tarras-Wahlberg, H., Everard, M., Harper, D.M., 2002. Geochemical and physical characteristics of river and lake sediments at Naivasha, Kenya. Hydrobiologia, 488 (1-3), 27-41.

Taub, F.B., 1996. Lakes and reservoirs. In: Goodhall, D.W. (Ed.) Ecosystems of the world, 23. Elsevier, Amsterdam.

Telford, R.J., Lamb, H.F., 1999. Groundwater-mediated response to Holocene climatic change recorded by the diatom stratigraphy of an Ethiopian crater lake. Quaternary Research, 52, 63-75.

Thompson, A.D., Dodson, R., 1963. Geology of the Naivasha Area. Geological Survey of Kenya Report, 55, Nairobi, Kenya.

Tiercelin, J.-J., Lezzar, K.-E., 2002. A 300 million years history of rift lakes in Central and East Africa: an updated broad review. In: Odada, E.O., Olago, D.O. (Eds.), The East African great lakes: Limnology, paleolimnology and biodiversity. Advances in Global Change Research, 12, 3-60.

Trauth, M.H., 1992. Tektonik und Sedimentation im Olkaria Gebiet, südlich Lake Naivasha, Kenia. Unpublished diploma thesis, University of Karlsruhe.

Trauth, M.H., Strecker, M.R., 1996. Late Pleistocene lake level fluctuations in the Naivasha basin, Kenya. In: Johnson, T. C., Odada, E. (Eds.), The limnology, climatology and paleoclimatology of the Eastern African lakes. Gordon and Breach Publishers, Amsterdam, 549-557.

Trauth, M.H., Deino, A., Strecker, M.R., 2001. Response of the East African climate to orbital forcing during the last interglacial (130-117 ka) and the early last glacial (117-60 ka). Geology, 29, 499-502.

Trauth, M.H., Deino, A.L., Bergner, A.G.N., Strecker, M.R., 2003. East African climate change and orbital forcing during the last 175 kyr BP. Earth and Planetary Science Letters, 206, 297-313.

Troll, C., 1959. Die tropischen Gebirge, Ihre dreidimensionale klimatische und pflanzengeographische Gliederung. Bonner Geographische Abhandungen, 25.

United Nations, 2003. Population, Land Management and Environment Change. United Nations University Publications.

van Dam, H., Mertens, A., Sinkeldam, J., 1994. A coded checklist and ecological indicator values of freshwater diatoms from The Netherlands. Netherlands Journal of aquatic ecology, 28 (1), 117-133.
Verschuren, D., 1999. Sedimentation controls on the preservation and time resolution of climate-proxy records from shallow fluctuating lakes. Quaternary Science Reviews, 18, 821-837.

Verschuren, D., Laird, K.R., Cumming, B.F., 2000. Rainfall and drought in equatorial Africa during the past 1,100 years. Nature, 403, 410-413.

Vincent, C.E., Davies, T.D., Beresford, A.K.C, 1979. Recent Changes in the level of Lake Naivasha, Kenya, as an indicator of Equatorial Westerlies over East Africa. Climatic Change, 2, 175-189.

Vincent, C.E., Davies, T.D., Primblecombe, P., Beresford, A.K.C., 1989. Lake Levels and glaciers: Indicators of the changing rainfall in the mountains of East Africa. In: Mahaney, W.C., ed. Quaternary and environmental research on East African Mountains, York University, North York, Canada, 199-216.

Vincent, D.G., 1994. The South Pacific Convergence Zone (SPCZ): a review. Monthly Weather Reviews, 124, 1949-1970.

Vrba, E., Denton, G., Burckle, L., Partridge, T. (Eds.), 1995. Paleoclimate and Evolution With Emphasis on Human Origins. Yale University Press, New Haven.

Waliser, D.E., Gautier, C., 1993. A satellite derived climatology of the ITCZ. Journal of Climatology, 6, 2162-2174.

Washbourn-Kamau, C., 1970. Late Quaternary chronology of the Nakuru-Elmenteita Basin, Kenya. Nature, 226, 253-254.

Washbourn- Kamau, C., 1971. Late Quaternary lakes in the Nakuru-Elmenteita Basin, Kenya. Geographical Journal, 137 (4,4), 522-535.

Washbourn-Kamau, C.K., 1975. Late Quaternary Shorelines of Lake Naivasha, Kenya. Azania, X, 77-92.

Washbourn-Kamau, C.K., 1977. The Ol Njorowa Gorge, Lake Naivasha basin, Kenya. In: Greer, D.C. (Ed.), Desertic Terminal Lakes. Utah Water Research Laboratory, 297-307.

Wessel, P., Bercovici, D., 1998. Interpolation with Splines in Tension: A Green's Function Approach. Mathematical Geology, 30 (1), 77-93.

Wise, B.M., Gallagher, N.B., Bro, R., Shaver, J.M., 2002. PLS Toolbox for use with Matlab, Version 3.0, Software. Eigenvector Research, Inc.

Yan, J.P., Hinderer, M., Einsele, G., 2002. Geochemical evolution of closed-basin lakes: general model and application to Lakes Quinghai and Turkana. Sedimentary Geology, 148, 105-122.

Yuretich, R.F., 1982. Possible influences upon lake development in the East African Rift valleys. Journal of Geology, 90, 329-337.

Yuretich, R.F., Ervin, C.R., 2002. Clay minerals as paleoenvironmental indicators in two large lakes of the African rift valleya: lake Malawi and Lake Turkana. In: Renaut, R.W., Ashley, G.M., (Eds.), 2002. Sedimentation in continental rifts. SEPM Special Publications, 73, 221-232.

APPENDIX

APPENDIX A – *stratigraphic profiles*

* for stratigraphic profiles of the Naivasha basin confer Fig. 3.3, p. 28 and references

APPENDIX B – *paleolimnological data*

Appendix A.1 Catalog of investigated diatomite sequences in the Naivasha basin

outcrop (nr., local name)	top. hight	longitude				(UTM)	latitude				(UTM)	diatom occurence					
												MP	LP	HV	HIV	HII	H
Ol Njorowa Gorge																	
101 Punkt 20/A	1770 b	E	36	°	18,76 '	200.903	S	0	°	55,29 '	9.898.078						
102 22/A	1830 b	E	36	°	19,90 '	203.011	S	0	°	54,37 '	9.899.774			x	x		
103 22/B	1840 t	E	36	°	19,02 '	201.386	S	0	°	54,35 '	9.899.817				x		
104 22/C	1860 b	E	36	°	19,15 '	201.621	S	0	°	53,81 '	9.900.803						
105 22/Cb		E	36	°	19,19 '	201.692	S	0	°	53,73 '	9.900.952					x	
Sahra Higgins																	
121 *GW I*		E	36	°	25,24 '	212.920	S	0	°	46,57 '	9.914.150						-
Sven's Boreholes																	
122 *GW II*		E	36	°	25,65 '	213.679	S	0	°	40,87 '	9.924.669						-
further ...																	
107 Oserian		E	36	°	18,56 '	200.521	S	0	°	49,19 '	9.909.325						x
106 Munyu railway		E	36	°	27,62 '	217.331	S	0	°	47,71 '	9.912.058						?
131 Malewa River 1	1940 t	E	36	°	25,77 '	213.895	S	0	°	37,58 '	9.930.735				x		
132 Malewa River 2	1910 b	E	36	°	25,31 '	213.045	S	0	°	39,24 '	9.927.673				x		
133 Old diatomite		E	36	°	15,31 '	194.490	S	0	°	47,90 '	9.911.703						x
Reference profiles (e.g., sediment cores)																	
Richardson & Richardson, 1973																	
123 Crescent Island		E	36	°	24,57 '	211.666	S	0	°	45,94 '	9.915.314						x
Clarke et al., 1990																	
108 Maasai Gorge		E	36	°	19,15 '	201.621	S	0	°	53,81 '	9.900.803						-
109 Clarke profile 9		E	36	°	19,03 '	201.400	S	0	°	54,36 '	9.899.800						-
110 Eburu Escarpment		E	36	°	21,62 '	206.200	S	0	°	35,75 '	9.934.100						-
Bone's Profiles																	
111 Lolonito		E	36	°	17,31 '	198.200	S	0	°	54,52 '	9.899.500						-
112 Ololbutot		E	36	°	18,22 '	199.900	S	0	°	53,54 '	9.901.300						-
113 Gorge Farm		E	36	°	20,24 '	203.650	S	0	°	51,21 '	9.905.600						-
114 Naivasha Southh		E	36	°	21,19 '	205.400	S	0	°	50,07 '	9.907.700			-			-
Washbourn-Kamau																	
133 Gilgil river		E	36	°	21,24 '	205.500	S	0	°	34,72 '	9.936.000						-
134 Malewa river		E	36	°	23,67 '	210.000	S	0	°	34,45 '	9.936.500						-

Appendix A.2 Catalog of investigated diatomite sequences in the Nakuru-Elmenteita basin

outcrop (nr., local name)		top. height	longitude				(UTM R)	latitude				(UTM H)	diatom occurence					
221	Mirian Karterit	1930 b	E	36 °	16,63 '		196.948	S	0 °	30,22 '		9.944.298						x
222	Lemulug	1930 b	E	36 °	14,62 '		193.222	S	0 °	30,06 '		9.944.595						x
223	Paladini		E	36 °	14,41 '		192.825	S	0 °	34,41 '		9.936.569						?
224	Paladini 2		E	36 °	15,88 '		195.560	S	0 °	34,21 '		9.936.949						?
201	Kariandusi, mine	1855 b	E	36 °	16,93 '		197.492	S	0 °	27,08 '		9.950.088	x	x				
202	Kar., Prehistoric site	1900 t	E	36 °	17,04 '		197.707	S	0 °	27,10 '		9.950.044		x				
203	Kar., Prehistoric top	1900 t	E	36 °	16,97 '		197.571	S	0 °	27,17 '		9.949.915		x				
211	Kariandusi, road cut	1875 s	E	36 °	15,78 '		195.360	S	0 °	25,75 '		9.952.527		x				x
215	Elmenteita, beach	1790 t	E	36 °	14,83 '		193.603	S	0 °	25,77 '		9.952.503	x					
217	Elmenteita, beach II	1830 b	E	36 °	15,11 '		194.119	S	0 °	25,86 '		9.952.334	?					
212	Elmenteita, gorge	1855 t	E	36 °	16,56 '		196.809	S	0 °	27,38 '		9.949.528	x	x		?		
213	Elmenteita, road cut	1865 s	E	36 °	16,58 '		196.851	S	0 °	27,20 '		9.949.861		x		?		
214	Elmenteita, river gully	1865 b	E	36 °	16,65 '		196.979	S	0 °	27,53 '		9.949.260	x					
216	Kariandusi, river gully		E	36 °	16,87 '		197.395	S	0 °	26,89 '		9.950.440		x				
231	Profile 24 (P.Blisniuk)	1950 s	E	36 °	18,03 '		199.536	S	0 °	28,11 '		9.948.177						
225	Soysambu	1920 t	E	36 °	10,43 '		185.443	S	0 °	25,60 '		9.952.818			x			
232	Nakuru, Baboon Cliff	2010 s	E	36 °	3,12 '		171.884	S	0 °	23,51 '		9.956.665	x					

t = top
s = road
b = base

General legend for stratigraphic profiles:

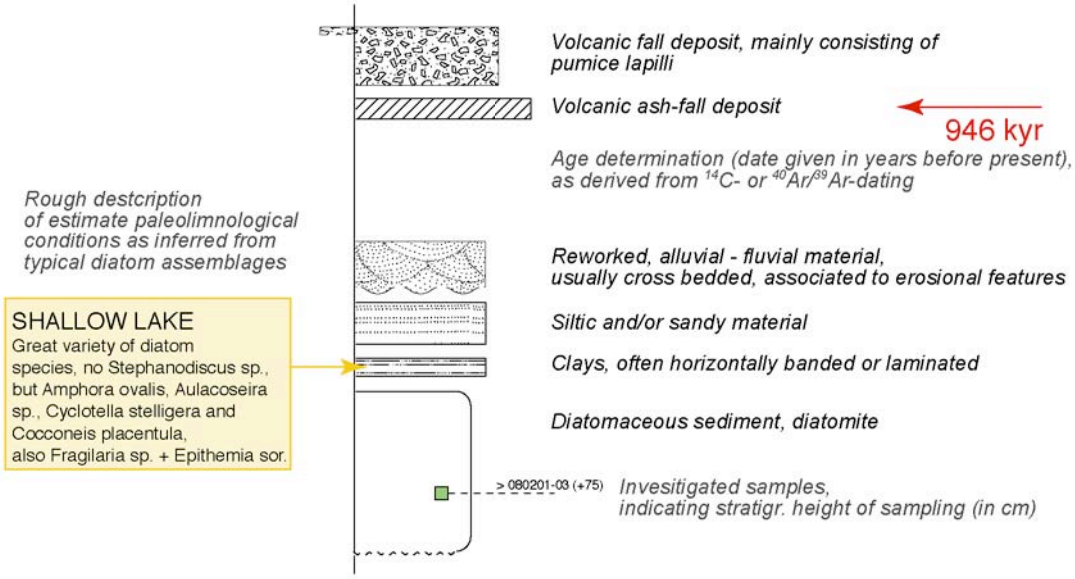

Appendix A.3 Profile legend for stratigraphic profiles

201

Kariandusi Diatomite Mine
(upper part)

sampled the
19.09.00 08.02.01
18.02.02 28.01.03
based on diploma thesis
by Peter Blisniuk (Profile 23)
Blisniuk, 1988

Coordinates:

UTM **H**	9.950.088
UTM **R**	197.492
height **base**	1855 m

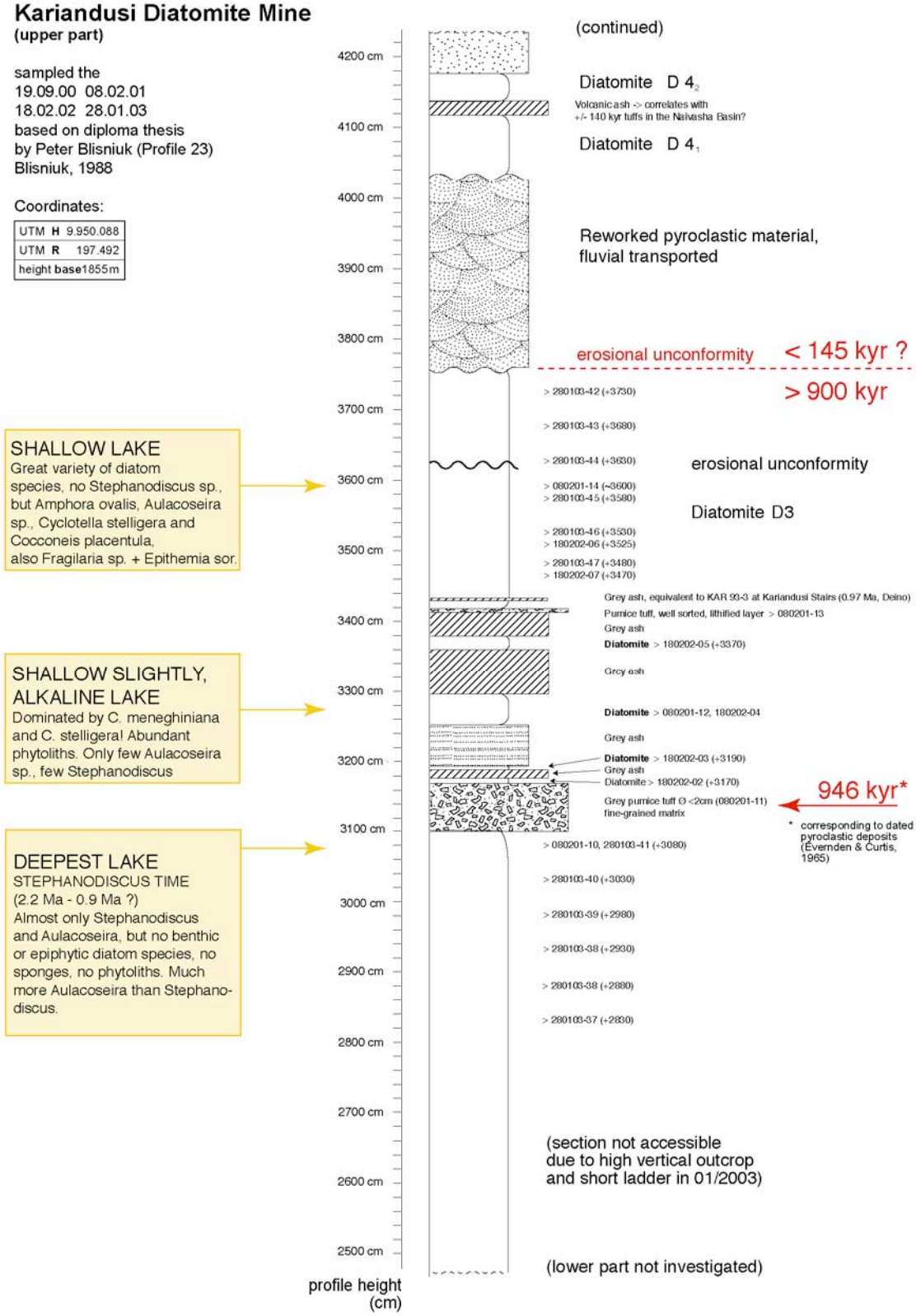

Appendix A.4 Stratigraphic profile of sediment sequence at Kariandusi diatomite mine (see Appendix A.2 for location data and A.3 for profile legend)

202

Kariandusi Prehistoric site
(on top of diatomite mine)

sampled the
19.09.00
08.02.01

Coordinates:

UTM **H**	9.950.044
UTM **R**	197.707
height **top**	1900 m

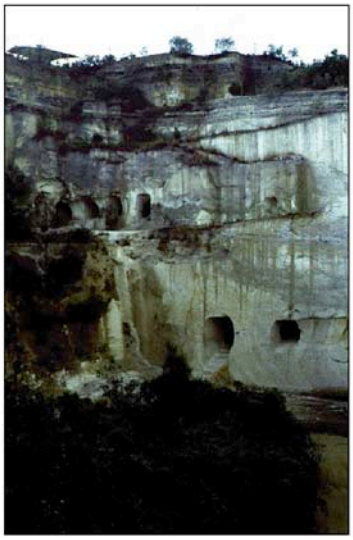

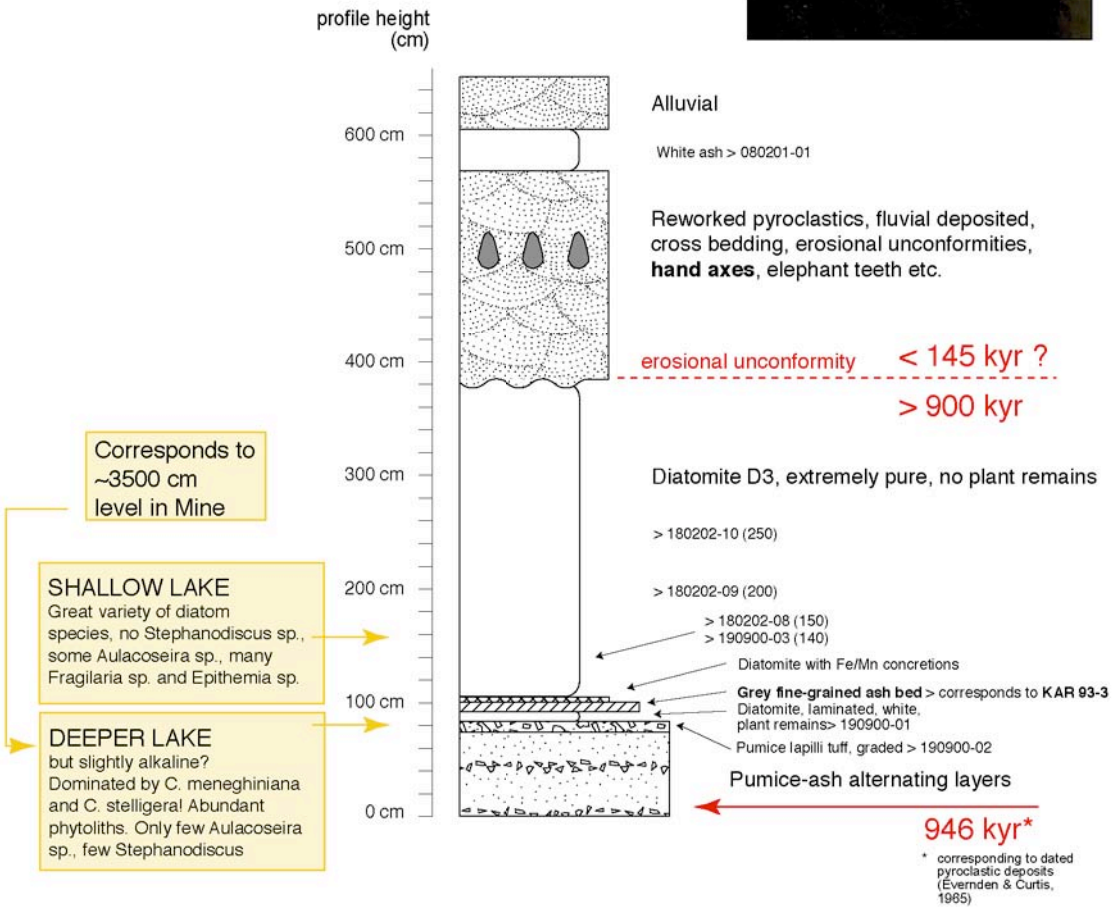

Appendix A.5 Stratigraphic profile of sediment sequence at Kariandusi prehistoric site (near stairs) (see Appendix A.2 for location data and A.3 for profile legend)

203

Kariandusi Prehistoric top

sampled the
08.02.01

Coordinates:

UTM **H**	9.949.915
UTM **R**	197.571
height **top**	1900 m

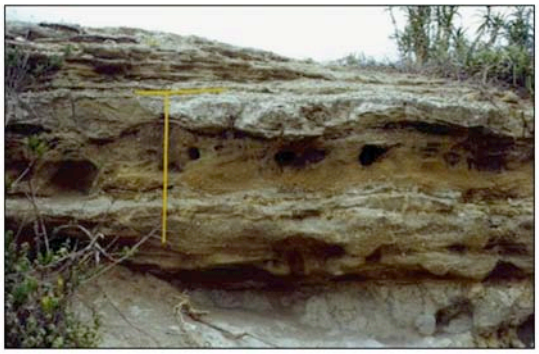

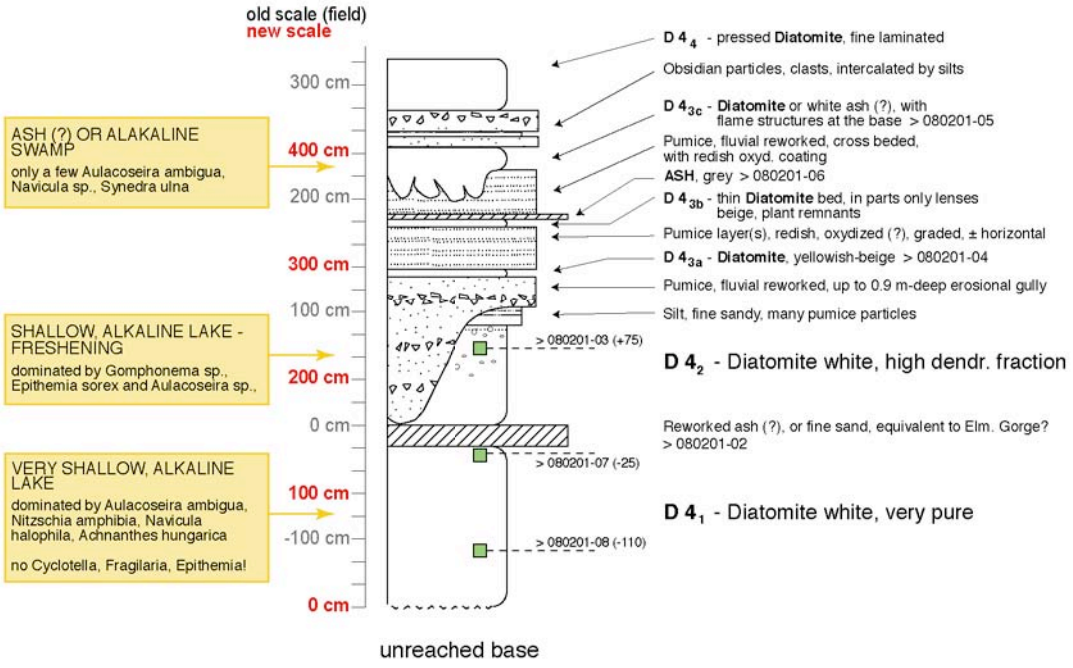

Appendix A.6 Stratigraphic profile of sediment sequence at Kariandusi prehistoric top (behind museum) (see Appendix A.2 for location data and A.3 for profile legend)

211

Kariandusi road cut
(Eisbacher)

sampled the
21.09.00, 09.02.01
based on diploma thesis
by Peter Blisniuk (Profile 31)
Blisniuk, 1988

Coordinates:

UTM **H**	9.952.527
UTM **R**	197.360
height **road**	1875 m

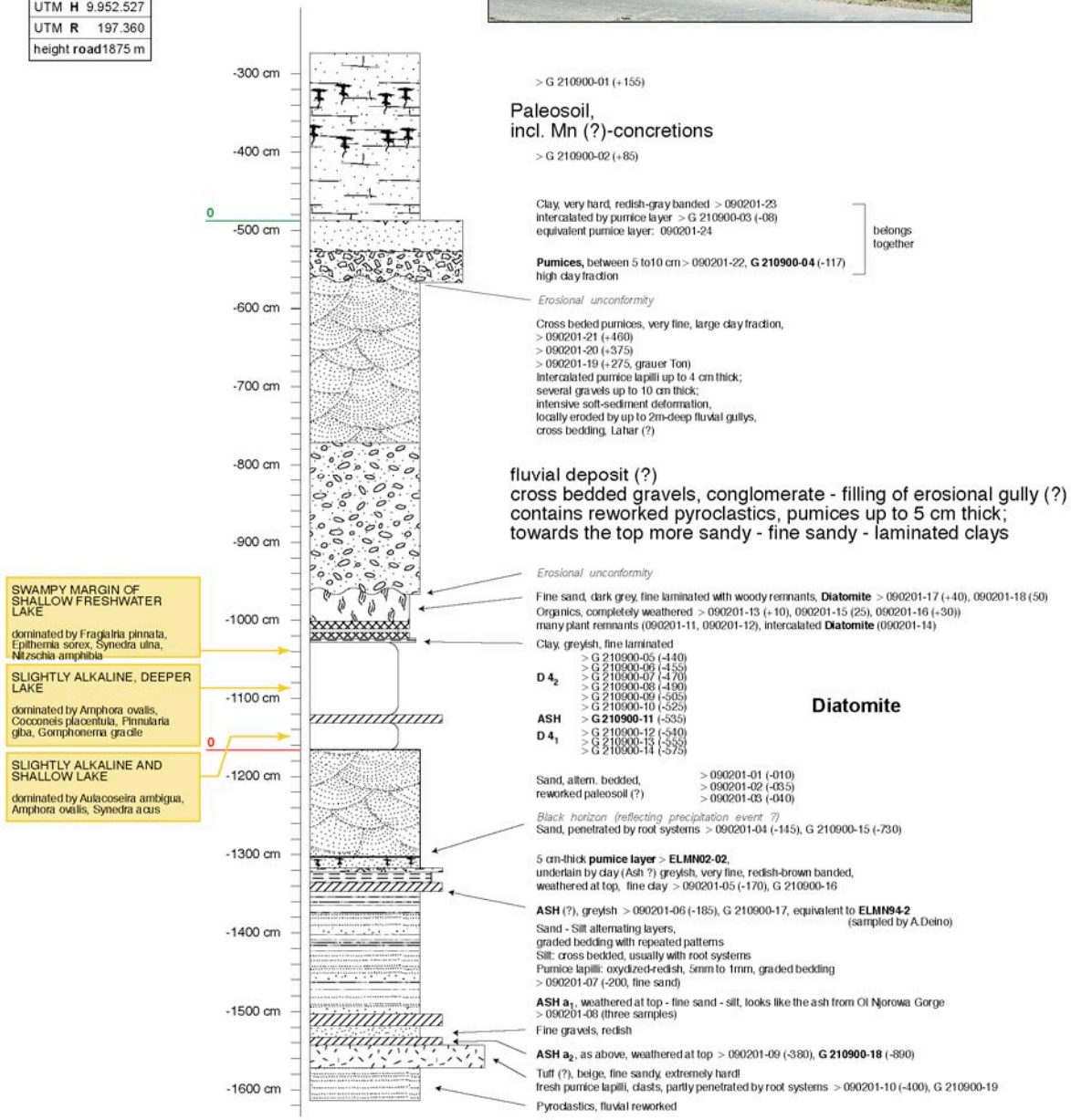

Appendix A.7 Stratigraphic profile of sediment sequence at road cut, north of Kariandusi
(see Appendix A.2 for location data and A.3 for profile legend)

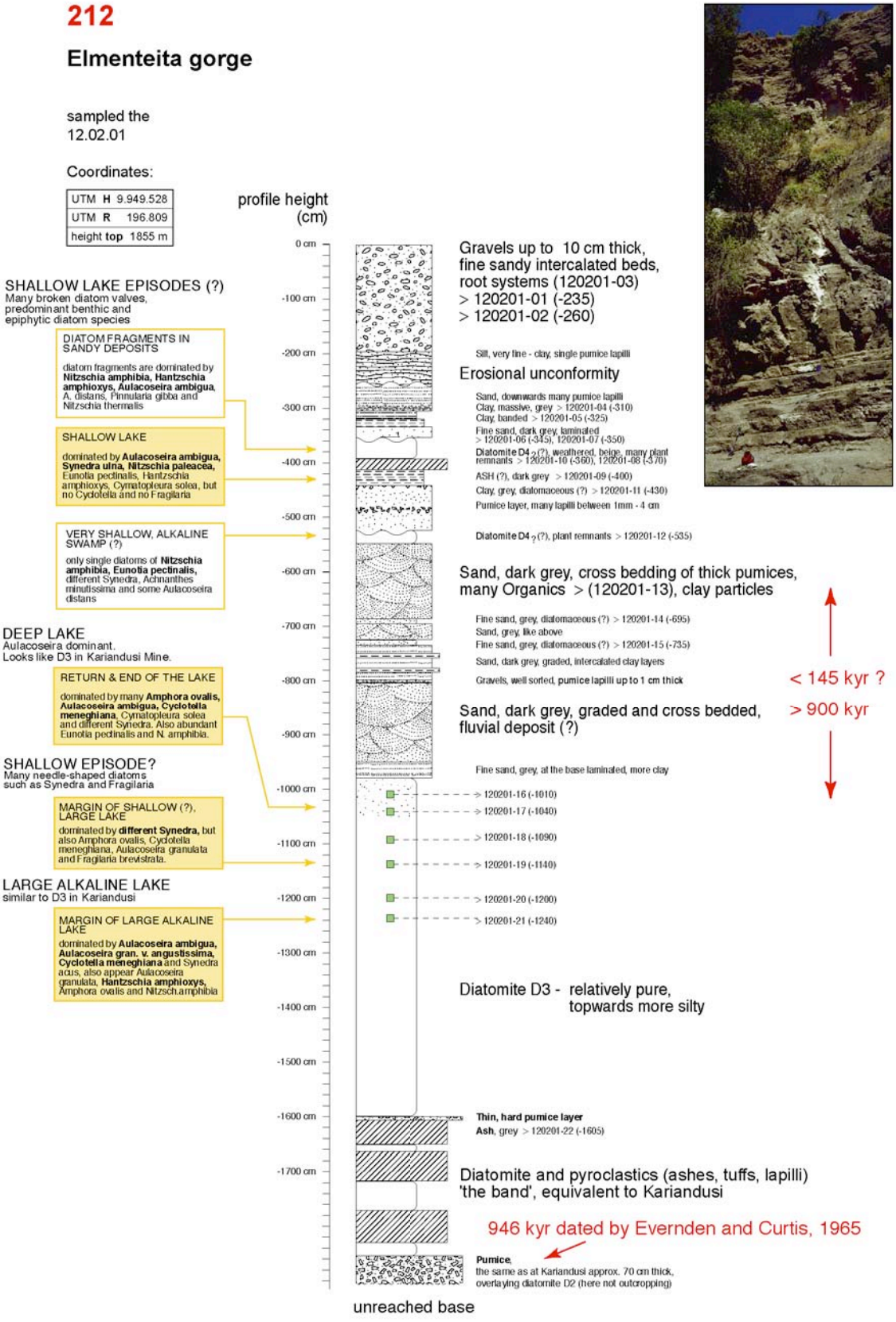

Appendix A.8 Stratigraphic profile of sediment sequence at the gorge of Kariandusi river (SW of Kariandusi village; see Appendix A.2 for location data and A.3 for profile legend)

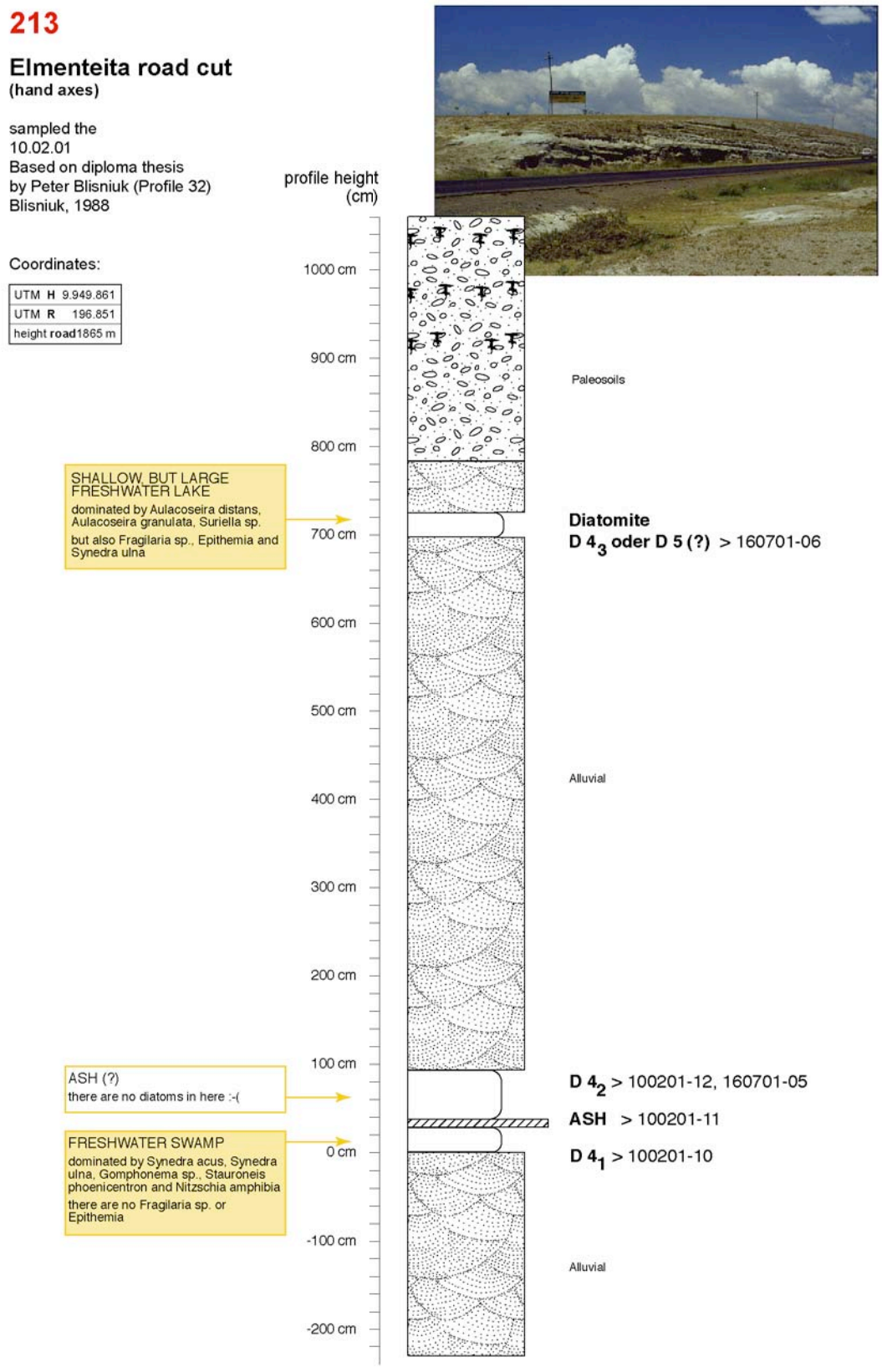

Appendix A.9 Stratigraphic profile of sediment sequence at the road cut, south of Kariandusi village (see Appendix A.2 for location data and A.3 for profile legend)

214

Elmenteita river gully
(dome)

sampled the
10.02.01

Coordinates:

UTM **H**	9.949.260
UTM **R**	196.979
height **top**	1865 m

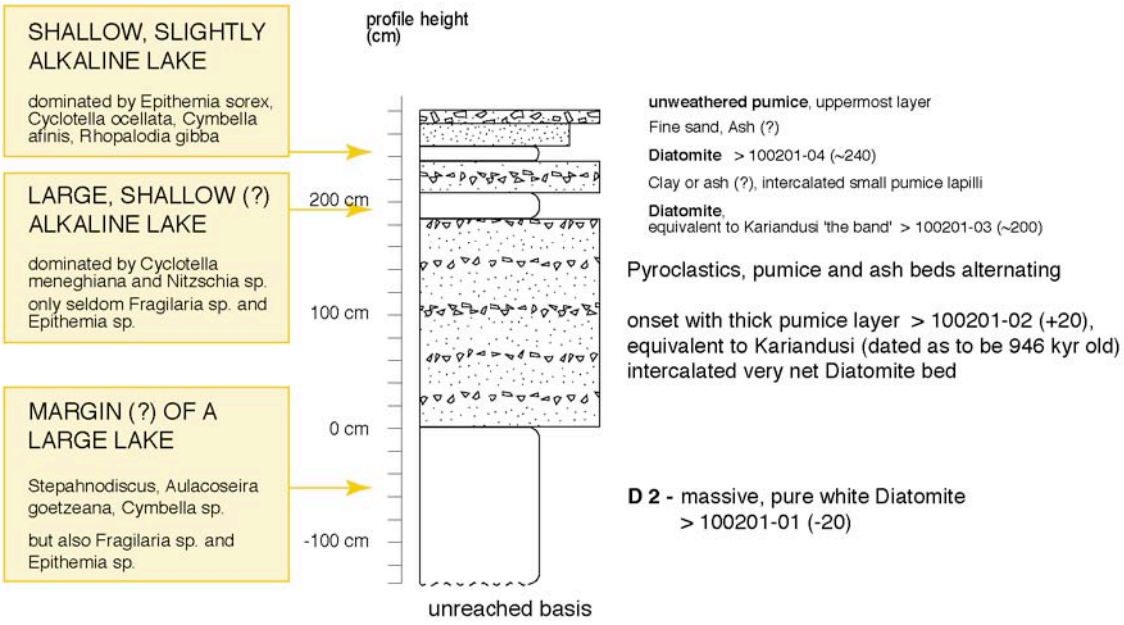

Appendix A.10 Stratigraphic profile of sediment sequence on top of the Elmenteita gorge (see Appendix A.2 for location data and A.3 for profile legend)

215

Elmenteita beach
(fishes)

sampled the
14.02.01

Coordinates:

UTM **H**	9.952.503
UTM **R**	193.603
height **top**	1790 m

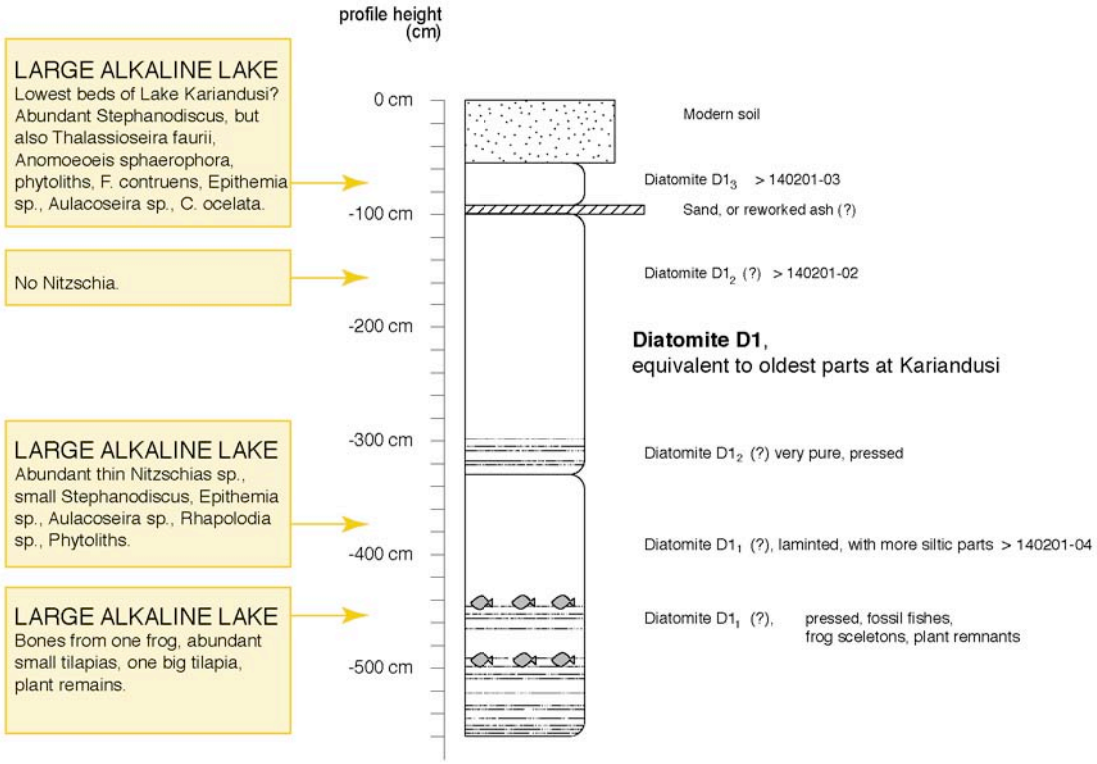

Appendix A.11 Stratigraphic profile of sediment sequence at the eastern shore of Lake Elmenteita (see Appendix A.2 for location data and A.3 for profile legend)

225

Soysambu diatomite mine

sampled the
17.09.00
13.02.01

Coordinates:

UTM **H**	9.952.818
UTM **R**	185.443
height **top**	1920 m

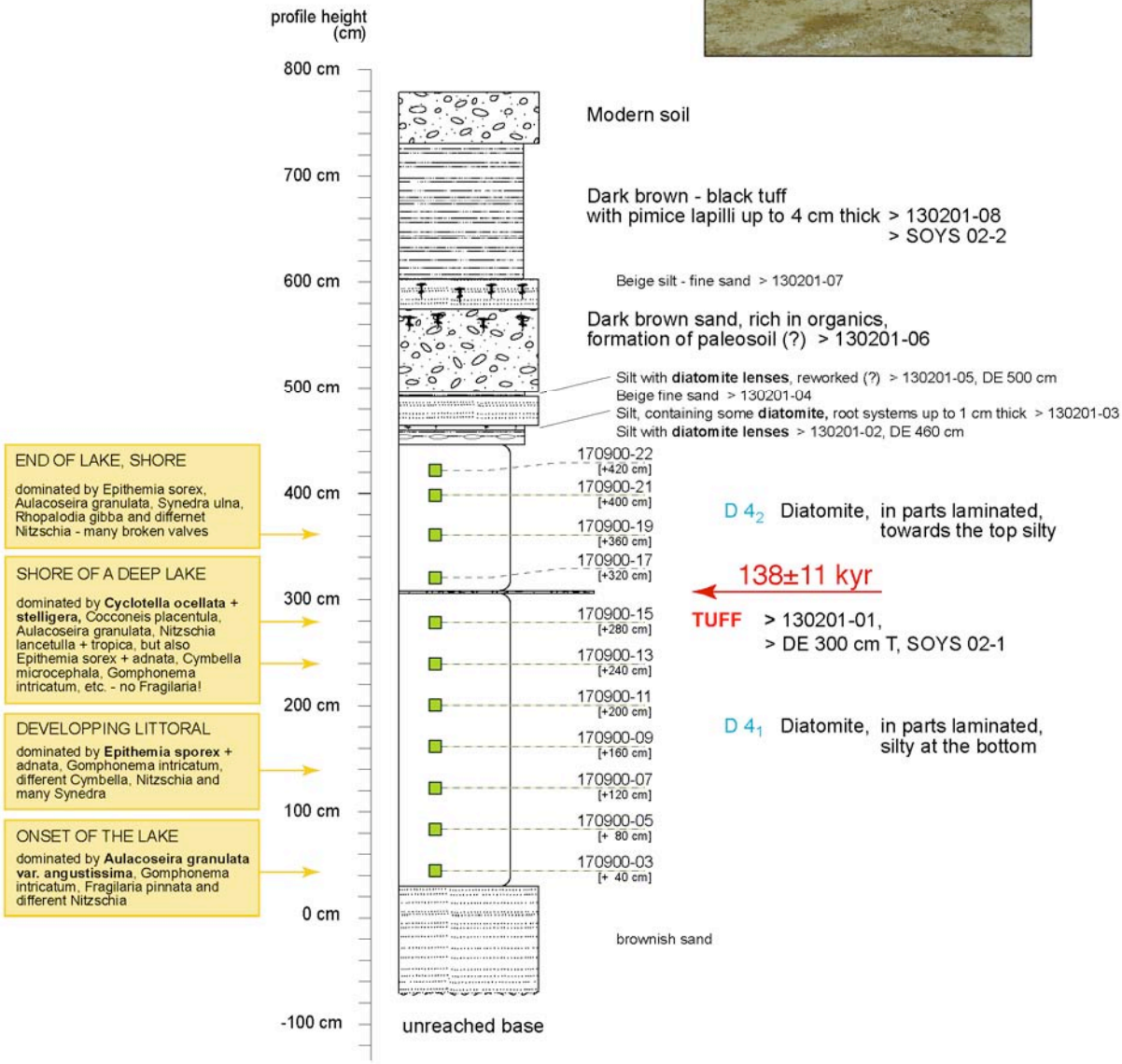

Appendix A.12 Stratigraphic profile of sediment sequence at the small diatomite mine west of Lake Elmenteita (see Appendix A.2 for location data and A.3 for profile legend)

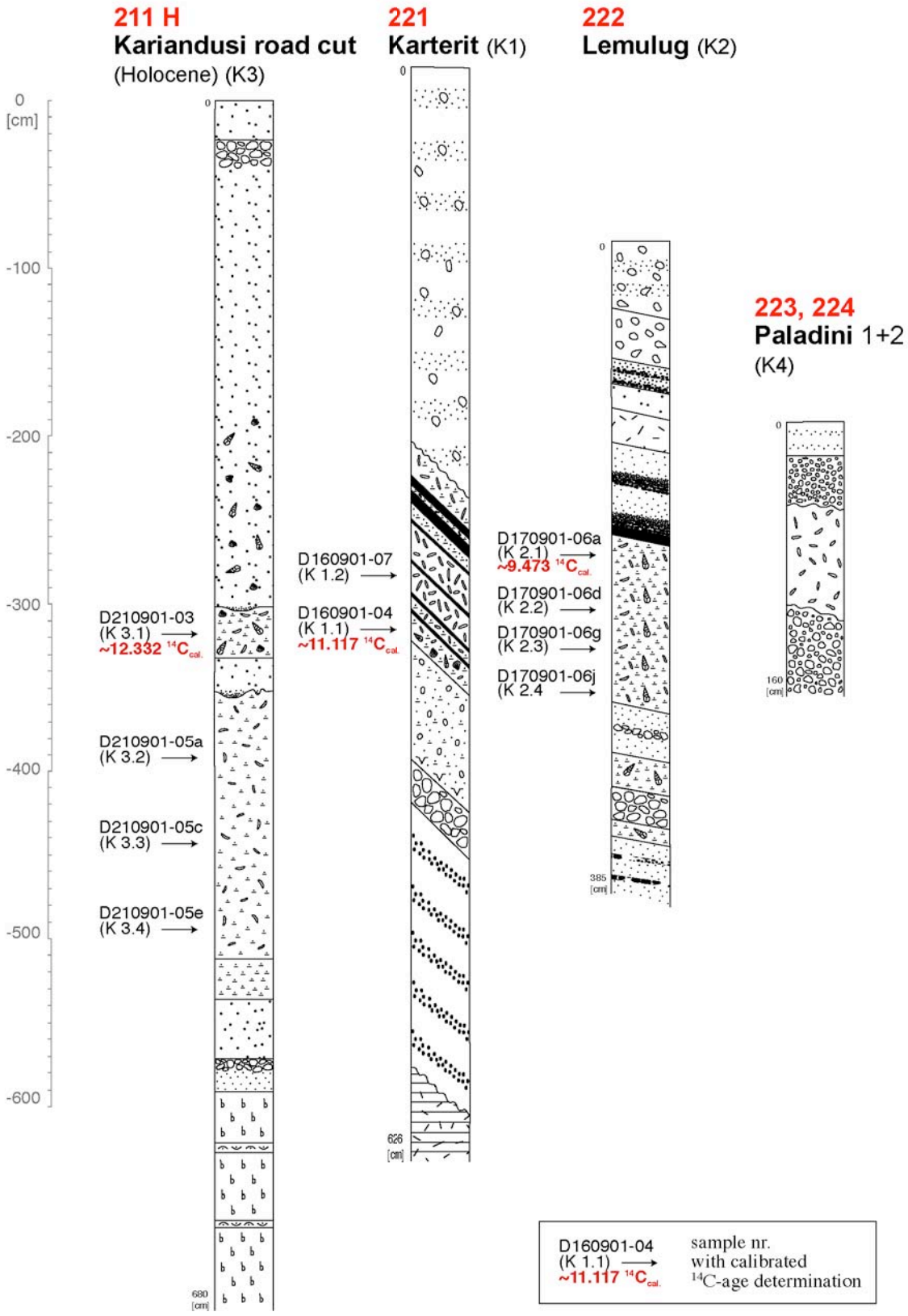

Appendix A.13 Copy of stratigraphic profiles of sediment sequence at Kariandusi road cut (Holocene section), Mt. Karterit and Mt. Lemulug volcanoes and two profiles south-west of Lake Elmenteita (Paladini 1 and 2) (from Dühnforth, 2001). See Appendix A.2 for location data and Dühnforth (2001) for profile legend and details.

Appendix B.1 Selected hydrochemical parameters of identified diatoms; data corresponding to the findings published by F. Gasse and their collegues (Gasse et al., 1995) as reference matrix for transfer functions

	Code after Gasse	Matlab-ID	Name	reference	ecological parameters								prevail.habit.					
					Conductivity		pH		Cat-Ratio		An.-Ratio		lit.	epi.	ben.	pel.	plan.	ID
					Optim.	Toler.	Optim.	Toler.	Optim.	Toler.	Optim.	Toler.						
1	0103	103	**Achnanthes clevei**	*Grunow*	**1,93**	1,04			**0,87**	0,72	**0,47**	0,34	*					1
2	0151	151	**Achnanthes conspicua + engelbrechtii**	*Mayer*										*				2
3	0104	104	**Achnanthes exigua**	*Grunow*	**3,21**	0,99	**8,62**	0,96	**1,00**	0,93	**0,46**	0,27	*	*				2
4	0107	107	**Achnanthes hungarica**	*Grunow*	**2,31**	0,7	**7,86**	1,07	**-0,33**	0,23	**1,49**	0,77		*				2
5	0108	108	**Achnanthes inflata**	*Kützing*									*	*				2
6	0113G	113	**Achnanthes minutissima var.**	*Kützing*	**2,42**	0,55	**7,93**	0,84	**0,52**	0,61	**0,40**	0,71	*	*				2
7	0118	118	**Achnanthes subhudsonis**	*Hustedt*	**1,79**	0,33	**6,54**	0,07	**0,45**	0,79	**0,59**	0,02		*				2
8	0311	311	**Amphora aequalis**	*Krammer*														0
9	0377	377	**Amphora inariensis**	*Krammer*	**4,84**	0,79	**8,77**	1,2	**0,65**	0,53	**-2,43**	0,72						0
10	0325	325	**Amphora ovalis** + A.lybica	*(Kütz.) Ehrenberg*	**2,86**	0,7	**7,44**	0,58	**0,27**	0,43	**-0,45**	0,75	*	*				2
11	0326	326	**Amphora pediculus**	*(Kütz.) Grunow*	**3,25**	0,73	**7,74**	0,59	**0,14**	0,34	**-0,61**	0,95		*		*		2
12	0370	370	**Amphora veneta**	*Kützing*	**4,38**	0,22	**9,05**	0,64	**0,39**	0,26	**-1,10**	0,82	*	*				2
13	0506	506	**Anomoeoneis sphaerphora**	*(Kütz.) Pfitzer*	**3,06**	0,64	**8,14**	0,72	**0,43**	0,49	**-0,29**	1,06	*					1
14	0503	503	**Anomoeoneis vitrea**	*(Grun)Ross*	**4,23**	0,43	**9,87**	0,71	**2,19**	0,56	**0,41**	0,41						0
15	3501	3501	**Aulacoseira agassizii + v.malayensis**	*Ostenfeld*	**2,20**	0,43	**7,77**	0,84	**0,01**	0,55	**0,73**	0,42					*	4
16	3502	3502	**Aulacoseira ambigua**	*(Grun.) Sim.*	**2,32**	0,4	**7,50**	0,68	**0,26**	0,45	**0,67**	0,27					*	4
17	3506	3506	**Aulacoseira goetzeana**	*(Müller) Sim.*	**2,36**	0,82	**7,82**	0,9	**0,05**	0,53	**0,66**	0,64					*	4
18	3507	3507	**Aulacoseira granulata + muzzanensis**	*(Ehr.) Ralfs*	**2,14**	0,46	**7,10**	0,68	**-0,10**	0,3	**0,56**	0,36					*	4
19	3508	3508	**Aulacoseira granulata** var.angustissima	*(Müller) Sim.*	**2,56**	0,47	**7,66**	0,75	**0,23**	0,65	**0,52**	0,6					*	4
20	3510G	3510	**Aulacoseira granulata** var.valida	*Hustedt*	**2,94**	1,31			**0,36**	1,78	**0,52**	0,27					*	4
21	0904G	904	**Caloneis bacillum**	*(Grun.) Mer.*	**2,90**	0,72	**7,67**	1,18	**0,47**	0,72	**0,08**	0,72	*			*		1
22	1401	1401	**Cocconeis diminuta**	*Pantocsek*	**2,47**	0,89	**9,06**	0,48	**0,25**	0,65	**0,16**	0,43	*	*				2
23	1403	1403	**Cocconeis placentula + v.euglypta**	*(Ehr.) Cleve*	**2,67**	0,76	**8,31**	0,93	**-0,12**	0,57	**0,08**	1,16	*	*				2
24	1405	1405	**Cocconeis thumensis**	*Mayer*	**1,84**	0,6	**7,49**	1,75	**0,74**	0,58	**0,55**	0,41		*				2
25	1610	1610	**Cyclotella glomerata**	*Bachmann*													*	4
26	1655	1655	**Cyclotella iris**	*Brun & Héribaud*	**4,01**	0,5	**9,58**	0,43	**2,57**	0,59	**0,61**	0,39						0
27	1620	1620	**Cyclotella meneghiniana + v.pumila**	*Kützing*	**3,78**	0,62	**8,85**	0,94	**0,67**	0,97	**-0,45**	0,86			*			3
28	1625	1625	**Cyclotella ocellata**	*Pantocsek*	**3,18**	0,7	**8,53**	0,91	**0,01**	1,17	**0,54**	1,02	*				*	5
29	1635	1635	**Cyclotella stelligera + v.tenuis**	*Cl. & Grunow*	**2,41**	0,32	**7,82**	0,92	**-0,10**	0,14	**0,60**	0,29	*				*	5
30	1901	1901	**Cymbella affinis**	*Kützing*	**2,41**	0,73	**7,20**	1,39	**0,14**	0,4	**-0,05**	0,51	*	*				2
31	1904	1904	**Cymbella cistula**	*(Hempr.) Grunow*									*	*				2
32	1911G	1911	**Cymbella microcephala**	*Grunow*	**3,21**	0,44	**8,00**	0,61	**0,04**	0,41	**-0,44**	0,93	*	*				2
33	1912	1912	**Cymbella muellerii**	*Müller*	**2,81**	0,52	**8,58**	0,94	**0,35**	0,92	**0,77**	0,39	*					1
34	1913	1913	**Cymbella naviculiformis**	*Auerswald*	**2,77**	0,69	**8,17**	1,08	**-0,11**	0,18	**-0,34**	0,11	*					1
35	1920	1920	**Cymbella pusilla**	*Grunow*	**3,96**	0,43	**7,78**	0,88	**0,31**	0,69	**-1,47**	0,59				*		1
36	1917	1917	**Cymbella turgida**	*Greg.*	**2,53**	0,6	**8,04**	1,08	**0,58**	0,88	**0,47**	0,37	*	*				2
37	1946	1946	**Cymbella turgidula**	*Grunow*														0
38	1918	1918	**Cymbella ventricosa** + C.silesiaca	*Agardh*	**2,33**	0,37	**7,88**	1,06	**0,30**	0,37	**0,39**	0,51	*	*				2
39	2301	2301	**Diploneis elyptica**	*(Kütz.) Cleve*									*					1
40	2303	2303	**Diploneis ovalis**	*(Hilse) Vleve*	**3,57**	0,8	**8,00**	0,54	**0,59**	0,74	**-1,17**	0,94	*					1
41	2406	2406	**Epithemia adnata + var.**	*Ehrenberg*	**2,42**	0,26	**8,27**	0,52	**-0,18**	0,35	**0,70**	0,35	*					1
42	2402	2402	**Epithemia argus**	*(Ehr.) Kützing*	**4,05**	1,17	**8,28**	1,23	**0,66**	0,89	**-0,97**	1,93	*					1
43	2404	2404	**Epithemia sorex + v.gracilis**	*Kützing*	**3,00**	0,65	**8,07**	1,25	**0,50**	0,77	**0,10**	0,35	*					1

Appendix B.1 (continued) Selected hydrochemical parameters of identified diatoms; data corresponding to the findings published by F. Gasse and their collegues (Gasse et al., 1995) as reference matrix for transfer functions

	Code after Gasse	Matlab-ID	Name	reference	ecological parameters								prevail.habit.					
					Conductivity		pH		Cat-Ratio		An.-Ratio		lit.	epi.	ben.	pel.	plan.	ID
					Optim.	Toler.	Optim.	Toler.	Optim.	Toler.	Optim.	Toler.						
44	2405	2405	**Epithemia turgida**	*Ehrenberg*	**2,66**	0,29	**8,01**	0,28	**0,23**	0,56	**0,28**	0,31	*					1
45	2504	2504	**Eunotia curvata**	*(Kütz.) Lagerstedt*	**2,34**	0,65	**6,64**	0,66	**0,92**	0,85	**0,82**	0,5						0
46	2503	2503	**Eunotia flexuosa**	*(Bréb)Kützing*	**2,34**	0,15			**0,03**	0,21	**0,83**	0,93						0
47	2506G	2506	**Eunotia pectinalis**	*(Dyllwyn) Rabenh.*	**2,26**	0,28	**6,99**	0,57	**0,31**	0,73	**0,46**	0,57	*	*				2
48	2516	2516	**Eunotia praerupta**	*Ehrenberg*	**1,78**	2,74	**6,00**	0,78										0
49	2601	2601	**Fragilaria africana**	*Hustedt*	**2,76**	0,8	**7,82**	1,02	**0,10**	0,67	**-0,14**	0,89			*		*	4
50	2602	2602	**Fragilaria brevistrata + var.**	*Grunow*	**2,53**	0,34	**8,42**	0,58	**0,00**	0,5	**0,33**	0,67	*				*	5
51	2606	2606	**Fragilaria construens + v.venter**	*(Ehr.) Grunow*	**2,54**	0,6	**8,76**	1,25	**-0,25**	0,54	**-0,43**	1,26	*				*	5
52	2611	2611	**Fragilaria lapponica**	*Grunow*	**2,14**	0,41	**7,97**	0,63	**0,06**	0,4	**0,49**	0,61	*					1
53	2612	2612	**Fragilaria leptostauron + var. dubia**	*(Ehr.) Hust.*	**2,16**	0,46	**8,17**	0,83	**0,16**	0,57	**0,47**	0,56	*					1
54	2613	2613	**Fragilaria pinnata**	*Ehrenberg*	**2,33**	0,67	**8,30**	0,61	**0,26**	0,71	**0,79**	0,15	*				*	5
55	2615	2615	**Fragilaria virescens**	*Ralfs*									*				*	5
56	2603G	2603	**Fragilaria zeilleri** +v.africana+elliptica G.	*Héribaud*	**2,01**	0,36	**7,21**	0,61	**0,03**	0,39	**0,57**	0,72						0
57	2910	2910	**Gomphonema affine**	*Kützing*														0
58	2917G	2917	**Gomphonema clavatum**	*Ehrenberg*	**2,67**	0,37	**8,63**	0,6	**0,31**	0,43	**0,13**	0,74	*	*				2
59	2904	2904	**Gomphonema clevei v. javanica**	*Hustedt*	**2,65**	0,56	**7,01**	1,25	**0,14**	0,91	**0,45**	0,42	*	*				2
60	2908G	2908	**Gomphonema gracile** + G.lanceolatum	*Ehrenberg*	**2,71**	0,59	**7,76**	0,96	**0,54**	0,46	**0,22**	0,69	*	*				2
61	2912G	2912	**Gomphonema intricatum/ angustum**	*(Agardh)*	**2,84**	0,87	**8,33**	1,04	**0,32**	0,63	**-0,08**	0,83	*	*				2
62	2923	2923	**Gomphonema parvulum**	*Kützing*	**2,42**	0,58	**7,63**	0,81	**0,52**	0,64	**0,54**	0,74	*	*				2
63	3201	3201	**Hantzschia amphioxys**	*(Ehr.) Grunow*	**2,68**	0,8	**7,57**	1,34	**0,72**	0,97	**0,34**	0,54	*					1
64	3302	3302	**Mastogloia braunii**	*Grunow*	**3,78**	0,22	**7,44**	0,48	**0,04**	0,22	**-1,57**	0,28	*					1
65	3303	3303	**Mastogloia elliptica + v.dansei + v.ellipt.**	*(Ag.) Cleve*	**3,32**	0,64	**7,65**	0,9	**0,44**	0,4	**-0,59**	0,98	*					1
66	3305G	3305	**Mastogloia smithi + var.**	*Thwaites*	**3,61**	0,22	**7,40**	0,27	**-0,12**	0,48	**-1,23**	0,51	*					1
67	3607G	3607	**Navicula cari + graciloides**	*Ehrenberg*	**3,76**	0,94	**8,97**	1,31	**1,75**	0,97	**0,13**	1,01	*					1
68	3613	3613	**Navicula cryptocephala** + v.lancettula	*Kützing*	**2,61**	0,74	**7,62**	0,85	**0,27**	0,61	**0,11**	0,83	*					1
69	3615	3615	**Navicula cryptocephala var. veneta**	*Kützing*	**3,25**	0,66	**7,46**	0,71	**0,19**	0,42	**-0,74**	1	*					1
70	3617G	3617	**Navicula cuspidata + var. ambigua**	*Kützing*	**3,26**	0,75	**8,37**	0,7	**0,81**	0,79	**0,28**	0,6	*					1
71	3620	3620	**Navicula damasii + vitabunda**	*Hustedt*	**3,21**	0,38	**9,35**	0,4	**0,83**	0,88	**0,47**	0,35	*					1
72	3621G	3621	**Navicula decussis**	*Oestrup*	**2,52**	0,46	**7,82**	0,98	**0,19**	0,82	**0,79**	0,4						0
73	3622	3622	**Navicula elkab**	*Müller*	**4,14**	0,6	**9,36**	0,62	**2,00**	0,44	**0,09**	0,5	*					1
74	9991	9991	**Navicula globosa**	*Meister*														0
75	9992	9992	**Navicula modica**	*Hustedt*														0
76	3712G	3712	**Navicula mutica + vars**	*Kützing*	**2,96**	0,88	**7,94**	1,13	**0,57**	0,68	**-0,06**	0,86	*			*		1
77	3767	3767	**Navicula oblonga**	*Kützing*	**3,26**	0,2	**7,70**	0,78	**0,04**	0,35	**-0,92**	0,17						0
78	3728	3728	**Navicula pupula + platycephala**	*Kützing*	**3,41**	0,79	**8,44**	1,12	**0,31**	0,66	**0,12**	0,69	*			*		1
79	3730	3730	**Navicula radiosa**	*Kützing*	**3,20**	1,01	**7,87**	0,65	**0,14**	0,39	**0,29**	1,04	*					1
80	3732	3732	**Navicula rhyncocephala**	*Hustedt*	**3,34**	0,84	**8,16**	0,95	**-0,02**	0,3	**-0,62**	0,69	*					1
81	3738	3738	**Navicula schoenfeldii + var. pusilla**	*Hustedt*									*					1
82	3742	3742	**Navicula seminuloides**	*Hustedt*	**2,99**	0,98	**8,37**	1,33	**0,39**	0,65	**0,68**	0,51	*					1
83	3743	3743	**Navicula seminulum**	*Grunow*	**2,34**	0,69	**7,56**	1,28	**0,54**	0,68	**0,45**	0,83	*					1
84	3606	3606	**Navicula sp. aff. bacilum**	*Ehrenberg*														0
85	3638	3638	**Navicula sp. aff. hungarica**	*Grunow*	**3,49**	0,63	**7,40**	0,49	**0,03**	0,28	**-1,09**	0,6						0
86	3627G	3627	**Navicula subminuscula + perparva**	*Manguin*	**2,51**	0,7	**8,32**	0,8	**0,60**	0,46	**0,44**	0,41						0
87	3739G	3739	**Navicula tenella** + Nav.cryptotenella	*Brébisson*	**3,58**	0,65	**7,77**	0,61	**0,20**	0,35	**-1,54**	0,91						0
88	3757	3757	**Navicula ventralis + pseudoventralis**	*Krasske*	**2,45**	0,58	**7,42**	0,91	**1,07**	0,24	**0,58**	0,79						0

Appendix B.1 (continued) Selected hydrochemical parameters of identified diatoms; data corresponding to the findings published by F. Gasse and their collegues (Gasse et al., 1995) as reference matrix for transfer functions

	Code after Gasse	Matlab-ID	Name	reference	ecological parameters: Conductivity Optim.	Conductivity Toler.	pH Optim.	pH Toler.	Cat-Ratio Optim.	Cat-Ratio Toler.	An.-Ratio Optim.	An.-Ratio Toler.	prevail.habit.: lit.	epi.	ben.	pel.	plan.	ID
89	**3906**	3906	**Nitzschia amphibia** + f.frauenfeldii	*Grunow*	**3,42**	0,14	**7,00**	0,78	**-0,26**	0,01	**-1,14**	0,13	*					1
90	**3922**	3922	**Nitzschia bacilum + fonticola**	*Hustedt*	**3,62**	0,69	**9,07**	1,07	**1,46**	0,88	**0,18**	0,73						0
91	**3918**	3918	**Nitzschia epiphytica**	*Müller*	**3,01**	0,04	**8,80**	0,28	**1,00**	0,77	**0,81**	0,09	*				*	5
92	**3925**	3925	**Nitzschia frustulum sp.**	*(Kütz.) Grun.*	**2,39**	0,68							*				*	5
93	**3942G**	3942	**Nitzschia frustulum sp.aff. inconspicua**	*Grunow*	**3,61**	0,57	**7,66**	1,06	**0,52**	0,91	**-0,73**	0,7	*				*	5
94	**3936**	3936	**Nitzschia goetzeana**	*Hustedt*	**2,70**	0,41	**7,52**	0,62	**0,03**	0,46	**0,73**	0,65					*	4
95	**3932G**	3932	**Nitzschia gracilis agg.**	*Hantzsch*	**4,65**	0,25	**8,91**	0,56	**0,73**	0,11	**-2,78**	0,33	*					1
96	**3946**	3946	**Nitzschia lacuum**	*Lange-Bertalot*	**2,86**	0,82	**7,34**	0,79	**-0,19**	0,13	**-0,79**	0,99						0
97	**4003**	4003	**Nitzschia lancettula**	*O. Müller*	**3,28**	0,8	**8,51**	0,76	**1,15**	1	**0,20**	0,5					*	4
98	**4012**	4012	**Nitzschia palea**	*(Kütz.) Smith*	**3,58**	0,55	**7,68**	1,16	**0,14**	0,45	**-0,78**	0,86	*					1
99	**4016**	4016	**Nitzschia paleacea**	*Grunow*	**3,46**	0,56	**7,22**	0,55	**-0,06**	0,14	**-1,16**	0,28	*					1
100	**4042G**	4042	**Nitzschia thermalis + var.**	*(Ehr.) Auerswald*	**2,82**	0,97	**7,66**	1,29	**0,12**	0,37	**0,23**	0,42	*					1
101	**4037**	4037	**Nitzschia tropica**	*Grunow*	**2,71**	0,76	**7,81**	0,83	**0,32**	0,95	**0,35**	0,69					*	4
102	**4070**	4070	**Nitzschia vanoyei**	*Cholnoky*													*	4
103	**4201**	4201	**Pinnularia acrosphaeria**	*Rabenhorst*	**2,26**	0,83	**7,18**	1,02	**-0,12**	0,33	**0,65**	0,09	*					1
104	**4208**	4208	**Pinnularia gibba** +var. sancta+v.linearis	*Ehrenberg*	**2,53**	0,5			**0,61**	0,69	**-0,94**	0,41	*					1
105	**4230**	4230	**Pinnularia intermedia**	*(Lagerst.) Cleve*	**1,78**	0,6	**6,00**	0,78										0
106	**4220**	4220	**Pinnularia maior**	*Rabenhorst*	**1,82**	0,3	**7,41**	1,1	**1,12**	0,92	**0,78**	0,5	*					1
107	**3647**	3647	**Pinnularia sp. aff. Nav.digitoradiata**	*(Greg.) Ralfs*	**2,99**	0,53	**8,18**	0,54	**1,32**	0,6	**-0,49**	0,48						0
108	**4240**	4240	**Pinnularia subcapitata**	*Gregory*	**3,32**	0,82	**7,78**	1,09	**0,57**	0,97	**-0,22**	0,52						0
109	**4250**	4250	**Pinnularia tropica**	*Hustedt*	**1,92**	0,33	**6,72**	0,46	**0,74**	0,86	**0,68**	0,45						0
110	**4501**	4501	**Rhoicosphenia abbreviata**	*(Agardh) Lange-B.*	**3,23**	0,82	**8,05**	0,99					*					1
111	**4602**	4602	**Rhopalodia gibba + var.minuta**	*(Ehr.) Müller*	**2,80**	0,68	**8,14**	0,96	**0,45**	0,78	**0,30**	0,35	*					1
112	**4603G**	4603	**Rhopalodia gibberula**	*(Ehr.) Müller*	**3,91**	0,46	**9,24**	0,96	**1,75**	0,79	**0,32**	0,7	*		*			1
113	**4601G**	4601	**Rhopalodia vermicularis**	*Müller*	**2,78**	0,7	**8,58**	1,31	**0,25**	1,19	**0,55**	0,47	*					1
114	**4802**	4802	**Stauroneis anceps** +var. linearis +f.gracilis	*Ehrenberg*	**2,16**	0,35	**6,95**	0,81	**0,06**	0,56	**0,47**	0,29	*					1
115	**4808**	4808	**Stauroneis phoenicenteron**	*(Nitzsch) Ehr.*	**2,55**	0,53	**7,03**	1,02	**0,24**	0,55	**0,69**	0,56	*					1
116	**5325**	5325	**Surirella linearis**	*Smith*	**2,25**	0,39	**6,84**	0,78	**0,40**	0,24	**0,49**	0,24	*					1
117	**5300**	5300	**Surirella sp.**	*Lange-Bertalot*									*				*	5
118	**5401G**	5401	**Synedra acus**, *bzw. F. tenera*	*Kützing*	**2,38**	0,38	**7,61**	0,64	**0,22**	0,45	**0,59**	0,34	*				*	5
119	**5402**	5402	**Synedra acus v. angustissima**	*Grunow*	**2,40**	0,03	**7,82**	0,42	**0,77**	0,76	**0,90**	0,05	*	*				2
120	**5403**	5403	**Synedra acus v. radians**	*(Kütz.) Hustedt*	**2,58**	0,27	**8,56**	0,57	**0,35**	0,44	**0,55**	0,57	*	*				2
121	**5417G**	5417	**Synedra rumpens**, *bzw. F. capucina var.*	*Kützing*	**2,34**	0,29	**7,80**	0,65	**0,43**	0,57	**0,55**	0,68	*	*				2
122	**5424**	5424	**Synedra ulna var. ulna**	*(Nitzsch) Ehr.*	**2,59**	0,6	**7,71**	0,89	**0,14**	0,49	**-0,09**	0,75	*				*	5
123	**5701**	5701	**Thalossiosira faurii**	*(Gasse) Hasle*	**3,95**	0,61	**9,19**	0,44	**1,49**	1,24	**0,21**	0,23					*	4
124	**5702**	5702	**Thalassiosira rudolfi**	*Bachmann*	**4,06**	0,61	**9,60**	0,6	**2,36**	0,65	**0,35**	0,21			*		*	4

Results of diatom counts for quantitative reconstruction of paleolimnological conditions during lake-highstand periods of paleo-Lake Naivasha at ~135, ~110 and ~80 kyr B.P.

Listen are results of cummulative counts (total and % of sum) for
- 19 samples for highstand IX
- 10 samples for highstand VIII
- 9 samples for highstand V
- 18 samples for part of high-resolution analyses in highst. IX.

Confer interpretation of these counts in chapter 3 'Quantitative reconstruction of paleohydrologic and hydrochemical characteristics during lake-highstand periods of Lake Naivasha'.

Appendix B.2 Results of diatom counts on Late Pleistocene sediments, paleo-Lake Naivasha
profile nr. 102 - Ol Njorowa Gorge, highstands IX, VIII
profile nr. 105 - Ol Njorowa Gorge, highstand V

nr.	ID after Gasse, 1995	Matlab ID	taxa name	sample: HIX_7.5-10.0 depth (cm) **9** reference		%		HIX_22.5-25.0 **24** %
			counted valves <total>:	**30.369**	total:	473,5	total:	347
1	**0103**	103	**Achnanthes clevei**	*Grunow*	8,0	1,690	1,5	0,432
2	**0151**	151	**Achnanthes conspicua + engelbrechti!**	*Mayer*		0,000		0,000
3	**0104**	104	**Achnanthes exigua**	*Grunow*		0,000		0,000
4	**0107**	107	**Achnanthes hungarica**	*Grunow*		0,000		0,000
5	**0108**	108	**Achnanthes inflata**	*Kützing*		0,000		0,000
6	**0113G**	113	**Achnanthes minutissima var.**	*Kützing*	4,0	0,845	2,0	0,576
7	**0118**	118	**Achnanthes subhudsonis**	*Hustedt*		0,000		0,000
8	**0311**	311	**Amphora aequalis**	*Krammer*		0,000		0,000
9	**0377**	377	**Amphora inariensis**	*Krammer*		0,000		0,000
10	**0325**	325	**Amphora ovalis + A.lybica**	*(Kütz.) Ehrenberg*	4,0	0,845		0,000
11	**0326**	326	**Amphora pediculus**	*(Kütz.) Grunow*		0,000		0,000
12	**0370**	370	**Amphora veneta**	*Kützing*		0,000		0,000
13	**0506**	506	**Anomoeoneis sphaerphora**	*(Kütz.) Pfitzer*		0,000		0,000
14	**0503**	503	**Anomoeoneis vitrea**	*(Grun)Ross*	1,0	0,211	3,0	0,865
15	**3501**	3501	**Aulacoseira agassizii + v.malayensis**	*Ostenfeld*		0,000		0,000
16	**3502**	3502	**Aulacoseira ambigua**	*(Grun.) Sim.*		0,000		0,000
17	**3506**	3506	**Aulacoseira goetzeana**	*(Müller) Sim.*		0,000	1,0	0,288
18	**3507**	3507	**Aulacoseira granulata + muzzanensis**	*(Ehr.) Ralfs*	9,0	1,901	2,0	0,576
19	**3508**	3508	**Aulacoseira granulata var.angustissima**	*(Müller) Sim.*	2,0	0,422		0,000
20	**3510G**	3510	**Aulacoseira granulata var.valida**	*Hustedt*		0,000		0,000
21	**0904G**	904	**Caloneis bacillum**	*(Grun.) Mer.*		0,000		0,000
22	**1401**	1401	**Cocconeis diminuta**	*Pantocsek*	1,0	0,211		0,000
23	**1403**	1403	**Cocconeis placentula + v.euglypta**	*(Ehr.) Cleve*	11,0	2,323	1,0	0,288
24	**1405**	1405	**Cocconeis thumensis**	*Mayer*	11,0	2,323	3,0	0,865
25	**1610**	1610	**Cyclotella glomerata**	*Bachmann*		0,000		0,000
26	**1655**	1655	**Cyclotella iris**	*Brun & Héribaud*		0,000		0,000
27	**1620**	1620	**Cyclotella meneghiniana + v.pumila**	*Kützing*		0,000		0,000
28	**1625**	1625	**Cyclotella ocellata**	*Pantocsek*		0,000	4,0	1,153
29	**1635**	1635	**Cyclotella stelligera + v.tenuis**	*Cl. & Grunow*	5,0	1,056	5,0	1,441
30	**1901**	1901	**Cymbella affinis**	*Kützing*	5,0	1,056		0,000
31	**1904**	1904	**Cymbella cistula**	*(Hempr.) Grunow*	6,0	1,267	4,5	1,297
32	**1911G**	1911	**Cymbella microcephala**	*Grunow*	2,0	0,422	4,0	1,153
33	**1912**	1912	**Cymbella muellerii**	*Müller*	11,0	2,323	4,0	1,153
34	**1913**	1913	**Cymbella naviculiformis**	*Auerswald*	1,0	0,211		0,000
35	**1920**	1920	**Cymbella pusilla**	*Grunow*		0,000		0,000
36	**1917**	1917	**Cymbella turgida**	*Greg.*		0,000		0,000
37	**1946**	1946	**Cymbella turgidula**	*Grunow*		0,000		0,000
38	**1918**	1918	**Cymbella ventricosa + C.silesiaca**	*Agardh*				
39	**2301**	2301	**Diploneis elyptica**	*(Kütz.) Cleve*	2,0	0,422		0,000
40	**2303**	2303	**Diploneis ovalis**	*(Hilse) Vleve*				
41	**2406**	2406	**Epithemia adnata + var.**	*Ehrenberg*	38,0	8,025	10,5	3,026
42	**2402**	2402	**Epithemia argus**	*(Ehr.) Kützing*		0,000		0,000
43	**2404**	2404	**Epithemia sorex + v.gracilis**	*Kützing*	13,5	2,851	3,0	0,865
44	**2405**	2405	**Epithemia turgida**	*Ehrenberg*	2,0	0,422		0,000
45	**2504**	2504	**Eunotia curvata**	*(Kütz.) Lagerstedt*				
46	**2503**	2503	**Eunotia flexuosa**	*(Bréb)Kützing*		0,000		0,000
47	**2506G**	2506	**Eunotia pectinalis**	*(Dyllwyn) Rabenh.*		0,000		0,000
48	**2516**	2516	**Eunotia praerupta**	*Ehrenberg*		0,000		0,000
49	**2601**	2601	**Fragilaria africana**	*Hustedt*	13,5	2,851	14,0	4,035
50	**2602**	2602	**Fragilaria brevistrata + var.**	*Grunow*	92,0	19,430	78,0	22,478
51	**2606**	2606	**Fragilaria construens + v.venter**	*(Ehr.) Grunow*	15,0	3,168	44,0	12,680
52	**2611**	2611	**Fragilaria lapponica**	*Grunow*		0,000		0,000
53	**2612**	2612	**Fragilaria leptostauron + var. dubia**	*(Ehr.) Hust.*		0,000		0,000
54	**2613**	2613	**Fragilaria pinnata**	*Ehrenberg*	102,0	21,542	92,0	26,513
55	**2615**	2615	**Fragilaria virescens**	*Ralfs*		0,000		0,000
56	**2603G**	2603	**Fragilaria zeilleri +v.africana+elliptica G**	*Héribaud*	2,0	0,422		0,000
57	**2910**	2910	**Gomphonema affine**	*Kützing*				
58	**2917G**	2917	**Gomphonema clavatum**	*Ehrenberg*		0,000		0,000
59	**2904**	2904	**Gomphonema clevei v. javanica**	*Hustedt*		0,000	6,0	1,729
60	**2908G**	2908	**Gomphonema gracile + G.lanceolatum**	*Ehrenberg*	8,5	1,795		0,000
61	**2912G**	2912	**Gomphonema intricatum/ angustum**	*(Agardh)*	4,0	0,845	6,0	1,729
62	**2923**	2923	**Gomphonema parvulum**	*Kützing*	2,0	0,422	2,0	0,576
63	**3201**	3201	**Hantzschia amphioxys**	*(Ehr.) Grunow*		0,000		0,000
64	**3302**	3302	**Mastogloia braunii**	*Grunow*		0,000		0,000
65	**3303**	3303	**Mastogloia elliptica + v.dansei + v.ellipt.**	*(Ag.) Cleve*	13,0	2,746	2,5	0,720
66	**3305G**	3305	**Mastogloia smithi + var.**	*Thwaites*		0,000		0,000
67	**3607G**	3607	**Navicula cari + graciloides**	*Ehrenberg*		0,000		0,000
68	**3613**	3613	**Navicula cryptocephala + v.lancettula**	*Kützing*				

nr.	ID after Gasse, 1995	Matlab ID	taxa name	reference	sample: HIX_7.5-10.0 depth (cm) 9		HIX_22.5-25.0 24	
						%		%
69	**3615**	3615	**Navicula cryptocephala var. veneta**	*Kützing*		0,000		0,000
70	**3617G**	3617	**Navicula cuspidata + var. ambigua**	*Kützing*		0,000		0,000
71	**3620**	3620	**Navicula damasii + vitabunda**	*Hustedt*		0,000	1,0	0,288
72	**3621G**	3621	**Navicula decussis**	*Oestrup*		0,000		0,000
73	**3622**	3622	**Navicula elkab**	*Müller*		0,000		0,000
74	**---**	9991	**Navicula globosa**	*Meister*		0,000		0,000
75	**---**	9992	**Navicula modica**	*Hustedt*		0,000		0,000
76	**3712G**	3712	**Navicula mutica + vars**	*Kützing*				
77	**3767**	3767	**Navicula oblonga**	*Kützing*		0,000		0,000
78	**3728**	3728	**Navicula pupula + platycephala**	*Kützing*	1,0	0,211		0,000
79	**3730**	3730	**Navicula radiosa**	*Kützing*		0,000	1,0	0,288
80	**3732**	3732	**Navicula rhyncocephala**	*Hustedt*		0,000		0,000
81	**3738**	3738	**Navicula schoenfeldii + var. pusilla**	*Hustedt*		0,000	3,0	0,865
82	**3742**	3742	**Navicula seminuloides**	*Hustedt*	1,0	0,211	5,0	1,441
83	**3743**	3743	**Navicula seminulum**	*Grunow*	2,0	0,422	6,0	1,729
84	**3606**	3606	**Navicula sp. aff. bacilum**	*Ehrenberg*		0,000		0,000
85	**3638**	3638	**Navicula sp. aff. hungarica**	*Grunow*		0,000		0,000
86	**3627G**	3627	**Navicula subminuscula + perparva**	*Manguin*				
87	**3739G**	3739	**Navicula tenella + Nav.cryptotenella**	*Brébisson*		0,000	1,0	0,288
88	**3757**	3757	**Navicula ventralis + pseudoventralis**	*Krasske*		0,000	2,0	0,576
89	**3906**	3906	**Nitzschia amphibia + f.frauenfeldii**	*Grunow*	8,5	1,795	4,5	1,297
90	**3922**	3922	**Nitzschia bacilum + fonticola**	*Hustedt*	2,0	0,422		0,000
91	**3918**	3918	**Nitzschia epiphytica**	*Müller*	2,0	0,422		0,000
92	**3925**	3925	**Nitzschia frustulum sp.**	*(Kütz.) Grun.*	2,0	0,422		0,000
93	**3942G**	3942	**Nitzschia frustulum sp.aff. inconspicua**	*Grunow*	4,0	0,845		0,000
94	**3936**	3936	**Nitzschia goetzeana**	*Hustedt*				
95	**3932G**	3932	**Nitzschia gracilis agg.**	*Hantzsch*				
96	**3946**	3946	**Nitzschia lacuum**	*Lange-Bertalot*	2,0	0,422		0,000
97	**4003**	4003	**Nitzschia lancettula**	*O. Müller*	6,0	1,267	12,0	3,458
98	**4012**	4012	**Nitzschia palea**	*(Kütz.) Smith*				
99	**4016**	4016	**Nitzschia paleacea**	*Grunow*		0,000		0,000
100	**3954**	4042	**Nitzschia thermalis + var.**	*(Ehr.) Auerswald*				
101	**4037**	4037	**Nitzschia tropica**	*Grunow*	3,0	0,634		0,000
102	**4070**	4070	**Nitzschia vanoyei**	*Cholnoky*	15,0	3,168	8,0	2,305
103	**4201**	4201	**Pinnularia acrosphaeria**	*Rabenhorst*		0,000		0,000
104	**4208**	4208	**Pinnularia gibba +var. sancta+v.linearis**	*Ehrenberg*	2,0	0,422		0,000
105	**4230**	4230	**Pinnularia intermedia**	*(Lagerst.) Cleve*	1,0	0,211		0,000
106	**4220**	4220	**Pinnularia maior**	*Rabenhorst*				
107	**3647**	3647	**Pinnularia sp. aff. Nav.digitoradiata**	*(Greg.) Ralfs*				
108	**4240**	4240	**Pinnularia subcapitata**	*Gregory*				
109	**4250**	4250	**Pinnularia tropica**	*Hustedt*		0,000		0,000
110	**4501**	4501	**Rhoicosphenia abbreviata**	*(Agardh) Lange-B.*		0,000		0,000
111	**4602**	4602	**Rhopalodia gibba + var.minuta**	*(Ehr.) Müller*	7,5	1,584	1,5	0,432
112	**4603G**	4603	**Rhopalodia gibberula**	*(Ehr.) Müller*		0,000		0,000
113	**4614**	4601	**Rhopalodia vermicularis**	*Müller*		0,000	2,0	0,576
114	**4802**	4802	**Stauroneis anceps +var. linearis +f.gracil**	*Ehrenberg*		0,000		0,000
115	**4808**	4808	**Stauroneis phoenicenteron**	*(Nitzsch) Ehr.*		0,000		0,000
116	**5325**	5325	**Surirella linearis**	*Smith*				
117	**5300**	5300	**Surirella sp.**	*Lange-Bertalot*		0,000		0,000
118	**5401G**	5401	**Synedra acus, bzw. F. tenera**	*Kützing*	6,5	1,373	2,0	0,576
119	**5402**	5402	**Synedra acus v. angustissima**	*Grunow*				
120	**5403**	5403	**Synedra acus v. radians**	*(Kütz.) Hustedt*				
121	**5417G**	5417	**Synedra rumpens, bzw. F. capucina var.**	*Kützing*	0,5	0,106	3,5	1,009
122	**5424**	5424	**Synedra ulna var. ulna**	*(Nitzsch) Ehr.*	19,0	4,013	1,5	0,432
123	**5701**	5701	**Thalossiosira faurii**	*(Gasse) Hasle*		0,000		0,000
124	**5702**	5702	**Thalassiosira rudolfi**	*Bachmann*				
					0	100	0	100

ID after Gasse, 1995	HIX_37.5-40.0 **39**		HIX_52.5-55.0 **54**		HIX_67.5-70.0 **69**		HIX_72.5-75.0 **74**		HIX_107.5-110.0 **109**		HIX_137.5-140.0 **139**	
		%		%		%		%		%	numb.	%
	total:	484,5	total:	337,5	total:	691,5	total:	309	total:	832,5	total:	1179
0103	3,0	0,619	2,0	0,593	3,0	0,434		0,000		0,000	14,0	1,187
0151		0,000		0,000		0,000		0,000		0,000		0,000
0104		0,000		0,000		0,000		0,000		0,000	1,0	0,085
0107		0,000		0,000		0,000		0,000		0,000	6,0	0,509
0108		0,000		0,000		0,000		0,000		0,000		0,000
0113G	38,0	7,843	8,5	2,519	12,5	1,808	5,0	1,618	52,0	6,246	30,0	2,545
0118		0,000		0,000		0,000		0,000		0,000		0,000
0311		0,000		0,000		0,000		0,000		0,000		0,000
0377		0,000		0,000		0,000		0,000		0,000	2,0	0,170
0325		0,000		0,000		0,000		0,000		0,000		0,000
0326		0,000	1,0	0,296		0,000		0,000	2,0	0,240	4,0	0,339
0370		0,000		0,000		0,000		0,000		0,000		0,000
0506		0,000		0,000		0,000	0,5	0,162		0,000	0,5	0,042
0503	10,5	2,167		0,000		0,000		0,000		0,000		0,000
3501		0,000		0,000		0,000		0,000		0,000		0,000
3502		0,000		0,000		0,000		0,000		0,000		0,000
3506		0,000	1,0	0,296		0,000	2,0	0,647		0,000		0,000
3507	5,0	1,032	10,0	2,963	3,0	0,434	10,0	3,236	15,0	1,802	22,0	1,866
3508		0,000		0,000		0,000	1,0	0,324		0,000		0,000
3510G		0,000		0,000		0,000		0,000	2,0	0,240		0,000
0904G		0,000		0,000		0,000		0,000		0,000		0,000
1401		0,000	1,0	0,296		0,000		0,000		0,000		0,000
1403	5,0	1,032	1,0	0,296	2,5	0,362	15,0	4,854	5,0	0,601	114,5	9,712
1405		0,000		0,000		0,000		0,000		0,000	2,0	0,170
1610	3,0	0,619		0,000	2,0	0,289	3,0	0,971	3,0	0,360	5,0	0,424
1655		0,000		0,000		0,000		0,000		0,000		0,000
1620		0,000		0,000		0,000		0,000		0,000		0,000
1625	22,0	4,541	18,0	5,333	21,0	3,037	21,0	6,796	106,0	12,733	101,0	8,567
1635	3,5	0,722	5,0	1,481	4,0	0,578	2,0	0,647	12,0	1,441	17,0	1,442
1901	2,0	0,413		0,000	1,0	0,145		0,000	13,0	1,562	11,0	0,933
1904	9,0	1,858	7,5	2,222		0,000	5,0	1,618	9,0	1,081	6,0	0,509
1911G	7,0	1,445	4,0	1,185	2,0	0,289	3,0	0,971	4,0	0,480	2,0	0,170
1912	4,0	0,826	1,0	0,296		0,000	3,0	0,971	5,0	0,601	16,5	1,399
1913		0,000		0,000		0,000		0,000	1,0	0,120		0,000
1920	3,0	0,619		0,000		0,000		0,000		0,000		0,000
1917	2,0	0,413		0,000		0,000		0,000		0,000		0,000
1946	4,5	0,929		0,000		0,000		0,000		0,000		0,000
1918												
2301		0,000		0,000		0,000		0,000		0,000		0,000
2303												
2406	60,5	12,487	9,5	2,815	19,5	2,820	5,0	1,618	56,0	6,727	19,0	1,612
2402		0,000		0,000		0,000		0,000	27,0	3,243		0,000
2404	20,5	4,231	10,5	3,111	10,0	1,446	12,0	3,883	7,5	0,901	37,0	3,138
2405	1,5	0,310	2,5	0,741		0,000		0,000		0,000	1,0	0,085
2504												
2503		0,000		0,000		0,000		0,000		0,000		0,000
2506G		0,000		0,000		0,000		0,000		0,000	6,5	0,551
2516		0,000		0,000		0,000		0,000	0,5	0,060		0,000
2601	1,0	0,206	3,5	1,037	1,0	0,145		0,000	6,0	0,721	1,0	0,085
2602	27,0	5,573	53,0	15,704	27,0	3,905	16,0	5,178	58,0	6,967	82,0	6,955
2606	13,0	2,683	40,0	11,852	275,0	39,769	60,0	19,417	48,0	5,766	136,0	11,535
2611		0,000		0,000		0,000		0,000		0,000		0,000
2612		0,000	1,0	0,296	2,0	0,289		0,000		0,000	7,0	0,594
2613	30,0	6,192	60,0	17,778	261,0	37,744	52,0	16,828	70,0	8,408	187,0	15,861
2615		0,000		0,000		0,000		0,000		0,000		0,000
2603G		0,000		0,000		0,000		0,000		0,000	6,0	0,509
2910												
2917G		0,000		0,000		0,000		0,000		0,000		0,000
2904	2,0	0,413	8,5	2,519	1,5	0,217	1,0	0,324	19,0	2,282		0,000
2908G	21,5	4,438		0,000		0,000		0,000	19,5	2,342	7,5	0,636
2912G	86,0	17,750	17,0	5,037	3,5	0,506	46,0	14,887	129,0	15,495	138,0	11,705
2923		0,000	1,0	0,296	2,0	0,289		0,000		0,000	4,0	0,339
3201		0,000		0,000		0,000		0,000		0,000		0,000
3302		0,000		0,000		0,000		0,000		0,000		0,000
3303	14,0	2,890	6,0	1,778	1,0	0,145	3,0	0,971	14,0	1,682	4,5	0,382
3305G		0,000		0,000		0,000		0,000		0,000		0,000
3607G		0,000		0,000		0,000		0,000		0,000		0,000
3613												

	HIX_37.5-40.0		HIX_52.5-55.0		HIX_67.5-70.0		HIX_72.5-75.0		HIX_107.5-110.0		HIX_137.5-140.0	
ID after	**39**		**54**		**69**		**74**		**109**		**139**	
Gasse, 1995		%		%		%		%		%	numb.	%
3615		0,000		0,000		0,000		0,000		0,000		0,000
3617G		0,000		0,000		0,000		0,000		0,000		0,000
3620		0,000		0,000		0,000		0,000		0,000		0,000
3621G		0,000		0,000		0,000		0,000		0,000	7,0	0,594
3622		0,000		0,000		0,000		0,000		0,000	1,0	0,085
---		0,000		0,000		0,000	1,0	0,324		0,000	1,0	0,085
---		0,000		0,000		0,000		0,000		0,000		0,000
3712G												
3767		0,000		0,000		0,000		0,000		0,000	4,5	0,382
3728		0,000		0,000		0,000		0,000		0,000	4,5	0,382
3730	4,5	0,929	1,5	0,444	3,0	0,434	2,0	0,647	5,0	0,601	3,0	0,254
3732		0,000		0,000		0,000		0,000		0,000		0,000
3738	1,0	0,206		0,000		0,000		0,000		0,000		0,000
3742	1,0	0,206	1,0	0,296	1,0	0,145	2,0	0,647		0,000		0,000
3743	6,0	1,238	5,0	1,481	2,0	0,289	2,0	0,647		0,000	4,0	0,339
3606		0,000		0,000		0,000		0,000		0,000		0,000
3638		0,000		0,000		0,000		0,000		0,000		0,000
3627G												
3739G	8,0	1,651	2,0	0,593		0,000		0,000	6,0	0,721	2,0	0,170
3757		0,000		0,000	2,0	0,289		0,000	1,0	0,120	6,5	0,551
3906	17,5	3,612	9,0	2,667	5,5	0,795	3,0	0,971	45,0	5,405	68,0	5,768
3922		0,000		0,000		0,000		0,000		0,000	3,0	0,254
3918	2,0	0,413	2,0	0,593	2,0	0,289		0,000	3,0	0,360		0,000
3925		0,000		0,000		0,000		0,000		0,000		0,000
3942G		0,000	3,0	0,889		0,000		0,000	4,0	0,480	5,5	0,466
3936												
3932G												
3946		0,000		0,000	2,0	0,289		0,000	1,0	0,120		0,000
4003	4,0	0,826	5,0	1,481	3,0	0,434	9,0	2,913		0,000	3,0	0,254
4012												
4016		0,000		0,000		0,000		0,000		0,000		0,000
3954												
4037	2,5	0,516	1,0	0,296		0,000	5,0	1,618	4,5	0,541	24,0	2,036
4070	1,0	0,206	19,0	5,630	4,0	0,578	1,0	0,324	2,0	0,240	3,0	0,254
4201		0,000		0,000		0,000		0,000		0,000		0,000
4208	3,0	0,619		0,000		0,000		0,000		0,000		0,000
4230		0,000		0,000	1,0	0,145		0,000		0,000	0,5	0,042
4220												
3647												
4240												
4250		0,000		0,000		0,000		0,000		0,000		0,000
4501	2,0	0,413		0,000		0,000		0,000		0,000		0,000
4602	12,5	2,580	5,5	1,630	1,5	0,217	6,5	2,104		0,000	14,0	1,187
4603G		0,000		0,000		0,000		0,000	54,0	6,486		0,000
4614	1,0	0,206	2,0	0,593		0,000		0,000		0,000	3,0	0,254
4802		0,000		0,000		0,000		0,000		0,000		0,000
4808		0,000		0,000		0,000		0,000		0,000		0,000
5325												
5300		0,000		0,000		0,000		0,000		0,000	2,0	0,170
5401G	11,0	2,270	3,0	0,889	3,0	0,434	2,5	0,809	6,5	0,781	10,5	0,891
5402												
5403												
5417G	2,5	0,516	0,5	0,148		0,000		0,000	2,0	0,240		0,000
5424	6,5	1,342	5,5	1,630	7,0	1,012	9,5	3,074	15,0	1,802	18,0	1,527
5701		0,000		0,000		0,000		0,000		0,000		0,000
5702												
	0	100	0	100	0	100	0	100	0	100	0	100

ID after Gasse, 1995	HIX_162.5-165.0 **164**		HIX_175.0-177.5 **176**		HIX_187.5-190.0 **189**		HIX_195.0-197.5 **196**		HIX_202.5-205.0 **204**		HIX_212.5-215.0 **214**	
	numb.	%	numb.	%	numb.	%	numb.	%	numb.	%	numb.	%
	total:	751	total:	233,5	total:	1712	total:	235,5	total:	2385	total:	1975
0103	1,0	0,133	1,0	0,428	8,0	0,467	2,0	0,849	2,0	0,084	5,0	0,253
0151		0,000	2,0	0,857		0,000		0,000		0,000		0,000
0104		0,000		0,000		0,000		0,000		0,000		0,000
0107		0,000		0,000		0,000	1,0	0,425	5,0	0,210	4,0	0,203
0108		0,000		0,000		0,000		0,000		0,000		0,000
0113G	8,0	1,065	3,0	1,285	14,0	0,818	17,0	7,219	49,0	2,055	40,5	2,051
0118		0,000		0,000		0,000		0,000		0,000		0,000
0311		0,000		0,000		0,000		0,000		0,000		0,000
0377	13,0	1,731		0,000		0,000		0,000		0,000	8,0	0,405
0325	2,0	0,266		0,000		0,000		0,000	2,0	0,084	6,0	0,304
0326	3,0	0,399	6,0	2,570	1,0	0,058		0,000	53,0	2,222	6,0	0,304
0370		0,000		0,000		0,000		0,000		0,000		0,000
0506		0,000		0,000		0,000		0,000		0,000		0,000
0503		0,000		0,000		0,000	1,5	0,637		0,000		0,000
3501		0,000		0,000		0,000		0,000		0,000		0,000
3502		0,000		0,000		0,000		0,000		0,000		0,000
3506		0,000	2,0	0,857	46,5	2,716	4,0	1,699	25,0	1,048	30,0	1,519
3507	43,5	5,792	15,0	6,424	145,0	8,470	29,0	12,314	239,0	10,021	83,0	4,203
3508	10,0	1,332	1,0	0,428	37,0	2,161		0,000	5,0	0,210	18,0	0,911
3510G	6,0	0,799	10,0	4,283	80,0	4,673	13,0	5,520	365,0	15,304	307,0	15,544
0904G		0,000		0,000		0,000		0,000		0,000		0,000
1401		0,000		0,000		0,000		0,000		0,000		0,000
1403	122,0	16,245	24,5	10,493	11,5	0,672	37,5	15,924	258,0	10,818	131,0	6,633
1405		0,000	1,0	0,428		0,000		0,000	1,0	0,042	2,0	0,101
1610		0,000	5,0	2,141	4,0	0,234	18,0	7,643	11,0	0,461	69,0	3,494
1655		0,000		0,000		0,000		0,000		0,000		0,000
1620		0,000		0,000		0,000		0,000		0,000		0,000
1625	58,0	7,723	15,0	6,424	131,0	7,652	22,0	9,342	403,0	16,897	219,0	11,089
1635	7,0	0,932	2,0	0,857	25,0	1,460	9,0	3,822	91,5	3,836	97,0	4,911
1901	14,0	1,864		0,000	17,0	0,993		0,000	7,0	0,294	6,5	0,329
1904	5,5	0,732	2,0	0,857	8,0	0,467	2,0	0,849	1,5	0,063	18,0	0,911
1911G		0,000		0,000		0,000	1,0	0,425		0,000	2,0	0,101
1912	10,0	1,332	4,5	1,927		0,000	1,0	0,425	5,0	0,210	5,0	0,253
1913	1,0	0,133		0,000		0,000		0,000		0,000		0,000
1920		0,000		0,000		0,000		0,000		0,000		0,000
1917		0,000		0,000		0,000	1,0	0,425		0,000		0,000
1946		0,000		0,000		0,000		0,000		0,000		0,000
1918												
2301	2,0	0,266		0,000	3,5	0,204		0,000		0,000	1,0	0,051
2303												
2406	55,5	7,390	6,0	2,570	37,0	2,161	2,5	1,062	141,0	5,912	41,0	2,076
2402		0,000		0,000		0,000		0,000		0,000		0,000
2404	24,5	3,262	3,0	1,285	46,5	2,716	1,0	0,425	16,5	0,692	18,0	0,911
2405	4,0	0,533	1,0	0,428		0,000	1,0	0,425	1,5	0,063	2,0	0,101
2504												
2503		0,000		0,000		0,000		0,000		0,000		0,000
2506G	1,5	0,200		0,000	1,0	0,058		0,000	3,5	0,147	5,0	0,253
2516		0,000		0,000		0,000		0,000		0,000		0,000
2601	4,0	0,533	6,0	2,570	4,0	0,234		0,000	10,5	0,440	13,0	0,658
2602	31,5	4,194	32,0	13,704	201,0	11,741	10,0	4,246	87,0	3,648	123,0	6,228
2606	26,5	3,529	25,0	10,707	309,5	18,078	3,0	1,274	96,0	4,025	131,0	6,633
2611		0,000	1,0	0,428		0,000		0,000		0,000		0,000
2612		0,000		0,000		0,000		0,000	3,0	0,126	2,0	0,101
2613	72,0	9,587	16,0	6,852	342,0	19,977	4,0	1,699	81,0	3,396	211,0	10,684
2615		0,000		0,000		0,000		0,000		0,000		0,000
2603G		0,000		0,000	1,0	0,058		0,000		0,000		0,000
2910												
2917G		0,000		0,000		0,000		0,000		0,000		0,000
2904	5,5	0,732		0,000	13,5	0,789	4,0	1,699	35,0	1,468	2,5	0,127
2908G	1,0	0,133	1,0	0,428	9,5	0,555	1,0	0,425	2,0	0,084	11,5	0,582
2912G	97,0	12,916	6,0	2,570	79,5	4,644	26,0	11,040	154,0	6,457	165,0	8,354
2923		0,000		0,000	1,0	0,058		0,000	3,0	0,126	3,0	0,152
3201		0,000		0,000		0,000		0,000		0,000		0,000
3302		0,000		0,000		0,000		0,000		0,000		0,000
3303	3,0	0,399	1,5	0,642	17,0	0,993	4,0	1,699	18,0	0,755	25,5	1,291
3305G		0,000		0,000		0,000		0,000		0,000		0,000
3607G		0,000		0,000		0,000		0,000		0,000	2,0	0,101
3613												

ID after Gasse, 1995	HIX_162.5-165.0 **164**		HIX_175.0-177.5 **176**		HIX_187.5-190.0 **189**		HIX_195.0-197.5 **196**		HIX_202.5-205.0 **204**		HIX_212.5-215.0 **214**	
	numb.	%	numb.	%	numb.	%	numb.	%	numb.	%	numb.	%
3615		0,000		0,000		0,000		0,000		0,000		0,000
3617G		0,000		0,000		0,000		0,000		0,000		0,000
3620		0,000		0,000		0,000		0,000		0,000		0,000
3621G	2,0	0,266		0,000		0,000		0,000		0,000		0,000
3622		0,000		0,000		0,000		0,000		0,000		0,000
---		0,000		0,000	1,0	0,058		0,000	1,0	0,042		0,000
---		0,000		0,000		0,000		0,000		0,000		0,000
3712G												
3767		0,000		0,000		0,000		0,000		0,000		0,000
3728		0,000		0,000		0,000	1,0	0,425		0,000	0,5	0,025
3730		0,000		0,000	5,5	0,321		0,000	3,5	0,147	6,5	0,329
3732		0,000		0,000		0,000		0,000		0,000		0,000
3738		0,000	1,0	0,428		0,000		0,000	5,0	0,210	2,0	0,101
3742	1,0	0,133		0,000		0,000		0,000		0,000	2,0	0,101
3743		0,000	3,0	1,285	4,0	0,234	1,0	0,425	1,0	0,042		0,000
3606	2,5	0,333		0,000	2,0	0,117		0,000	5,0	0,210		0,000
3638		0,000		0,000		0,000		0,000		0,000		0,000
3627G												
3739G	5,5	0,732		0,000	2,0	0,117	3,5	1,486	8,0	0,335	3,0	0,152
3757		0,000		0,000	1,0	0,058	1,0	0,425	1,0	0,042	1,0	0,051
3906	14,0	1,864	4,5	1,927	24,5	1,431	1,0	0,425	25,5	1,069	30,0	1,519
3922	3,0	0,399	1,0	0,428	2,0	0,117	1,0	0,425	18,0	0,755	5,0	0,253
3918	11,0	1,465		0,000		0,000		0,000		0,000		0,000
3925		0,000		0,000		0,000		0,000		0,000		0,000
3942G		0,000		0,000	7,0	0,409		0,000	15,0	0,629	7,0	0,354
3936												
3932G												
3946		0,000		0,000	4,0	0,234		0,000	41,0	1,719	20,0	1,013
4003	4,5	0,599	3,0	1,285	20,0	1,168		0,000	5,0	0,210	5,5	0,278
4012												
4016		0,000		0,000		0,000		0,000		0,000		0,000
3954												
4037	24,0	3,196	11,5	4,925	4,0	0,234	3,0	1,274	16,0	0,671	16,5	0,835
4070	1,0	0,133	10,0	4,283	8,0	0,467	3,0	1,274	4,0	0,168	1,0	0,051
4201		0,000		0,000		0,000		0,000		0,000		0,000
4208		0,000		0,000	4,5	0,263		0,000		0,000		0,000
4230		0,000		0,000		0,000		0,000		0,000	0,5	0,025
4220												
3647												
4240												
4250		0,000		0,000		0,000		0,000		0,000		0,000
4501	2,0	0,266		0,000		0,000		0,000		0,000		0,000
4602	15,5	2,064	1,0	0,428	9,0	0,526	1,0	0,425	23,0	0,964	12,5	0,633
4603G		0,000		0,000		0,000		0,000		0,000		0,000
4614		0,000		0,000		0,000		0,000		0,000		0,000
4802		0,000		0,000		0,000		0,000		0,000		0,000
4808	6,5	0,866		0,000		0,000		0,000		0,000		0,000
5325												
5300		0,000		0,000	0,5	0,029		0,000		0,000		0,000
5401G	6,5	0,866		0,000	11,5	0,672		0,000	21,0	0,881	23,0	1,165
5402												
5403												
5417G	7,0	0,932	1,0	0,428		0,000	1,0	0,425	7,0	0,294	4,0	0,203
5424	13,0	1,731	5,0	2,141	7,5	0,438	3,5	1,486	10,0	0,419	21,5	1,089
5701		0,000		0,000		0,000		0,000		0,000		0,000
5702												
	0	100	0	100	0	100	0	100	0	100	0	100

ID after Gasse, 1995	HIX_225.0-227.5 **226** numb.	%	HIX_237.5-240.0 **239** numb.	%	HIX_262.5-265.0 **264**	%	HIX_292.5-295.0 **294**	%	HIX_312.5-315.0 **314**	%	HIX_302 **211,8** numb.	%
	total:	309,5	total:	1393,5		289,5		277,5		636	total:	207
0103	2,0	0,646	4,0	0,287		0,000		0,000		0,000		0,000
0151	5,0	1,616	3,0	0,215		0,000		0,000		0,000		0,000
0104	2,0	0,646		0,000		0,000		0,000		0,000		0,000
0107		0,000		0,000		0,000		0,000		0,000		0,000
0108		0,000		0,000		0,000		0,000		0,000		0,000
0113G	2,0	0,646	13,5	0,969	1,0	0,345	1,0	0,360	2,0	0,314	3,5	1,691
0118		0,000	1,0	0,072		0,000		0,000		0,000		0,000
0311		0,000		0,000		0,000		0,000	2,0	0,314		0,000
0377	0,5	0,162	3,0	0,215		0,000		0,000		0,000		0,000
0325		0,000	4,0	0,287		0,000		0,000	2,0	0,314		0,000
0326		0,000	10,0	0,718		0,000		0,000		0,000		0,000
0370		0,000	1,0	0,072		0,000		0,000		0,000		0,000
0506		0,000		0,000		0,000		0,000	2,0	0,314		0,000
0503		0,000		0,000		0,000	1,0	0,360		0,000		0,000
3501		0,000		0,000		0,000		0,000		0,000		0,000
3502		0,000		0,000		0,000		0,000		0,000		0,000
3506		0,000	40,0	2,870		0,000	3,0	1,081		0,000		0,000
3507	19,0	6,139	89,0	6,387	7,0	2,418	23,0	8,288	3,0	0,472	4,0	1,932
3508	1,0	0,323		0,000	1,0	0,345	3,0	1,081	1,0	0,157		0,000
3510G	31,0	10,016	114,0	8,181	39,0	13,472	15,0	5,405	3,0	0,472	8,0	3,865
0904G		0,000		0,000		0,000		0,000		0,000		0,000
1401		0,000		0,000		0,000		0,000		0,000		0,000
1403	5,0	1,616	108,5	7,786	7,0	2,418	8,0	2,883	10,0	1,572	12,5	6,039
1405		0,000	3,0	0,215		0,000		0,000	1,0	0,157		0,000
1610	3,0	0,969	24,0	1,722	1,0	0,345	2,0	0,721	2,0	0,314		0,000
1655		0,000		0,000		0,000		0,000		0,000		0,000
1620		0,000		0,000		0,000		0,000		0,000		0,000
1625	33,0	10,662	127,5	9,150	26,0	8,981	34,0	12,252	27,0	4,245	31,0	14,976
1635	3,0	0,969	78,0	5,597	3,0	1,036	11,0	3,964	5,0	0,786	4,0	1,932
1901		0,000	2,0	0,144	4,0	1,382	4,0	1,441	5,0	0,786	1,0	0,483
1904	1,0	0,323	1,0	0,072		0,000	1,5	0,541	1,0	0,157	3,0	1,449
1911G		0,000		0,000	1,0	0,345		0,000	2,0	0,314	1,0	0,483
1912	1,0	0,323	5,0	0,359	2,0	0,691	4,0	1,441	5,0	0,786		0,000
1913		0,000		0,000	1,0	0,345	1,0	0,360	4,0	0,629		0,000
1920		0,000		0,000		0,000		0,000		0,000		0,000
1917		0,000		0,000		0,000		0,000		0,000	1,0	0,483
1946		0,000		0,000		0,000		0,000		0,000		0,000
1918												
2301		0,000	0,5	0,036		0,000		0,000		0,000	1,5	0,725
2303												
2406	2,0	0,646	40,5	2,906	16,5	5,699	15,5	5,586	23,5	3,695	9,5	4,589
2402		0,000	4,5	0,323		0,000		0,000		0,000		0,000
2404	0,5	0,162		0,000	1,0	0,345	2,0	0,721		0,000	1,0	0,483
2405	1,0	0,323	0,5	0,036		0,000	1,5	0,541	1,5	0,236		0,000
2504												
2503		0,000		0,000		0,000	1,0	0,360		0,000		0,000
2506G		0,000		0,000		0,000	4,5	1,622	1,0	0,157		0,000
2516		0,000		0,000		0,000	1,0	0,360		0,000		0,000
2601	4,0	1,292	10,0	0,718	5,5	1,900	3,0	1,081	21,5	3,381	2,0	0,966
2602	42,0	13,570	88,0	6,315	21,0	7,254	10,0	3,604	70,0	11,006	19,0	9,179
2606	50,0	16,155	211,0	15,142	73,0	25,216	38,0	13,694	229,0	36,006	15,0	7,246
2611	4,0	1,292		0,000		0,000		0,000		0,000		0,000
2612		0,000	9,5	0,682		0,000		0,000	1,0	0,157	4,0	1,932
2613	68,0	21,971	194,0	13,922	46,0	15,889	44,0	15,856	127,0	19,969	49,0	23,671
2615		0,000		0,000		0,000		0,000	2,0	0,314		0,000
2603G		0,000		0,000		0,000	1,0	0,360	1,0	0,157		0,000
2910												0,000
2917G		0,000		0,000		0,000		0,000		0,000		0,000
2904		0,000	2,5	0,179		0,000		0,000	1,0	0,157		0,000
2908G		0,000		0,000	3,5	1,209	3,0	1,081	2,5	0,393		0,000
2912G	2,0	0,646	56,5	4,055	4,5	1,554	7,0	2,523	16,0	2,516	18,0	8,696
2923		0,000		0,000		0,000		0,000		0,000		0,000
3201		0,000		0,000		0,000		0,000		0,000		0,000
3302		0,000		0,000		0,000		0,000		0,000		0,000
3303		0,000	4,5	0,323	1,0	0,345	1,5	0,541	0,5	0,079	4,0	1,932
3305G		0,000		0,000		0,000		0,000		0,000		0,000
3607G		0,000		0,000		0,000		0,000		0,000		0,000
3613												

ID after Gasse, 1995	HIX_225.0-227.5 **226** numb.	%	HIX_237.5-240.0 **239** numb.	%	HIX_262.5-265.0 **264**	%	HIX_292.5-295.0 **294**	%	HIX_312.5-315.0 **314**	%	HIX_302 **211,8** numb.	%
3615		0,000		0,000		0,000		0,000		0,000		0,000
3617G		0,000		0,000		0,000		0,000		0,000		0,000
3620		0,000		0,000		0,000	5,0	1,802	2,0	0,314		0,000
3621G		0,000		0,000		0,000		0,000	2,0	0,314		0,000
3622		0,000		0,000		0,000		0,000		0,000		0,000
---	1,0	0,323	3,0	0,215	3,0	1,036	1,0	0,360	8,0	1,258		0,000
---		0,000		0,000		0,000		0,000		0,000		0,000
3712G												
3767		0,000		0,000		0,000		0,000		0,000		0,000
3728	1,0	0,323	1,0	0,072		0,000	1,5	0,541	2,5	0,393		0,000
3730	0,5	0,162	1,5	0,108		0,000	1,5	0,541	0,5	0,079		0,000
3732		0,000		0,000		0,000		0,000		0,000		0,000
3738	1,0	0,323		0,000		0,000		0,000		0,000		0,000
3742	3,0	0,969	1,0	0,072	1,0	0,345	1,0	0,360		0,000		0,000
3743	2,0	0,646	5,0	0,359		0,000		0,000	1,0	0,157	1,0	0,483
3606		0,000		0,000	1,0	0,345		0,000		0,000		0,000
3638		0,000		0,000		0,000	1,0	0,360		0,000		0,000
3627G												
3739G	1,0	0,323	7,0	0,502		0,000		0,000	0,5	0,079	0,5	0,242
3757	2,0	0,646	10,0	0,718		0,000		0,000		0,000		0,000
3906		0,000	17,0	1,220	5,0	1,727	3,0	1,081	5,0	0,786		0,000
3922		0,000	6,0	0,431		0,000	2,0	0,721	1,0	0,157		0,000
3918	3,0	0,969	7,0	0,502	2,0	0,691		0,000	2,0	0,314		0,000
3925		0,000		0,000		0,000		0,000		0,000		0,000
3942G		0,000	4,0	0,287	1,0	0,345		0,000	1,0	0,157		0,000
3936												
3932G												
3946		0,000	6,0	0,431		0,000		0,000		0,000		0,000
4003	3,0	0,969	19,0	1,363	8,0	2,763		0,000	7,0	1,101	2,0	0,966
4012												
4016		0,000		0,000		0,000		0,000		0,000		0,000
3954												0,000
4037	1,5	0,485	15,0	1,076		0,000	2,5	0,901	2,0	0,314	3,0	1,449
4070	7,0	2,262	19,0	1,363	1,0	0,345	3,0	1,081	10,0	1,572	2,0	0,966
4201		0,000		0,000		0,000	1,0	0,360		0,000		0,000
4208		0,000		0,000		0,000	1,0	0,360		0,000		0,000
4230		0,000		0,000		0,000		0,000	1,0	0,157		0,000
4220												
3647												0,000
4240												
4250		0,000		0,000		0,000		0,000	1,0	0,157		0,000
4501		0,000		0,000		0,000		0,000		0,000		0,000
4602	0,5	0,162	5,0	0,359	0,5	0,173	4,0	1,441	6,5	1,022	3,5	1,691
4603G		0,000		0,000		0,000		0,000		0,000		0,000
4614		0,000		0,000		0,000		0,000		0,000	0,5	0,242
4802		0,000		0,000		0,000		0,000		0,000		0,000
4808		0,000		0,000		0,000		0,000		0,000		0,000
5325												
5300		0,000		0,000		0,000		0,000	0,5	0,079		0,000
5401G		0,000	7,5	0,538	2,0	0,691	2,0	0,721	2,0	0,314	1,0	0,483
5402												
5403												
5417G		0,000	1,5	0,108		0,000	0,5	0,180	0,5	0,079		0,000
5424	1,0	0,323	4,5	0,323		0,000	3,0	1,081	5,5	0,865	1,5	0,725
5701		0,000		0,000		0,000		0,000		0,000		0,000
5702												
	0	100	0	100	0	100	0	100	0	100	0	100

	HIX_303		HIX_304		HIX_305		HIX_306		HIX_307		HIX_08	
ID after	**212,25**		**212,75**		**213,25**		**214**		**215**		**215,75**	
Gasse, 1995	numb.	%	numb.	%	numb.	%	numb.	%	numb.	%	numb.	%
	total:	208	total:	249	total:	244	total:	265,5	total:	230,5	total:	200
0103	1,0	0,481		0,000		0,000		0,000		0,000		0,000
0151		0,000		0,000		0,000		0,000		0,000		0,000
0104		0,000		0,000		0,000		0,000		0,000		0,000
0107		0,000		0,000		0,000		0,000		0,000		0,000
0108		0,000		0,000		0,000		0,000		0,000		0,000
0113G	2,0	0,962	2,0	0,803		0,000	5,0	1,883	4,0	1,735	3,0	1,500
0118		0,000		0,000		0,000		0,000		0,000		0,000
0311		0,000		0,000		0,000		0,000		0,000		0,000
0377	2,0	0,962		0,000		0,000		0,000	2,0	0,868		0,000
0325		0,000	1,0	0,402		0,000	1,0	0,377		0,000		0,000
0326		0,000		0,000		0,000	2,0	0,753	3,0	1,302		0,000
0370		0,000		0,000		0,000		0,000		0,000		0,000
0506		0,000		0,000		0,000		0,000		0,000		0,000
0503		0,000		0,000		0,000		0,000		0,000		0,000
3501	6,0	2,885		0,000		0,000		0,000		0,000		0,000
3502		0,000		0,000		0,000		0,000		0,000		0,000
3506		0,000		0,000		0,000	15,0	5,650	14,0	6,074	10,0	5,000
3507		0,000	4,0	1,606	18,0	7,377	29,0	10,923	14,0	6,074	9,0	4,500
3508		0,000		0,000		0,000		0,000		0,000		0,000
3510G	24,0	11,538	14,0	5,622	40,0	16,393	47,0	17,702	28,0	12,148	28,0	14,000
0904G		0,000		0,000		0,000		0,000		0,000		0,000
1401		0,000		0,000		0,000		0,000		0,000		0,000
1403	20,0	9,615	20,0	8,032	13,0	5,328	36,5	13,748	40,5	17,570	31,0	15,500
1405		0,000		0,000		0,000	3,0	1,130		0,000		0,000
1610		0,000	8,0	3,213	4,0	1,639	13,0	4,896	7,0	3,037	8,0	4,000
1655		0,000		0,000	2,0	0,820	2,0	0,753		0,000		0,000
1620		0,000		0,000		0,000		0,000		0,000		0,000
1625	21,0	10,096	31,0	12,450	27,0	11,066	44,0	16,573	45,0	19,523	34,0	17,000
1635	2,0	0,962	11,0	4,418	2,0	0,820	9,0	3,390	12,0	5,206	9,0	4,500
1901	1,0	0,481	3,0	1,205	2,0	0,820	10,5	3,955		0,000		0,000
1904	2,0	0,962	7,0	2,811	5,5	2,254		0,000	1,0	0,434		0,000
1911G		0,000	1,0	0,402		0,000		0,000		0,000		0,000
1912		0,000		0,000		0,000		0,000		0,000	1,0	0,500
1913		0,000		0,000		0,000		0,000		0,000		0,000
1920		0,000		0,000		0,000		0,000		0,000		0,000
1917		0,000		0,000		0,000		0,000		0,000	1,0	0,500
1946		0,000		0,000		0,000		0,000		0,000		0,000
1918												
2301	1,0	0,481	0,5	0,201		0,000		0,000		0,000		0,000
2303												
2406	12,0	5,769	3,0	1,205	14,0	5,738		0,000	13,5	5,857	1,0	0,500
2402		0,000		0,000		0,000		0,000		0,000		0,000
2404	2,0	0,962	1,0	0,402	3,0	1,230		0,000		0,000		0,000
2405	0,5	0,240	1,0	0,402	1,0	0,410		0,000	0,5	0,217	1,5	0,750
2504												
2503		0,000		0,000		0,000		0,000		0,000		0,000
2506G		0,000		0,000		0,000		0,000		0,000		0,000
2516		0,000		0,000		0,000		0,000		0,000		0,000
2601		0,000		0,000	3,0	1,230		0,000		0,000		0,000
2602	29,0	13,942	26,0	10,442	27,0	11,066	8,0	3,013	8,0	3,471	7,0	3,500
2606	18,0	8,654	30,0	12,048	25,0	10,246	7,0	2,637	3,0	1,302	8,0	4,000
2611		0,000		0,000		0,000		0,000		0,000		0,000
2612	2,0	0,962		0,000		0,000		0,000		0,000		0,000
2613	22,0	10,577	28,0	11,245	28,0	11,475	11,0	4,143	5,0	2,169	16,0	8,000
2615		0,000		0,000		0,000		0,000		0,000		0,000
2603G		0,000		0,000		0,000		0,000		0,000		0,000
2910		0,000		0,000		0,000		0,000		0,000		0,000
2917G		0,000		0,000		0,000		0,000		0,000		0,000
2904		0,000	3,0	1,205		0,000	1,0	0,377		0,000		0,000
2908G		0,000	5,0	2,008	2,0	0,820	1,0	0,377		0,000	1,0	0,500
2912G	20,0	9,615	14,0	5,622	15,0	6,148	9,0	3,390	14,0	6,074	14,0	7,000
2923		0,000		0,000		0,000		0,000		0,000		0,000
3201		0,000		0,000		0,000		0,000		0,000		0,000
3302		0,000		0,000		0,000		0,000		0,000		0,000
3303	7,0	3,365	1,0	0,402		0,000		0,000	1,5	0,651		0,000
3305G		0,000		0,000		0,000		0,000		0,000		0,000
3607G		0,000		0,000		0,000		0,000		0,000		0,000
3613												

	HIX_303		HIX_304		HIX_305		HIX_306		HIX_307		HIX_08	
ID after	**212,25**		**212,75**		**213,25**		**214**		**215**		**215,75**	
Gasse, 1995	numb.	%	numb.	%	numb.	%	numb.	%	numb.	%	numb.	%
3615		0,000		0,000		0,000		0,000		0,000		0,000
3617G		0,000		0,000		0,000		0,000		0,000		0,000
3620		0,000		0,000		0,000		0,000		0,000		0,000
3621G		0,000		0,000		0,000		0,000		0,000		0,000
3622		0,000		0,000		0,000		0,000		0,000		0,000
---		0,000		0,000		0,000		0,000		0,000		0,000
---		0,000		0,000		0,000		0,000		0,000		0,000
3712G												
3767		0,000		0,000		0,000		0,000		0,000		0,000
3728		0,000	2,0	0,803		0,000		0,000		0,000		0,000
3730	2,0	0,962	2,5	1,004		0,000	1,5	0,565		0,000	1,5	0,750
3732		0,000		0,000		0,000		0,000		0,000		0,000
3738		0,000		0,000		0,000		0,000		0,000		0,000
3742		0,000	3,0	1,205	1,0	0,410		0,000		0,000	1,0	0,500
3743		0,000	2,0	0,803		0,000		0,000		0,000		0,000
3606		0,000		0,000		0,000		0,000		0,000		0,000
3638		0,000		0,000		0,000		0,000		0,000		0,000
3627G												
3739G		0,000	1,5	0,602	1,0	0,410		0,000	1,0	0,434	1,0	0,500
3757		0,000		0,000		0,000		0,000		0,000		0,000
3906	5,5	2,644	7,5	3,012	0,5	0,205		0,000	3,5	1,518	2,5	1,250
3922		0,000		0,000	1,0	0,410		0,000		0,000		0,000
3918		0,000		0,000		0,000		0,000		0,000		0,000
3925		0,000		0,000		0,000		0,000	2,0	0,868		0,000
3942G		0,000	2,0	0,803		0,000		0,000		0,000		0,000
3936												
3932G												
3946		0,000	2,0	0,803		0,000	1,0	0,377	2,0	0,868	3,0	1,500
4003		0,000		0,000		0,000		0,000		0,000	1,0	0,500
4012												
4016		0,000		0,000		0,000		0,000		0,000		0,000
3954		0,000		0,000		0,000		0,000		0,000		0,000
4037	2,0	0,962		0,000	1,0	0,410	7,0	2,637	3,5	1,518	4,0	2,000
4070		0,000	2,0	0,803	1,0	0,410	2,0	0,753		0,000	1,0	0,500
4201		0,000		0,000		0,000		0,000		0,000		0,000
4208		0,000		0,000		0,000		0,000		0,000		0,000
4230	1,0	0,481	0,5	0,201		0,000		0,000		0,000		0,000
4220												
3647		0,000		0,000		0,000		0,000		0,000		0,000
4240												
4250		0,000		0,000		0,000		0,000		0,000		0,000
4501		0,000		0,000		0,000		0,000		0,000		0,000
4602	1,0	0,481	3,5	1,406	3,0	1,230		0,000		0,000		0,000
4603G		0,000		0,000		0,000		0,000		0,000		0,000
4614	0,5	0,240	0,5	0,201		0,000		0,000		0,000		0,000
4802		0,000	0,5	0,201		0,000		0,000		0,000		0,000
4808		0,000		0,000		0,000		0,000		0,000		0,000
5325												
5300		0,000		0,000		0,000		0,000		0,000		0,000
5401G	0,5	0,240	2,0	0,803	0,5	0,205		0,000	0,5	0,217	1,5	0,750
5402												
5403												
5417G		0,000		0,000		0,000		0,000		0,000		0,000
5424	1,0	0,481	3,0	1,205	3,5	1,434		0,000	2,0	0,868	1,0	0,500
5701		0,000		0,000		0,000		0,000		0,000		0,000
5702												
	0	100	0	100	0	100	0	100	0	100	0	100

	HIX_309		HIX_201		HIX_310		HIX_202		HIX_311		HIX_203	
ID after	**216**		**216,5**		**216,5**		**217,5**		**217,5**		**218,3**	
Gasse, 1995	numb.	%	numb.	%	numb.	%	numb.	%	numb.	%	numb.	%
	total:	197	total:	1129	total:	229,5	total:	644,5	total:	206,5	total:	930,5
0103		0,000	5,0	0,443		0,000	4,0	0,621	1,0	0,484	5,0	0,537
0151		0,000		0,000		0,000		0,000		0,000		0,000
0104		0,000	3,0	0,266		0,000		0,000		0,000	1,0	0,107
0107		0,000		0,000		0,000		0,000		0,000		0,000
0108		0,000		0,000		0,000		0,000		0,000		0,000
0113G	2,0	1,015	11,0	0,974	4,0	1,743	4,0	0,621		0,000	2,0	0,215
0118		0,000		0,000		0,000		0,000		0,000		0,000
0311		0,000		0,000		0,000		0,000		0,000		0,000
0377		0,000	2,0	0,177		0,000		0,000		0,000		0,000
0325	1,0	0,508	4,0	0,354		0,000	3,0	0,465		0,000	8,0	0,860
0326	4,0	2,030		0,000		0,000	8,0	1,241	2,0	0,969	4,0	0,430
0370	2,0	1,015		0,000		0,000		0,000		0,000		0,000
0506		0,000		0,000		0,000		0,000		0,000		0,000
0503		0,000		0,000		0,000		0,000		0,000		0,000
3501		0,000		0,000		0,000		0,000		0,000		0,000
3502		0,000		0,000		0,000	2,0	0,310		0,000		0,000
3506	15,0	7,614	7,0	0,620	12,0	5,229	3,0	0,465	6,0	2,906	10,0	1,075
3507	8,0	4,061	28,0	2,480	19,0	8,279	50,0	7,758	16,0	7,748	95,0	10,210
3508		0,000		0,000	1,0	0,436		0,000		0,000		0,000
3510G	40,0	20,305	95,0	8,415	30,0	13,072	141,0	21,877	40,0	19,370	235,0	25,255
0904G		0,000		0,000		0,000		0,000		0,000		0,000
1401		0,000		0,000		0,000		0,000		0,000		0,000
1403	26,5	13,452	42,0	3,720	23,0	10,022	64,0	9,930	17,5	8,475	47,0	5,051
1405		0,000	5,0	0,443	1,0	0,436	1,0	0,155		0,000		0,000
1610	7,0	3,553	14,0	1,240	5,0	2,179	1,0	0,155	3,0	1,453	6,0	0,645
1655		0,000		0,000		0,000	1,0	0,155		0,000	1,0	0,107
1620		0,000		0,000		0,000		0,000		0,000		0,000
1625	26,0	13,198	75,0	6,643	31,0	13,508	113,0	17,533	35,0	16,949	155,0	16,658
1635	13,0	6,599	10,0	0,886	9,0	3,922	39,0	6,051	6,0	2,906	12,0	1,290
1901		0,000		0,000		0,000	1,5	0,233		0,000	1,0	0,107
1904	1,0	0,508	3,0	0,266	3,0	1,307		0,000		0,000		0,000
1911G		0,000		0,000		0,000		0,000		0,000		0,000
1912	1,0	0,508	3,0	0,266		0,000	4,5	0,698		0,000	1,0	0,107
1913		0,000		0,000		0,000		0,000		0,000		0,000
1920		0,000		0,000		0,000		0,000		0,000		0,000
1917		0,000		0,000		0,000		0,000		0,000		0,000
1946		0,000	2,0	0,177		0,000		0,000		0,000		0,000
1918												
2301		0,000	2,5	0,221		0,000	1,5	0,233	2,0	0,969		0,000
2303												
2406	11,0	5,584	5,5	0,487	2,0	0,871	21,5	3,336	3,0	1,453	18,5	1,988
2402		0,000		0,000		0,000		0,000		0,000		0,000
2404	1,0	0,508	4,0	0,354		0,000		0,000		0,000	1,0	0,107
2405		0,000		0,000	0,5	0,218	0,5	0,078	1,0	0,484	4,0	0,430
2504												
2503		0,000		0,000		0,000		0,000		0,000		0,000
2506G		0,000		0,000		0,000		0,000		0,000		0,000
2516		0,000	0,5	0,044		0,000	0,5	0,078		0,000	0,5	0,054
2601	1,0	0,508	20,0	1,771	1,0	0,436		0,000		0,000	8,5	0,913
2602	4,0	2,030	282,0	24,978	31,0	13,508	50,0	7,758	24,0	11,622	62,0	6,663
2606		0,000	177,0	15,678	18,0	7,843	30,0	4,655	24,0	11,622	51,0	5,481
2611		0,000		0,000		0,000		0,000		0,000		0,000
2612		0,000	1,0	0,089		0,000	2,0	0,310		0,000		0,000
2613	6,0	3,046	247,0	21,878	14,0	6,100	25,0	3,879	12,0	5,811	121,0	13,004
2615		0,000		0,000		0,000		0,000		0,000		0,000
2603G		0,000		0,000		0,000		0,000		0,000	2,0	0,215
2910		0,000		0,000		0,000				0,000		
2917G		0,000		0,000		0,000		0,000		0,000		0,000
2904		0,000		0,000		0,000	1,0	0,155	1,0	0,484	4,0	0,430
2908G	2,0	1,015	1,0	0,089	2,0	0,871	3,0	0,465		0,000	1,5	0,161
2912G	8,0	4,061	17,0	1,506	8,0	3,486	21,5	3,336	6,0	2,906	6,0	0,645
2923		0,000		0,000		0,000	2,0	0,310		0,000	1,0	0,107
3201		0,000		0,000		0,000		0,000		0,000		0,000
3302		0,000		0,000		0,000		0,000		0,000		0,000
3303		0,000	1,5	0,133	0,5	0,218	0,5	0,078		0,000	3,5	0,376
3305G		0,000		0,000		0,000		0,000		0,000		0,000
3607G		0,000		0,000		0,000		0,000		0,000		0,000
3613												

	HIX_309		HIX_201		HIX_310		HIX_202		HIX_311		HIX_203	
ID after	**216**		**216,5**		**216,5**		**217,5**		**217,5**		**218,3**	
Gasse, 1995	numb.	%	numb.	%	numb.	%	numb.	%	numb.	%	numb.	%
3615		0,000		0,000		0,000		0,000		0,000		0,000
3617G		0,000		0,000		0,000		0,000		0,000		0,000
3620		0,000		0,000	2,0	0,871		0,000		0,000		0,000
3621G		0,000		0,000		0,000		0,000		0,000		0,000
3622		0,000		0,000		0,000		0,000		0,000		0,000
---		0,000		0,000		0,000	2,0	0,310		0,000	1,0	0,107
---		0,000		0,000		0,000	1,0	0,155		0,000		0,000
3712G												
3767		0,000		0,000		0,000		0,000		0,000		0,000
3728		0,000	0,5	0,044		0,000		0,000		0,000		0,000
3730		0,000	2,0	0,177	0,5	0,218	1,5	0,233		0,000	2,5	0,269
3732		0,000		0,000		0,000		0,000		0,000		0,000
3738		0,000		0,000		0,000	4,0	0,621		0,000		0,000
3742	1,0	0,508	3,0	0,266	2,0	0,871	1,0	0,155		0,000	4,0	0,430
3743		0,000	4,0	0,354	1,0	0,436	5,0	0,776	1,0	0,484	6,0	0,645
3606		0,000		0,000		0,000		0,000		0,000		0,000
3638		0,000		0,000		0,000		0,000		0,000		0,000
3627G												
3739G		0,000		0,000		0,000		0,000		0,000		0,000
3757		0,000	16,5	1,461		0,000	1,0	0,155		0,000	1,0	0,107
3906	2,5	1,269	3,5	0,310	0,5	0,218	2,0	0,310		0,000	8,5	0,913
3922		0,000		0,000		0,000		0,000		0,000		0,000
3918		0,000	2,0	0,177		0,000		0,000		0,000	6,0	0,645
3925		0,000		0,000	2,0	0,871		0,000		0,000		0,000
3942G		0,000		0,000		0,000		0,000		0,000	2,0	0,215
3936												
3932G												
3946	3,0	1,523	2,0	0,177	1,0	0,436	2,0	0,310		0,000		0,000
4003	1,0	0,508	3,0	0,266		0,000	3,0	0,465	1,0	0,484	3,0	0,322
4012												
4016		0,000		0,000		0,000		0,000		0,000		0,000
3954		0,000		0,000		0,000				0,000		
4037	2,0	1,015	0,5	0,044	0,5	0,218	7,0	1,086	1,5	0,726	7,0	0,752
4070	1,0	0,508	16,0	1,417		0,000	8,0	1,241	2,0	0,969	9,0	0,967
4201		0,000		0,000		0,000		0,000		0,000		0,000
4208	2,0	1,015	1,0	0,089		0,000		0,000		0,000		0,000
4230		0,000	0,5	0,044		0,000		0,000		0,000		0,000
4220												
3647		0,000		0,000		0,000				0,000		
4240												
4250		0,000		0,000		0,000		0,000		0,000		0,000
4501		0,000		0,000		0,000		0,000		0,000		0,000
4602		0,000	1,0	0,089	1,5	0,654	1,0	0,155		0,000		0,000
4603G		0,000		0,000		0,000		0,000		0,000		0,000
4614		0,000		0,000		0,000	1,0	0,155		0,000	3,0	0,322
4802		0,000		0,000		0,000		0,000		0,000		0,000
4808		0,000		0,000		0,000		0,000		0,000		0,000
5325												
5300		0,000		0,000		0,000		0,000		0,000		0,000
5401G	0,5	0,254	2,0	0,177	1,0	0,436	1,5	0,233		0,000	4,0	0,430
5402												
5403												
5417G		0,000		0,000		0,000		0,000		0,000		0,000
5424	4,5	2,284	3,5	0,310	2,5	1,089	4,5	0,698	1,5	0,726	6,0	0,645
5701		0,000		0,000		0,000		0,000		0,000		0,000
5702												
	0	100	0	100	0	100	0	100	0	100	0	100

	HIX_204		HIX_312		HIX_205		HIX_206		HIX_207		HIX_208	
ID after	**219**		**219**		**219,8**		**220,5**		**220,8**		**221,3**	
Gasse, 1995	numb.	%	numb.	%	numb.	%	numb.	%	numb.	%	numb.	%
	total:	785,5	total:	177	total:	330,5	total:	397	total:	594	total:	520
0103	4,0	0,509		0,000	1,0	0,303	2,0	0,504	1,0	0,168	9,0	1,731
0151		0,000		0,000		0,000		0,000		0,000		0,000
0104		0,000		0,000		0,000	2,0	0,504		0,000		0,000
0107		0,000		0,000		0,000		0,000		0,000		0,000
0108		0,000		0,000		0,000		0,000		0,000		0,000
0113G		0,000		0,000		0,000	2,0	0,504		0,000		0,000
0118		0,000		0,000		0,000		0,000		0,000		0,000
0311		0,000		0,000		0,000		0,000		0,000		0,000
0377		0,000	2,0	1,130		0,000		0,000		0,000		0,000
0325	4,0	0,509		0,000	2,0	0,605	0,5	0,126		0,000		0,000
0326		0,000		0,000		0,000		0,000		0,000		0,000
0370		0,000		0,000		0,000		0,000		0,000		0,000
0506		0,000		0,000		0,000		0,000		0,000		0,000
0503		0,000		0,000		0,000		0,000		0,000		0,000
3501		0,000		0,000		0,000		0,000		0,000		0,000
3502		0,000		0,000		0,000		0,000		0,000		0,000
3506	7,0	0,891	5,0	2,825	16,0	4,841	24,0	6,045	9,0	1,515	30,0	5,769
3507	85,0	10,821	18,0	10,169	14,0	4,236	22,0	5,542	16,0	2,694	4,0	0,769
3508		0,000		0,000		0,000		0,000		0,000		0,000
3510G	145,0	18,460	50,0	28,249	63,0	19,062	51,0	12,846	84,0	14,141	48,0	9,231
0904G		0,000		0,000		0,000	2,0	0,504		0,000		0,000
1401		0,000		0,000		0,000		0,000		0,000		0,000
1403	63,5	8,084	5,5	3,107	20,0	6,051	20,0	5,038	7,0	1,178	11,5	2,212
1405		0,000	1,0	0,565		0,000		0,000		0,000	2,0	0,385
1610	3,0	0,382	2,0	1,130	5,0	1,513		0,000	3,0	0,505	3,0	0,577
1655		0,000		0,000		0,000		0,000	2,0	0,337		0,000
1620		0,000		0,000		0,000		0,000		0,000		0,000
1625	143,5	18,269	34,0	19,209	76,0	22,995	77,0	19,395	28,0	4,714	74,0	14,231
1635	12,0	1,528	1,0	0,565	3,0	0,908	8,0	2,015	2,0	0,337	4,0	0,769
1901	1,0	0,127		0,000		0,000		0,000		0,000		0,000
1904		0,000		0,000	0,5	0,151	1,5	0,378	0,5	0,084	0,5	0,096
1911G		0,000		0,000		0,000		0,000		0,000		0,000
1912	7,5	0,955		0,000	5,0	1,513	1,0	0,252	1,0	0,168		0,000
1913		0,000		0,000		0,000		0,000		0,000		0,000
1920		0,000		0,000	1,0	0,303		0,000		0,000		0,000
1917		0,000		0,000	1,0	0,303		0,000		0,000		0,000
1946		0,000		0,000		0,000		0,000		0,000		0,000
1918												
2301	1,0	0,127		0,000		0,000	3,0	0,756	7,0	1,178	0,5	0,096
2303												
2406	18,5	2,355	5,0	2,825	4,5	1,362	1,5	0,378	2,0	0,337	3,0	0,577
2402		0,000		0,000		0,000		0,000		0,000		0,000
2404	3,0	0,382		0,000	2,0	0,605	4,5	1,134	2,0	0,337	2,5	0,481
2405	3,5	0,446	1,0	0,565	1,0	0,303	2,5	0,630	1,5	0,253	2,0	0,385
2504												
2503		0,000		0,000		0,000		0,000		0,000		0,000
2506G		0,000		0,000		0,000		0,000		0,000		0,000
2516	2,5	0,318		0,000	0,5	0,151	2,0	0,504		0,000	0,5	0,096
2601	3,0	0,382	3,0	1,695	3,0	0,908	7,0	1,763	8,0	1,347	7,0	1,346
2602	68,0	8,657	10,0	5,650	37,0	11,195	49,0	12,343	100,0	16,835	78,0	15,000
2606	53,0	6,747	22,0	12,429	38,0	11,498	45,0	11,335	89,0	14,983	105,0	20,192
2611		0,000		0,000	20,0	6,051		0,000		0,000		0,000
2612		0,000		0,000		0,000		0,000	1,0	0,168	1,0	0,192
2613	84,0	10,694	11,0	6,215		0,000	35,0	8,816	180,0	30,303	105,0	20,192
2615		0,000		0,000		0,000		0,000		0,000		0,000
2603G		0,000		0,000		0,000		0,000		0,000		0,000
2910				0,000								
2917G		0,000		0,000		0,000		0,000		0,000		0,000
2904	3,0	0,382		0,000		0,000	2,5	0,630		0,000		0,000
2908G		0,000		0,000		0,000		0,000		0,000		0,000
2912G	14,5	1,846		0,000	1,5	0,454	10,0	2,519	1,0	0,168	2,5	0,481
2923		0,000		0,000		0,000		0,000		0,000		0,000
3201		0,000		0,000		0,000		0,000		0,000		0,000
3302		0,000		0,000		0,000		0,000		0,000		0,000
3303	2,0	0,255	0,5	0,282	1,0	0,303	1,0	0,252	1,0	0,168	0,5	0,096
3305G		0,000		0,000		0,000		0,000		0,000	1,0	0,192
3607G		0,000		0,000		0,000		0,000		0,000		0,000
3613												

	HIX_204		HIX_312		HIX_205		HIX_206		HIX_207		HIX_208	
ID after	**219**		**219**		**219,8**		**220,5**		**220,8**		**221,3**	
Gasse, 1995	numb.	%	numb.	%	numb.	%	numb.	%	numb.	%	numb.	%
3615		0,000		0,000		0,000		0,000		0,000		0,000
3617G		0,000		0,000		0,000		0,000		0,000		0,000
3620	4,0	0,509		0,000		0,000		0,000		0,000	1,0	0,192
3621G		0,000		0,000		0,000		0,000		0,000		0,000
3622		0,000		0,000		0,000		0,000		0,000		0,000
---	1,0	0,127		0,000		0,000		0,000	3,0	0,505	4,0	0,769
---		0,000	1,0	0,565		0,000	1,0	0,252		0,000		0,000
3712G												
3767		0,000		0,000		0,000		0,000		0,000		0,000
3728	1,0	0,127		0,000		0,000		0,000		0,000		0,000
3730		0,000		0,000		0,000		0,000	1,0	0,168	2,0	0,385
3732		0,000		0,000		0,000		0,000		0,000		0,000
3738		0,000		0,000	2,0	0,605	3,0	0,756	12,0	2,020	3,0	0,577
3742	7,0	0,891		0,000	1,0	0,303	2,0	0,504	4,0	0,673	3,0	0,577
3743	4,0	0,509	1,0	0,565	1,0	0,303	6,5	1,637	11,0	1,852	1,0	0,192
3606		0,000		0,000		0,000		0,000		0,000		0,000
3638		0,000		0,000		0,000		0,000		0,000		0,000
3627G												
3739G		0,000		0,000	0,5	0,151	0,5	0,126		0,000		0,000
3757	1,0	0,127		0,000	1,5	0,454		0,000	1,0	0,168	1,0	0,192
3906	7,0	0,891	1,5	0,847	3,0	0,908	1,0	0,252	3,0	0,505	4,0	0,769
3922		0,000		0,000		0,000		0,000		0,000		0,000
3918	4,0	0,509		0,000		0,000	1,0	0,252	2,0	0,337		0,000
3925		0,000		0,000		0,000		0,000		0,000		0,000
3942G	2,0	0,255		0,000		0,000		0,000		0,000		0,000
3936												
3932G												
3946	2,0	0,255		0,000		0,000		0,000		0,000		0,000
4003		0,000	1,0	0,565	2,0	0,605	1,0	0,252		0,000		0,000
4012												
4016		0,000		0,000		0,000		0,000		0,000		0,000
3954				0,000								
4037		0,000	1,0	0,565	2,0	0,605	0,5	0,126	2,0	0,337	1,0	0,192
4070	14,0	1,782		0,000		0,000		0,000	3,0	0,505	1,0	0,192
4201		0,000		0,000		0,000		0,000		0,000		0,000
4208		0,000		0,000		0,000		0,000		0,000	1,0	0,192
4230		0,000		0,000		0,000		0,000		0,000		0,000
4220												
3647				0,000								
4240												
4250		0,000		0,000		0,000		0,000		0,000		0,000
4501		0,000		0,000		0,000		0,000		0,000		0,000
4602	0,5	0,064		0,000	1,0	0,303	3,0	0,756	2,5	0,421	0,5	0,096
4603G		0,000		0,000		0,000		0,000		0,000		0,000
4614		0,000	0,5	0,282		0,000		0,000		0,000		0,000
4802		0,000		0,000		0,000		0,000		0,000		0,000
4808		0,000		0,000		0,000		0,000		0,000		0,000
5325												
5300		0,000		0,000		0,000		0,000		0,000		0,000
5401G	3,0	0,382		0,000		0,000	1,0	0,252		0,000	1,0	0,192
5402												
5403												
5417G		0,000		0,000		0,000		0,000		0,000		0,000
5424	3,5	0,446		0,000	0,5	0,151	0,5	0,126	3,5	0,589	2,0	0,385
5701		0,000		0,000		0,000		0,000		0,000		0,000
5702												
	0	100	0	100	0	100	0	100	0	100	0	100

	HIX_209		HIX_210		HVIII_12.5-15.0		HVIII_20.0-22.5		HVIII_30		HVIII_37.5-40.0	
ID after	**221,8**		**222,8**		**14**		**21**		**30**		**39**	
Gasse, 1995	numb.	%	numb.	%	numb.	%	numb.	%	numb.	%	numb.	%
	total:	517,5	total:	868,5	total:	705,5		313,5		348		541
0103	6,0	1,159	9,0	1,036	9,0	1,276		0,000		0,000	1,0	0,185
0151		0,000		0,000		0,000		0,000		0,000		0,000
0104		0,000		0,000	1,0	0,142		0,000		0,000		0,000
0107	2,0	0,386	13,0	1,497		0,000		0,000	1,0	0,287		0,000
0108		0,000		0,000	14,5	2,055		0,000		0,000	3,0	0,555
0113G		0,000	9,0	1,036	1,0	0,142	1,0	0,319	2,0	0,575		0,000
0118		0,000		0,000		0,000		0,000		0,000		0,000
0311		0,000		0,000		0,000		0,000		0,000		0,000
0377		0,000		0,000	7,0	0,992		0,000	1,0	0,287		0,000
0325		0,000	4,0	0,461	5,0	0,709		0,000	1,0	0,287		0,000
0326	2,0	0,386		0,000	5,0	0,709		0,000		0,000		0,000
0370		0,000		0,000		0,000		0,000		0,000		0,000
0506		0,000		0,000		0,000		0,000		0,000		0,000
0503		0,000		0,000		0,000		0,000		0,000		0,000
3501		0,000		0,000		0,000		0,000		0,000		0,000
3502	1,0	0,193		0,000		0,000		0,000		0,000		0,000
3506	10,0	1,932	13,0	1,497		0,000		0,000		0,000		0,000
3507	20,0	3,865	26,0	2,994	15,0	2,126	7,0	2,233	17,0	4,885	13,0	2,403
3508		0,000		0,000	2,0	0,283	2,0	0,638	8,0	2,299	11,0	2,033
3510G	68,0	13,140	61,0	7,024	7,0	0,992		0,000		0,000	1,0	0,185
0904G		0,000	1,5	0,173		0,000		0,000		0,000		0,000
1401		0,000		0,000	69,0	9,780		0,000		0,000		0,000
1403	10,5	2,029	32,0	3,685	5,0	0,709	2,0	0,638	3,5	1,006		0,000
1405	1,0	0,193	10,0	1,151		0,000		0,000		0,000		0,000
1610	2,0	0,386	5,0	0,576		0,000		0,000		0,000		0,000
1655		0,000		0,000		0,000		0,000		0,000		0,000
1620		0,000		0,000		0,000		0,000		0,000		0,000
1625	90,0	17,391	99,0	11,399	49,0	6,945	4,0	1,276	32,0	9,195	21,0	3,882
1635	4,0	0,773	23,0	2,648	20,0	2,835	9,0	2,871	6,0	1,724	1,0	0,185
1901		0,000	1,0	0,115	1,5	0,213		0,000		0,000		0,000
1904		0,000		0,000		0,000	6,0	1,914		0,000	1,0	0,185
1911G		0,000		0,000		0,000	1,0	0,319	8,0	2,299	1,0	0,185
1912	3,0	0,580	7,0	0,806		0,000		0,000	1,0	0,287	4,0	0,739
1913		0,000		0,000		0,000		0,000	1,0	0,287		0,000
1920		0,000		0,000	1,0	0,142		0,000		0,000		0,000
1917		0,000		0,000		0,000		0,000		0,000		0,000
1946		0,000		0,000		0,000		0,000		0,000		0,000
1918												
2301	1,0	0,193	0,5	0,058	8,5	1,205		0,000		0,000	1,0	0,185
2303												
2406	4,0	0,773	7,5	0,864	42,0	5,953	8,5	2,711	18,5	5,316	13,0	2,403
2402		0,000		0,000		0,000		0,000	0,5	0,144	2,0	0,370
2404		0,000	2,0	0,230	2,0	0,283	16,5	5,263	1,5	0,431	14,5	2,680
2405	0,5	0,097	2,0	0,230	27,0	3,827	1,5	0,478		0,000		0,000
2504												
2503		0,000		0,000		0,000		0,000		0,000		0,000
2506G	1,0	0,193	0,5	0,058	2,5	0,354		0,000		0,000		0,000
2516		0,000		0,000		0,000		0,000		0,000		0,000
2601	4,0	0,773	16,5	1,900	3,0	0,425		0,000	3,0	0,862	2,0	0,370
2602	74,0	14,300	177,0	20,380	34,0	4,819	17,0	5,423	25,0	7,184	57,0	10,536
2606	86,0	16,618	107,0	12,320	127,0	18,001	56,0	17,863	59,0	16,954	79,0	14,603
2611		0,000		0,000		0,000		0,000		0,000		0,000
2612	1,0	0,193	4,0	0,461		0,000		0,000		0,000	1,0	0,185
2613	105,0	20,290	149,0	17,156	155,0	21,970	116,0	37,002	93,0	26,724	209,0	38,632
2615		0,000		0,000	5,0	0,709		0,000		0,000	10,0	1,848
2603G		0,000	2,0	0,230	4,0	0,567		0,000	1,0	0,287	1,0	0,185
2910						0,000		0,000		0,000	2,0	0,370
2917G		0,000		0,000		0,000		0,000		0,000	4,5	0,832
2904		0,000	2,0	0,230		0,000	1,0	0,319		0,000		0,000
2908G		0,000		0,000	11,0	1,559	22,5	7,177	12,0	3,448	31,0	5,730
2912G	3,0	0,580	13,0	1,497		0,000	9,0	2,871	12,0	3,448	10,5	1,941
2923		0,000		0,000	1,0	0,142		0,000		0,000		0,000
3201		0,000		0,000		0,000		0,000		0,000		0,000
3302		0,000		0,000		0,000		0,000		0,000		0,000
3303		0,000	1,0	0,115	1,0	0,142		0,000		0,000	3,5	0,647
3305G		0,000		0,000		0,000		0,000		0,000		0,000
3607G		0,000		0,000		0,000		0,000		0,000		0,000
3613												

	HIX_209		HIX_210		HVIII_12.5-15.0		HVIII_20.0-22.5		HVIII_30		HVIII_37.5-40.0	
ID after	**221,8**		**222,8**		**14**		**21**		**30**		**39**	
Gasse, 1995	numb.	%	numb.	%	numb.	%	numb.	%	numb.	%	numb.	%
3615		0,000		0,000		0,000		0,000		0,000		0,000
3617G		0,000		0,000		0,000		0,000		0,000		0,000
3620		0,000	3,0	0,345		0,000		0,000		0,000		0,000
3621G		0,000		0,000		0,000		0,000	1,0	0,287		0,000
3622		0,000		0,000		0,000		0,000		0,000		0,000
---		0,000	2,0	0,230		0,000		0,000	1,0	0,287	2,0	0,370
---		0,000	1,0	0,115		0,000		0,000		0,000		0,000
3712G												
3767		0,000		0,000		0,000		0,000		0,000		0,000
3728	1,0	0,193		0,000	0,5	0,071		0,000		0,000		0,000
3730		0,000	1,0	0,115	1,5	0,213	2,5	0,797	2,0	0,575	2,0	0,370
3732		0,000		0,000	1,0	0,142		0,000		0,000		0,000
3738	1,0	0,193	9,0	1,036	2,0	0,283		0,000		0,000		0,000
3742	2,5	0,483	1,0	0,115		0,000		0,000		0,000	1,0	0,185
3743	2,0	0,386	6,0	0,691		0,000		0,000		0,000	2,0	0,370
3606		0,000		0,000		0,000		0,000		0,000		0,000
3638		0,000		0,000		0,000		0,000		0,000		0,000
3627G												
3739G		0,000		0,000		0,000		0,000		0,000		0,000
3757	1,0	0,193	3,0	0,345		0,000		0,000		0,000		0,000
3906	2,0	0,386	9,0	1,036	1,5	0,213	3,0	0,957	5,5	1,580	2,0	0,370
3922		0,000		0,000	6,0	0,850		0,000	1,0	0,287		0,000
3918	2,0	0,386	12,0	1,382	3,0	0,425	1,0	0,319	5,0	1,437		0,000
3925		0,000		0,000	2,0	0,283		0,000		0,000		0,000
3942G		0,000	1,0	0,115	2,0	0,283	1,0	0,319	2,0	0,575		0,000
3936												
3932G												
3946		0,000		0,000		0,000		0,000	2,0	0,575		0,000
4003	3,0	0,580	9,0	1,036	10,0	1,417	3,0	0,957	4,0	1,149	14,0	2,588
4012												
4016		0,000		0,000		0,000		0,000		0,000		0,000
3954						0,000		0,000		0,000		0,000
4037		0,000	3,0	0,345		0,000		0,000		0,000		0,000
4070		0,000	4,0	0,461		0,000	9,0	2,871	4,0	1,149	6,0	1,109
4201		0,000		0,000		0,000		0,000		0,000		0,000
4208	1,0	0,193		0,000		0,000		0,000	2,5	0,718		0,000
4230		0,000	1,0	0,115		0,000		0,000		0,000		0,000
4220												
3647					11,5	1,630		0,000	1,0	0,287	1,0	0,185
4240												
4250		0,000		0,000		0,000		0,000		0,000		0,000
4501		0,000		0,000		0,000		0,000		0,000		0,000
4602	0,5	0,097	2,0	0,230	10,5	1,488	9,0	2,871		0,000	1,0	0,185
4603G		0,000		0,000		0,000		0,000		0,000		0,000
4614		0,000		0,000	4,5	0,638		0,000		0,000		0,000
4802		0,000		0,000		0,000		0,000		0,000		0,000
4808		0,000		0,000		0,000		0,000		0,000		0,000
5325												
5300		0,000		0,000		0,000		0,000		0,000		0,000
5401G	1,5	0,290	0,5	0,058	0,5	0,071	2,5	0,797	1,5	0,431	1,5	0,277
5402												
5403												
5417G		0,000		0,000	1,0	0,142		0,000		0,000	0,5	0,092
5424	1,0	0,193	3,5	0,403	13,0	1,843	2,5	0,797	8,5	2,443	10,0	1,848
5701		0,000		0,000		0,000		0,000		0,000		0,000
5702												
	0	100	0	100	0	100	0	100	0	100	0	100

	HVIII_50		HVIII_62.5-65.0		HVIII_75.0-77.5		HVIII_87.5-90.0		HVIII_100.0-102.5		HVIII_112.5-115.0	
ID after	**50**		**64**		**76**		**89**		**101**		**114**	
Gasse, 1995	numb.	%	numb.	%	numb.	%	numb.	%	numb.	%	numb.	%
		306,5		414,5		241		357		124		346,5
0103		0,000	2,0	0,483		0,000		0,000		0,000		0,000
0151		0,000		0,000		0,000		0,000		0,000		0,000
0104		0,000		0,000		0,000		0,000		0,000	2,0	0,577
0107		0,000		0,000		0,000		0,000		0,000	1,0	0,289
0108	7,0	2,284		0,000		0,000		0,000		0,000		0,000
0113G		0,000	1,0	0,241		0,000	3,0	0,840	1,5	1,210	1,0	0,289
0118		0,000		0,000		0,000		0,000		0,000		0,000
0311		0,000		0,000		0,000		0,000		0,000		0,000
0377		0,000		0,000		0,000		0,000		0,000		0,000
0325		0,000	1,0	0,241		0,000		0,000		0,000		0,000
0326		0,000		0,000		0,000		0,000		0,000	1,0	0,289
0370		0,000		0,000	1,0	0,415		0,000		0,000		0,000
0506		0,000		0,000		0,000	1,0	0,280		0,000		0,000
0503		0,000		0,000		0,000		0,000		0,000		0,000
3501		0,000		0,000		0,000		0,000		0,000		0,000
3502		0,000		0,000		0,000		0,000		0,000		0,000
3506		0,000		0,000		0,000		0,000		0,000		0,000
3507	10,0	3,263	6,0	1,448	6,0	2,490	3,0	0,840	2,0	1,613	1,0	0,289
3508		0,000	6,0	1,448	2,0	0,830	7,0	1,961		0,000	6,0	1,732
3510G		0,000	5,0	1,206		0,000	5,0	1,401		0,000	4,0	1,154
0904G		0,000		0,000		0,000		0,000		0,000		0,000
1401		0,000		0,000		0,000		0,000		0,000		0,000
1403	4,5	1,468	5,5	1,327	2,5	1,037	8,5	2,381	2,5	2,016	6,5	1,876
1405		0,000		0,000		0,000		0,000		0,000		0,000
1610		0,000		0,000		0,000		0,000		0,000		0,000
1655		0,000		0,000		0,000		0,000		0,000		0,000
1620		0,000		0,000		0,000		0,000		0,000		0,000
1625	22,0	7,178	21,0	5,066	21,0	8,714	18,0	5,042	10,0	8,065	22,0	6,349
1635	4,0	1,305	3,0	0,724	1,0	0,415	3,0	0,840		0,000	2,0	0,577
1901		0,000	1,0	0,241		0,000	1,0	0,280		0,000	3,0	0,866
1904	2,0	0,653	6,0	1,448	5,0	2,075	3,0	0,840	2,0	1,613	2,5	0,722
1911G		0,000		0,000		0,000		0,000		0,000		0,000
1912	1,5	0,489		0,000		0,000	2,0	0,560	1,0	0,806	5,0	1,443
1913		0,000		0,000		0,000		0,000		0,000		0,000
1920		0,000		0,000		0,000		0,000		0,000		0,000
1917		0,000		0,000		0,000		0,000		0,000		0,000
1946		0,000		0,000		0,000		0,000		0,000		0,000
1918												
2301		0,000		0,000		0,000	0,5	0,140		0,000		0,000
2303												
2406	11,0	3,589	31,0	7,479	7,0	2,905	30,5	8,543	2,5	2,016	14,0	4,040
2402		0,000	3,5	0,844		0,000		0,000		0,000		0,000
2404		0,000	16,5	3,981	8,5	3,527	14,5	4,062	5,5	4,435	20,0	5,772
2405	3,0	0,979	1,0	0,241	1,0	0,415	0,5	0,140	0,5	0,403		0,000
2504												
2503		0,000		0,000		0,000		0,000		0,000		0,000
2506G		0,000	1,0	0,241		0,000	2,0	0,560		0,000	5,0	1,443
2516		0,000		0,000		0,000		0,000		0,000		0,000
2601	1,0	0,326		0,000		0,000	2,0	0,560	1,0	0,806	1,0	0,289
2602	23,0	7,504	16,0	3,860	11,0	4,564	14,0	3,922	10,0	8,065	10,0	2,886
2606	62,0	20,228	49,0	11,821	52,0	21,577	47,0	13,165	33,0	26,613	59,0	17,027
2611		0,000	4,0	0,965		0,000		0,000		0,000	1,0	0,289
2612		0,000	1,0	0,241		0,000		0,000		0,000		0,000
2613	94,0	30,669	139,0	33,534	81,0	33,610	116,0	32,493	36,0	29,032	107,0	30,880
2615		0,000	8,0	1,930		0,000	3,0	0,840		0,000	2,0	0,577
2603G		0,000	2,0	0,483		0,000		0,000		0,000		0,000
2910		0,000	7,5	1,809		0,000	5,0	1,401		0,000		0,000
2917G		0,000		0,000		0,000		0,000		0,000		0,000
2904		0,000	1,0	0,241		0,000		0,000		0,000	2,0	0,577
2908G	18,5	6,036	20,5	4,946	14,0	5,809	15,0	4,202	6,0	4,839	25,0	7,215
2912G	15,0	4,894	16,0	3,860	5,0	2,075	12,0	3,361	2,0	1,613	16,0	4,618
2923		0,000		0,000		0,000		0,000		0,000		0,000
3201		0,000		0,000		0,000		0,000		0,000		0,000
3302		0,000		0,000		0,000		0,000		0,000		0,000
3303		0,000	2,0	0,483		0,000	4,0	1,120	0,5	0,403	1,0	0,289
3305G		0,000		0,000		0,000		0,000		0,000		0,000
3607G		0,000		0,000		0,000		0,000		0,000	3,0	0,866
3613												

	HVIII_50		HVIII_62.5-65.0		HVIII_75.0-77.5		HVIII_87.5-90.0		HVIII_100.0-102.5		HVIII_112.5-115.0	
ID after	**50**		**64**		**76**		**89**		**101**		**114**	
Gasse, 1995	numb.	%	numb.	%	numb.	%	numb.	%	numb.	%	numb.	%
3615		0,000		0,000		0,000		0,000		0,000		0,000
3617G		0,000		0,000		0,000		0,000		0,000		0,000
3620		0,000		0,000		0,000		0,000		0,000		0,000
3621G		0,000		0,000		0,000		0,000		0,000		0,000
3622		0,000		0,000		0,000		0,000		0,000		0,000
---		0,000		0,000	1,0	0,415		0,000		0,000	1,0	0,289
---		0,000		0,000		0,000		0,000		0,000	1,0	0,289
3712G												
3767		0,000		0,000		0,000		0,000		0,000		0,000
3728		0,000		0,000		0,000		0,000		0,000		0,000
3730	1,5	0,489	1,0	0,241	2,5	1,037	2,0	0,560		0,000		0,000
3732		0,000		0,000		0,000		0,000		0,000		0,000
3738		0,000		0,000		0,000	1,0	0,280		0,000		0,000
3742		0,000		0,000		0,000		0,000		0,000		0,000
3743	1,0	0,326		0,000		0,000		0,000		0,000		0,000
3606		0,000		0,000		0,000		0,000		0,000		0,000
3638		0,000		0,000		0,000		0,000		0,000		0,000
3627G												
3739G		0,000	1,0	0,241	2,0	0,830	3,0	0,840		0,000		0,000
3757	1,0	0,326		0,000		0,000		0,000		0,000	1,0	0,289
3906	4,5	1,468	4,0	0,965		0,000	2,0	0,560	1,0	0,806	4,5	1,299
3922		0,000	1,0	0,241		0,000		0,000		0,000		0,000
3918		0,000	2,0	0,483	4,0	1,660		0,000		0,000		0,000
3925		0,000	1,0	0,241		0,000		0,000		0,000		0,000
3942G	2,0	0,653	1,0	0,241		0,000		0,000		0,000		0,000
3936												
3932G												
3946		0,000		0,000		0,000		0,000		0,000		0,000
4003	7,0	2,284	7,0	1,689	7,0	2,905	8,0	2,241	3,0	2,419	2,0	0,577
4012												
4016		0,000		0,000		0,000		0,000		0,000		0,000
3954		0,000	1,5	0,362		0,000		0,000		0,000	0,5	0,144
4037		0,000		0,000		0,000	1,0	0,280	1,0	0,806		0,000
4070	3,0	0,979	5,0	1,206	1,0	0,415	2,0	0,560		0,000	1,0	0,289
4201		0,000		0,000		0,000		0,000		0,000		0,000
4208		0,000		0,000		0,000		0,000		0,000		0,000
4230		0,000		0,000		0,000		0,000		0,000		0,000
4220	0,5											
3647		0,000		0,000		0,000	2,5	0,700		0,000		0,000
4240												
4250		0,000		0,000		0,000	2,0	0,560		0,000		0,000
4501		0,000		0,000		0,000		0,000		0,000		0,000
4602	2,0	0,653	4,5	1,086	2,5	1,037	2,5	0,700	0,5	0,403	3,5	1,010
4603G		0,000		0,000		0,000		0,000		0,000		0,000
4614		0,000	0,5	0,121		0,000	0,5	0,140		0,000	1,5	0,433
4802		0,000		0,000		0,000		0,000		0,000		0,000
4808		0,000		0,000		0,000		0,000		0,000		0,000
5325												
5300		0,000	1,0	0,241		0,000		0,000		0,000		0,000
5401G		0,000	3,0	0,724	0,5	0,207	5,0	1,401	0,5	0,403	1,5	0,433
5402												
5403												
5417G		0,000	1,0	0,241	0,5	0,207	0,5	0,140		0,000	1,0	0,289
5424	5,5	1,794	3,5	0,844	2,0	0,830	4,5	1,261	2,0	1,613	5,0	1,443
5701		0,000		0,000		0,000		0,000		0,000		0,000
5702												
	0	99,837	0	100	0	100	0	100	0	100	0	100

	HV_270103-19		HV_270103-18		HV_270103-15		HV_270103-14		*HV* _7.5-10.0		HV_10.0-12.5	
ID after	**11**		**13**		**50**		**55**		**58**		**60**	
Gasse, 1995	numb.	%	numb.	%	numb.	%	numb.	%	numb.	%	numb.	%
		419		184		421		429,5		261,5		335,5
0103		0,000		0,000		0,000	1,0	0,233	1,0	0,382		0,000
0151		0,000		0,000		0,000		0,000		0,000		0,000
0104		0,000		0,000		0,000		0,000		0,000		0,000
0107		0,000		0,000		0,000		0,000		0,000	1,0	0,298
0108		0,000		0,000		0,000		0,000		0,000		0,000
0113G		0,000		0,000	5,0	1,188	3,0	0,698	2,0	0,765	1,0	0,298
0118		0,000		0,000		0,000		0,000		0,000		0,000
0311		0,000		0,000		0,000		0,000		0,000		0,000
0377		0,000		0,000		0,000		0,000		0,000		0,000
0325		0,000		0,000	2,0	0,475	2,0	0,466		0,000		0,000
0326		0,000		0,000		0,000		0,000		0,000		0,000
0370		0,000		0,000		0,000		0,000		0,000		0,000
0506		0,000		0,000	2,0	0,475	2,0	0,466	2,0	0,765	3,0	0,894
0503		0,000		0,000		0,000		0,000		0,000	2,0	0,596
3501		0,000		0,000		0,000		0,000		0,000		0,000
3502		0,000		0,000		0,000		0,000	31,0	11,855	117,0	34,873
3506		0,000		0,000		0,000		0,000	1,0	0,382		0,000
3507	1,0	0,239	4,0	2,174		0,000		0,000		0,000	2,0	0,596
3508		0,000		0,000		0,000	2,0	0,466	3,0	1,147		0,000
3510G		0,000		0,000		0,000		0,000		0,000		0,000
0904G		0,000		0,000		0,000		0,000		0,000		0,000
1401		0,000		0,000		0,000		0,000		0,000		0,000
1403	1,0	0,239	3,0	1,630	0,5	0,119		0,000		0,000	2,0	0,596
1405		0,000		0,000		0,000		0,000		0,000		0,000
1610		0,000		0,000		0,000	1,0	0,233	2,0	0,765		0,000
1655		0,000		0,000		0,000		0,000		0,000		0,000
1620		0,000		0,000		0,000		0,000	10,0	3,824	2,0	0,596
1625	4,0	0,955	5,0	2,717	31,0	7,363	14,0	3,260	14,0	5,354	11,0	3,279
1635		0,000		0,000	1,0	0,238	2,0	0,466	3,0	1,147	6,0	1,788
1901		0,000		0,000		0,000		0,000		0,000		0,000
1904	1,5	0,358	4,0	2,174	4,5	1,069	4,5	1,048	1,5	0,574	6,0	1,788
1911G		0,000		0,000		0,000		0,000	1,0	0,382		0,000
1912	2,0	0,477	1,0	0,543		0,000	3,0	0,698	7,5	2,868	4,5	1,341
1913		0,000		0,000		0,000	2,0	0,466		0,000		0,000
1920		0,000		0,000		0,000		0,000		0,000		0,000
1917		0,000		0,000		0,000		0,000		0,000		0,000
1946		0,000		0,000		0,000		0,000		0,000		0,000
1918												
2301		0,000		0,000		0,000		0,000	1,0	0,382		0,000
2303												
2406		0,000		0,000		0,000	3,5	0,815	1,5	0,574	3,0	0,894
2402		0,000		0,000		0,000		0,000	2,0	0,765		0,000
2404	5,5	1,313	5,0	2,717	17,5	4,157	20,0	4,657	8,5	3,250	17,5	5,216
2405		0,000		0,000		0,000		0,000	0,5	0,191	1,0	0,298
2504												
2503		0,000		0,000		0,000		0,000		0,000		0,000
2506G		0,000		0,000		0,000		0,000		0,000		0,000
2516		0,000		0,000		0,000		0,000		0,000		0,000
2601	10,0	2,387		0,000		0,000	3,0	0,698		0,000	1,0	0,298
2602	105,0	25,060	34,0	18,478	36,0	8,551	5,0	1,164	29,0	11,090	13,0	3,875
2606	175,0	41,766	109,0	59,239	199,0	47,268	259,0	60,303	89,0	34,034	66,0	19,672
2611	5,0	1,193		0,000		0,000		0,000		0,000		0,000
2612		0,000		0,000		0,000		0,000		0,000		0,000
2613	105,0	25,060	15,0	8,152	47,0	11,164	36,0	8,382	8,0	3,059	24,0	7,154
2615		0,000		0,000		0,000		0,000	1,0	0,382		0,000
2603G		0,000		0,000		0,000		0,000	2,0	0,765		0,000
2910		0,000		0,000		0,000		0,000		0,000		0,000
2917G		0,000		0,000		0,000		0,000		0,000		0,000
2904		0,000		0,000		0,000		0,000		0,000		0,000
2908G		0,000	0,5	0,272	5,5	1,306	4,0	0,931	3,0	1,147	4,0	1,192
2912G		0,000		0,000	5,5	1,306	2,0	0,466	4,0	1,530	4,0	1,192
2923		0,000		0,000		0,000		0,000	3,0	1,147		0,000
3201		0,000		0,000	1,0	0,238		0,000		0,000		0,000
3302		0,000		0,000		0,000		0,000		0,000		0,000
3303	0,5	0,119	0,5	0,272	3,5	0,831	6,5	1,513	3,0	1,147	4,0	1,192
3305G	2,0	0,477	1,5	0,815	14,0	3,325	9,0	2,095	2,0	0,765	2,0	0,596
3607G		0,000		0,000		0,000		0,000		0,000		0,000
3613												

	HV_270103-19		HV_270103-18		HV_270103-15		HV_270103-14		*HV* _7.5-10.0		HV_10.0-12.5	
ID after	**11**		**13**		**50**		**55**		**58**		**60**	
Gasse, 1995	numb.	%	numb.	%	numb.	%	numb.	%	numb.	%	numb.	%
3615		0,000		0,000		0,000		0,000		0,000		0,000
3617G		0,000		0,000		0,000		0,000		0,000		0,000
3620		0,000		0,000	2,0	0,475		0,000		0,000		0,000
3621G		0,000		0,000		0,000		0,000		0,000		0,000
3622		0,000		0,000		0,000		0,000		0,000		0,000
---		0,000		0,000		0,000	2,0	0,466	1,0	0,382		0,000
---		0,000		0,000		0,000		0,000		0,000		0,000
3712G												
3767		0,000		0,000		0,000		0,000		0,000		0,000
3728		0,000		0,000	4,5	1,069	1,0	0,233	1,0	0,382		0,000
3730		0,000	1,0	0,543	6,5	1,544	1,0	0,233	0,5	0,191	2,5	0,745
3732		0,000		0,000		0,000		0,000		0,000		0,000
3738		0,000		0,000		0,000		0,000		0,000		0,000
3742		0,000		0,000		0,000		0,000		0,000		0,000
3743		0,000		0,000	1,0	0,238	1,0	0,233		0,000		0,000
3606		0,000		0,000		0,000		0,000		0,000		0,000
3638		0,000		0,000		0,000		0,000		0,000		0,000
3627G												
3739G		0,000		0,000		0,000		0,000	1,0	0,382		0,000
3757		0,000		0,000	1,0	0,238		0,000		0,000		0,000
3906	0,5	0,119		0,000	19,0	4,513	25,5	5,937	6,0	2,294	14,5	4,322
3922		0,000		0,000		0,000		0,000		0,000		0,000
3918		0,000		0,000		0,000	4,0	0,931		0,000		0,000
3925		0,000		0,000		0,000		0,000	1,0	0,382		0,000
3942G		0,000		0,000		0,000		0,000		0,000		0,000
3936												
3932G												
3946		0,000		0,000		0,000		0,000		0,000		0,000
4003		0,000		0,000	2,0	0,475		0,000		0,000	2,0	0,596
4012												
4016		0,000		0,000		0,000		0,000		0,000		0,000
3954		0,000		0,000		0,000		0,000		0,000		0,000
4037		0,000		0,000		0,000		0,000		0,000		0,000
4070		0,000		0,000		0,000	3,0	0,698		0,000		0,000
4201		0,000		0,000		0,000		0,000		0,000		0,000
4208		0,000		0,000		0,000	2,0	0,466		0,000		0,000
4230		0,000		0,000		0,000		0,000		0,000		0,000
4220												
3647		0,000		0,000		0,000		0,000		0,000		0,000
4240												
4250		0,000		0,000		0,000		0,000		0,000		0,000
4501		0,000		0,000		0,000		0,000		0,000		0,000
4602	0,5	0,119		0,000	5,0	1,188		0,000	3,0	1,147	6,5	1,937
4603G		0,000		0,000		0,000		0,000	1,0	0,382		0,000
4614		0,000		0,000		0,000		0,000		0,000		0,000
4802		0,000		0,000		0,000		0,000		0,000		0,000
4808		0,000		0,000		0,000		0,000		0,000		0,000
5325												
5300		0,000		0,000		0,000		0,000		0,000		0,000
5401G		0,000	0,5	0,272	4,5	1,069	3,0	0,698	1,0	0,382	4,5	1,341
5402												
5403												
5417G		0,000		0,000		0,000		0,000	1,0	0,382		0,000
5424	0,5	0,119		0,000	0,5	0,119	2,5	0,582	2,0	0,765	4,0	1,192
5701		0,000		0,000		0,000		0,000	6,5	2,486	4,5	1,341
5702												
	0	100	0	100	0	100	0	100	0	100	0	100

	HV_270103-13		HV_12.5-15.0		HV_17.5-20.0		mod_CB3 [39]		mod_CB4 [40]		mod_H1 [133]	
ID after	**62**		**64**		**68**		**1**		**2**		**3**	
Gasse, 1995	numb.	%	numb.	%	numb.	%	numb.	%	numb.	%	numb.	%
		260		215		162,5						
0103		0,000		0,000		0,000		0,000		0,000		0,000
0151		0,000		0,000		0,000		0,000		0,000		0,000
0104		0,000		0,000		0,000		0,000		0,000		0,000
0107		0,000		0,000		0,000		0,000		0,000		0,000
0108		0,000		0,000		0,000		0,000		0,000		0,000
0113G		0,000	3,0	1,395	2,0	1,231		0,000		0,000		0,000
0118		0,000		0,000		0,000		0,000		0,000		0,000
0311		0,000		0,000		0,000		0,000		0,000		0,000
0377		0,000		0,000		0,000		0,000		0,000		0,000
0325		0,000		0,000	1,0	0,615		0,180		0,000		0,000
0326		0,000		0,000		0,000		0,000		0,000		0,000
0370		0,000		0,000		0,000		0,000		0,000		0,000
0506		0,000	0,5	0,233	1,0	0,615		0,180		0,000		0,000
0503		0,000	7,5	3,488		0,000		0,000		0,000		0,000
3501		0,000		0,000		0,000		0,000		0,000		0,000
3502	106,0	40,769	13,0	6,047	3,0	1,846		72,970		74,690		61,280
3506	1,0	0,385		0,000		0,000		0,000		0,000		0,000
3507	3,0	1,154	3,0	1,395		0,000		0,360		0,200		0,000
3508	6,0	2,308		0,000	1,0	0,615		5,050		7,140		15,950
3510G		0,000		0,000		0,000		0,000		0,000		0,000
0904G		0,000		0,000		0,000		0,000		0,000		0,000
1401		0,000		0,000		0,000		0,000		0,000		0,000
1403	0,5	0,192	0,5	0,233	4,0	2,462		0,180		0,000		0,000
1405		0,000		0,000		0,000		0,000		0,000		0,000
1610	1,0	0,385		0,000	1,0	0,615		0,000		0,000		0,000
1655		0,000		0,000		0,000		0,000		0,000		0,000
1620	2,0	0,769		0,000	4,0	2,462		0,000		0,000		0,000
1625	14,0	5,385	22,0	10,233	9,0	5,538		4,320		1,220		0,000
1635	1,0	0,385	1,0	0,465		0,000		0,000		0,000		0,000
1901		0,000		0,000		0,000		0,000		0,000		0,000
1904	4,5	1,731	3,5	1,628	2,5	1,538		0,000		0,000		0,000
1911G	3,0	1,154	1,0	0,465		0,000		0,000		0,000		0,000
1912	1,0	0,385	1,0	0,465	1,0	0,615		0,540		0,820		0,000
1913		0,000		0,000		0,000		0,000		0,000		0,000
1920		0,000		0,000		0,000		0,000		0,000		0,000
1917		0,000		0,000		0,000		0,000		0,410		0,000
1946		0,000		0,000		0,000		0,000		0,000		0,000
1918		0,000		0,000		0,000		0,360		0,200		
2301	1,0	0,385		0,000		0,000		0,000		0,000		0,000
2303		0,000		0,000		0,000		0,000		0,000		0,000
2406		0,000	3,0	1,395	4,0	2,462		0,720		0,200		0,000
2402		0,000		0,000		0,000		0,000		0,000		0,000
2404	7,5	2,885	4,5	2,093	4,0	2,462		0,000		0,000		0,000
2405		0,000	1,5	0,698		0,000		0,000		0,000		0,000
2504		0,000		0,000		0,000		0,000		0,000		0,000
2503		0,000		0,000		0,000		0,000		0,000		0,000
2506G		0,000		0,000		0,000		0,000		0,000		0,000
2516		0,000		0,000		0,000		0,000		0,000		0,000
2601		0,000		0,000	1,0	0,615		0,000		0,000		0,000
2602	34,0	13,077	26,0	12,093	23,0	14,154		0,000		0,000		0,000
2606	27,0	10,385	61,0	28,372	59,0	36,308		0,000		0,000		0,000
2611		0,000		0,000		0,000		0,000		0,000		0,000
2612		0,000		0,000		0,000		0,000		0,000		0,000
2613	12,0	4,615	24,0	11,163	14,0	8,615		0,000		0,000		0,000
2615		0,000	1,0	0,465	4,0	2,462		0,000		0,000		0,000
2603G		0,000	1,0	0,465		0,000		0,000		0,000		0,000
2910	1,0	0,385		0,000		0,000		0,000		0,000		0,000
2917G		0,000		0,000		0,000		0,000		0,000		0,000
2904		0,000		0,000	2,0	1,231		0,000		0,000		0,000
2908G		0,000		0,000	3,0	1,846		0,180		0,200		0,000
2912G	2,5	0,962	2,0	0,930	3,0	1,846		0,360		0,410		0,000
2923		0,000		0,000	1,0	0,615		0,000		0,000		0,000
3201		0,000		0,000		0,000		0,000		0,000		0,000
3302		0,000		0,000		0,000		0,000		0,000		0,000
3303	1,0	0,385	5,0	2,326	1,5	0,923		0,000		0,000		0,000
3305G	2,0	0,769	1,5	0,698	2,0	1,231		0,000		0,000		0,000
3607G		0,000		0,000		0,000		0,000		0,000		0,000
3613		0,000		0,000		0,000		0,360				

	HV_270103-13		HV_12.5-15.0		HV_17.5-20.0		mod_CB3 [39]		mod_CB4 [40]		mod_H1 [133]	
ID after	**62**		**64**		**68**		**1**		**2**		**3**	
Gasse, 1995	numb.	%	numb.	%	numb.	%	numb.	%	numb.	%	numb.	%
3615		0,000		0,000		0,000		0,000		0,000		0,000
3617G		0,000		0,000		0,000		0,000		0,000		0,000
3620	1,0	0,385		0,000		0,000		0,000		0,000		0,000
3621G		0,000		0,000		0,000		0,000		0,000		0,000
3622		0,000		0,000		0,000		0,000		0,000		0,000
---		0,000	3,0	1,395		0,000		0,000		0,000		0,000
---		0,000		0,000		0,000		0,000		0,000		0,000
3712G	1,0	0,385		0,000		0,000		0,000		0,000		0,000
3767		0,000		0,000		0,000		0,000		0,000		0,000
3728		0,000		0,000		0,000		0,000		0,000		0,000
3730	1,0	0,385	0,5	0,233	1,0	0,615		0,000		0,000		0,000
3732		0,000		0,000		0,000		0,000		0,000		0,000
3738		0,000		0,000		0,000		0,000		0,000		0,000
3742		0,000		0,000		0,000		0,000		0,000		0,000
3743		0,000		0,000		0,000		0,000		0,000		0,000
3606		0,000		0,000		0,000		0,000		0,000		0,000
3638		0,000		0,000		0,000		0,000		0,000		0,000
3627G		0,000		0,000		0,000		0,720		0,000		0,000
3739G	0,5	0,192	4,0	1,860		0,000		0,000		0,000		0,000
3757		0,000		0,000		0,000		0,000		0,000		0,000
3906	10,5	4,038	8,0	3,721	3,0	1,846		0,180		0,000		0,000
3922		0,000		0,000		0,000		0,000		0,000		0,000
3918		0,000		0,000		0,000		0,000		0,000		0,000
3925		0,000		0,000		0,000		0,000		0,000		0,000
3942G	2,0	0,769		0,000		0,000		0,000		0,000		0,000
3936		0,000		0,000		0,000		0,900		0,820		0,000
3932G		0,000		0,000		0,000		0,720		0,820		0,000
3946		0,000		0,000		0,000		0,000		0,000		0,000
4003	1,0	0,385		0,000		0,000		0,000		0,000		0,000
4012		0,000		0,000		0,000						
4016		0,000		0,000		0,000		3,060		0,000		0,000
3954		0,000		0,000		0,000		0,000		0,000		0,000
4037		0,000	3,0	1,395		0,000		0,000		0,000		0,000
4070	1,0	0,385		0,000		0,000		0,000		0,000		0,000
4201		0,000		0,000		0,000		0,000		0,000		0,000
4208		0,000		0,000		0,000		0,000		0,000		0,000
4230		0,000		0,000		0,000		0,000		0,000		0,000
4220	0,5	0,192		0,000		0,000		0,000		0,000		0,000
3647		0,000		0,000		0,000		0,000		0,000		0,000
4240		0,000		0,000		0,000		0,000		0,000		0,000
4250		0,000		0,000		0,000		0,000		0,000		0,000
4501		0,000		0,000		0,000		0,000		0,410		0,000
4602	3,0	1,154	3,5	1,628	1,5	0,923		0,000		0,000		0,000
4603G		0,000		0,000	4,0	2,462		0,180		0,000		0,000
4614		0,000		0,000		0,000		0,000		0,000		0,000
4802		0,000		0,000		0,000		0,000		0,000		0,000
4808		0,000		0,000		0,000		0,000		0,000		0,000
5325		0,000		0,000		0,000		0,360		0,000		0,000
5300		0,000		0,000		0,000		0,000		0,000		0,000
5401G	1,5	0,577	2,5	1,163	0,5	0,308		0,000		0,410		0,000
5402		0,000		0,000		0,000		0,000		0,000		10,120
5403		0,000		0,000		0,000		5,410		2,450		6,030
5417G		0,000	0,5	0,233		0,000		1,080		1,430		0,000
5424	3,0	1,154	3,5	1,628	1,5	0,923		1,260		1,840		0,000
5701	3,0	1,154		0,000		0,000		0,000		0,000		0,000
5702		0,000		0,000		0,000		0,000		3,670		0,000
	0	100	0	100	0	100	0	99,63	0	97,34	0	93,38

	mod_H2 [148]		mod_H3 [150]		mod_JK2 [155]		mod_JK3 [156]		mod_JK4 [157]		mod_JK5 [158]	
ID after	**4**		**5**		**6**		**7**		**8**		**9**	
Gasse, 1995	numb.	%	numb.	%	numb.	%	numb.	%	numb.	%	numb.	%
0103		0,000		0,000		0,000		0,000		0,000		0,000
0151		0,000		0,000		0,000		0,000		0,000		0,000
0104		0,000		0,520		0,000		0,000		0,000		0,000
0107		0,000		0,000		0,000		0,000		0,000		0,000
0108		0,000		0,000		0,000		0,000		0,000		0,000
0113G		0,000		0,000		0,000		0,000		0,000		0,990
0118		0,000		0,000		0,000		0,000		0,000		0,000
0311		0,000		0,000		0,000		0,000		0,000		0,000
0377		0,000		0,000		0,000		0,000		0,000		0,000
0325		0,000		1,220		0,000		0,000		0,000		0,000
0326		0,000		0,000		0,000		0,000		0,000		0,000
0370		0,000		0,000		0,000		0,000		0,000		0,000
0506		0,000		0,000		0,000		0,000		0,000		0,000
0503		0,000		0,000		0,000		0,000		0,000		0,000
3501		0,000		0,350		0,000		0,000		0,000		0,000
3502		6,630		12,060		58,610		17,550		75,750		22,520
3506		0,000		0,000		0,000		0,000		0,000		0,000
3507		0,000		0,870		0,990		0,000		0,000		0,000
3508		1,530		1,750		2,650		0,660		0,000		3,640
3510G		0,000		0,000		0,000		0,000		0,000		0,000
0904G		0,000		0,000		0,000		0,000		0,000		0,000
1401		0,000		0,000		0,000		0,000		0,000		0,000
1403		0,000		0,000		0,000		0,000		0,000		0,000
1405		0,000		0,000		0,000		0,000		0,000		0,000
1610		0,000		0,000		0,000		0,000		0,000		0,000
1655		0,000		0,000		0,000		0,000		0,000		0,000
1620		0,260		0,000		0,000		0,000		0,660		0,000
1625		0,000		0,350		0,000		0,000		0,000		0,000
1635		0,000		0,000		0,000		0,000		0,000		0,000
1901		0,000		0,000		0,000		0,000		0,000		0,000
1904		0,000		0,000		0,000		0,000		0,000		0,000
1911G		0,000		0,000		0,000		0,000		0,000		0,000
1912		0,000		0,000		0,660		0,000		0,000		0,000
1913		0,000		0,000		0,000		0,000		0,000		0,000
1920		0,000		0,000		0,000		0,000		0,000		0,000
1917		0,000		0,350		0,000		0,000		1,000		0,000
1946		0,000		0,000		0,000		0,000		0,000		0,000
1918				0,350								
2301		0,000		0,000		0,000		0,000		0,000		0,000
2303		0,000		0,000		0,000		0,000		0,000		0,000
2406		0,000		0,350		0,000		0,000		0,000		0,000
2402		0,000		0,170		0,000		0,000		0,000		0,000
2404		0,000		0,870		0,000		0,000		0,000		0,000
2405		0,000		0,000		0,000		0,000		0,000		0,000
2504		0,000		0,350		0,000		0,000		0,000		0,000
2503		0,000		0,000		0,000		0,000		0,000		0,000
2506G		0,000		0,170		0,000		0,000		0,000		0,000
2516		0,000		0,000		0,000		0,000		0,000		0,000
2601		0,000		0,000		0,000		0,000		0,000		0,000
2602		0,000		0,000		0,000		0,000		0,000		0,000
2606		0,000		0,000		0,000		0,000		0,000		0,000
2611		0,000		0,000		0,000		0,000		0,000		0,000
2612		0,000		0,000		0,000		0,000		0,000		0,000
2613		0,000		0,000		0,000		0,000		0,000		0,990
2615		0,000		0,000		0,000		0,000		0,000		0,000
2603G		0,000		0,000		0,000		0,000		0,000		0,000
2910		0,000		0,000		0,000		0,000		0,000		0,000
2917G		0,000		0,000		0,000		0,000		0,000		0,000
2904		0,000		0,000		0,000		0,000		0,000		0,000
2908G		0,000		0,870		0,000		0,000		0,000		0,000
2912G		0,000		0,520		0,000		0,000		0,000		0,000
2923		0,000		1,750		0,000		0,000		0,000		0,000
3201		0,000		0,520		0,000		0,000		0,000		0,000
3302		0,000		0,000		0,000		0,000		0,000		0,000
3303		0,000		0,000		0,000		0,000		0,000		0,000
3305G		0,000		0,000		0,000		0,000		0,000		0,000
3607G		0,000		0,000		0,000		0,000		0,000		0,000
3613				0,870								

	mod_H2 [148]		mod_H3 [150]		mod_JK2 [155]		mod_JK3 [156]		mod_JK4 [157]		mod_JK5 [158]	
ID after	**4**		**5**		**6**		**7**		**8**		**9**	
Gasse, 1995	numb.	%	numb.	%	numb.	%	numb.	%	numb.	%	numb.	%
3615		0,000		0,870		0,000		0,000		0,000		0,000
3617G		0,000		0,000		0,000		0,000		0,000		0,000
3620		0,000		0,000		0,000		0,000		0,000		0,000
3621G		0,000		0,000		0,000		0,000		0,000		0,000
3622		0,000		0,000		0,000		0,000		0,000		0,000
---		0,000		0,000		0,000		0,000		0,000		0,000
---		0,000		0,000		0,000		0,000		0,000		0,000
3712G		0,000		2,270		0,000		0,000		0,000		0,000
3767		0,000		0,000		0,000		0,000		0,000		0,000
3728		0,000		0,000		0,000		0,000		0,000		0,000
3730		0,000		0,000		0,000		0,000		0,000		0,000
3732		0,000		0,000		0,000		0,000		0,000		0,000
3738		0,000		0,000		0,000		0,000		0,000		0,000
3742		0,000		0,000		0,000		0,000		0,000		0,000
3743		0,000		0,000		0,000		0,000		0,000		0,000
3606		0,000		0,000		0,000		0,000		0,000		0,000
3638		0,000		0,000		0,000		0,000		0,000		0,000
3627G		0,000		0,000		0,000		0,000		0,000		0,000
3739G		0,000		0,000		0,000		0,000		0,000		0,000
3757		0,000		0,700		0,000		0,000		0,000		0,000
3906		0,000		0,000		0,000		0,660		0,000		0,000
3922		0,000		0,000		0,000				0,000		0,000
3918		0,000		0,000		0,000		0,000		0,000		0,000
3925		0,000		0,000		0,000		0,000		0,000		0,000
3942G		0,000		0,000		0,000		0,000		0,000		0,000
3936		0,000		0,350		0,000		0,990		1,000		0,000
3932G		0,000		0,170		0,000		0,000		0,000		0,000
3946		0,000		0,000		0,000		0,000		0,000		0,000
4003		0,000		0,000		0,000		0,000		0,000		0,000
4012				0,700						1,000		0,990
4016		0,000		0,000		0,000		0,000		0,000		0,000
3954		0,000		0,000		0,000		0,000		0,000		0,000
4037		0,000		0,000		0,000		0,000		0,000		0,000
4070		0,000		0,000		0,000		0,000		0,000		0,000
4201		0,000		0,000		0,000		0,000		0,000		0,000
4208		0,000		0,170		0,000		0,000		0,000		0,000
4230		0,000		0,000		0,000		0,000		0,000		0,000
4220		0,000		0,170		0,000		0,000		0,000		0,000
3647		0,000		0,000		0,000		0,000		0,000		0,000
4240		0,000		0,000		0,000		0,000		0,000		0,000
4250		0,000		0,000		0,000		0,000		0,000		0,000
4501		0,000		0,000		0,000		0,000		0,000		0,000
4602		0,000		0,000		0,000		0,000		0,000		0,000
4603G		0,000		0,000		0,000		0,000		0,000		0,000
4614		0,000		0,000		0,000		0,000		0,000		0,000
4802		0,000		0,000		0,000		0,000		0,000		0,000
4808		0,000		0,000		0,000		0,000		0,000		0,000
5325		0,000		0,000		0,000		0,000		0,000		0,000
5300		0,000		0,000		0,000		0,000		0,000		0,000
5401G		0,000		0,350		31,460		78,480		19,930		70,200
5402		0,000		0,000		0,000		0,000		0,000		0,000
5403		91,330		11,010		0,000		0,000		0,000		0,000
5417G		0,000		50,000		0,000		0,000		0,000		0,000
5424		0,000		1,220		4,970		0,660		0,000		0,660
5701		0,000		0,000		0,000		0,000		0,000		0,000
5702		0,000		0,000		0,000		0,000		0,000		0,000
	0	99,75	0	92,24	0	99,34	0	99	0	99,34	0	99,99